MODERN DEVELOPMENT OF MAGNETIC RESONANCE

abstracts

2021

KAZAN ∗ RUSSIA

MODERN DEVELOPMENT OF MAGNETIC RESONANCE

KAZAN 2021

MODERN DEVELOPMENT OF MAGNETIC RESONANCE

ABSTRACTS OF THE INTERNATIONAL CONFERENCE

Editors:
ALEXEY A. KALACHEV
KEV M. SALIKHOV

KAZAN, NOVEMBER 1–5, 2021

CHAIRMEN

Alexey A. Kalachev
Kev M. Salikhov

PROGRAM COMMITTEE

Kev Salikhov, chairman (Russia)
Vadim Atsarkin (Russia)
Elena Bagryanskaya (Russia)
Pavel Baranov (Russia)
Marina Bennati (Germany)
Robert Bittl (Germany)
Bernhard Blümich (Germany)
Michael Bowman (USA)
Gerd Buntkowsky (Germany)
Sergei Demishev (Russia)
Sabine Van Doorslaer (Belgium)
Rushana Eremina (Russia)
Jack Freed (USA)
Alexey Kalachev (Russia)
Vladislav Kataev (Germany)
Walter Kockenberger (Great Britain)
Wolfgang Lubitz (Germany)
Anders Lund (Sweden)
Sergei Nikitin (Russia)
Klaus Möbius (Germany)
Hitoshi Ohta (Japan)
Igor Ovchinnikov (Russia)
Vladimir Skirda (Russia)
Alexander Smirnov(Russia)
Graham Smith (Great Britain)
Mark Smith (Great Britain)
Murat Tagirov (Russia)
Takeji Takui (Japan)
Valery Tarasov (Russia)
Violeta Voronkova (Russia)

LOCAL ORGANIZING COMMITTEE

Khantimerov S.M., chairman
Latypov V.A., vice-chairman
Mamin R.F., vice-chairman
Voronkova V.K., scientific secretary
Akhmetgalieva A.M.
Falin M.L.
Fazlizhanov I.I.
Garipov R.R.
Gubaidulina A.Z.
Guseva R.R.
Khabibullina V.I.
Khakimova L.N.

Konovalov D.A.
Kupriyanova O.O.
Kurkina N.G.
Mukhtasarova Kh.L.
Oladoshkin Yu.V.
Pushkova V.V.
Salikhov K.M.
Sukhanov A.A.
Tarasov V.F.
Vorobeva V.E.
Yanduganova O.B.
Zaripov R.B.

SCIENTIFIC SECRETARIAT

Violeta K. Voronkova
Laila V. Mosina
Vladislav A. Latypov

The conference is organized under the auspices of the AMPERE Society

ORGANIZERS

Zavoisky Physical-Technical Institute, FRC Kazan Scientific Center of RAS
Kazan Federal University
The Academy of Sciences of the Republic of Tatarstan

SUPPORTED BY

The Government of the Republic of Tatarstan
The Russian Science Foundation (Project No. 20-63-46034)

CONTENTS

SECTION 5
NEW TRENDS IN SPIN CHEMISTRY

ZAVOISKY AWARD LECTURES

Magnetic Resonance One Spin at a Time

J. Wrachtrup

University of Stuttgart, 3rd Institute of Physics and Center for Applied Quantum Technology, Stuttgart, Germany

Single spin resonance has found its way into ultrasensitive spectroscopy and quantum applications. Single spins and few spin clusters e.g. are ideal playgrounds to explore fundamental properties of quantum physics, like e.g. probing the "quantumness" of a system or understand the measurement process with unprecedented accuracy [1, 2]. Beyond that, spins are leading contenders in the race for practical quantum computers. Good photonic interfaces as well as excellent spin coherence properties and coherent control make them close to ideal candidates for small scale quantum registers needed for scaling quantum networks [3].

Single spin probes also are developing into versatile use to measure the properties of materials with high spatial resolution. Besides measuring single spin detected NMR [4], specifically magnetic materials lend themselves as interesting objects to be investigated by single spin quantum probes [5]. To this end a single spin, like a single nitrogen vacancy centre in diamond, is scanned across a sample while at the same time measuring its electron spin resonance frequency as a probe for local magnetic fields.

1. Vorobyov V. *et al.*: arxiv2104.04507 (2021)
2. Pfender M. *et al.*: Nature Comm. **10**, 594 (2019)
3. Henson B. *et al.*: Nature **526**, 682 (2015)
4. Aslam N.: *et al.*: Science **357**, 6346, 67 (2017)
5. Qi-Chao Sun *et al.*: Nature Comm. **12**, 1989 (2021)

EPR Adventures in the Strongly Correlated World: Quantum Materials and Quantum Critical Systems

S. V. Demishev

Prokhorov General Physics Institute of Russian Academy of Sciences, Vavilov street 38, Moscow 119991, Russian Federation, demis@lt.gpi.ru

Recent progress in the application of the electron paramagnetic resonance (EPR) method for the investigation of various strongly correlated materials, quantum materials, and quantum critical phenomena is discussed [1–3]. Special attention is paid to the case of metallic systems including CeB_6, $Mn_{1-x}Fe_xSi$, and metallic surface of topological Kondo insulator SmB_6. A new technique of EPR measurements and data analysis in strongly correlated metals, which allows finding the full set of spectroscopic parameters including oscillating magnetization, relaxation parameter (line width), and hyromagnetic ratio (g-factor) is described. It is shown that EPR in strongly correlated and quantum materials provides a unique tool for studying short-range correlations at the nanoscale of a spin polaron type, spin nematic effects, and spin fluctuation transitions. Application of EPR technique opens new opportunities for investigation of quantum criticality in strongly correlated metals and doped quantum spin chains observation of quantum critical points, including hidden ones. In many cases, it is exactly the EPR method, which either indicates the necessity for clarification or deep revision of the prevailing paradigm or constitutes the basis for a new concept of magnetic properties of various strongly correlated and quantum materials. However, in spite of achieved considerable progress in experimental studies, several breakthroughs, and very valuable theoretical results, the ESR research on the considered class of objects is still awaiting Columbus, who will map the new beautiful islands of scientific knowledge.

1. Demishev S.V.: Appl. Magn. Reson. **51**, 473 (2020)
2. Demishev S.V., Semeno A.V., Ohta H.: Appl. Magn. Reson. **52**, 379 (2021)
3. Semeno A.V., Okubo S., Ohta H., Demishev S.V.: Appl. Magn. Reson. **52**, 459 (2021)

PLENARY LECTURES

Compact Magnetic Resonance: Progress and Applications

B. Blümich

ITMC, RWTH Aachen University, Aachen 52159, Germany, bluemich@rwth-aachen.de

The era of compact NMR started in the 1970ties with the advent of tabletop NMR relaxometers [1]. In took about 50 years to learn how to make compact permanent magnets with fields sufficiently homogeneous to resolve the ^{1}H chemical shifts. Today multi-nuclear tabletop NMR spectrometers are used routinely for chemical analysis [2]. Arguably the miniaturization of precision compact permanent magnets benefitted from the advances in shaping the strayfield of inside-out NMR sensors used for oil-well logging and nondestructive materials testing [3, 4].

Recent progress in instrumentation and applications of compact NMR is reported. In particular, methods of mapping the sensitive volume of strayfield-sensors like the NMR-MOUSE and compact magnets have been developed [5], the NMR-MOUSE has been employed in unconventional outdoor measurements like in Yellowstone National Park and the fire damaged library of the Glasgow School of Art [6]. Moreover, a compact and open permanent magnet has been built and passively shimmed for chemical-shift resolved Overhauser-DNP experiments [7], and a high-pressure setup has been constructed and tested for compositional analysis of gas mixtures at pressures of up to 200 bar [8]. Current work concerns the development of a compact and robust prototype stray-field sensor for outdor measurements [9].

1. Blümich B.: J. Magn. Reson. **306**, 27–35 (2019)
2. Blümich B., Singh K.: Angew. Chem. Int. Ed. **57**, 6996–7010 (2018)
3. Jackson J.A., Burnett L.J., Harmon J.F., J. Magn. Reson. **41**, 411–421 (1980)
4. Blümich B., Perlo J., Casanova F.: Prog. Nucl. Magn. Reson. Spectr. **52**, 197–269 (2008)
5. Überrück T., Rehorn C., Höhner R., Blümich B.: J. Magn. Reson. **296**, 169–175 (2018)
6. Blümich B., Jaschtschuk D., Rehorn C., in: S. Haber-Pohlmeier, B. Blümich, L. Ciobanu, eds., Magnetic Resonance Microscopy. Instrumentation and Applications in Engineering, Life Science and Energy Research, Wiley-VCH, Weinheim, 2021, in press.
7. Überrück T., Adams M., Granwehr J., Blümich B.: J. Magn. Reson. **314**, 10267 (2021)
8. Duchowny A., Dupuy P.M., Widerøe H.C., Berg O.J., Fanes A., Paulsen A., Thern H., Mohnke O., Blümich B., Adams A.: J. Magn. Reson. **329**, 107025 (2021)
9. Blümich B., Anders J.: Magnetic Resonance **2**, 149–160 (2021)

CW and Pulse EPR of Radicals in Solutions Undergoing Exchange

M. K. Bowman[1], B. Bales[2], R. N. Schwartz[3]

[1] Novosibirsk Institute of Organic Chemistry, Novosibirsk 630090, Russia;
Chemistry & Biochemistry Dept., University of Alabama, Tuscaloosa, AL 35487,
USA, mkbowman@ua.edu
[2] Department of Physics and Astronomy, The Center for Biological Physics,
California State University at Northridge, Northridge, CA 91330, USA, barney.bales@csun.edu
[3] Electrical and Computer Engineering Department, University of California, Los Angeles,
Los Angeles, CA 90095, USA, rnschwartz@msn.com

Paramagnetic systems have a very wide range of behaviors and properties that make them both scientifically interesting and technologically useful in fields as diverse as: dosimetry, archeological dating, single molecular magnets, atomic clocks, masers, dynamic and chemical spin polarization, magnetic resonance imaging, and quantum computing/communication. The classic Bloch equations are a convenient basis for summarizing or predicting the EPR properties of some of these paramagnetic systems and for interpreting their CW and pulse EPR spectroscopy. The Bloch equations are widely used for free radicals in liquid solution.

We show, using simple solutions of Galvinoxyl radical, how exchange during simple collisions in solution alter the spin behavior as predicted by Prof. Salikhov's new paradigm. The more complex spin behavior provides an opportunity to experimentally measure the dynamics and kinetic properties of radicals and non-radicals in these solutions.

The classic Bloch equations require that each spin packet or 'isochromat' acts independently of all other spin packets so that the CW or FT-EPR spectra depend on three properties of the radicals: the resonance frequencies, T_1 and T_2. Exchange destroys the independence of each spin packet and makes the behavior of each spin packet depend on the magnetization of every other spin packet. In CW spectra, we see changes in the shape, position, and number of lines and in the ease of saturation; while in pulse spectra, there is spectral diffusion, magnetization transfer, and changes in line shape and position. When exchange is added to make a set of 'modified' Bloch equations, the solutions at short times describing pulse EPR spectra can be quite different from the steady-state solutions describing the CW spectra. The ease of saturating the CW spectrum may not be simply related to the relaxation of Mz in pulse experiments.

Radical SAM Enzymes, and the Jahn-Teller Effect Hiding in Plain Sight

B. M. Hoffman

Northwestern University, 2145 Sheridan Road, Evanston 60208, Il, USA,
bmh@northwestern.edu

Integrative Structural Ensemble Biology Based on EPR-Derived Distance Distributions

G. Jeschke, L. Esteban-Hofer

[1] Department of Chemistry and Applied Biosciences, ETH Zurich, CH-8093, Switzerland, gjeschke@ethz.ch

The function of proteins and their interactions with other molecules depend on an interplay between precisely structured and flexible parts. This leads to heterogeneously distributed structure, which can be modeled by ensembles of conformers. Methodology for doing so is still in its infancy. On the one hand, most experimental techniques provide only ensemble averages of parameters. They are thus deficient in information on the width of the ensemble. On the other hand, parametrization of force fields for molecular dynamics simulations is not usually sufficiently good for making valid predictions on disordered regions. Dipolar spectroscopy techniques of EPR can provide distance distributions between spin labels. They thus provide exactly the missing information on ensemble width, and they do so even with site-pair resolution. However, sample preparation is tedious, so that only a small number of distance distribution restraints (DDRs) is usually available. Further, uncertainty in modeling spin-label sidechain conformation limits effective resolution of such restraints in terms of backbone conformation. Finally, DDRs are measured on freeze-quenched samples, raising the question whether they are representative for the conformer ensemble at ambient temperature. For all these reasons, the DDRs should be integrated with restraints from other techniques

In this contribution, we discuss our general approach for doing this. In this approach, we first use DDRs alone in generation of a raw ensemble. Second, we use them again, now together with other restraints in ensemble fitting and contraction. Examples for other restraints are small-angle scattering curves and NMR paramagnetic relaxation enhancement data. Further, we discuss the RigiFlex approach. This approach partitions the system into rigid bodies, whose structures can be determined with established approaches, and flexible parts. We thus separate the rigid-body arrangement problem and the modeling of each individual flexible part. The fully scriptable modeling suite MMMx implements such ensemble generation, fitting and ensemble analysis.

Our concepts are illustrated by elastic network modeling of a structural transition and by an ensemble model of the RNA-binding protein SRSF1 in complex with a short RNA.

Liquid-Liquid Phase Separation of the N-Terminal Domain of CPEB4 via the Good Old CW EPR and the Help of DEER

D. Goldfarb

Department of Chemical and Biological Physics, Weizmann Institute of Science, Rehovot 7510001, Israel, Daniella.goldfarb@weizmann.ac.il

Knowledge about the structural and dynamic properties of proteins that form membrane-less organelles in cells via liquid-liquid phase separation (LLPS) is required for understanding the process at a molecular level. We used spin labeling and electron paramagnetic resonance (EPR) spectroscopy, complemented by double-electron-electron resonance (DEER) to investigate the dynamic properties (rotational diffusion) of the low complexity N-terminal domain of cytoplasmic polyadenylation element binding-4 protein ($CPEB4_{NTD}$) across its LLPS transition, which takes place with increasing temperature. We report coexistence of three spin labeled $CPEB4_{NTD}$ (CPEB4*) populations with distinct dynamic properties representing different conformational spaces, both before and within LLPS state. Monomeric CPEB4* exhibiting fast motion defines population **I** and shows low abundance prior to and following LLPS. Population **II** and **III** are part of a CPEB4* assembly where **II** corresponds to loose conformations with intermediate range motions and population **III** represents compact conformations with strongly attenuated motions. As the temperature increased the population of component **II** increased reversibly at the expense of component **III**, indicating the existence of an **III** $\rightleftharpoons$ **II** equilibrium. We correlated the macroscopic LLPS properties with the **III** $\rightleftharpoons$ **II** exchange process upon varying temperature and CPEB4* and salt concentrations and hypothesized that weak transient intermolecular interactions facilitated by component **II** lead to LLPS, with the small assemblies integrated within the droplets. The LLPS transition, however, was not associated with a clear discontinuity in the correlation times and population of the three components. Importantly, $CPEB4_{NTD}$ exhibits unique LLPS properties where droplet formation occurs from a preformed microscopic assembly rather than the monomeric protein molecules.

Recent Advances in Multinuclear Solid-State NMR of Inorganic Materials

M. E. Smith[1-3]

[1] President and Vice-Chancellor's Office and Department of Chemistry, University of Southampton, University Road, Southampton, SO17 1BJ, UK
[2] Department of Chemistry, Lancaster University, Bailrigg, Lancaster, LA1 4YB, UK
[3] Department of Physics, University of Warwick, Coventry, CV4 7AL, UK

The family of oxynitride ceramics β′-sialons, a solid solution with the unit cell changing continuously with z ($Si_{6-z}Al_zO_zN_{8-z}$, where $0 \leq z \leq {\sim}4.2$), which were originally studied by solid-state NMR in the mid-1980s has recently been re-investigated. The significant methodological progress since the 1980s is discussed (e.g. fields of up to 20 T, multiple quantum approaches, Density Functional Theory (DFT) calculations). These advances have greatly enhanced the ability to probe and understand atomic ordering in oxynitrides by solid-state NMR. Four structural models of the possible atomic ordering in β′-sialons have been proposed, which result in differing distributions of the local coordination units present. The latest NMR work can distinguish between these distributions [1]. Further recent work on other closely related oxynitrides using the same methodology is presented [2]. Advances in NMR capability towards observation of nuclei with small magnetic moments (termed low-γ), especially those that experience the quadrupolar interaction are also examined. Illustrative examples will be given from work on ^{43}Ca [3] (including with magnetic fields up to 35.2 T [4]) and ^{105}Pd [3, 5]. The ability to better observe more nuclei allows a more comprehensive multinuclear approach. When experimental observation is coupled with DFT calculations there are cases where the low-γ nucleus provides the crucial information at distinguishing different potential structural models.

1. Seymour V.R., Smith M.E.: J. Phys. Chem. A **123**, 9729 (2019)
2. Seymour V.R., Griffin J.M., Griffith B.E., Page S.J., Iuga D., Hanna J.V., Smith M.E.: J. Phys. Chem. C **124**, 23976 (2020)
3. Smith M.E.: Magn. Reson. Chem. (Early View) DOI: 10.1002/mrc.5116
4. Bonhomme C., Wang X., Hung I., Gan Z., Gervais C., Sassoye C., Rimza J., Du J., Smith M.E., Hanna J.V., Sarda S., Gras P., Combes C., Laurencin D.: Chem. Comm. **54**, 9595 (2018)
5. Hooper T.J.N., Partridge T.A., Rees G.J., Keeble D.S., Powell N.A., Smith M.E., Mikheenko I.P., Macaskie L.E., Bishop P.T., Hanna J.V.: Phys. Chem. Chem. Phys. **41**, 26734 (2018)

NMR and MRI Studies of Catalytic Processes
Taking Advantage of Nuclear Spin Hyperpolarization

I. V. Koptyug

International Tomography Center, SB RAS, Novosibirsk 630090, Russian Federation,
koptyug@tomo.nsc.ru

It is well established today that parahydrogen can be a useful and powerful source of hyperpolarization of nuclear spins for boosting sensitivity in numerous applications of NMR spectroscopy and imaging (MRI). A number of variants of parahydrogen-based techniques are used today to achieve this goal. Furthermore, it is quite remarkable that parahydrogen can be applied to study the mechanisms of important catalytic processes that involve H_2 as a reactant. In particular, hydrogenation processes of unsaturated hydrocarbons are of great fundamental and practical importance. Already in the 1930s (i.e., before the NMR era) para-hydrogen was actively used in catalysis to study the features and mechanisms of H_2 activation and hydrogenation processes on metals [1]. In 1987 it was shown [2] that the use of parahydrogen in homogeneous hydrogenations can lead to a significant enhancement of the NMR signals of reaction products and intermediates. The observation of this effect requires that both hydrogen atoms that end up in the product molecule come from the same H_2 molecule. This pairwise H_2 addition mechanism, characteristic of metal complexes in solution, is fundamentally different from the mechanism of hydrogenation on the surface of metals formulated by Horiuti and Polanyi [3], which is based exclusively on the hydrogenation of a substrate with random individual hydrogen atoms on the metal surface. Nevertheless, in 2008 it was experimentally established that pairwise hydrogen addition is in fact possible on supported metal catalysts [4], which is unambiguously confirmed by the significant enhancements of the NMR signals during such processes. The substantiation of such an unexpected reaction mechanism and the establishment of its contribution requires not only a detailed study of the features of the ortho-para conversion of hydrogen on the surface of metals in the presence of reacting substrates and of the amplification of the NMR signal of the products, but also a critical analysis of the existing catalytic literature. If pairwise hydrogen addition process over metal-based catalysts may, under favorable conditions, compete successfully with the non-pairwise Horiuti-Polanyi mechanism, significant improvements in signal enhancement levels using heterogeneous hydrogenations are likely possible.

In addition to mechanistic studies, parahydrogen-based hyperpolarization can help address a number of major challenges encountered in the applications of NMR and MRI to the studies of heterogeneous systems, including multiphase reacting media and model operating reactors. In particular, the use of para-drogen can provide a useful sensitivity boost when one deals with gases or low-concentrated solutions, or with the spatially resolved MRI studies where the sensitivity issue is even more demanding. In particular, parahydrogen-induced

polarization (PHIP) is particularly suited for the studies of chemical processes that involve activation and chemical transformations of molecular hydrogen. Examples to be presented will include the visualization of operating model reactors [5] and development of SABRE approaches for heteronuclear MRI [6]. In addition, it will be shown that hyperpolarized xenon is a useful probe for heterogeneous processes including thermometry of a granular catalyst bed under operating conditions [7].

Another major complication associated with multiphase systems is that they tend to severely perturb an applied permanent magnetic field, leading to the loss of spectral resolution. Possible approaches to address this issue will be addressed based on the suitable design of NMR/MRI-compatible model reactors [5] as well as on performing the reaction studies at zero and ultra-low magnetic fields [8] where sample heterogeneity does not limit the spectral resolution that can be achieved.

1. Farkas A., Farkas L.: J. Am. Chem. Soc. **60**, 22 (1938)
2. Bowers C.R., Weitekamp D.P.: J. Am. Chem. Soc. **109**, 5541 (1987)
3. Horiuti I., Polanyi M.: Trans. Faraday Soc. **30**, 1164 (1934)
4. Kovtunov K.V., Beck I.E., Bukhtiyarov V.I., Koptyug I.V.: Angew. Chem. Int. Ed. **47**, 1492 (2008)
5. Svyatova A., Kononenko E.S., Kovtunov K.V., Lebedev D., Gerasimov E.Y., Bukhtiyarov A., Prosvirin I., Bukhtiyarov V., Muller C.R., Fedorov A., Koptyug I.V.: Catal. Sci. Technol. **10**, 99 (2020)
6. Salnikov O.G., Chukanov N.V., Svyatova A., Trofimov I.A., Kabir M.S.H., Gelovani J.G., Kovtunov K.V., Koptyug I.V., Chekmenev E.Y.: Angew. Chem. Int. Ed. **60**, 2406 (2021)
7. Burueva D.B., Pokochueva E.V., Wang X., Filkins M., Svyatova A., Rigby S.P., Wang C., Pavlovskaya G.E., Kovtunov K.V., Meersmann T., Koptyug I.V.: ACS Catal. **10**, 1417 (2020)
8. Burueva D.B., Eills J., Blanchard J.W., Garcon A., Picazo-Frutos R., Kovtunov K.V., Koptyug I.V., Budker D.: Angew. Chem. Int. Ed. **59**, 17026 (2020)

SECTION 1

PERSPECTIVES OF MAGNETIC RESONANCE IN SCIENCE AND SPIN TECHNOLOGY

Spin in Singlet Fission – Identification and Dynamics of Singlet, Triplet and Quintet States

D. McCamey

University of New South Wales, Sydney, Australia,
dane.mccamey@unsw.edu.au

High-Frequency Rapid Scan Electron Spin Resonance Spectroscopy

A. Sojka, M. Šedivý, A. Solodovnik, A. Lagin, T. Láznička, V. Santana, A. Marko, O. Laguta, <u>P. Neugebauer</u>

Central European Institute of Technology, Magneto-Optical and Terahertz Spectroscopy Group, Brno University of Technology, Purkynova 123, 61200 Brno, Czech Republic.
petr.neugebauer@ceitec.vutbr.cz

We report on the recent development of a high-frequency rapid scan electron spin resonance (FRASCAN) spectrometer at the Brno University of Technology. The basic principle of frequency rapid scan will be explained and compared to conventional methods. The FRASCAN operates in induction mode using quasi-optics with a superheterodyne detection scheme. Fast frequency sweeps of the order of 1000 THz/s allows to access spin relaxation of the order of 1 ns [1], in a frequency range of 80 GHz to 1100 GHz [2], at temperatures from 1.8 K to 300 K, and at magnetic fields up to 16 T. We developed several sample holders for performing measurements on liquids, oriented single crystals, and air-sensitive samples, including the possibility of photo-excitation [3]. In addition, we developed a carousel sample holder for pressed powders that accommodates up to 6 samples, avoiding the time-consuming event of loading the probe into the cryostat and cooling down process. The carousel holder can be used for quantitative ESR. The FRASCAN is controlled by a home-written software in LabView, allowing to run experiments in an automatic mode controlled by scripts. Multi-frequency rapid scan experiments on an oriented single crystal of LiPc will be presented along with simulation for calculation of the relaxation times. Furthermore, additional capabilities of FRASCAN are demonstrated using frequency-detected magnetic resonance spectra as a function of the orientation for a single-crystal of copper acetate and frequency-field ESR maps for Mn12 and TEMPO.

1. Laguta O., Tuček M., van Slageren J., Neugebauer P.: J. Magn. Reson. **296**, 138–142 (2018)
2. Neugebauer P., Bloos D., Marx R., Lutz P., Kern M., Aguila D., Vaverka J., Laguta O., Dietrich C., Clérac R., van Slageren J.: Phys.Chem.Chem.Phys. **20**, 15528 (2018)
3. Sojka A., Šedivý M., Solodovnik A., Lagin A., Láznička T., Santana V., Marko A., Laguta O., Neugebauer P., to be published

FRaScan Spectrometer.

^{1}H, ^{13}C NMR for Testing of Edible Oils

<u>G. S. Kupriyanova</u>^{2}, G. V. Mozzhukhin^1, I. G. Mershiev^2,
M. L. Smirnov^2, B. Z. Rameev^{1,3}

^{1} Department of Physics, Gebze Technical University, 41400 Gebze/Kocaeli, Turkey.
^{2} Immanuel Kant Baltic Federal University, 236041 Kaliningrad, Russian Federation
^{3} Zavoisky Physical-Technical Institute, FRC Kazan Scientific Center of RAS, Kazan 420029,
Russian Federation, galkupr@yandex.ru, mgeorge@gtu.edu.tr, rameev@gtu.edu.tr

It is known that high resolution ^{1}H, ^{13}C NMR spectroscopy is used in a broad range of scientific and various technological applications, e.g. food, petrochemistry, pharmaceutics, medicine, etc [1, 2]. In recent years, much attention has been paid to the study of vegetable oils, which is associated with an increase in the growth of cases of falsification of high-quality oils. For the analysis of oils, typical target compounds in their composition are fatty acids, triacylglycerol, sterols, volatiles, phenolic compounds, phospholipids. They serve as markers characterizing the quality of vegetable oils, determining their authenticity, and revealing falsification. Techniques based on high resolution ^{1}H NMR are used as a powerful tool for quantification of the composition of fatty acids in vegetable oils without the need for any sample processing. However, high resolution NMR is a rather expensive method that requires significant costs to maintain the stable operation of the superconducting magnet, as well as the costs of using deuterated solvents.

Along with high-resolution NMR methods, time-domain methods (TD ^{1}H NMR) in a low magnetic field are being developed to determine the quality of food products and their composition [3]. The development of permanent magnets systems with a magnetic field of up to 1 Tesla contributed to the creation of relatively cheap compact NMR relaxometers. ^{1}H NMR relaxometry methods have been used to study various varieties of technical oils, polymer products from the point of view of their degradation [4]. In recent years, NMR relaxation methods in low field have been intensively developing, using fast Laplace transform algorithms that make it possible to extract in addition to the T_1, T_2 relaxation times also the data on T_1-T_2, T_2-T_2 correlations [5]. The main advantage of this method is the low cost of testing and portability of the equipment. From the point of view of solving the problem of identifying counterfeit products among high-quality oils, it is important to find the main identification features for various kinds of vegetable oils and their mixtures that would form the basis for determining their quality and adulteration degree. However, the conventional relaxation experiments requires rather long measurement times.

This paper presents the results of an experimental study various types of oils, such as flax seed oil, bone oil, olive oils made in Italy, Turkey, vegetable oils and their mixtures, as well as processed soybean oils by TD ^{1}H NMR in a relatively low magnetic field as well as ^{13}C, ^{1}H, ^{31}P NMR spectroscopy in a high magnetic field. The results of measurements of the longitudinal and transverse relaxation times of various types of oils (olive, linseed oils, bone oil, flax seed,
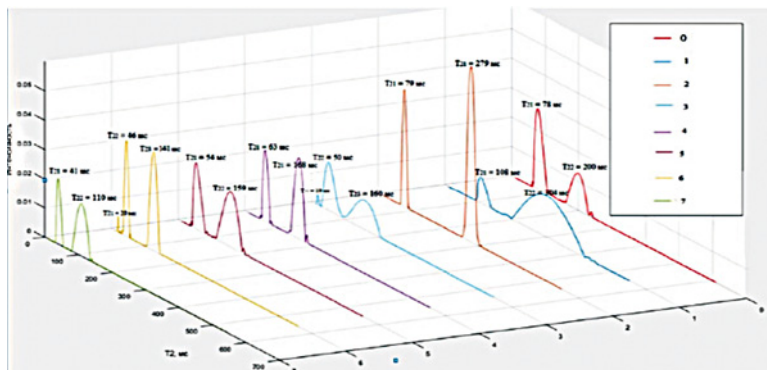
Fig. 1. The distribution functions of ^{1}H transverse relaxation times for various oils.

soybean, sunflower) made by different methods have been studied and compared to evaluate the possibility of distinguishing between them. As example, the distribution function of ^{1}H transverse relaxation times obtained using of fast Laplace transform algorithms for various oils are shown in Fig. 1. ^{1}H, ^{13}C high resolution NMR have been also used as a reference to determine the oil quality and composition.

The main goal of this research has been to optimize the parameters of the relaxation experiment, shorten the experimental time and conduct a relaxation study of various oils. The second task has consisted of a deeper study of edible oils from the point of view of analyzing their quality and composition and the possibility of applying the relaxation spectroscopy method with using Laplace transform to distinguish between different substances to detect counterfeit and substandard products among Turkish olive oils. It is known that the detection of counterfeit substances and adulterated food products is a very important problem nowadays. On the other hand, the solutions related to the low field TD NMR could be used in very various technological applications, e.g. food, petrochemistry, pharmaceutics, medicine, etc.

1. Mannina L., Sobolev A.P.: Special Issue Review Magn. Reson. Chem. **49**, S3–S11 (2011)
2. Pauli G.F., Gödecke T., Jaki B.U., Lankin D.C.: J. Nat. Prod. **75**(4): 834–851 (2012)
3. Blümich B., Haber-Pohlmeier S., Zia W.: Compact NMR. Berlin.Boston, Walter de Gruyter GmbH, 2014. 276 p
4. Sinyavsky N.Ya., Mershiev I.G., Kupriyanova G.S.: Marine intelligent technology. VI International Baltic Marine Forum. **4** (42), T. 3. 2018.

Spin-Electric Coupling in a Copper(II)-Based Spin Triangle Revealed by Electric-Field-Modulated Electron Spin Resonance Spectroscopy

M. Fittipaldi[1], A. Cini[1,2], M. Perfetti[2], B. Kintzel[3], M. Böhme[3], W. Plass[3], R. Sessoli[2]

[1] Department of Physics and Astronomy and INSTM Research Unit, University of Florence, via Sansone 1, I-50019 Sesto Fiorentino, Italy, maria.fittipaldi@unifi.it

[2] Department of Chemistry 'Ugo Schiff' and INSTM Research Unit, University of Florence, via della lastruccia 3-13, I-50019 Sesto Fiorentino, Italy

[3] Institute of Inorganic and Analytical Chemistry, Friedrich Schiller University Jena, Humboldt str. 8, 07743 Jena, Germany.

The possibility to operate on magnetic materials through the application of electric rather than magnetic fields – promising faster, more space confined and energy efficient circuits – continues to spur the investigation of magnetoelectric (ME) effects [1]. Symmetry considerations, in particular the lack of an inversion centre, characterize linear ME effect. In addition, spin–orbit coupling is generally considered necessary to make a spin system sensitive to a charge distribution. However, a ME effect not relying on spin–orbit coupling is appealing for spin-based quantum technologies. We have very recently reported the detection of a ME effect that we have attributed to an electric field modulation of the magnetic exchange interaction without atomic displacement [2]. The effect is visible in electron paramagnetic resonance (EPR) absorption of molecular helices
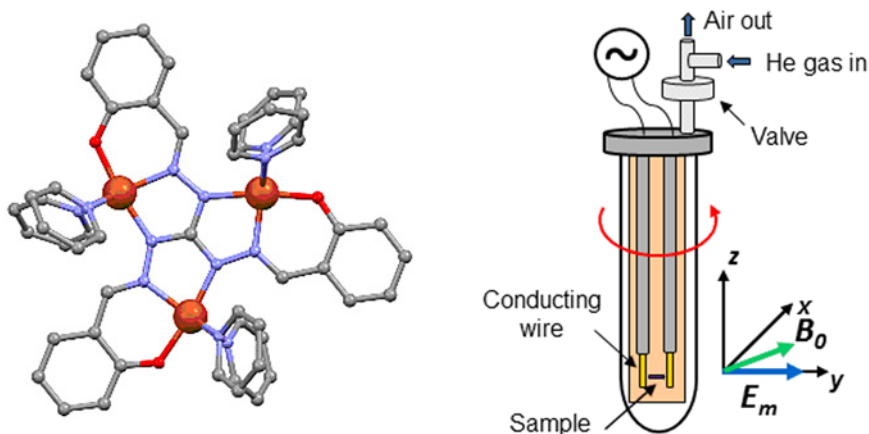
Fig. 1. Left: the molecular structure of the spin-frustrated Cu3, with a ground state $\underline{S}$ = 1/2. Right: schematic view of the modified version of the sample holder used for the EFM-EPR measurements. The orientations of the static magnetic field (B_0), and the electric field (E_m) are shown. E_m is obtained by applying an alternating voltage $V = V_0\cos(\omega t)$, with V_0 = 170 V over a distance of 1.5 mm, and $\omega = 2\pi \cdot 30$ kHz.

under electric field modulation (EFM-EPR) and confirmed by specific symmetry properties and spectral simulation.

After this report, an oscillating electric field ten times stronger was imparted to the sample by an improvement in the experimental setup. This made possible the observation of a ME effect in a single-crystal of a frustrated Cu3 triangle (Fig. 1). The orientation dependence of the effect was recorded, and fully analyzed by means of a phenomenological model as well as by extensive computational studies performed in order to investigate the EFM-ESR effect in silico. Therefore, the magnitude and the anisotropy of the variations of Hamiltonian tensors induced by the electric field has been revealed. This is a significant step forward for the design of new molecular-based spin-electric systems which may have an impact on information technology as well as for conceiving new devices based on them.

1. Spaldin N. A., Fiebig M.: Science **309**, 391–392 (2005)
2. Fittipaldi M., Cini A., Annino G., Vindigni A., Caneschi A., Sessoli R.: Nat. Mater. **18**, 329–334 (2019)

New DNP Results in Liquid State Samples at High Magnetic Fields

A. Kuzhelev, D. Dai, V. Denysenkov, <u>T. Prisner</u>

Institute of Physical and Theoretical Chemistry and Center of Biomolecular Magnetic Resonance,
Goethe University Frankfurt, Germany

Dynamic Nuclear Polarization (DNP) at high magnetic fields has become a very powerful technique with many applications in structural biology, chemistry, surface analytics, material sciences and medicine [1]. Most of these developments execute the polarization transfer step from the unpaired electron spin of the paramagnetic DNP agent to the nuclear spins of the target molecule in the solid state at temperatures below 110 K. The DNP mechanism which work in solid samples are the solid and the cross effect and thermal mixing. Applications on samples at high temperatures and in the liquid state are predominantly performed by other hyperpolarization methods or by fast dissolution of the solid sample [2]. We will report on some of our recent new results performing DNP directly at room temperature in liquid samples at a magnetic field of 9.4 T, corresponding to 260 GHz and 400 MHz resonance frequency for the electron and proton spin, respectively. To avoid sample heating of the liquid sample by the microwave irradiation a home-build Fabry-Pérot DNP resonator is used for efficient saturation of the electron spin transitions and for sensitive detection of proton and carbon nuclear spins [3]. We will show new applications based on our earlier results on lipid bilayer doped with paramagnetic radicals [4] and discuss the polarization transfer mechanism and efficiencies at high magnetic field as well as potential applications.

1. Corzilius B.: Annu. Rev. Phys. Chem. **71**, 143–170 (2020)
2. Ardenkjær-Larsen J.H., Golman K., Gram A., Lerche, M.H., Servin R., Thaning M., Wolber J.: Proc. Natl. Acad. Sci. **3** (19), 37–379 (2003)
3. Denysenkov V., Prisner T.: J. Magn. Reson. **217**, 1–5 (2012)
4. Jakdetchai O., Denysenkov V., Becker-Baldus J., Dutagaci B., Prisner T.F.; Glaubitz C.: J. Am. Chem. Soc. **136** (44), 15533–15536 (2014)
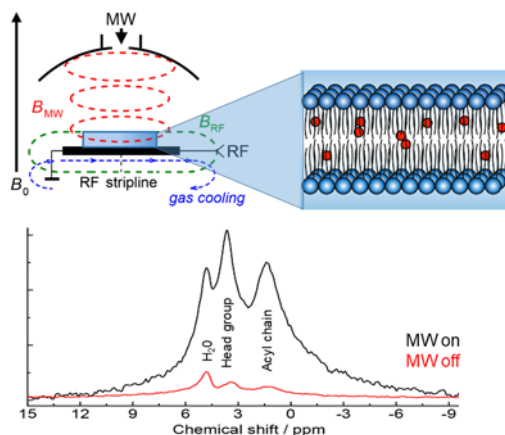
Update on Radical Pairs and Photo-CIDNP
to Commemorate Prof. Konstantin Ivanov

J. Matysik

Institute of Analytical Chemistry, Leipzig University, 04103 Leipzig, Germany,
jo-erg.matysik@uni-leipzig.de

A phenomenon allowing for nuclear polarization in NMR is called "photochemically induced dynamic nuclear polarization" (photo-CIDNP). Its occurrence relies on the dynamics of spin-correlated radical pairs which transfers electron hyperpolarization into nuclear hyperpolarization. Under solid-state conditions, detected by magic-angle spinning (MAS) NMR under in-situ illumination, the phenomenon was for many years confined to acceptor-blocked and frozen photosynthetic reaction center proteins. For recent review in the solid-state photo-CIDNP effect, see ref. [1]. Recently, it became evident that designed frozen flavoproteins also allow for the induction of the effect [2, 3]. These systems also provide plenty of opportunities to tailor the parameters and to optimize its occurrence for different conditions and experiments.

The presentation will discuss present developments and future plans on this research line. In particular, the great contributions of Prof. Konstantin Ivanov to this field will be remembered.

1. Matysik J., Ding Y., Kim Y., Kurle P., Yurkovskaya A., Ivanov K., Alia A.: "Photo-CIDNP in solid state" (Review) Applied Magnetic Resonance (2021) online. DOI: 10.1007/s00723-021-01322-5.
2. Ding Y., Kiryutin A.S., Zhao Z., Xu Q.Z., Zhao K.H., Kurle P., Bannister S., Kottke T., Sagdeev R.Z., Ivanov K.L., Yurkovskaya A.V., Matysik J.: Scientific Reports **10**, 18658 (2020)
3. Ding Y., Kiryutin A., Yurkovskaya A., Sosnovsky D., Sagdeev R.Z., Bannister S., Kottke T., Kar R., Schapiro I., Ivanov K., Matysik J.: Scientific Reports **9**, 18436 (2019)

Relaxation of Lanthanide Ions in Acidic Aqueous Ethanol Solutions

S. S. Eaton[1], G. R. Eaton[1], J. E. McPeak[1,2]

[1] Department of Chemistry and Biochemistry, University of Denver, Denver, Colorado, USA 80208, sandra.eaton@du.edu
[2] Berlin Joint EPR Laboratory and EPR4Energy, Department Spins in Energy Conversion and Quantum Information Science (ASPINS), Helmholtz-Zentrum Berlin für Materialien und Energie GmbH, Hahn-Meitner-Platz 1, Berlin 14109, Germany, joseph.mcpeak@helmholtz-berlin.de

Although lanthanides have been studied extensively in ionic lattices, there are relatively few reports of electron spin relaxation times for lanthanides in glassy solutions [1]. Electron spin relaxation times T_1 and T_m in acidified 1:1 solutions of water:ethanol for $4f^8$ S = 3, L = 3 Tb^{3+}, $4f^{12}$ S = 1, L = 5 Tm^{3+} [2], and $4f^5$ S = 5/2 Sm^{3+} were measured by inversion recovery and 2-pulse electron spin echo methods between about 4.2 and 10 K with B_1 perpendicular to B_0 (Fig. 1). The Tb^{3+} and Tm^{3+} cations are non-Kramers ions and the EPR signals are attributed to energy levels that are admixtures of $M_J = \pm 6$ [3]. Comparison studies were performed of $3d^5$ Mn^{2+} and Fe^{3+}. Phase memory times, T_m, are less than 1 µs at 4.2 K for all species in this study and is attributed to spectral diffusion within the electron spin system, such as by small librations of the highly anisotropic ions [4]. The wide distributions of inversion recovery time constants were
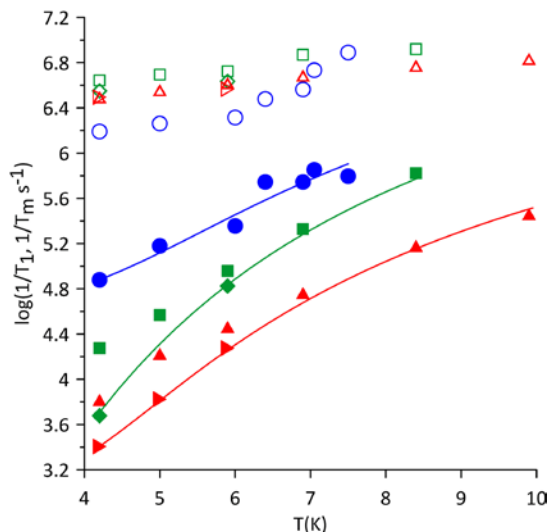
Fig. 1. Temperature dependence of relaxation rates in 1:1 water (pH ~ 1):ethanol. $1/T_m$ for (□) 10 mM Tb^{3+}, (◊) 1 mM Tb^{3+}, (Δ) 10 mM Tm^{3+}, (▷) 1 mM Tm^{3+}, (○) 1 mM Sm^{3+}; $1/T_1$ for (■) 10 mM Tb^{3+}, (♦) 1 mM Tb^{3+}, (▲) 10 mM Tm^{3+}, (▶) 1 mM Tm^{3+}, and (●) 1 mM Sm^{3+}. The solid lines are fits to the temperature dependence of $1/T_1$ including contributions from the direct and Raman processes.

analyzed with stretched exponentials and the uniform penalty (UPEN) method [5]. The T_1 values are much shorter than for 3d transition elements which is attributed to the large spin-orbit couplings for the lanthanides. The temperature dependence was modeled as the sum of the direct and Raman processes [4]. The process that is denoted as the direct process may be impacted by cross relaxation between neighboring paramagnetic centers which also depends linearly on temperature. The temperature range over which relaxation times were long enough to measure by spin echo was smaller for Sm^{3+} than for Tb^{3+} or Tm^{3+} so the Debye temperature was fixed at 54 K which was found previously for this acidic water:ethanol mixture [2]. The fit parameters were A_{dir} = 320., 0., and $1.6 \cdot 10^4$ s^{-1} for Tm^{3+}, Tb^{3+}, and Sm^{3+}, respectively and A_{Ram} = $3.2 \cdot 10^8$, $1.4 \cdot 10^9$, and $3.3 \cdot 10^9$ s^{-1}K^{-1} for Tm^{3+}, Tb^{3+}, and Sm^{3+}, respectively.

1. McPeak J.E., Eaton S.S., Eaton G.R.: Meth. Enzymol. 651, 63–101 (2021)
2. McPeak J., Alexander D., Joseph C., Eaton S.S., Eaton G.R.: Appl. Magn. Reson. **51**, 961–976 (2020)
3. Baker J.M., Hutchison J.C.A., Martineau P.M.:Proc. Roy. Soc. London. A, Math. Phys. Sci. **403**, 221–233 (1986)
4. Eaton S.S., Eaton G.R.: Biol. Magn. Reson. **19**, 29–154 (2000)
5. Borgia G.C., Brown R.J.S., Fantazzini P.: J. Magn. Reson. **147**, 273–285 (2000)

Influence of the Optical Configuration
of a Chiral Linked System on its Reactivity

T. Leshina[1], A. Ageeva[1], P. Kuznetsova[1,2], V. Plyusnin[1,2], A. Doktorov[1]

[1] Voevodsky Institute of Chemical Kinetics and Combustion SB RAS, Novosibirsk 630090,
Russian Federation
[2] Department of Natural Sciences, Novosibirsk State University, Novosibirsk 630090,
Russian Federation, leshina@ngs.ru

Establishing differences in the properties of L and D-tryptophan (Trp) that are part of various proteins, enzymes and receptors is an important fundamental and practical problem, since the optical isomers themselves are identical in physicochemical properties, while proteins containing L and D isomers of amino acids, in particular, Trp, are dramatically different [1]. Thus chiral inversion known to occur during aging of living organisms and lead to the replacement in a number of proteins L isomers of amino acids with D analogs, is currently considered one of the main causes of Alzheimer's, Parkinson's, type II diabetes and a number of other pathological conditions [1]. Due to the difficulties arising in the study of these highly disordered proteins by modern physicochemical methods, including high-resolution NMR spectroscopy, the model systems is proposed for studying the reasons of the abnormal behavior of proteins with D optical isomers of amino acids. In particular, the authors of [1] propose to apply mathematical modeling to study the role of the optical configuration of proteins using the example of short peptides. This report puts forward a modification of this approach: We will talk about photoinduced processes involving the transfer of an electron or a hydrogen atom that occurs in chiral linked systems: donor –acceptor dyads. One partner of dyad is a chiral drug- ketoprofen (KP), the other is D or L tryptophan (Trp) [2]. The fact that two of the three studied configurations of the dyad, in which L and D Trp are linked to S or R ketoprofen (KP-Trp), are enantiomers (RS and SR configurations) poses new problems. Comparison of the R,S and S,R enantiomers is important because, like enantiomers with one chiral carbon atom, they have completely identical physicochemical properties, with the exception of the direction of rotation of the plane of polarization. This also implies the identical reactivity. Meanwhile, the activity of chiral drugs enantiomers with several chiral atoms often differ by orders of magnitude. Studies have shown that a change in the configuration of even one chiral center changes the activity of Trp during quenching by the main mechanism, energy transfer. This also applies to enantiomers which are quenched with different efficiency. We tried to connect these results with the difference in conformations of dyad's in different optical configuration, which were calculated by quantum-chemical methods. As for quenching by the electron transfer mechanism, the enantiomers really demonstrate the same efficiency, but the S,S configuration shows an ET contribution that is almost an order of

magnitude larger. In order to quantitatively compare the contributions of ET, an original theory was developed that calculates the differences in the CIDNP effects of various optical configurations. Thus, we believe that, as a result, an approach has been developed to study the effect of optical configuration on reactivity, which can be applied to more complex and practically important systems, e.g. peptides.

1. Raskatov J., Teplow D.: Scientific Reports **7**: 12433, DOI:10.1038/s41598 -017-10525
2. Ageeva A., Babenko S., Magin I., Plyusnin V., Kuznetsova P., Stepanov A., Vasilevsky S., Polyakov N., Doktorov A., Leshina T.: Int. J. Mol. Sci. **21**, 5370 (2020); doi:10.3390/ijms21155370.

Optically Active Spin Centers in Silicon Carbide for Sensing and Quantum Computing Applications: a Study of Double Resonances

P. G. Baranov[1], A. N. Anisimov[1], I. D. Breev[1], V. A. Soltamov[1], R. A. Babunts[1], S. B. Orlinskii[2]

[1] Ioffe Institute, Politekhnicheskaya 26, Saint Petersburg 194021, Russian Federation
[2] Federal Center of Shared Facilities of Kazan State University, Kazan 420008, Russian Federation,
pavel.baranov@mail.ioffe.ru

The unique quantum properties of the nitrogen-vacancy (NV) color center in diamond have motivated efforts to find defects with similar properties in silicon carbide (SiC), which can extend the functionality of such systems [1]. SiC is a well-developed wide-band-gap semiconductor widely used for applications in high-frequency, high-temperature, high-power, and radiation-resistant electronic devices. SiC is taking on a new role as a flexible and practical platform for harnessing the new quantum technologies. Atomic-scale color centers in bulk and nanocrystalline SiC are promising systems for spintronics, photonics compatible with fiber optics, quantum information processing and sensing at ambient conditions. Their spin state can be initialized, manipulated and readout by means of optically detected magnetic resonance (ODMR), level anticrossing and cross-relaxation. It has been shown that there are at least two families of color centers in SiC with $S = 1$ and $S = 3/2$, which have the property of optical alignment of the spin levels and allow a spin manipulation. For the $S = 3/2$ family, the ground state and the excited state were demonstrated to have spin $S = 3/2$ and a population inversion in the ground state can be generated using optical pumping, leading to stimulated microwave emission even at room temperature and above.

The uniqueness of the SiC is also manifested in the presence of silicon and carbon isotopes with both nuclear angular ($I = 1/2$) and, therefore, magnetic moments, and isotopes with zero angular (magnetic) moments. This makes it possible to widely use isotope engineering, that is, the modification of the isotopic composition of silicon and carbon in solving certain applied problems. An important area of research is the determination of hyperfine interactions, which are realized for silicon and carbon nuclei located both in the immediate environment of the spin center and in distant positions. The main method for such studies is electron-nuclear double resonance (ENDOR), in which the radio-frequency quantum of nuclear magnetic resonance is replaced by a microwave EPR quantum, which sharply increases the NMR sensitivity, according to the same principle as in ODMR, where the microwave quantum is replaced by an optical quantum.

High-frequency pulsed ENDOR was used to determine electron-nuclear interactions on remote ligand shells of silicon and carbon in spin-3/2 color centers with an optically induced high-temperature spin alignment in hexagonal 4H-, 6H- and rhombic 15R- SiC polytypes. The EPR and ENDOR experimental data relate

unambiguously to spin-3/2 centers in which the optically induced alignment of the spin level populations occurs. The identification is based on resolved ligand hyperfine interactions with carbon and silicon nearest, next nearest and the more distant neighbors and on the determination of the unpaired electron spin densities. The hyperfine interactions with ^{29}Si and ^{13}C nuclei are unambiguously separated due to the selective population of the fine structure levels with certain values of MS. The signs of these interactions and, as a result, the signs of oscillating spin density at ^{29}Si and ^{13}C nuclei, are determined. On the basis of the EPR and optically induced ENDOR measurements, signs of the fine structure splitting for all the centers were demonstrated, which made it possible to establish the character of optically induced spin alignment, including the inverse populations of the spin levels for these centers. The values of hyperfine interaction with ^{29}Si and ^{13}C nuclei, including those remote from the localization of the spin-3/2 center, are tabulated, which can be used by a number of algorithms in quantum information processing as long-term memory.

The experimental achievements in all-optical magnetometry and thermometry with submicron resolution based on the spin state mixing at level anticrossings and cross-relaxation in an external magnetic field will be discussed. Fabricating various types of microstructures and nanostructures in SiC with spin color centers, has increasingly attracted owing to their potential applications in electronic and photonic devices. The successful use of metamaterials with NV centers provides a basis for suggesting a similar combination for color centers in SiC whose radiation extends to a near infrared range of 800–1600 nm which is area of transparency for fiber optics and living systems.

In conclusion, we note that one of the main directions in the development of technologies based on silicon carbide is the creation and study of optically active spin structures in silicon carbide and related semiconductors as a material platform for spintronics, nanoscale sensing, quantum information processing, and the development of hybrid quantum systems.

1. Baranov P.G., von Bardeleben H.-J., Jelezko F., Wrachtrup J.: Magnetic Resonance of Semiconductors and Their Nanostructures: Basic and Advanced Applications: Springer Series in Materials Science **253**, 2017.

Electrically Detected Non-Linear Electron Paramagnetic Magnetic Resonance

Ch. Boehme

Department of Physics and Astronomy, University of Utah 115S, 1400E, Salt Lake City, USA,
boehme@physics.utah.edu

In materials where electronic states generally experience weak spin-orbit coupling, e.g. organic semiconductors, spin-selection rules emerge which allow for spin-dependent electric current that are sensitive of spin-permutation symmetry and other quantum mechanical observables. This presentation is about using these spectroscopic probes to detect magnetic resonance at very low magnetic fields/Zeeman energies [1, 2] for the study of the non-perturbative drive regime of magnetic dipole excitations. These experiments have revealed previously not accessible magnetic resonant strong-drive phenomena, including spin-collectivity effects [3], multiple-quantum transitions occurring at integer and fractional *g*-factors, as well as a magnetic resonant Bloch-Siegert Shift [4, 5].

1. McCamey D.R. *et al.*: Phys. Rev. Lett. **104** (1), 017601.
2. Baker W.J. *et al.*: Nature Commun. **3**, 898, (2012
3. Waters D.P. *et al.*: Nat. Phys. **11**, 910 (2015)
4. Jamali S. *et al.*: Nano Lett. **17**, 4648 (2017)
5. Jamali S. *et al.*: Nature Commun. **12** (1), 1 (2021)

Free Radicals within Active Layers of Organic Solar Cells and Their Effect on Photoinduced Charge Carriers

D. A. Nevostruev[1], A. V. Kulikova[1,2], D. S. Baranov[1], <u>M. N. Uvarov</u>[1]

[1] Voevodsky Institute of Chemical Kinetics and Combustion,
Siberian Branch of the Russian Academy of Sciences, Institutskaya Str. 3, Novosibirsk 630090,
Russian Federation, uvarov@kinetics.nsc.ru
[2] Novosibirsk State University, Pirogova Str. 2, Novosibirsk 630090, Russian Federation

Photocurrent generation in organic solar cells (OSC) is rather interesting and important phenomenon which should be investigated and described to manufacture stable and effective thin-film electronic devices. Under visible light illumination active layer of OSC is full by photoinduced charge carriers. The propose of the present study is to reveal and describe any effects related charge dissociation and photocurrent generation due to doping of free radicals into the active layer of OSC by continuous wave and pulse EPR techniques. One of such radicals was galvinoxyl radical **Gx** (Fig. 1) which was successfully used to improve efficiency of OSC based an active layer of polymer/fullerene composite [1]. New tetraazapyrene-based compound **1** was synthesized by its modification by nitroxide radical. The compound **1** has branched substituent and heterocyclic moiety which allows to avoid undesirable effects of aggregation within polymer/fullerene blend. Spin relaxation of photoinduced fullerene anions could be enhanced by **Gx** radical but not by nitroxide **1**, therefore doped stable radicals could manage of photocurrent generation process within OSCs.

1. Zhang Y., Basel T.P., Gautam B.R., Yang X., Mascaro D.J., Liu F., Vardeny Z.V.: Nat. Commun. **3**, 1043 (2012)
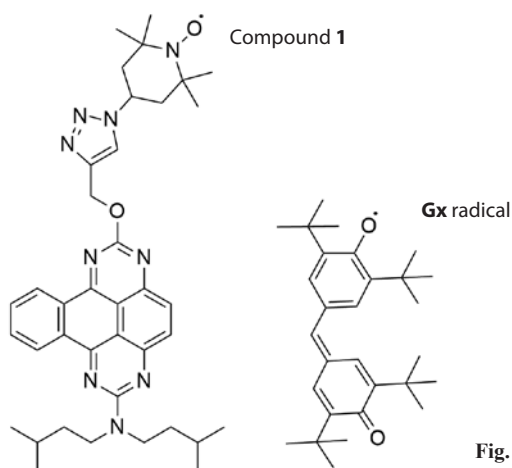
Fig. 1. Stable radicals investigated.

Spin Echo Studies in GaN:Fe: Spin-Phonon Relaxation and Ligand Hyperfine Interactions

D. V. Azamat[1,2,3], A. G. Badalyan[1], N. G Romanov[1], M. Hrabovsky[2], L. Jastrabik[3], A. Dejneka[3], D. R. Yakovlev[1,4], M. Bayer[1,4]

[1] Ioffe Institute, Russian Academy of Sciences, St. Petersburg 194021, Russian Federation
[2] Palacky University, Joint Laboratory of Optics, 17. listopadu 12, 771 46 Olomouc, Czech Republic
[3] Institute of Physics of the Czech Academy of Sciences, 182 21, Prague 8, Czech Republic
[4] Experimentelle Physik 2, Technische Universitaet Dortmund, D-44221 Dortmund, Germany,
dv.azamat@gmail.com

Gallium nitride is a wide bandgap semiconductor extensively used in high-power, high-frequency electronics [1]. A maser action in the $GaN:Fe^{3+}$ system can be considered in view of the ground state level multiplicity (electron spin $S = 5/2$)
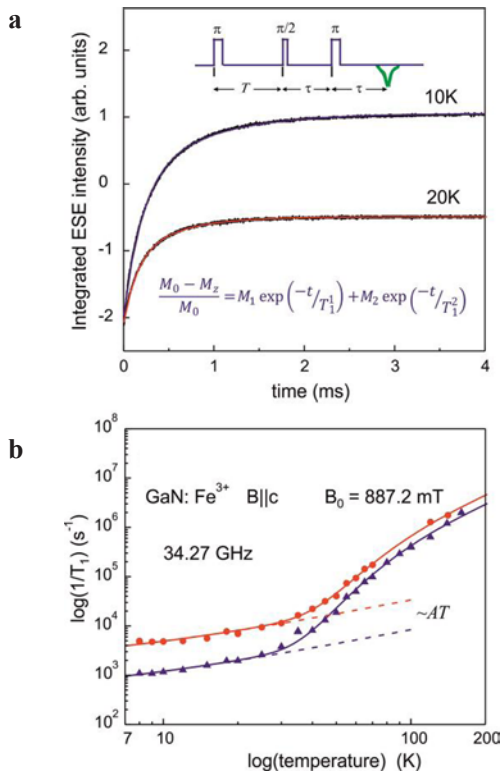
Fig. 1. a Inversion recovery measurements of spin-lattice relaxation time T_1 in $GaN:Fe^{3+}$. Magnetization recovery curves measured at the temperatures 10 K and 20 K show the bi-exponential recovery of the magnetization. **b** The temperature dependence of the spin-lattice relaxation rate of Fe^{3+} ions in GaN. Below 25 K, a direct interaction mechanism of spin-lattice relaxation freezes out and shows $\sim T$ temperature variation. The spin-spin cross-relaxation in this multilevel system gives large contribution to the spin-lattice relaxation.

to get the population inversion throughout the resonance linewidth by a pulsed microwave pumping. So, microwave energy may be amplified by the stimulated emission of radiation in the Fe^{3+} spin system with nearly equally spaced energy levels at the Q-band.

The electron spin echo detected inversion recovery technique at the Q-band frequency was used to characterize spin diffusion effects in spin-lattice relaxation of compensating Fe^{3+} impurities in n-type doped GaN crystals. It was found that the selective saturation can be achieved in the GaN:Fe^{3+} system due to magnetization transfer based on the spin flip-flop cross-relaxation processes. The temperature dependence of $1/T_1$ can be explained by direct spin-phonon processes ($\sim T$) below 25 K and by Raman two-phonon processes ($\sim T^9$) at higher temperatures (Fig. 1). Spin diffusion in this system is characterized by an additional cross-relaxation rate which is weakly temperature dependent below 25 K. The transferred hyperfine interactions of Fe^{3+} centers with gallium and nitrogen neighbor nuclei were resolved using pulsed-electron nuclear double resonance. A comparative analysis of quadrupole interactions indicates the essential increase in the electric field gradients on the nearest nitrogen and gallium shells.

1. Baranov P.G., von Bardeleben H.J., F. Jelezko, Wrachtrup J., Magnetic Resonance of Semiconductors and Their Nanostructures. Springer, 2017.

A Convenient, Improved Calibration of EPR Rapid-Freeze Quench Times: Kinetics of EDTA Transfer from Calcium(II) to Copper(II)

P. E. Doan

Northwestern University, Department of Chemistry, Evanston, IL, 60208 USA
ped131@northwestern.edu

The kinetics of the transfer of the chelate, ethylenediamine tetraacetate (EDTA), from Calcium(II) to Copper(II) in imidazole (Im) buffers near neutral pH, corresponding to the conversion, $[Cu(II)Im_4]^{2+} \rightarrow [Cu(II)EDTA]^{2-}$, are characterized with stopped-flow absorption spectroscopy and implemented as a tool for calibrating the interval between mixing and freezing, the freeze-quench time (t_Q), of a rapid freeze-quench (RFQ) apparatus. The kinetics of this reaction are characterized by monitoring changes in UV-visible spectra (300 nm) due to changes in the charge-transfer band associated with the Cu^{2+} ions upon EDTA binding. Stopped-flow measurements show that the rates of conversion of the Cu^{2+} ions exhibit exponential kinetics on millisecond time scales at pH values less than 6.8. In parallel we have developed a simple but precise method to quantitate the speciation of frozen solution mixtures of $[Cu(II)(EDTA)]^{2-}$ and tetraimidazole Cu(II) ($[Cu(Im)_4]^{2+}$) in X-band EPR spectra. The results are implemented in a simple high-precision 'recipe' for determining t_Q. These procedures are more accurate and precise than the venerable reaction of aquometmyoglobin with azide for calibrating RFQ apparatus, with the benefit of avoiding high-concentrations of toxic azide solutions.

SECTION 2

STRONGLY CORRELATED ELECTRON SYSTEMS

Interplay of Magnetism and Topological Electronic Structure in Magnetic van der Waals Compounds

V. Kataev

Leibniz Institute for Solid State and Materials Research IFW Dresden,
01069 Dresden, Germany, v.kataev@ifw-dresden.de

Layered van der Waals magnetic compounds attract currently large attention as they may display an intrinsically low-dimensional magnetic behavior and as such offer an extensive materials base for exploring fundamental magnetic properties of strongly correlated two-dimensional (2D) electron systems. Here, the results of a detailed electron spin resonance (ESR) spectroscopic study of the prominent representatives of this family will be discussed:

$Cr_2Ge_2Te_6$ is a quasi-2D magnet showing intriguing intrinsic ferromagnetism down to atomically thin films [1]. We could obtain new detailed insights into the magnetocrystalline anisotropy of this compound which should be responsible for the stabilization of magnetic order in the 2D limit and find evidence for an intrinsically 2D character of the dynamics of Cr spins even in bulk single crystals [2, 3]. These results are supported by calculations of the electronic structure revealing that the low-lying conduction band carries almost completely spin-polarized, quasi-homogeneous, two-dimensional states [2].

$MnBi_2Te_4$ [4, 5] is the first antiferromagnetic topological insulator featuring Dirac cones in the electronic structure due to the topological surface states [5, 6]. In this material we observe a surprisingly anisotropic spin dynamics of bulk conduction electrons and Mn localized states which, as we argue, could be responsible for the persistence of the band gap in the topological surface state even above the magnetic ordering temperature [5, 7].

1. Gong C. *et al.*: Nature **546**, 265 (2017)
2. Zeisner J. *et al.*: Phys. Rev. B **99**, 165109 (2019)
3. Sakurai T. *et al.*: Phys. Rev. B **103**, 024404 (2021)
4. Zeugner A. *et al.*: Chem. Mater. **31**, 2795 (2019)
5. Otrokov M. *et al.*: Nature **576**, 416 (2019)
6. Lee S.H. *et al.*: Phys. Rev. Research **1**, 012011(R) (2019)
7. Alfonsov A. *et al.*: Phys. Rev. B (Letter) **103**, L180403 (2021)

Multi-Frequency ESR Study of *S* = 1/2 Antiferromagnetic Chain with Staggered Field System KCuMoO$_4$(OH) by Force Detection ESR Method Using Single Microcrystal

S. Okubo[1,2], K. Tsuneishi[2], H. Takahashi[1,3], Y. Saito[4,*], S. Hara[4],
T. Sakurai[4], E. Ohmichi[2], K. Takahashi[2], H. Ohta[1,2], K. Nawa[5],
T. Yajima[6], Y. Okamoto[7], Z. Hiroi[6]

[1] Molecular Photoscience Research Center, Kobe University, Kobe 657-8501, Japan,
sokubo@kobe-u.ac.jp
[2] Graduate School of Science, Kobe University, Kobe 657-8501, Japan
3 PREST, Japan Science and Technology, Tokyo 102-0076, Japan
[4] Research Facility Center for Science and Technology, Kobe University, Kobe 657-8501, Japan
[5] institute of Multidisciplinary Research for Advanced Materials, Tohoku University, Sendai 980-8577,
Japan
[6] Institute of Solid State Physics, University of Tokyo, Kashiwa 277-8581, Japan
[7] Department of Applied Physics, Nagoya University, Nagoya 464-8603, Japan
[*] Current address: Department of Materials and Life Sciences, Sophia University,
Tokyo 102-8554, Japan

It is well known that quantum effect appears strongly in low-dimensional spin systems. Electron spin resonance (ESR) is a highly sensitive probe of local anisotropic fields. From the quantum field theory, as known as Oshikawa-Affleck theory (OA theory) [1, 2], soliton, antisoliton and breather excitations for low-energy excitations are expected in $S = 1/2$ Heisenberg antiferromagnetic chain with staggered fields [3–5]. KCuMoO$_4$(OH) has a one-dimensional chains with corner-shared CuO$_6$ octahedra along the *b*-axis [6]. From structural symmetry, the Dzyaloshinsky-Moriya interaction with the alternative *D*-vector and the alternative *g*-tensor are expected. Therefore, KCuMoO$_4$(OH) becomes a model substance for $S = 1/2$ Heisenberg antiferromagnetic chain with staggered fields, which is yielded by alternative *D*-vector and *g*-tensor. The specific heats and the magnetic susceptibilities as macroscopic properties were interpreted by soliton, antisoliton and breather excitations [7]. To obtain magnetic anisotropy from a microscopic viewpoint, multi-frequency ESR measurements of KCuMoO$_4$(OH) has been performed up to 15 T. The samples are synthesized by hydrothermal technique [6]. Temperature dependence measurements in the range from 300 K to 1.8 K have been performed using magnetically aligned powder samples and the pulsed magnetic fields. Frequency dependence measurements in the frequency range from 90 to 700 GHz at 1.8 K have been performed using single micro-crystal ($0.5 \times 0.3 \times 0.3$ mm^3) and the membrane force detection ESR method [8]. Fig. 1 shows the temperature dependence of ESR spectra of 160 GHz for *H*‖*a*. The linewidths changes dynamically and follow the OA theory. It shows clearly the spinon regime in higher temperature and the breather regime in lower temperature. From the frequency dependence measurements at 1.8 K (the breather regime), ESR spectra above 300 GHz show that several broad absorption lines are observed clearly. The frequency-field diagram shows nonlinear ESR modes.
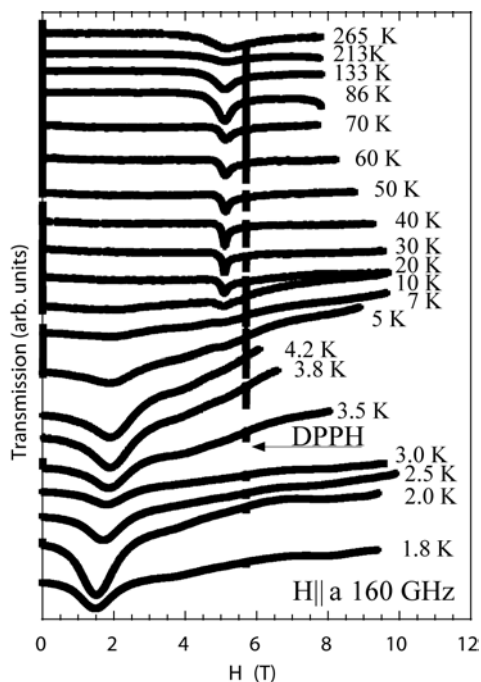
Fig. 1. Temperature dependence of ESR spectra of 160 GHz for $H\|a$.

These ESR modes can be fitted using only one soliton mass as the boundary bound resonances for the OA theory of finite length chains [9]. The magnetic anisotropy and microscopic parameters such as the effective staggered fields will also be discussed.

1. Oshikawa M., Affleck I.: Phys. Rev. Lett. **79**, 2883 (1997)
2. Oshikawa M., Affleck I.: Phys. Rev. Lett. **82**, 5136 (1999)
3. Asano T., Nojiri H., Inagaki Y., Boucher J.P., Sakon T., Ajiro Y., Motokawa M.: Phys. Rev. Lett. **84**, 5880 (2000)
4. Okubo S., Fukuoka D., Kimata M., Ohta H., Inagaki Y., Kunimoto T., Koyama K., Motokawa M., Hiroi Z.: J. Phys. Soc. Jpn. Suppl. **74**, 80 (2005)
5. Umegaki I., Tanaka H., Ono T., Uekusa H., Nojiri H.: Phys. Rev. B **79**, 184401 (2009)
6. Nawa K., Yajima T., Okamoto Y., Hiroi Z.: Inorg. Chem. **54**, 5566 (2015)
7. Nawa K., Janson O., Hiroi Z.: Phys. Rev. B **96**, 104429 (2017)
8. Takahashi H., Okamoto T., Ishimura K., Hara S., Ohmichi E., Ohta H.: Rev. Sci. Instrum. **89**, 083905 (2018)
9. Furuya S.C., Oshikawa M.: Phys. Rev. Lett. **109**, 247603 (2012)

Strongly Correlated Fermi Systems as New State of Matter

V. R. Shaginyan

Petersburg Nuclear Physics Institute, NRC Kurchatov Institute, Gatchina 188300,
Russian Federation

We focus on the topological fermion condensation of quantum phase transition (FCQPT) that paves a new avenue in modern condensed matter physics. Such a transition belongs to the unique type of quantum phase transitions, and leads to the topological reconstruction of the Fermi surface. The idea of such a phase transition, making flat bands, started long ago, in 1990 [1], at first as a curious mathematical option, and now it is a rapidly expanding, vibrant field with uncountable applications. We discuss the modification of the systems under the action of FCQPT that leads to a "second edition" of condensed matter theory, presenting a new state of matter [2, 3]. Further, we demonstrate that topological FCQPT takes place in many strongly correlated Fermi-systems like heavy fermion metals, high-temperature superconductors, new-type quantum spin liquids in insulators, quasicrystals and two-dimensional systems, and explains their thermodynamic and transport properties [2, 3].

FCQPT forms a new state of matter by making the behavior of strongly correlated Fermi systems universal. In order to describe the new state of matter it is necessary to have a new version of the theory of condensed matter physics that is represented by the fermion condensation theory [2, 3]. The new state presents all the aspects of traditional condensed matter physics that are significantly modified by FCQPT. The fermion condensation theory also explains striking non-Fermi liquid behavior of strongly correlated Fermi systems that are not observed in the common solid state physics. The theory allows one to analyze such anomalies as asymmetric tunneling conductivity with respect to change of the bias voltage V to $-V$. We show that this asymmetry points to a violation of both the time and charge symmetries.

1. Khodel V.A., Shaginyan V.R.: JETP Lett. **51**, 553 (1990)
2. Amusia M.Ya., Popov K.G., Shaginyan V.R., Stephanowich W.A.: Theory of Heavy-Fermion Compounds; Theory of Strongly Correlated Fermi-Systems, Springer Series in Solid-State Sciences, Vol. 182, 2015.
3. Amusia M.Ya., Shaginyan V.R.: Strongly Correlated Fermi Systems: A New State of Matter, Springer Tracts in Modern Physics, Vol. 283, 2020.

Magnetic Properties of $Mn_{1.5}Co_{1.5}BO_5$ Ludwigite Compound

D. V. Popov[1], T. P. Gavrilova[1], I. V. Yatsyk[1], M. A. Cherosov[2], E. M. Moshkina[3], V. A. Shustov[1], <u>R. M. Eremina</u>[1]

[1] Zavoisky Physical-Technical Institute, FRC Kazan Scientific Center of RAS, Kazan 420029, Russian Federation, REremina@yandex.ru

[2] Institute of Physics, Kazan Federal University, Kazan 420008, Russian Federation

[3] Kirensky Institute of Physics, Federal Research Center KSC SB RAS, Akademgorodok 50, Krasnoyarsk 660036, Russian Federation

Ludwigites are oxyborates with structural formula $(M^{2+})_2(M'^{3+})BO_5$ with (M^{2+}) and (M^{3+}) stand for divalent and trivalent metals, respectively. Ludwigites have an orthorhombic crystal structure with symmetry space group Pbam. The metal ions can occupy four nonequivalent positions. Mixed valence, random magnetic ions distribution and strong electronic correlation lead to the existence of different magnetic states, charge ordering, structure and magnetic transitions in ludwigites. Their extremely unusual magnetic properties are related to the presence of zigzag walls in their crystal structure formed by the metal ions of different valence and up to twelve magnetic ions in the unit cell.

Here we present the results of the flux crystal growth of Mn-Co heterovalent ludwigite $Mn_{1.5}Co_{1.5}BO_5$ and the study of its magnetic behavior by ESR methods. In addition to magnetization measurements, thermodynamic properties of $Mn_{1.5}Co_{1.5}BO_5$ were investigated, that allowed us to determine the features of magnetic ordering in this compound. Detailed investigations of magnetic properties were performed using a commercial PPMS-9 platform (Quantum Design) in the temperature range of 2 to 300 K in the zero-field-cooling (ZFC) and field-cooling (FC) regimes. A magnetic ferromagnetic transition was obtained at $T = 43.9$ K in this compound. The EPR spectra were measured at temperature range from 5 to 300K in the continuous wave mode in the X-band using an EMXPlus spectrometer. The temperature dependence of the magnetic resonance spectra of these samples was studied. It was found that the magnetic resonance spectrum contains one signal belonging to exchange interaction spin system of manganese and cobalt spins. The signal has a strong temperature dependence of the *g*-factor and a linewidth. The magnetic nature in $Mn_{1.5}Co_{1.5}BO_5$ is discussed.

Nonstoichiometry, Ground State and Temperature Transformation of the Frustrated Magnet $Li_{0.8}Ni_{0.6}Sb_{0.4}O_2$

E. Vavilova[1], T. Salikhov[1], M. Iakovleva[1], T. Vasilchikova[2], I. Shukaev[3], V. Nalbandyan[3], A. Vasiliev[2], E. Zvereva[2]

[1] Zavoisky Physical-Technical Institute, FRC Kazan Scientific Center of RAS, Kazan 420029, Russian Federation
[2] Moscow State University, Moscow 119991, Russian Federation
[3] SFU, Rostov-na-Donu 344090, Russian Federation

The problem of the disorder in the frustrated magnets attracts a lot of interest both due to fundamental aspects and because the real samples always contain the defects. Of particular interest, in our opinion, is the situation where the level of disorder, on the one hand, is high enough to destroy the long-range homogeneity, and, on the other hand, not enough to destroy the two-dimensionality of the magnetic structure,so the homogeneity survives on the short-range scale. In such compounds, the combination of two-dimensionality, frustrations and a short-range scale of interactions give rise to a nontrivial phase diagram and unusual states. For investigation of this problem we have chosen the complex transition metal oxide compound $Li_{0.8}Ni_{0.6}Sb_{0.4}O_2$. It is a Li-deficient derivative of zig-zag antiferromagnet $Li_3Ni_2SbO_6$, which has 2D structural order of magnetic Ni^{2+} ($S = 1$) ions on a honeycomb lattice with non-magnetic Sb in the middle, while honeycomb layers being separated by Li ions. Using a combination of bulk and local experimental techniques, we studied non-trivial magnetic properties of $Li_{0.8}Ni_{0.6}Sb_{0.4}O_2$, in particular, a nonconventional cluster spin-glass state.

High-Field Magnetic Structure of the Triangular Antiferromagnet RbFe(MoO$_4$)$_2$ Studied by ^{87}Rb NMR

Yu. A. Sakhratov[1,2], A. Ya. Shapiro[3], H. D. Zhou[4], A. P. Reyes[1], <u>L. E. Svistov[5]</u>

[1] National High Magnetic Field Laboratory, Tallahassee, Florida 32310, USA
[2] Kazan State Power Engineering University, Kazan 420066, Russian Federation
[3] A. V. Shubnikov Institute of Crystallography RAS, Moscow 119333, Russian Federation
[4] Department of Physics and Astronomy, University of Tennessee, Knoxville, Tennessee 37996, USA
[5] P. L. Kapitza Institute for Physical Problems, RAS, Moscow 119334, Russian Federation

RbFe(MoO$_4$)$_2$ is an example of a quasi-two-dimensional antiferromagnet ($S = 5/2$) with a regular triangular lattice structure. In this compound the antiferromagnetic inter-planar exchange interaction is approximately a hundred times weaker than the dominant in-plane interaction .

The sufficiently strong single-ion easy plane anisotropy governs the resemblance of the main features of RbFe(MoO$_4$)$_2$ H-T phase diagram with the model phase diagram of the XY 2D triangular lattice antiferromagnet for the moderate static magnetic field applied within triangular plane.

The ^{87}Rb study of the magnetic phase diagram of RbFe(MoO$_4$)$_2$ within the field range from one third of saturation field ($H_{sat}/3$) up to saturation shows four magnetic phases with a distinct NMR spectra.

The modeling of the NMR spectra allows for a verification of the magnetic structures, it also provides the values of the ordered component of the magnetic moment on Fe^{3+} ions for the whole set of the magnetic structures studied. In the figure the experimental and model spectra (solid and dashed lines) are presented for three commensurate phases Up-Up-Down, V and PM.

The analysis of the experimental spectra allows to conclude, that the high field phase ($0.75\ H_{sat} < H < H_{sat}$) is the so-called fan-phase. In contrast to other lower field phases this phase is stabilized due to week frustrated inter-plane interactions. The nature of this phase is discussed.
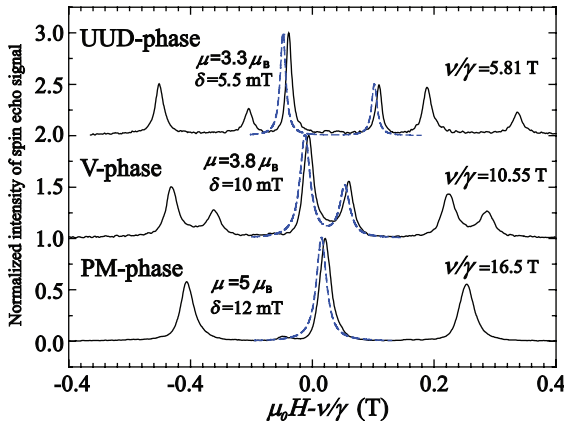
Influence of Electric Field on the Dynamics
of the Multiferroic LiCuVO$_4$

S. K. Gotovko[1,2], L. E. Svistov[1]

[1] P. L. Kapitza Institute for Physical Problems, RAS, Moscow 119334, Russian Federation
[2] National Research University Higher School of Economics, Moscow 101000, Russian Federation,
sofyagotovko@gmail.com

We present an electron spin resonance (ESR) study of multiferroic quantum spin-chain compound LiCuVO$_4$ in presence of an external electric field combined with the theoretical analysis conducted within the framework of phenomenological description. Below $T_N < 2.3$ K simultaneously with the helical magnetic order the crystal acquires the electric polarization connected with the magnetic structure. It has been shown that the ESR spectra of LiCuVO$_4$ depend on both applied magnetic and electric fields.

Our macroscopic analysis has shown that the value and orientation of electric polarization $\mathbf{P}$ in LiCuVO$_4$ depend on the orientation of the spin plane, and this result coincides with the results of microscopic approach [1] that showed that $\mathbf{P}$ is directed within the helix spin plane and perpendicular to the wave vector of the magnetic structure $\mathbf{k}$.
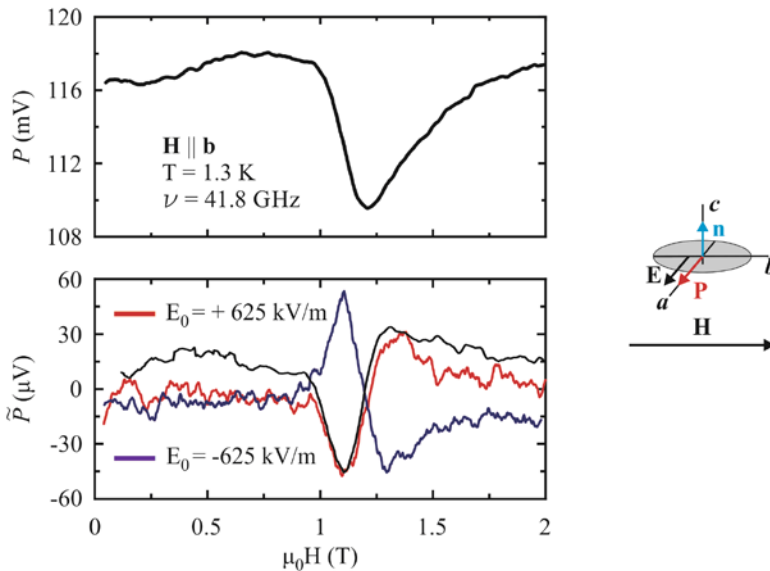
Fig. 1. Upper panel: field scan of the transmitted through the resonator UHF power. Bottom panel: responses of transmitted power on alternating electric field (red line: $E_0 = +625$ kV/m, blue line: $E_0 = -625$ kV/m). Black line – scaled derivative of absorption line. Inset: mutual orientation of crystallographic axes, external $\mathbf{H}$ and $\mathbf{E}$ fields, electric polarization $\mathbf{P}$. Grey ellipse illustrates helical magnetic structure, $\mathbf{n}$ is the vector product of spins on neighbor copper ions.

ESR study of LiCuVO$_4$ was conducted with use of a multiple-mode rectangular resonator at T = 1.3 K and at frequencies f = 17.2 GHz, 36.2 GHz, and 41.8 GHz at **H**$\|$**b**, and at f = 42 GHz at **H**$\|$**c**. The shifts of resonance fields were observed with use of modulation technique: both static and low-frequency alternating electric fields **E$_0$** and **E$_a$** were applied to the sample, and the oscillating part of resonance line at the frequency of the electric field modulation was measured. To control the direction of electric polarization **P** the electric field E0 was applied to the sample. The field dependence of transmitted through the resonator UHF power at f = 41.8 GHz is shown on the upper panel of Fig. 1, the responses of transmitted power on the alternating electric field are shown on the bottom panel. Orientation of **H**, **E**, and **P** in respect to crystallographic axes is shown in the inset to Fig. 1. The responses measured on the frequency of **E$_a$** replicate the shape of the derivative of the absorption line. Switch of the sign of **P** leads to change of the response sign (red and blue lines). The amplitudes of responses allow determining the shift of the resonance fields. The results of the experiments at different frequencies demonstrate that electric field influences the dynamic properties of the magnetic system in LiCuVO$_4$.

1. Katsura H., Nagaosa N., Balatsky A.V.: Phys. Rev. Lett. **95**, 057205 (2005)

Electron Spin Resonance of the Eu^{2+} Ions in 122-type Iron Pnictides

I. Gimazov[1], Yu. Talanov[1], G. Teitel'baum[1], R. Zaripov[1], K. Pervakov[2], V. Pudalov[2]

[1] Zavoisky Physical-Technical Institute, FRC Kazan Scientific Center of RAS, Kazan 420029, Russian Federation, gimazov@kfti.knc.ru
[2] P. N. Lebedev Physical Institute, Moscow, 119333, Russian Federation

Some compounds from the family of iron-containing high-temperature superconductors demonstrate various types of magnetic ordering along with superconducting state (see, for example, [1,2]). The magnetic state data of the corresponding parent compounds make a significant contribution to understanding this coexistence of phases, despite the absence of superconductivity in them. Among the parent compounds of iron pnictide superconductors, $EuFe_2As_2$ stands out due to the presence of both the Fe spin density waves and the antiferromagnetic (AFM) ordering of the Eu^{2+} localized moments. Long-range ordering of the Fe and Eu spins is observed below 190 K and 19 K, respectively.

The presence of spin moments in the Fe^{2+} and Eu^{2+} ions indicates that ESR spectroscopy is promising for studying $EuFe_2As_2$. However, the strong antiferromagnetic interaction of iron ions does not allow one to observe the resonance signal of these ions. At the same time, europium ions remain paramagnetic (disordered) in a wide temperature range above 19 K, and the ESR signal of these ions is well observed [3], which made it possible to establish interesting properties of the magnetic state with a spin density wave.

Our report presents the results of the first magnetic resonance study of the features of the $EuFe_2As_2$ antiferromagnetic phase, which is realized at temperatures below 19 K. The studies were carried out on the X-band ESR spectrometers at the frequency of 9.35 and 9.77 GHz in the field range from 0 to 1.8 T at temperatures below 19 K.

Since there is no intrinsic magnetostructural anisotropy in the case of europium ions, the antiferromagnetic resonance parameters are determined by the effective anisotropy due to the biquadratic exchange interaction of these ions with iron ions [4]. It is significant that the structural transition at $T_s = 190$ °K from a tetragonal to an orthorhombic lattice leads to the formation of twins whose magnetizations are perpendicular to each other.

In order to understand the complex intertwining of numerous interactions, we obtained and analyzed the angular dependences (both in-plane and out-of-plane one) of magnetic resonance spectra at different temperatures. The performed analysis showed that the magnetic structure of the europium ion sublattice belongs to the class of easy-plane magnets with weak uniaxial anisotropy in the easy plane. It is essential that the axes of this anisotropy for each type of twins are directed at the angle of 90 degrees to each other.

The temperature dependence of the effective anisotropy parameters made it possible to determine the variation in the relative fraction of different twins with temperature.

1. Nandi S., Jin W.T., Y. Xiao *et al.*: Phys. Rev. B **89**, 014512 (2014)
2. Kim T.K., Pervakov K.S., Evtushinsky D.V. *et al.*: Phys. Rev. B **103**, 174517 (2021)
3. Dengler E., Deisenhofer J., Krug von Nidda H.-A. *et al.*: Phys. Rev. B **81**, 024406 (2010)
4. Maiwald J., Mazin I.I., Gegenwart P.: Phys. Rev. X **8**, 011011 (2018)

SECTION 3

OTHER APPLICATIONS OF MAGNETIC RESONANCE

Spin-Probe EPR of Nanoporous Materials

M. V. Fedin

International Tomography Center SB RAS, Novosibirsk 630090, Russian Federation,
mfedin@tomo.nsc.ru

Stable organic radicals are well-known multifunctional spin probes, which are widely employed in EPR studies of various materials, including nanoporous media of a diverse nature. In general, nanoporous materials draw significant attention in science and industry and are prospective in fields of catalysis, separations, gas storage, drug delivery, etc.

In a series of recent works, using various radical spin probes and pulse/CW EPR techniques, we have investigated such nanoporous compounds as metal-organic frameworks (MOFs) [1], ionic liquid (IL) glasses and composites on their basis [2], as well as organosilica materials [3]. This report briefly overviews the above research and highlights promising implications for separation/molecular sieving [1], design of smart materials [2] and quantum computing [3].

1. Polyukhov D.M. *et al.*: Nano Lett. **19**, 6506 (2019); Poryvaev A.S. *et al.*: ACS Appl. Mater. Interf. **12**, 16655 (2020); Polyukhov D.M. *et al.*: ACS Appl. Mater. Interf. **13** (2021)
2. Ivanov M.Yu. *et al.*: Nanoscale **12**, 23480 (2020); Bakulina O.D. *et al.*: Nanoscale **12**, 19982 (2020)
3. Poryvaev A.S. *et al.*: Angew. Chem. Int. Ed. **60**, 8683 (2021)

Selective Ionic and Molecular Transport in Nanochannels of Sulfocation Exchange Membranes Studied by NMR

V. I. Volkov[1,2], A. V. Chernyak[1,2], N. A. Slesarenko[1]

[1] Institute of Problems of Chemical Physics RAS, Chernogolovka, Russian Federation
[2] Science Center in Chernogolovka RAS, Chernogolovka, Russian Federation, vitwolf@mail.ru

The interconnection of transport channel structure, counter ion hydration and mobility in sulfonic cation exchange membranes were revealed. The hydration numbers h of H$^+$, alkaline and alkaline-earth metal cation were calculated. The h values are 2, 5±1, 6±1 and 1±0.2 for H$^+$, Li$^+$, Na$^+$ and Cs$^+$ cation in Nafion membrane [1–3] and 2, 4±1, 5±1 and 3±1 in membranes (MSC) based on polyethylene and sulfonated grafted polystyrene [2, 4], correspondingly. Cation hydration numbers in MSC membrane are close to ones in aqueous salt solutions [4]. Self-diffusion coefficients of Li$^+$, Na$^+$, Cs$^+$ counter ions were measured for the first time by pulsed field gradient NMR technique on ^{7}Li$^+$, ^{23}Na$^+$, ^{133}Cs$^+$ nuclei. Experimental self-diffusion coefficients and self-diffusion coefficients calculated from translation jump correlation times of counter ions (measured by NMR relaxation techniques) were compared. It was concluded that macroscopic water and ionic transfer is controlled by translational jumping between membrane sulfonate groups [2, 3]. Cation translation mobility is governed by ionic hydration. Cation self-diffusion coefficients are changed in the next row H$^+ \gg$ Li$^+ \leq$ Na$^+ >$ Cs$^+$ in Nafion compare to membrane MSC with more water-absorbing ability [2, 4] and chloride aqueous solutions where Li$^+ <$ Na$^+ <$ Cs$^+$. Low mobility of Cs+ ion in Nafion is a result of Cs$^+ \rightarrow$ SO$_3^{3-}$ group contact ionic pair forming. Ionic conductivities calculated from self-diffusion coefficients on the basis of Nernst-Einstein equation are in good agreement with experimental values. As it was shown by ^{23}Na and ^{133}Cs NMR in mixture Na$^+$-Cs$^+$ Nafion membrane ionic form a presence of sodium cation increases cesium cation mobility because of additional membrane hydration compare to Cs$^+$ ionic form only. Therefore the detailed NMR investigations gave opportunity to understand the microscopic mechanism of membrane selectivity of sulfo containing membranes to the alkaline metal cations. These results may be a guide for new materials creation.

1. Chernyak A.V., Vasiliev S.G., Avilova I.A., Volkov V.I.: Appl. Magn. Res. **50**, 667–693 (2019)
2. Volkov V. I., Chernyak A. V., Avilova I. A., Slesarenko N. A., Melnikova D.L., Skirda V.D.: Membranes **11**(6), 385 (2021)
3. Volkov V. I., Chernya A. V., Gnezdilov O. I., Skirda V. D.: Solid State Ionics **364**, 115627 (2021)
4. Volkov V.I., Chernyak A.V., Golubenko D.V., Tverskoy V.A., Lochin G.A., Odjigaeva E.S., Yaroslavtsev A.B.: Membranes **10**, 272 (2020)

Possibilities for Integrating Dielectric Scanning and Nuclear Magnetic Logging to Assess the Type of Fluid in the Well

V. M. Murzakaev[1], N. B. Belousova[1], A. V. Bragin[1], D. A. Kisler[1], V. D. Skirda[2], A. A. Alexandrov[2], Ya. V. Fattakhov[3]

[1] TNG-Group, Bugulma, Russian Federation, Murzakaev.VM@tng.ru
[2] Institute of Physics, Kazan Federal University, Kazan, Russian Federation, kazanvs@mail.ru
[3] Zavoisky Physical-Technical Institute, FRC Kazan Scientific Center of RAS, Kazan 420029, Russian Federation, fattakhov@kfti.knc.ru

The Nuclear Magnetic Resonance method has found wide application in many fields of science and technology. In addition to physics and chemistry, in geology, with the use of new knowledge about NMR, significant progress has been made in studying the composition and properties of the formation fluid that saturates the pore space of rocks. More detailed information about the properties of the studied object together with multi-dimensional presentation of the results allows interpreters to better understand properties of the fluid in the reservoir and get more reliable information about the potential of production in difficult geological conditions. This is very important in the study of unconventional oil and gas reserves, in the conditions of a thin-layered section of wells, as well as in new areas where there are no petrophysical dependencies yet.

Using Nuclear Magnetic Logging we can identify intervals with mobile fluid, determine its type (oil, gas) and volume, and predict recoverability of hydrocarbons. Information about the type of fluid in the formation can be acquired using 2D relaxation time distributions obtained with NMR equipment. The method for
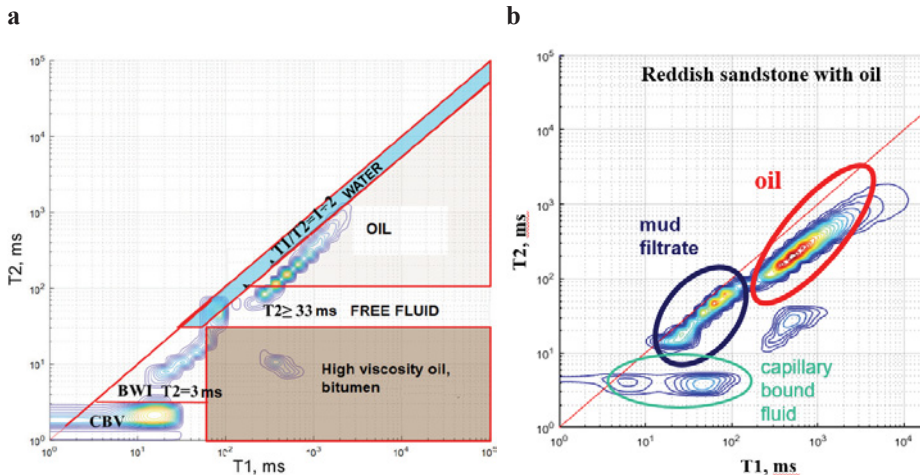
Fig. 1. a Method for analysis of 2D maps of T_1-T_2 distribution. **b** Example of using the method for T_1-T_2 maps analysis.
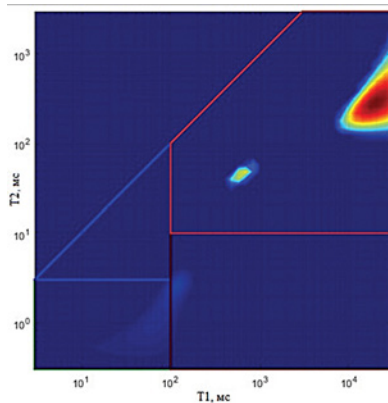
Fig. 2. Oil & gas in formation.

analyzing such maps is shown in Fig. 1a. This technique was tested not only in a downhole tool, but also in a ground-based NMR unit for core analysis. By means of appropriate spot analysis, presence of hydrocarbon in the test object can be assessed. So Fig. 1b shows one of the many examples of this technique being applied, which highlights the following parameters: drilling mud filtrate, mobile oil and bound fluid. This method has not only visible advantages, but it also has a serious drawback associated with the fact that the time spectrum of oil is much wider than that of water. If the object under study contains both water and oil in free form, then it can be difficult to distinguish one component against the other. It is possible to reduce this uncertainty by using additional research methods for interpretation. One of the well logging methods that is directly related to reservoir saturation estimation is Multi-frequency Waveform Dielectric Logging.

Since the dielectric constant of water and oil differ greatly (up to 5 units for oil and over 50 units for water, in the range of 6–10 units for the rock matrix), this fact can be useful for identification of hydrocarbons in the formation [1].

Figure 2 shows an example where, with the help of additional data acquired during processing of Multi-frequency Waveform Dielectric Logging data, the "spot" was explained in the upper right corner on the T_1-T_2 map, which corresponds to residual (non-displaced) gas. Also on the T_1-T_2 distribution map there is an oil spot (highlighted in red) in the formation corresponding to OBM filtrate that was used for well drilling.

The research data confirm good prospects of integrated interpretation of well logging methods aimed at assessing the type of fluid to increase reliability of Well Reports issued, in this case the Nuclear Magnetic Resonance and Multi-frequency Waveform Dielectric Logging.

1.   Itenberg S.S.: Interpretation of Well Logging Data, Nedra, Moscow, 1978, 389 p.

SECTION 4

CHEMICAL AND BIOLOGICAL SYSTEMS

DEER/PELDOR Study of Supramolecular Assemblies of Human Ribosome and RNAs

E. G. Bagryanskaya[1], I. O. Timofeev[2,3], K. N. Bulygin[4], A. A. Malygin[3,4], D. M. Graifer[3,4], M. I. Meschaninova[4], A. G. Venyaminova[4], O. A. Krumkacheva[2,3], M. V. Fedin[2,3], L. Yu. Frolova[5], G. G. Karpova[4]

[1] N. N. Vorozhtsov Novosibirsk Institute of Organic Chemistry SB RAS, Novosibirsk 630090, Russia, egbagryanskaya@nioch.nsc.ru
[2] International Tomography Center SB RAS, Novosibirsk 630090, Russian Federation, olesya@tomo.nsc.ru
[3] Novosibirsk State University, Novosibirsk 630090, Russian Federation
[4] Institute of Chemical Biology and Fundamental Medicine SB RAS, Novosibirsk 630090, Russian Federation, karpova@niboch.nsc.ru
[5] Engelhardt Institute of Molecular Biology RAS, Moscow 119991, Russian Federation

Ribosomes are giant cellular machines that translate genetic information encoded in nucleotide sequences of messenger RNAs (mRNAs) into amino acid sequences of proteins. We used pulse dipolar EPR to investigated structural rearrangements in mRNA upon its binding to human 80S ribosomes [1–3]. The model mRNA (MR), 11-mer RNA containing two nitroxide spin labels at the 5- and 3-terminal nucleotides and prone to form a stable homodimer (MR)2, was used. Intramolecular spin-spin distances were measured by DEER/PELDOR spectroscopy in model complexes mimicking different states of the 80S ribosome during elongation and termination of translation. The formation of two different types of ribosomal complexes with MR was observed [1]. First, there were stable complexes where MR was fixed in the ribosomal mRNA-binding channel by the codon-anticodon interaction(s) with cognate tRNA(s). Second, we for the first time detected complexes assembled without tRNA due to the binding of MR most likely to an exposed peptide of ribosomal protein uS3
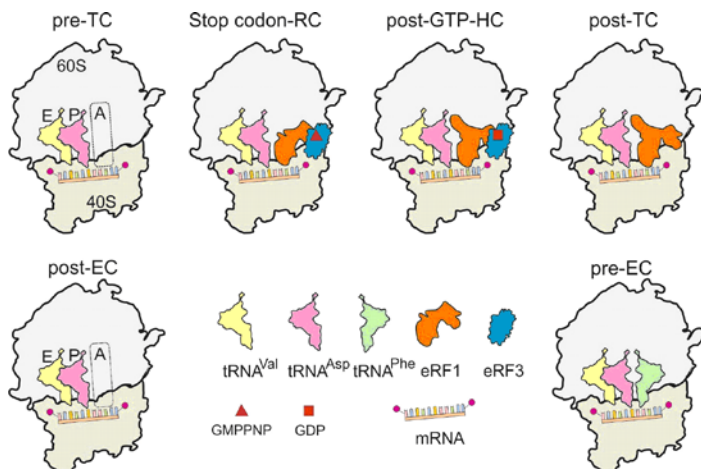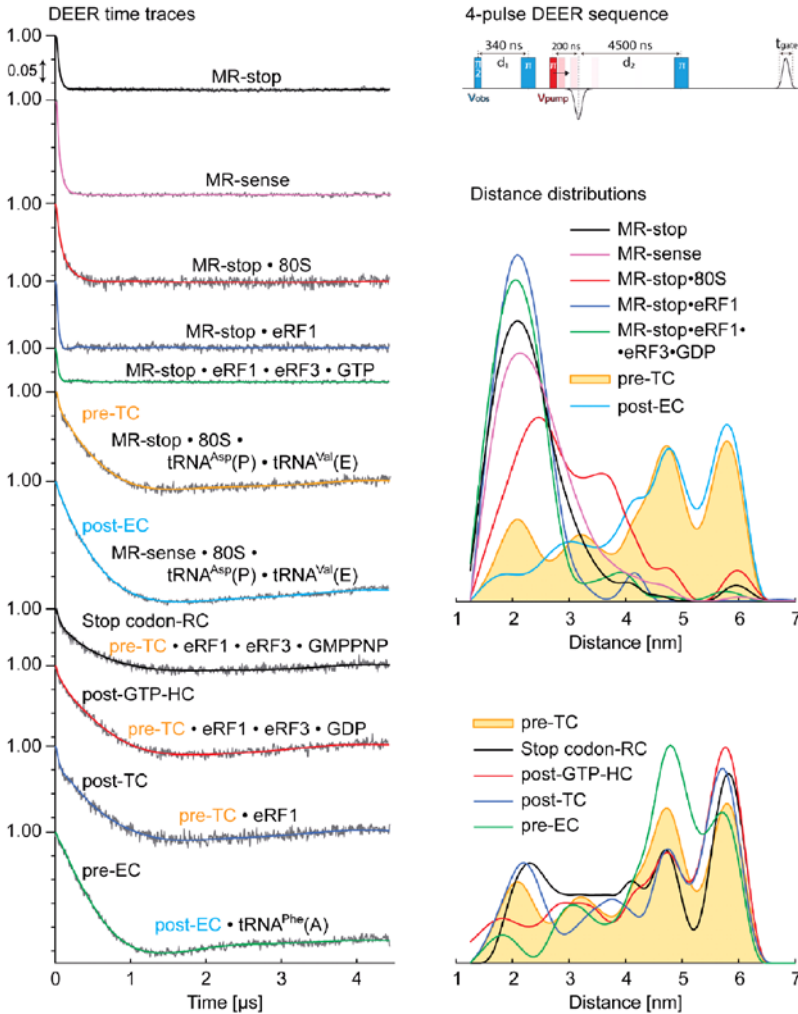
away from the mRNA channel. The analysis of interspin distances allowed the conclusion that 80S ribosomes facilitate dissociation of the duplex (MR)2: the equilibrium between the duplex and the single-stranded MR shifts to MR due to its efficient binding with ribosomes. Furthermore, we observed a significant influence of tRNA bound at the ribosomal exit (E) and/or aminoacyl (A) sites on the stability of ribosomal complexes. Our findings showed that a part of mRNA bound in the ribosome channel, which is not involved in codon-anticodon interactions, has more degrees of freedom than that interacting with tRNAs. The features of labile complexes of human 40S ribosomal subunits with RNAs, whose formation is manifested in the cross-linking of aldehyde derivatives of RNAs to the ribosomal protein uS3 through its peptide 55–64 located outside the mRNA channel [2].

The measurements revealed that in all studied complexes, mRNA exists in two alternative conformations, whose ratios are different in post-translocation, pre-translocation and termination complexes. We found that the presence of aminoacyl-tRNA at the ribosomal A site decreases the relative share of the more extended mRNA conformation, whereas the binding of eRF1 (alone or in a complex with eRF3) results in the opposite effect. In the termination complexes, the ratios of mRNA conformations are practically the same, indicating that a part of mRNA bound in the ribosome channel does not undergo significant structural alterations in the course of completion of the translation. Our results contribute to the understanding of mRNA molecular dynamics in the mammalian ribosome channel during translation [3].

1. Malygin A.A., Krumkacheva O.A., Graifer D.M., Timofeev I.O., Ochkasova A.S., Meschaninova M.I., Venyaminova A.G., Fedin M.V., Bowman M., Karpova G.G., Bagryanskaya E.G.: NAR **47**, 11850 (2019)
2. Malygin A.A., Graifer D.M., Meschaninova M.I., Venyaminova A.G., Timofeev I.O., Kuzhelev A.A., Krumkacheva O.A., Fedin M.V., Karpova G.G., Bagryanskaya E.G.: NAR **46**, 897 (2018)
3. Bulygin K.N., Timofeev I. O., Malygin A.A., Graifer D.M., Meschaninova M.I., Venyaminova A.G., Krumkacheva O.A., Fedin M.V., Frolova L.Yu., Karpova G.G., Bagryanskaya E.G.: Computational and Structural Biotechnology Journal **19**, 4702 (2021)

Parahydrogen Induced Polarization Enhanced NMR of Peptides and Biomarkers

G. Buntkowsky

Technische Universität Darmstadt, Eduard-Zintl-Institut für Anorganische und Physikalische Chemie, Alarich-Weiss-Straße 8, Darmstadt 64287, Germany

Since many years PHIP (Parahydrogen Induced Polarization) and its reversible variant SABRE (Signal Amplification By Reversible Exchange) are among the most versatile tools for NMR signal enhancement in solution NMR. In the present talk we first give a short introduction into PHIP and SABRE, followed by a number of examples from our recent work. The first example shows results from our investigations of a bioactive derivative of the sunflower trypsin inhibitor-1 (SFTI-1), which inhibits matriptase, a colon cancer related enzyme. The PHIP activity of the inhibitor was achieved by labeling the tetradecapeptide with O-propargyl-L-tyrosine. Employing a carefully optimized automatized PHIP setup [1]. In 1D-PHIP experiments an enhancement of up to ca. 1200 compared to normal NMR was found [2, 3]. This huge enhancement factor permitted the ultrafast single scan detection of 2D-TOCSY spectra of micromole solutions of the PHIP labelled inhibitor [3]. The second example discusses the application of parahydrogen for the detection of low-concentrated intermediates of hydrogenation reactions via the PANEL (PArtial NEgative Line experiment) [4]. The last example describes some recent results on the hyperpolarization of fumarate as a possible sensor for tumor diagnosis in MRT [5].

We present results of the application of parahydrogen hyperpolarization for the signal enhancement of a bioactive derivative of the sunflower trypsin inhibitor-1 (SFTI-1). In 1D-PHIP experiments an enhancement of up ca. 1200 was found, permitting the ultrafast single scan detection of 2D-TOCSY spectra of micromole solutions. We discuss the detection of low-concentrated intermediates of hydrogenation reactions and report some recent results on the hyperpolarization of fumarate as a possible sensor for tumor diagnosis in MRT.

1. Kiryutin A., Sauer G., Hadjiali S., Yurkovskaya A.V., Breitzke H., Buntkowsky G.: J. Magn. Res. **285**, 26–36 (2017)
2. Sauer G., Nasu D., Tietze D., Gutmann T., Englert S., Avrutina O., Kolmar H., Buntkowsky G.: Angewandte Chemie Int. Ed. **53**, 12941–12945 (2014)
3. Kiryutin A.S., Sauer G., Tietze D., Brodrecht M., Knecht S., Yurkovskaya A.V., Ivanov K.L., Avrutina O., Kolmar H., Buntkowsky G., Chemistry Eur. J. **25**, 4025–4030 (2019)
4. Kiryutin A.S., Sauer G., Yurkovskaya A.V., Limbach H.-H., Ivanov K.L., Buntkowsky G.J. Phys. Chem. C **121**, 9879–9888 (2017)
5. Eills J., Cavallari E., Kirchner R., Di Matteo G., Carrera C., Dagys L., Levitt M.H., Ivanov K., Aime S., Reineri F., Münnemann K., Budker D., Buntkowsky G., Knecht S.: Angewandte Chemie Int. Ed., **60**, 6791–6798 (2021)

Insights into Redox Active Proteins in Respiration and Photosynthesis from EPR Spectroscopy

K. H. Richardson[1,2], G. T. Hanke[1], M. M. Roessler[2]

[1] School of Biological and Behavioural Sciences, Queen Mary University London, UK
[2] Department of Chemistry, Imperial College London, UK, m.roessler@imperial.ac.uk

In respiration and photosynthesis large bioenergetic machines use electron-transfer centres to build up the electrochemical gradient required for ATP synthesis. EPR has long been a powerful technique used to understand the role of such centres, including in respiratory complex I. However, these membrane proteins are often tightly regulated, labile and limiting to cell growth, hindering our ability to isolate and characterise them. Photosynthetic complex I (PS-CI, Fig. 1), the photosynthetic homologue of respiratory complex I, is a prominent example of these limitations and consequently its mechanism is not well understood.

Using the methodology developed for respiratory complex I [1] and exploiting recent EPR sensitivity advancements [2], we are able to characterise the three overlapping [4Fe-4S] cluster EPR signals from PS-CI in two cyanobacterial strains at low concentration (<10 μM) using relaxation-filtered pulse EPR, and to determine their structural position with orientation selective DEER. Using small volume potentiometric EPR titrations [3] we establish the reduction potentials of the Fe-S clusters, placing PS-CI into the biogenetic map of photosynthesis [4].

1. Roessler M.M. *et al.*: PNAS, **107**, 1930–35 (2010)
2. Šimenas M. *et al.*: J. Magn. Reson. **322**, 106876 (2021)
3. Wright J. *et al.*: Inorg. Biochem. **162**, 201–206 (2016)
4. Richardson K. *et al.*: Functional basis of electron transport within photosynthetic complex I, Nat. Commun. (accepted)
5. Schuller J.M. *et al.*: Science **260**, 257–260 (2019)
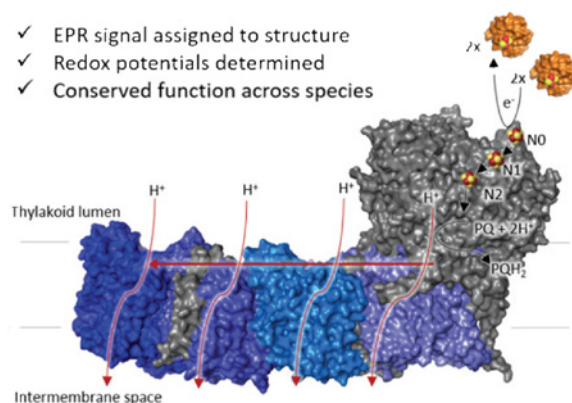
Fig. 1. Structure and proposed catalysis of *T. elongatus* PS-CI (PDB: 6HUM) [5]. Proton pumping subunits (blue) and putative proton movement indicated by red arrows. Electron transfer from ferredoxin (orange) to plastoquinone (PQ) is indicated by black arrows.

Recent EPR Insights into Earth Abundant Metal Catalysis

<u>B. E. Bode</u>[1,2], S. Chabbra[3], M. Bühl[1,2], D. J. Cole-Hamilton[1], D. Smith[4], A. J. B. Watson[1]

[1] EaStCHEM School of Chemistry and [2]Centre of Magnetic Resonance, University of St Andrews, St Andrews, KY16 9ST, Scotland, beb2@st-andrews.ac.uk
[3] Max-Planck Institute for Chemical Energy Conversion, Mülheim 45470, Germany
[4] Drochaid Ltd, St Andrews, KY16 9ST, Scotland

Earth abundant 3d metals are gaining increasing importance in catalysis as alternative to e.g., well-established but expensive platinum group metal catalysts. However, mechanisms for catalysis involving first row transition metals can be quite unique and frequently involve paramagnetic states hampering NMR analysis. Electron paramagnetic resonance (EPR) spectroscopy results showcasing different catalysis applications using copper and chromium will be presented.

EPR on copper-catalysts has informed Chan-Lam N-arylation reactions [1]. cross-coupling reactions to form to nitrilium and pyridinium products [2], and late-stage N-arylation for formation of antiparasitic agents [3]. Furthermore, recent insights on the chromium catalyst system that underpins the commercially important selective ethylene oligomerisation (>1 Mton a^{-1}) will be presented. The use of selectively isotope labelled substrates and catalyst precursors in EPR time course experiments has provided unequivocal evidence for the transient formation of a bis-ethylene chromium species that has been postulated early in the catalytic cycle but had until now eluded structural characterisation [4].

1. Vantourout J.C., Li L., Bendito-Moll E., Chabbra S., Arrington K., Bode B.E., Isidro-Llobet A., Kowalski J.A., Nilson M., Wheelhouse K., Woodward J.L., Xie S., Leitch D.C., Watson A.J.B.: ACS Catal. **8**, 9560 (2018)
2. Bell N.L., Xu C., Fyfe J.W.B., Vantourout J.C., Brais J., Chabbra S., Bode B.E., Cordes D.B., Slawin A.M.Z., McGuire T.M., Watson A.J.B.: Angew. Chem. Int. Ed. **60**, 7935 (2021)
3. Robertson J., Ungogo M.A., Aldfer M.M., Lemgruber L., McWhinnie F.S., Bode B.E., Jones K.L., Watson A.J.B., de Koning H.P., Burley G.A.: ChemMedChem in press.
4. Chabbra S., Smith D.M., Bell N.L., Watson A.J.B., Bühl M., Cole-Hamilton D.J., Bode B.E.: Sci. Adv. **6**, eabd7057 (2020)

Spin Polarized Triplet States and Radical Pair States in Heliobacterial Reaction Centres

A. van der Est[1], A. Agostini[2], D. K. Matta[1], B. Ferlez[3], T. Biskup[4], S. Weber[4], J. Golbeck[3], D. Carbonera[2]

[1] Brock University, St. Catharines, ON, Canada
[2] University of Padova, Padova, Italy
[3] Penn State University, University Park, PA, USA
[4] University of Freiburg, Freiburg, Germany

Heliobacteria are soil-dwelling strictly anaerobic photosynthetic bacteria that live in a symbiotic relationship with plants and play an important role in nitrogen fixation. To deal with the low intensity infrared light present in the soil environment they are the only organism to use bacterial chlorophyll g (BChl g) as the main chromophore for photosynthesis. The heliobacterial reaction centre (HbRC) is a homodimeric protein with exact C_2 symmetry that performs light-induced electron transfer (Fig. 1). If HbRC are exposed to oxygen, the BChl g isomerizes to chlorophyll a_F (Chl a_F). This naturally occurring process, provides a unique opportunity to study the effect of subtle changes in the chlorophyll on the energy and electron transfer in the RC without resorting to mutations. We have used transient EPR, pulsed ENDOR and ODMR spectroscopy to study the changes in the HbRC as the BChl g is converted to Chl a_F. The transient EPR data show that electron transfer kinetics are altered and suggest that this occurs when one of the chlorophylls of the primary donor, P_{800}^+ is converted creating a heterodimer. This is borne out by the ENDOR studies and DFT calculations that show greater localization of the unpaired electron of the donor radical cation in the heterodimer. Triplet states are also observed in the antenna chlorophylls of the complex. The ODMR measurements reveal that there are two pools of BChl g molecules in different local environments that form triplet states with different zero-field splitting parameters. Moreover, these two pools have different sensitivities to oxygen. Using the recently published X-ray structure [1] and estimates of the excitonic coupling between the antenna chlorophylls we propose possible sites for the triplet states.

1. S Gisriel C., Sarrou I., Ferlez B., Golbeck J.H., Redding K.E., Fromme R.: Science **357**, 1021 (2017)
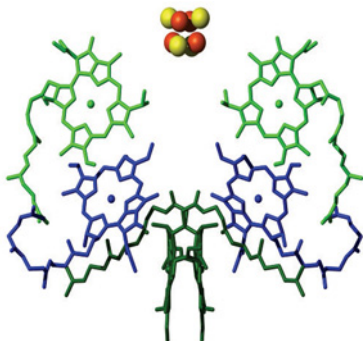
Fig. 1. Structure of the electron-transfer cofactors of HbRC's [1].

CRISPR Target Recognition Investigated Using Site-Directed Spin Labeling: Mechanistic Insights Informing Applications

P. Z. Qin[1,2]

[1] Department of Chemistry and [2] Department of Biological Sciences, University of Southern California, Los Angeles, CA, 90089, USA; pzq@usc.edu

CRISPR (Clustered-Regularly-Interspaced-Short-Palindromic-Repeats) systems have been adapted into programmable agents for genome-wide manipulation of nucleic acids in many organisms, unleashing a revolution in genome editing and manipulation that is still rapidly advancing. Mechanistic understanding on specific CRISPR target recognition sets the foundation for CRISPR revolution, and is critical for overcoming remaining obstacles, such as the "off-target effects" that result in undersigned aberrant actions. Our group has been studying mechanisms of CRISPR-Cas9 and Cas12a that target double-stranded DNA, with a focus on elucidating the roles of intrinsic physical properties of DNA duplex (i.e., DNA shape) in target discrimination. In this presentation, I will describe recent work on using site-directed spin-labeling in conjuction with fluorescence spectroscopy, enzymology, and cell-based gene editing to reveal the connection between DNA shape, Cas9-induced DNA unwinding, and Cas9 activities; as well as our on-going efforts to integrate these mechanistic findings into Cas9 target design for gene editing applications.

Spin Centers in Titania Nanotubes
with Different Chemical Composition

E. A. Konstantinova[1], E. V. Kytina[1], A. A. Dronov[2], A. I. Kokorin[3]

[1] Physics Department, M.V. Lomonosov Moscow State University, Russian Federation, liza35@mail.ru
[2] National Research University of Electronic Technology – MIET, Zelenograd, Moscow, Russian Federation
[3] N.N. Semenov Federal Research Center for Chemical Physics, RAS, Moscow, Russian Federation

Titania (TiO_2) is a widely investigated semiconductor for photocatalytic decomposition of organic impurities in air and water and photoelectrochemical water splitting due to its chemical stability, photocorrosion resistance, low cost, and a large specific surface area with a high density of defects – own and adsorptive origin [1]. The type of defects and their properties are strongly depend on way of sample preparation and therefore are determined by the morphology of nanostructures [2].Therefore, the aim of this work was to identify the defects in the TiO_2 nanotubes (NTs) with different morphology and to study their peculiarities. Since the most of defects in the TiO_2 has a nonzero spin, we used EPR spectroscopy.

Multi-walled (MW) TiO_2 NTs were formed by Ti foil anodization in a potentiostatic mode at 60 V and temperature of 20°C for 60 minutes. Electrolyte solution consisted of 0.3 wt.% NH_4F in ethylene glycol with the addition of 2 wt.% of deionized water. The duration of the anodization of pretreated Ti foil was 60 minutes. The obtained samples (NTs) were cleaned in ethyl alcohol and dried in an argon stream. Vacuum heat treatment of TiO_2 NTs samples were carried out in a chamber of the vacuum-thermal evaporation unit at a temperature of 450 °C for 60 min with the residual gas pressure was $3 \cdot 10^{-5}$ Torr (NTs-1). Heat treatment in air of TiO_2 NTs samples were carried out in a muffle furnace at a temperature of 450 °C for 60 min (NTs-2). Also we have made combined annealing: first in vacuum at 450 °C for 60 min, then in air at 300 °C for 60 min (NTs-3) and first in vacuum at 450 °C for 60 min, then in air at 450 °C for 60 min (NTs-4). The single-walled (SW) TiO_2 nanotubes (NTs-5) were prepared using a technique similar to one described in [3]. Note that the multi-wall NTs means that ones have an outer layer of pure titania and an inner layer of carbon doped titania; single-wall NTs have only an outer layer. The EPR spectrum of NTs-1 and NTs-3 samples consists of a single line of high intensity, line width is approximately 4 G and the g-factor is 2.0027 ± 0.0005. According to the literature data, such signals are due to carbon dangling bonds [4]. The presence of carbon in the samples under the investigation is due to use of a polyethylene glycol in the synthesis process and is confirmed by our data of elemental analysis. Notice, that in NTs-1 and NTs-3 samples we have detected a slightly asymmetric EPR signal. Such form of EPR signal can be due to superposition of different EPR line. Origin of several EPR lines with close g-factors can be explained by the presence of carbon in various forms, which is confirmed by our structural investigation and Raman data, which indicate the presence of carbon

in the form of amorphous and crystalline inclusions. EPR spectrum of NTs-2 samples is a superposition of two signals originated from carbon dangling bond and Ti^{3+}/oxygen vacancies centers. The concentration of spin centers (Ns) in the synthesized samples is in the range of $10^{15} \div 10^{17}$ spin/g, depending on the conditions of thermal treatment. The highest Ns value is observed in the vacuum sample NTs-1, which contains the largest amount of carbon. In the NTs-3 and NTs-4 samples the Ns value is significantly lower because of the amount of carbon is less. NTs-5 samples has only Ti^{3+}/oxygen vacancies centers (Ns = 10^{15} g^{-1}). The energy position of the spin centers in the band gap of TiO_2 NTs was determined using our original EPR method with illumination of the samples in situ [1]. It is established that the energy level of carbon dangling bond is 2.1 eV below conduction band and the energy level of Ti^{3+}/oxygen vacancy is 2.9 eV above valence band. Analyzing the saturation curves (dependence of the EPR signal intensity vs the root of the microwave power), we found that the inner layer of NTs has a mesoporous structure.

The obtained results can be useful in developing light-driven titania nanotubes with optimal defect concentration for effective photocatalysis under visible light illumination. The study was supported by a grant from Russian Science Foundation № 21-19-00494, https://rscf.ru/en/project/21-19-00494/. The EPR spectra were recorded using Bruker spectrometer ELEXSYS-E500 (Physics Department, Moscow State University).

1. Konstantinova E.A., Minnekhanov A.A., Kokorin A.I., Sviridova T.V., Sviridov D.V.: J. Phys. Chem. C **122**, 10248 (2018)
2. Kokorin A.I. "Electron spin resonance of nanostructured oxide semiconductors", in: Chemical physics of nanostructured semiconductors (edited by Kokorin A.I.,. Bahnemann D.W.). VSP-Brill Academic Publishers, Boston 2003.
3. Gavrilin I., Dronov A., Volkov R., Savchuk T., Dronova D., Borgardt N., Pavlikov A., Gavrilov S., Gromov D.: Appl. Surf. Sci. **516**, 146120 (2020)

Spin Exchange and Chemical Exchange in Biradicals

A. I. Kokorin[1,2], E. N. Golubeva[3]

[1] Department of Dynamics of Chem-Bio Processes, N. N. Semenov Federal Research Center
for Chemical Physics RAS, Moscow 119991, Russian Federation, alex-kokorin@yandex.ru
[2] Dept. of Chemistry, Plekhanov Russian University of Economics, Moscow 115093,
Russian Federation
[3] Chemistry Department, Lomonosov Moscow State University, Moscow 119991,
Russian Federation, legol@mail.ru

The carbonate biradical $O=C(OR_6)_2$ (**B1**), where R_6 is 1-oxyl-2,2,6,6-tetramethyl-piperidine ring has been studied by the EPR spectroscopy, DFT calculations and X-ray analysis. The intramolecular electron spin exchange dynamics in diluted toluene and methanol solutions at the temperature range $263 < T < 353$ K demonstrated the slow spin exchange between two conformations of **B1**, which are characterized by the values of the exchange integral $J_1 = 0$ and $|J_2| = 2.78 \pm 0.05$ mT in toluene, 2.91 ± 0.05 mT in methanol, and by the ratio of the lifetimes of these conformations τ_2/τ_1 depended on temperature. Differences of enthalpies ΔH and entropies ΔS of these conformations were determined. Peculiarities of the dynamics in the case of fast and slow spin exchange are analyzed as the effect of the solvent nature.

Short nitroxide biradical R_6–O–CO–O–R_6, **B1**, was one of the first synthesized in 1964 and characterized in details in [1, 2] where the spin exchange
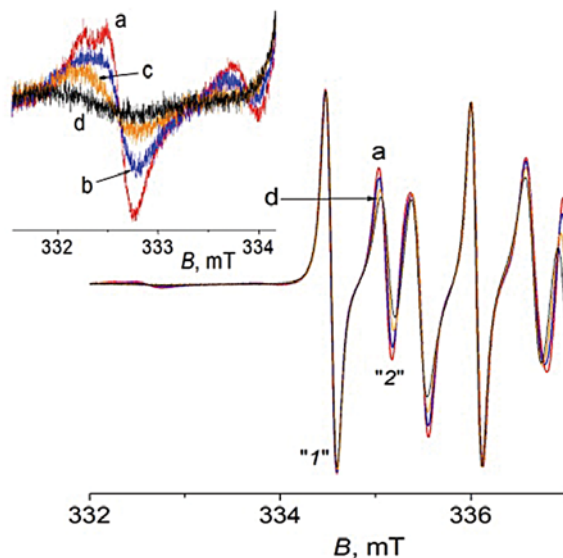
Fig. 1. Experimental EPR spectra of biradical **1** in toluene at 298 (**a**), 313 (**b**), 333 (**c**), and 353 K (**d**). Insert: enlarged low-field lines of the s-transitions in nitroxide biradical
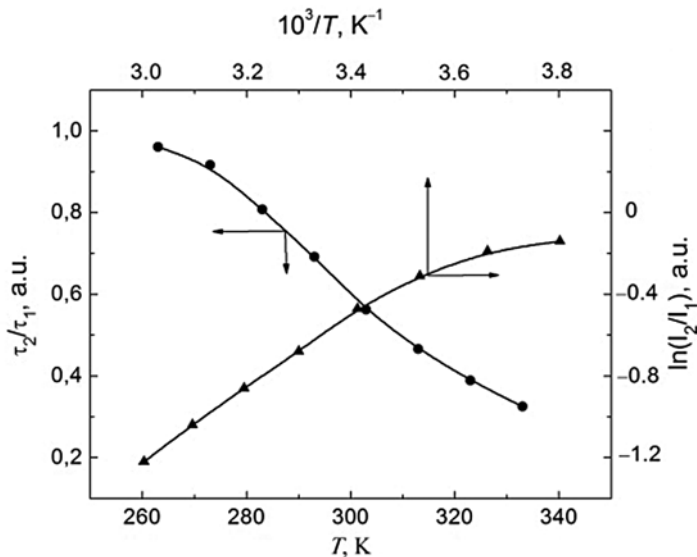
Fig. 2. Temperature dependences of parameters τ_2/τ_1 (●) and $\ln(I_2/I_1)$ (▲) for **B1** in methanol.

coupling between the unpaired electrons of **B1** was characterized by values of the exchange integral J measured at different temperatures in a very wide range of T. Three various regions of J changes vs. T were revealed but such behavior could not be described in terms of the existed theory based on the idea of fast spin exchange and a frequency parameter characterized transitions between conformations of **B1**.

The most intriguing temperature interval in which J-value depended on the solvent nature (polarity) but was constant in the error limits is at ca. $250 < T < 340$ K [1–3]. This effect has been successfully explained applying the idea of the slow electron spin exchange which characterized slow intramolecular transitions with $\Delta\omega \cdot \max\{\tau_1, \tau_2\} > 1$ [3, 4]. Here $\Delta\omega = |\omega_1 - \omega_2|$, ω_1 and ω_2 are the free electron frequencies of the first and second conformations, and τ_1, τ_2 are their life-times correspondingly.

In this work we present our results on studying biradical **B1** in toluene and methanol diluted solutions using X-band EPR spectroscopy and DFT calculations. Figure 1 illustrates typical changes in EPR spectra of **B1**, the presence of the isobestic points, hence, existence of **B1** in only two conformers confirming slow transitions between them. Experimental temperature dependences are shown in Fig. 2. DFT calculations have revealed a few conformations with similar values of the energy levels and estimated potential barriers for transitions.

Chemical exchange, CE, is usually observed in NMR spectra showing a transmission of magnetization from the state A with a chemical shift V_A to a

state B with a shift V_B, which are characterized also by the life-times τ_A and τ_B. The rate of CE increases with temperature, spin-spin interaction disappears, therefore, it can be sometimes observed upon cooling the sample. Note that CE can occur with any rate and can be studied in the case of slow exchange conditions as well as at fast chemical exchange.

The relationship between electron spin exchange and chemical exchange will be discussed.

1. Lemaire H.: J. Chim. Phys. **64**, 559 (1967)
2. Glarum S.H., Marshall J.H.: J. Chem. Phys. **47**, 1374 (1967)
3. Parmon V.N., Kokorin A.I., Zhidomirov G.M., Zamaraev K.I.: Molec. Phys. **26**, 1565 (1973)
4. Parmon V.N., Kokorin A.I., Zhidomirov G.M.: Stable Biradicals, pp. 72–86. Moscow: Nauka 1980.

Double Electron-Electron Resonance Revealing Heterogeneity of Model Biological Membranes

S. A. Dzuba[1,2], E. A. Golysheva[2], A. S. Smorygina[2], V. V. Unguryan[1,2]

[1] Department of Physics, Novosibirsk State University, Russian Federation
[2] Voevodsky Institute of Chemical Kinetics and Combustion, Russian Academy of Sciences, Novosibirsk, Russian Federation, dzuba@kinetics.nsc.ru

It is widely acknowledged that plasma membrane is highly compartmentalized, with lipids and proteins organized in specific domains, the so-called lipid rafts, with cholesterol (Chol) as an important constituent. Lipid rafts are thought to be small (10–200 nm), heterogeneous, highly dynamic, sterol- and sphingolipid-enriched domains that compartmentalize cellular processes. Their formation implies liquid ordered-disordered phase segregation in the membrane. Lipid rafts are assumed to be involved in different cellular processes, such as signal transduction, membrane trafficking, and protein activity. To elucidate the role of lipid rafts in more detail, a notion on the nanoscale lateral segregation in membranes and on the intrinsic raft structure is required.

Double electron-electron resonance spectroscopy (DEER, also known as PELDOR) is sensitive to spin-spin dipolar interactions between spin labels at the nanoscale range of distances. Here, DEER is applied to spin-labeled cholestane, 3β-doxyl-5α-cholestane (DChl), diluted in bilayers comprised of equimolar mixture of saturated dipalmitoyl-glycero-phosphocholine (DPPC) and unsaturated dioleoyl-glycero-phosphocholine (DOPC) phospholipids, with cholesterol (Chol) added in different proportions. The DEER data (see Fig. 1) were described in terms of enhanced local concentrations which allowed to detect clustering of DChl molecules. The lateral distribution in the clusters was found to change drastically with Chol content: in absence of Chol the DChl molecules are randomly distributed in the cluster while in presence of Chol the distribution becomes quasi-regular, with some area of inaccessibility appearing around each DChl molecule. DEER time traces in presence of Chol are fairly well simulated within a simple square superlattice model. For the 20 mol% Chol content, for which at physiological temperatures the lipid rafts are formed, the found superlattice parameter was 3.7 nm. Assuming that lipid rafts are captioned upon freezing at temperature of investigation (80 K), the found regularity of DChl lateral distribution was interpreted by raft sub-structuring, with DChl molecules embedded between the substructures [1].

Free fatty acids play various roles in biological membranes. Their functioning depends on intermolecular interactions. DEER was applied here to study spin-labeled stearic acids in gel-phase phospholipid bilayers composed either of equimolecular mixture of DPPC and DOPC lipids, or of 1-palmitoyl-2-oleoyl-sn-glycero-3-phosphocholine (POPC) lipid. The data obtained showed that in all cases stearic acids are assembled into lipid-mediated lateral clusters, with a characteristic intermolecular distance of ~2 nm. In two opposite leaflets of the
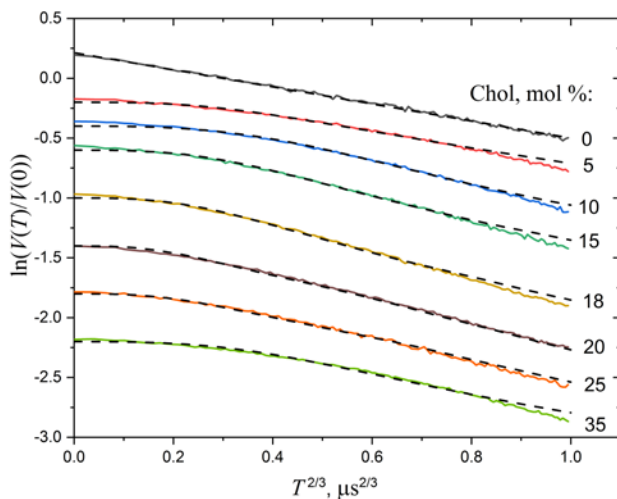
Fig. 1. DEER time traces for different Chol content in the DPPC/DOPC/Chol bilayer, with DChl added in concentration of 0.5 mol%. Dashed lines show results of simulation. Curves are vertically shifted for convenience of presentation.

bilayer the clustering was found to occur in an alternative way. For the mean concentration in the bilayer $\chi > 2$ mol%, molecules in the clusters stick together, forming oligomers.

CW EPR spectra taken for the bilayers at room temperature nicely support the results on the cluster formation obtained by DEER spectroscopy that operates at cryogenic temperatures (80 K). These spectra were found to change noticeably when concentration of spin-labeled stearic acid is increased above the value characteristic for this clustering (0.5 mol%), which may be explained by increasing anisotropy of rotational motion because of inter-cluster interactions between the stearic acid molecules.

1. Unguryan V.V., Golysheva E.A., Dzuba S.A.: J. Phys. Chem. B, 2021, DOI: 10.1021/acs.jpcb.1c05215.

Utilizing EPR Spectroscopy and Computational Modelling To Evaluate the Mechanism Underlying Metal Transcription Activators and De-Repressors

S. Ruthstein

Department of Chemistry, Faculty of Exact Sciences, Bar-Ilan University, Israel

Metal ions are essential for many important biological and chemical reactions that occur in the cell. However, if their concentration is not highly regulated, it can lead o toxicity and eventually to cell death. The situation of prokaryotic systems is more difficult than eukaryotic ones, since they are facing a changing environment depending on the host cell. Therefore, they have evolved a very sophisticated regulation system which is controlled by metal sensors.

Metal sensors are a unique class of metal regulators in pathogenic systems that sense specific metal ion with very high affinity (10^{-15}–10^{-21} M). When the protein chelates the specific metal ion, it induces changes in protein structure and/or dynamics, activates or prevents DNA binding and consequently regulate a transcription process of proteins that should shuttle the specific metal ion outside the cell.

There are four different families of metal sensors, each characterized by specific structure and metal site, that upon metal binding activate the transcription process. In our lab we are studying three out of these four families using EPR spectroscopy and computational modelling. We target various conformation states of the protein and the DNA during the transcription using various spin-labeling methods. In my talk, I will present our recent findings in this topic.

EPR and Quantum Chemical Studies of the Pirolidine Nitroxides with Bulky Substituents

A. Brovko[1,2], K. Lomanovich[1], S. Dobryunin[1], Yu. Polienko[1], I. Kirilyuk[1], E. Bagryanskaya[1]

[1] Novosibirsk Institute of Organic Chemistry SB RAS, Novosibirsk 630090, Russian Federation
lomanovich@nioch.nsc.ru; s.a.dobrynin@gmail.com; polienko@nioch.nsc.ru; kirilyuk@nioch.nsc.ru; egbagryanskaya@nioch.nsc.ru
[2] Department of Natural Sciences, Novosibirsk State University, Novosibirsk 630090, Russian Federation, a.brovko@g.nsu.ru

Stable free radicals are widely used as molecular probes and spin labels in various biophysical and biomedical research applications of magnetic resonance spectroscopy and imaging. Among these radicals, sterically shielded nitroxides of pyrrolidine series demonstrate the highest stability in biological systems. This was confirmed by the example of tetraethyl-substituted imidazoline and imidazolidine nitroxides [1] and later on the pyrrolidine [2].

It was shown that in the case of tetraethyl-substituted pH-sensitive nitroxyl radicals in the EPR spectrum, a triplet splitting of each line of ^{14}N ($I = 1$) of the N-O fragment occurs due to two hydrogens. Each hydrogen atom is one of four hydrogen atoms in the methylene groups of geminal ethyl substituents at positions 2 or 5 of the heterocycle [1]. To determine the exact positions of these hydrogen atoms, we studied radicals deuterated to different degrees and in different positions of ethyl group (Fig. 1). It is known that the hfs constant of
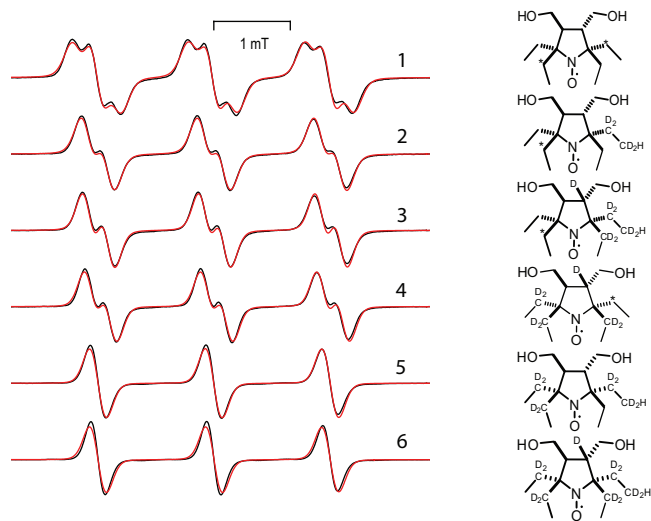
Fig. 1. Experimental (black) and calculated (red) EPR-spectra of nitroxide shown on right side.

Table 1. Parameters of EPR-spectra simulations.

Name	g	aN (mT)	a_1 (mT)	a_2 (mT)	Gauss (mT)	Lorenz (mT)
1	$2.0057 \pm 5 \cdot 10^{-5}$	$1.53 \pm 2 \cdot 10^{-3}$	0.23(H)	0.23(H)	0.21	0.05
2			0.23(H)	0.035(D)	0.19	0.05
3			0.23(H)	0.035(D)	0.18	0.05
4			0.035(D)	0.23(H)	0.19	0.03
5			0.035(D)	0.035(D)	0.16	0.05
6			0.035(D)	0.035(D)	0.14	0.05

deuterium is 6.5 times less than the hfs constant of hydrogen. All the obtained EPR spectra and simulated EPR spectra are shown in Fig. 1.

In nitroxide 2,3,4 hydrogen atoms are partly substituted by deuterium atoms. As a consequence, in the EPR spectrum, we observed the doublets of about 0.2 mT of three EPR lines corresponding to ^{14}N. Thus, there is only one proton with a significant constant hfs on both sides of the ring. For nitroxides 5 and 6 the EPR spectrum contains only lines corresponding to ^{14}N, since hydrogen atoms of methylene groups with a significant constant hfs are replaced by deuterium. Based on the above, we can conclude that only two protons have a significant hfs constant (0.2 mT), each of which is located in the methylene group of the ethyl substituent in the cis-position to the $-CH_2OH$ neighboring group.

Temperature dependence of electron spin relaxation times were measured and will be discussed.

1. Bobko A.A., Kirilyuk I.A., Gritsan N.P., Polovyanenko D.N., Grigor'ev I.A., Khramtsov V.V., Bagryanskaya E.G.: Appl. Magn. Reson. **39**, 437–451 (2010)
2. Roser P., Schmidt M.J., Drescher M.; Summerer D.: Org. Biomol. Chem. **14**, 5468–5476 (2016)

Spin Probe Approach for Studying Inhomogeneities in Solutions of Thermoresponsive Polymers

E. N. Golubeva[1], E. M. Zubanova[1], P. S. Timashev[1-3], A. I. Kokorin[3,4], M. Ya. Melnikov[1]

[1] Chemistry Department, Lomonosov Moscow State University, Moscow 119991, Russian Federation, legol@mail.ru

[2] Institute for Regenerative Medicine, Sechenov First Moscow State Medical University, Moscow 119991 Russian Federation, timashev_p_s@staff.sechenov.ru

[3] N.N. Semenov Federal Research Center for Chemical Physics, Russian Academy of Sciences, Moscow 119991, Russian Federation, alex-kokorin@yandex.ru

[4] Plekhanov Russian University of Economics, Moscow 117997, Russian Federation, alex-kokorin@yandex.ru

Thermoresponsive polymers are of great interest because they undergo coil-to-globule transitions of single polymer chains in polar solvents near the lower critical solution temperature (LCST). This peculiarity makes them perspective for biomedical and pharmaceutical applications such as drug and gene delivery, tissue engineering, and cell expansion. Macroscopic methods (turbidimetry, DSC, etc.) usually fix sharp and reversible changes of aqueous solutions or wet films of thermoresponsive polymers in the vicinity of LCST. Besides this, the formation of small, even nanoscopic inhomogeneities of polymer gels in different solvents before LCST is proved by continuous-wave electron paramagnetic resonance spectroscopy (CW EPR) [1–3].

In the present report, we discuss the features of the formation and structure of inhomogeneities of aqueous solutions of poly-N-isopropylacrylamide (PNIPAM) as one of the most applied and studied thermoresponsive polymers using spin
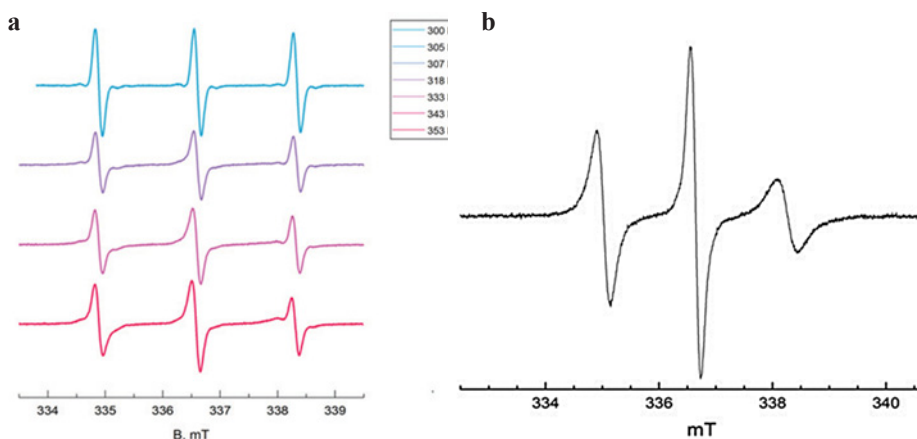
Fig. 1. a EPR spectra of TEMPO in 10wt% PNIPAM aqueous solutions at 300–353 K. **b** EPR spectrum of TEMPO in 10wt% PNIPAM aqueous solutions at 353 K in the presence of Cu(II) ions.

probe CW EPR. The effect is based on the greater affinity of TEMPO radical to hydrophobic media of the polymer associates. It manifests itself by appearing of the more broadened and hence less intensive signal of TEMPO radicals while heating compared to their water solutions at low temperatures (see Fig. 1). Using Cu(II) ions as "quencher" for fast-moving radicals in the liquid phase allowed us to obtain individual spectra of TEMPO in polymer globules and observe inhomogeneities in solutions before globule collapsing. Spin-Hamiltonian parameters of TEMPO in PNIPAM globules were obtained by modeling the spectra. The spectra simulations confirm the formation of molten globule at the first step with its further shrinkage due to coming out of water molecules, making it denser and more hydrophobic.

1. Antheunis H., van der Meer J.-C., de Geus M., Heise A., Koning C.E.: Biomacromolecules **11**, 1118 (2010)
2. Kurzbach D., Junk M.J.N., Hinderberger D.: Macromol. Rapid Commun. **34**, 119 (2013)
3. Winnik F.M., Ottaviani M.F., Bossmann S.H., Garcia-Garibay M., Turro N.J.: Macromolecules **25** (1992) 6007.

Electron Spin Resonance Study of the Epoxide Thiolysis Fe$_3$O$_4$ Magnetically Separable Catalyst

S. S. Yakushkin, V. L. Kirillov, A. A. Philippov, O. N. Martyanov

Boreskov Institute of Catalysis, Russian Academy of Sciences, Siberian Branch, Novosibirsk 630090, Russian Federation, stas-yk@catalysis.ru

Magnetically controllable colloidal nanoparticles are studied in a various fields of knowledge, including engineering, medicine, microbiology and catalysis. For the catalysis the advantage of magnetically separable nanoparticles is obvious. While the catalytical activity of such a system is close to the homogeneous catalysts [17], magnetic separation may drastically improve the usability of the catalyst, allowing one to perform synthesis with near zero loss.

One of the most common iron oxides used in magnetically controlled systems is magnetite Fe$_3$O$_4$. Magnetite shows promising properties regarding catalysis, since there is mix-valence iron in its structure. Iron oxides, magnetite in particular is known as promising inexpensive and environmental friendly organic synthesis catalyst.

New facile one step synthesis of few nanometers Fe$_3$O$_4$ particles colloid was suggested in the Boreskov Institute of Catalysis based on the modification of co-precipitation method proceeding in surfactant like environment. The method allows one to get colloids based on Fe$_3$O$_4$ nanoparticles with narrow size distribution that show superparamagnetic behavior at room temperature.

In the present study we compare two samples of magnetite nanoparticles, which were synthesized using original methods [1, 2]. Main attention has been paid to the changes in the nanoparticles magnetic properties during catalytical reaction and separation process, using electron spin resonance as the sensitive tool to study magnetic nanoparticles and their interactions with the reaction media and each other.

1. Kirillov V.L., Balaev D.A., Semenov S.V., Shaikhutdinov K.A., Martyanov O.N.: Mater. Chem. Phys. **145**, 75 (2014)
2. Kirillov V.L., Yakushkin S.S., D.A. Balaev D.A., Dubrovskiy A.A., Semenov S.V., Knyazev Y.V., Bayukov O.A., Velikanov D.A., Yatsenko D.A., Martyanov O.N.: Mater. Chem. Phys. **225**, 292 (2019)

In vivo Free Radicals Detection in Zebrafish Embryos with X band Electron Paramagnetic Resonance

K. Makarova[1], K. Zawada[1], M. Wiweger[2]

[1] Department of Physical Chemistry, Chair of Physical Pharmacy and Bioanalysis, Faculty of Pharmacy with Laboratory Medicine Division, Medical University of Warsaw, Banacha 1, Warsaw 02-097, Poland, katerina.makarova@gmail.com
[2] Laboratory of Neurodegeneration International Institute of Molecular and Cell Biology in Warsaw, 4 Ks. Trojdena Str., Warsaw 02-109, Poland

Oxidative stress, in which excessive reactive oxygen and nitrogen species cause cell damage, is a component of many diseases, including cancer. [1] Free radicals are an important group of these reactive species. Other free radicals, such as melanin radicals, are formed in the physiological and pathological processes. Electron Paramagnetic Resonance (EPR) is a technique that allows direct detection of free radicals, also *in vivo*.

Due to the high genetic similarity to humans, combined with a short reproductive cycle, high fecundity and easy observation of changes in transparent embryos, zebrafish (*Danio rerio*) is an attractive alternative to other vertebrate models. Zebrafish embryos are used to uncover the mechanisms of many diseases including oxidative stress studies [2, 3] Additionally, the zebrafish is one of the few laboratory animals whose size allows analyses to be performed using standard EPR resonators.

We have used a benchtop EPR X-band spectrometer (Magnettech/Adani, MS200) with a multi-harmonic analyzer eSpect+ (Novilet) and developed by us, a special flat EPR capillary for the *Danio rerio* embryos.

We detected melanin radical in zebrafish embryos >27 hours post fertilization (stages developing pigmentation). The signal from melanin was absent in pigment-free albino line (Fig. 1) and in wildtype embryos, where the synthesis
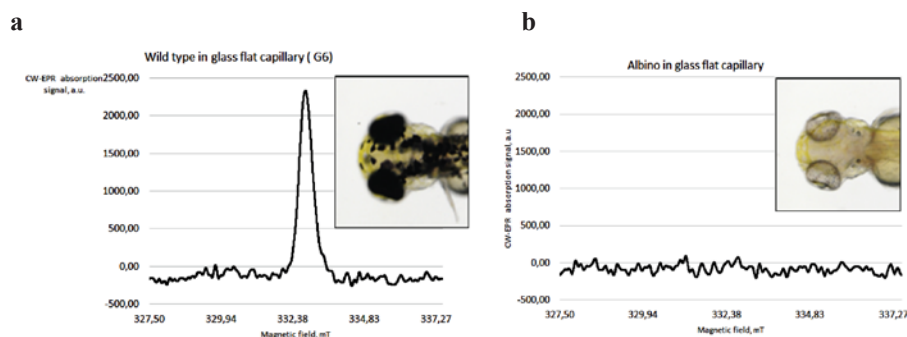
Fig. 1. Detection of the melanin in zebrafish embryos loaded into the specially shaped glass capillaries. EPR parameters were as follows: modulation amplitude 500 µT, range 10 mT, 16 scans, 25 dB, 11 s sweep time. Integrated CW X-band EPR with eSpect+ signal from melanin radical and representative bright field images of 3 days-old zebrafish larvae: **a** wild-type (WT), **b** albino

of melanin was inhibited chemically with Phenylthiourea. We also detected the incorporation of 5-DSA spin probe into zebrafish embryo membranes. In the presence of DMSO, the membrane fluidity of the zebrafish embryos changed as reflected in EPR spectra of 5-DSA. Thus, EPR spectroscopy could be used to access the level and monitor changes in the melanin radical in living zebrafish embryos as well as to monitor changes in membrane fluidity. This method allows repeated *in vivo* measurements for several subsequent days and opens new possibilities for melanoma studies.

1. Forman H.J., Zhang H.: Nature Reviews Drug Discovery **20**, 689–709 (2021)
2. Abbate F., Maugeri A., Laurà R., Levanti M., Navarra M., Cirmi S., Germanà A.: Antioxidants. **10**(5), 668 (2021)
3. Zhao S., Huang J., Ye J.: Journal of Experimental & Clinical Cancer Research **34**, 80 (2015)

Stereoselectivity, Spin Selectivity and Chiral Inversion in Diastereomers of Chiral Drugs. Spin Chemistry and Photochemistry Investigation

A. Ageeva[1,2], I. Magin[1], A. Stepanov[1], N. Polyakov[1], T. Leshina[1]

[1] Voevodsky Institute of Chemical Kinetics and Combustion, Novosibirsk 630090, Russian Federation, al.ageeva@gmail.com

[2] Natural Science Department, Novosibirsk State University, Novosibirsk 630090, Russian Federation

The difference in medical properties of enantiomers of many chiral drugs is well known fact. Widespread nonsteroidal anti-inflammatory drug – Naproxen (NPX) is the striking example of the drug, which enantiomers differ not only in degree but also in direction of therapeutic activity. To understand the origin of activity differences we have studied the photoinduced elementary processes in NPX-based dyads, modelling drug-receptor binding. These dyads are linked systems, with electron donors (S)-N-methylpyrrolidine and (S)-tryptophan and acceptors (S) and (R)-NPX.

The photochemistry and spin chemistry investigations of photoinduced electron transfer (ET) have shown stereoselectivity of rate constants of NPX excited state quenching and fluorescence quantum yields of local excited states and exciplex. In order to understand the nature of observed stereoselectivity the thorough analysis of spin effects have been performed. The comparison of CIDNP enhancement coefficients has demonstrated the twofold difference between dyads with (R)- and (S)-NPX. This was found to be the result of difference in spin density distribution that allows one to expect the difference in electron density distribution and the reactivity of enantiomers. Moreover, the ^{1}H NMR spectra of (R,S)-NPX-Trp dyad after the UV irradiation have demonstrated the appearance of new signals coincident with signals pattern for (S,S)-diastereomer. This fact points at spontaneous conversion of (R)-NPX to (S)- in diastereomers via reversible H atom transfer from NPX's chiral center.

Thus, on the example of NPX-Trp dyad two essential elementary processes have been established: photoinduced ET and reversible H atom transfer. The former process leads to stereoselectivity and spin selectivity, the latter results in unidirectional radical chiral inversion of (R)-NPX to (S)- in diastereomers. Note that observed peculiarities might be the reasons of sharp distinction in medical activity of drug enantiomers.

W-band ^{19}F ENDOR Spectroscopy for Distance Measurement Using Trityl Spin Probe

<u>N. B. Asanbaeva</u>[1,2], A. A. Sukhanov[3], A. A. Diveikina[1],
O. Yu. Rogozhnikova[1], D. V. Trukhin[1], V. M. Tormyshev[1],
A. S. Chubarov[4], A. G. Maryasov[1], A. M. Genaev[1], E. G. Bagryanskaya[1]

[1] Novosibirsk Institute of Organic Chemistry SB RAS, Novosibirsk, 630090, Russian Federation,
nasanbaeva@nioch.nsc.ru
[2] Physics Department, Novosibirsk State University, Novosibirsk 630090, Russian Federation
[3] Zavoisky Physical-Technical Institute, Kazan 420029, Russian Federation
[4] Institute of Chemical Biology and Fundamental Medicine SB RAS, Novosibirsk 630090,
Russian Federation

Due to the long electron spin relaxation times, low *g*-factor anisotropy and stability triarylmethyl (TAM) radicals have been successfully used to measure distances in biological objects by the PELDOR, DQC spectroscopy [1, 2]. These techniques allow measuring distance between spin labels in the range of 1.8–10.0 nm. Shorter distances are not determined because in this case the exchange coupling is added to the dipolar interaction, and rather strong microwave field is needed to obtain proper modulation depth [3]. Therefore, it is very difficult to accurately measure the distance between the paramagnetic centers. Then ENDOR method comes to the rescue that can elucidate of the hyperfine interactions or coupling (hfi) of an unpaired electron with surrounding nuclei. In concert with the use of ^{19}F labels, which are in short supply in biological systems and have large gyromagnetic ratio, the ENDOR method allows selective measurement of atomic distances up to 1.5 nm [4].

In the present work we focused on the use of ^{19}F nuclear spins and TAMs in combination with high-frequency (94 GHz/3.4 T) W-band ENDOR. Application of high magnetic fields allows separation of nuclear frequencies of ^{19}F and
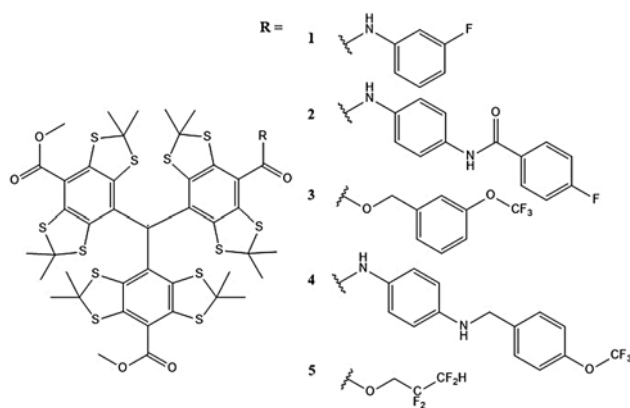
Fig. 1. Chemical structures of the model compounds **1-5**.
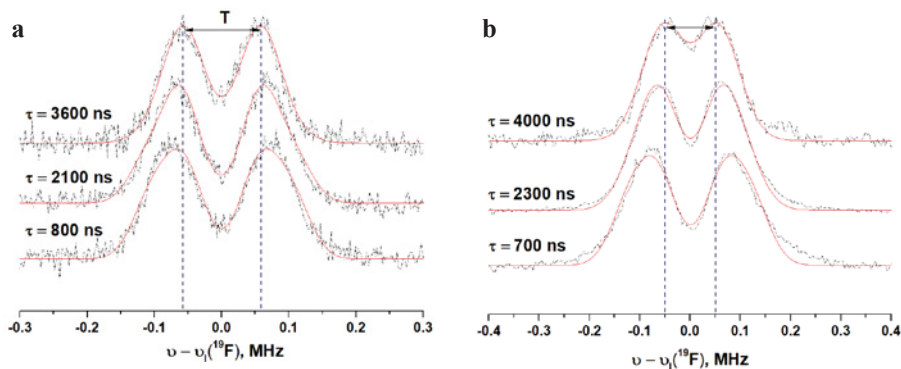
Fig. 2. 94 GHz ^{19}F Mims ENDOR spectra of **1** (**a**) and 5 (**b**) in [d$_6$]DMSO/[d$_4$]MeOD (2:3) were recorded at different values of τ.

protons with sufficient resolution. We demonstrated the possibilities of using this method on model compounds **1-5** (Fig. 1). Aromatic linkers of various lengths were used to obtain structures with a fixed distance "radical center–fluorine". For data processing the point dipole model ($T \sim 1/r^3$, r – inter-spin distance, T – dipolar part of hfi) was used in spite of the electron spin density distribution over the π-system of trityl. It was shown because symmetry of spin density distribution is high enough it is reasonable to account that in the system studied the vector **r** connects ^{19}F nucleus and the central carbon atom of TAM radical.

Mims ENDOR spectra were obtained at the EPR resonance at 80 K, where the echo signal is maximized. For all compounds, we do not observe an explicit Pake pattern, i.e. its parallel component does not show up. But to determine the spin-to-spin distance, we need only the $T_\perp$ component, which appears itself in the spectra of samples **1** and **5**. The values 129 ±15 and 136 ± 15 kHz were extracted from spectra (Fig. 2). Using the determined dipolar hyperfine interaction values the distances r of 8.3 ± 0.2 and 8.2 ± 0.3 Å were calculated for compounds 1 and 5 respectively. The structures **2-4** have ENDOR spectra with unresolved hyperfine structure. It can be assumed that these compounds can have conformations with distances of more than 10 Å, which is practically beyond the limits of applicability of this method.

1. Krumkacheva O.A. *et al.*: Nucleic Acids Res. **47**, 7767 (2019)
2. Shevelev G.Y. *et al.*: J. Phys. Chem. B. **122**, 137 (2018)
3. Tsvetkov Yu.D., Milov A.D., Maryasov A.G.: Russ. Chem. Rev. **77**, 487 (2008)
4. Meyer A. *et al.*: Angew. Chemie - Int. Ed. **59**, 373 (2020)

SECTION 5

NEW TRENDS IN SPIN CHEMISTRY

New Trends in CIDNP Study

A. Yurkovskaya, H.-M. Vieth, O. Morozova, K. Ivanov

International Tomography Center, Novosibirsk 630090, Russian Federation, yurk@tomo.nsc.ru

Chemically induced dynamic nuclear polarization (CIDNP) has emerged as a highly informative method to study spin-dependent radical reactions by analyzing enhanced NMR signals of their diamagnetic reaction products. In this way, one can probe the structure of elusive radical intermediates and determine their magnetic parameters. A careful examination of experimental CIDNP data at variable magnetic fields shows that formation of hyperpolarized molecules in a coherent state is a ubiquitous though rarely discussed phenomenon. The presence of nuclear spin coherences commonly leads to subsequent polarization transfer among coupled spins in the diamagnetic products of radical recombination reaction that must be taken into account when analyzing the results of CIDNP experiments at low magnetic field. Moreover, such coherent polarization transfer can be efficiently exploited to polarize spins, which do not acquire CIDNP directly. Here we explain under what conditions such coherences can be generated, focusing on the key role of level anti-crossings in coherent polarization transfer, and provide experimental approaches to probing nuclear spin coherences and their time evolution [1]. The relevance of polarization transfer in strongly coupled spin systems goes beyond the field of CIDNP: such polarization transfer is frequently exploited in PHIP experiments (and then it is often termed "spontaneous" polarization transfer) to polarize protons and heteronuclei (for review see [3]).

The key advantage of the time-resolved variant of CIDNP at biologically relevant conditions is the linear relationship between the CIDNP intensities in NMR spectra and hyperfine interaction constants in short-lived radicals as explained by Konstantin Ivanov in 2011 [2]. It is only applicable to the CIDNP of geminate diamagnetic products formed on the nanosecond time scale. Since its discovery, such linear relationship was widely used to characterize the spin-density distribution in transient radicals in multistage reactions (for review see [4]).

1. Ivanov K.L., Yurkovskya A.V., Fishman N.N., Kiryutin A.S., Sagdeev R.Z., Vieth H.-M.: Appl. Magn. Reson. DOI: 10.1007/s00723-021-01348-9 (2021)
2. Morozova O.B., Ivanov K.L., Kiryutin A.S., Sagdeev R.Z., Köchling T., Vieth H.-M., Yurkovskaya A.V.: Phys. Chem. Chem. Phys. **13**, 6619–6627 (2011)
3. Barskiy D.A., Knecht S., Yurkovskaya A.V., Ivanov K.L.: Prog. Nucl. Magn. Reson. Spectrosc. **114-115**, 33–70 (2019)
4. Morozova O.B., Ivanov K.L.: ChemPhysChem **20**, 197–215 (2019)

Simple Rules for Resolved Level Crossing Spectra in Magnetic Field Effects on Reaction Yields

D. V. Stass[1,2,3], V. A. Bagryansky[1], Yu. N. Molin[1]

[1] Voevodsky Institute of Chemical Kinetics and Combustion,
Novosibirsk 630090, Russian Federation,
[2] Novosibirsk State University, Novosibirsk 630090, Russian Federation,
[3] International Tomography Center, Novosibirsk 630090, Russian Federation,
stass@ns.kinetics.nsc.ru

Spin-correlated nature of radical (ion) pairs arising as intermediates in many chemical transformations gives rise to a host of "magnetic and spin effects" in chemical reactions. This talk deals with a curious bridge between the most humble magnetic field effect curves (MFE) and hyperpolarized NMR: additional sharp resonance-like lines that may occur against the smooth background of MFE due to genuine level crossings in the spin system of the radical pair. The lines for such purely spin level crossings were first discovered in zero magnetic field and attributed to interference of pair states similar to Hanle effect in atomic spectroscopy [1]. In that paper hyperfine-driven crossings at nonzero fields in MFE for a pair with equivalent nuclei in only one pair partner also first appeared in calculations, which were specifically explored later in [2] and then experimentally observed in several systems, turning MFE curves into "resolved MARY spectra". It was further suggested and checked that for very simple systems the hyperfine structure of the second pair partner may be revealed at the level crossing lines, which was termed "MARY ESR" [3]. In this work we explore conditions under which a level crossing line in magnetic field effect curve for a recombining radical pair will be equivalent to ESR spectrum, providing a full justification for the term "MARY ESR", and discuss three simple rules for qualitative prediction of the level crossing spectra [4].

1. Anisimov O.A., Grigoryants V.M., Kiyanov S.V., Salikhov K.M., Sukhenko S.A., Molin Y.N.: Theor. Exp. Chem. **18**, 256 (1983)
2. Sukhenko S.A., Purtov P.A., Salikhov K.M.: Sov. J. Chem. Phys. **2**, 29 (1985)
3. Tadjikov B.M., Stass D.V., Molin Yu.N.: Chem. Phys. Lett. **260**, 529 (1996)
4. Stass D.V., Bagryansky V.A., Molin Yu.N.: Magn. Reson. **2**, 77 (2021)

Pulse and AWG-based RF Magnetic Field Effects on Chemical Reaction Kinetics

K. Maeda

Department of Chemistry, Graduate School of Science and Engineering, Saitama University, Saitama 338-8570, Japan, kiminorimaeda@mail.saitama-u.ac.jp

Previously, many techniques to modulate the radical pair (RP) reactions by weak static, pulse and oscillating magnetic fields have been developed. Here, we present following two kinds of methods.

1. Static and pulse magnetic field effect measured by transient spectroscopy.

Magnetic field effect (MFE) measurement is one of the most direct diagnostic tests for the magnetoreception of biological systems. The MFEs are strongly related with the kinetic feature of the diffusion on the surface of biomolecular systems [1]. In this sense, the temporal measurement in the photochemical reaction measurement is very important. However, the usual transient absorption measurements often hardly distinguish the radical pair from the large background signal of the free radical and the triplet excited state. The Switched External Magnetic Field (SEMF) method [2] enable us to measure the decay kinetics of RP avoiding the interference by the background transient absorptions. Here, we present the results of SEMF in the system of RP on a protein surface and demonstrate the power of the technique for the analysis of inhomogeneous RP systems. Not only the kinetic information, the SEMF is also able to probe the coherent spin dynamics in low field regime.

2. Arbitrary waveform generator (AWG) based RYDMR (Reaction Yield Detected Magnetic Resonance)

Recently, AWG based pulse EPR and NMR have been developed for the manipulation of spin system. We are now proposing AWG based chemical reaction control of RPs both in low and high magnetic field regime. Here we present a theoretical calculation of the optimized RF field using the local control theory [3] and manifest AWG based reaction control. In high field, the selection of the hyperfine lines and anisotropic control in the rotating frame can be done by the optimized the RF(MW) field. In low magnetic field, an optimized RF field is calculated for a coherent control for a model RP [4].

1. Maeda K., Robinson A.J., Henbest K.B., Dell E.J., Timmel C.R.: J. Am. Chem. Soc. 132, 1466 (2010)
2. Suzuki T., Miura T., Maeda K., Arai T.: J. Phys. Chem. **109**(44), 9911 (2005)
3. Masuzawa K., Sato M., Sugawara M., Maeda K.: J. Chem. Phys. **152**, 14301 (2020)
4. Sugawara M.: J. Chem. Phys. **118**(15), 6784-6800 (2005)

The Review of Magnetic Field Effects in Charge Separated States of Rigidly Linked Donor-Acceptor Dyads

N. N. Lukzen

International Tomography Center SB RAS, Novosibirsk, Russian Federation, luk@tomo.nsc.ru

The magnetic field effects in charge separated states in rigidly linked by molecular bridge donor-acceptor dyads are reviewed. It includes: giant magnetic field effects in donor–acceptor triarylamine–naphthalenediimide triads with bis-diyprrinato-palladium(II), porphodimethenato-palladium(II) and palladium(II)–porphyrin as photosensitizers and linkers;

J-resonance lineshape of MARY spectrum from charge recombination in a linked donor/acceptor dyad and also nanoviscosity effect on the spin chemistry of an electron donor/Pt-complex /electron acceptor triad, its classical and quantum kinetics interpretation.

New Paradigm of Spin Exchange Opens Up New Horizons

K. M. Salikhov

Zavoisky Physical-Technical Institute, FRC Kazan Scientific Center of RAS, Kazan 420029, Russian Federation, kevsalikhov@mail.ru

There are presented new theoretical observations concerning manifestations of the spin exchange in steady state EPR spectra of dilute solutions of paramagnetic particles.

The analysis of the dependence of the width of the spectrum lines on the spin coherence transfer rate and on the microwave field power revealed the "destructive interference" of these factors in terms of their manifestation in the EPR spectra.

It is shown that the broadening of the spectral lines observed in the experiment under saturation conditions is not the additional homogeneous broadening of resonance transitions.

The results are presented and discussed of an attempt to find the effective time of spin-lattice relaxation of spins as a function of the spin exchange rate and of the microwave field strength.

Using stationary EPR spectra under saturation conditions and taking into account the spin exchange, the effective spin-lattice relaxation time is obtained. Conditions are found under which the effective spin-lattice relaxation time is practically equal to the spin-lattice relaxation time of isolated paramagnetic particles.

The report briefly presents the experiments that flow from the new paradigm of spin exchange, in particular, under the conditions of the saturation effect in strong microwave fields.

1. Salikhov K.M.: Fundamentals of spin exchange. Story of a paradigm shift. Springer Nature Switzerland AG (2019)
2. Salikhov K.M.: New Information About Manifestations of Spin Exchange in the EPR Spectra of Solutions of Paramagnetic Particles Under Saturation Conditions. Appl. Magn. Reson. **52**,1063–1093 (2021)

Modern Methods of Transferring Nuclear Polarization Induced by Parahydrogen Utilizing Ultra-Low Magnetic Fields

V. P. Kozinenko[1,2], A. S. Kiryutin[1,2], A. V. Yurkovskaya[1,2]

[1] International Tomography Center, Novosibirsk 630090, Russian Federation,
[2] Novosibirsk State University, Novosibirsk 630090, Russian Federation,
vitaly.kozinenko@gmail.com

Over the last decade, parahydrogen-induced polarization (PHIP) has revealed itself as an exceptionally powerful method of NMR signal enhancement. One of the reasons for that stems from its ability to effectively hyperpolarize biologically relevant molecules by using low-cost experimental equipment. Signal enhancement in PHIP method arises due to the non-equilibrium population of nuclear spin states in the para-hydrogen molecule and reaches a factor of 10^3–10^5 [1]. Moreover, PHIP build-up occurs on a timescale of several seconds, which makes a high throughput creation of hyperpolarized product possible. A particular interest is concentrated on the transfer of PHIP from protons to magnetic heteronuclei (^{13}C, ^{15}N, and others) [2]. Such heteronuclei are less susceptible to relaxation loss of polarization compared to protons and allow to record NMR spectra free of background signals.

Here, we perform a comprehensive analysis of a variety of PHIP transfer methods operating at ultra-low (B_0 < 1 uT) magnetic fields. Such magnetic fields correspond to the regime of strong coupling between protons and heteronucleus, which allows one to transform singlet order of parahydrogen protons into net magnetization of heteronucleus. We implement various experimental schemes, including continuous parahydrogen bubbling at ULF, adiabatic sweeping of the external magnetic field and coherent spin mixing at the optimal ULF. We optimize the experimental conditions to achieve the most efficient transfer of PHIP to the ^{13}C magnetization. We demonstrate the performance of these transfer schemes for both – model systems (ethyl cinnamate) and biologically relevant molecules (allyl pyruvate and fmoc-L-tyrosine-allyl).

1. Bowers C.R., Weitekamp D.P.: J. Am. Chem. Soc. **109**(18), 5541–5542 (1987)
2. Reineri F., Boi T., Aime S.: Nat Commun. **6**, 5858 (2015)

Determination of the Reorganization Energy in Degenerate Electron Exchange Reactions Involving Short-Lived Radicals by the Method of Time-Resolved CIDNP

M. Geniman

[1] Laboratory of Photochemical Radical Reactions, ITC SB RAS, Novosibirsk 630090, Russian Federation, m.geniman@g.nsu.ru

It is well known that oxidative damage to DNA, usually through structural changes in nucleotides and chain breaks, leads to mutations, cancer or other diseases. Guanine (G) has the lowest ionization potential among the DNA bases, so most oxidants attack G with the formation of the cation radical $G^{+\bullet}$, oxidative damage of other bases also can migrate to guanine. Guanine radicals can be reduced in electron transfer reaction with the amino acids tyrosine and tryptophan. Depending on the pH value of the solution the guanine radical exists in different forms, so the rate of its recovery depends on the pH.

According to the Marcus theory the activation energy E_a of electron transfer reaction is expressed in terms of the difference free energy of the initial and final states $\Delta G°$ and the reorganization energy λ – parameter that takes into account the difference in the solvation energies of the reactants and the transition state and the change in the geometry of the reactants when they are converted into products. For a degenerate electron exchange, when the donor and acceptor differ by only one electron, $\Delta G° = 0$ and $E_a = \lambda/4$. The Marcus cross-relation is used to estimate the rate constant of electron transfer reaction from the rate constants of the corresponding degenerate exchange reactions. Therefore, it is interesting to study the reactions of degenerate exchange.

The time-resolved CIDNP method can provide information about degenerate exchange reactions involving short-lived radicals. In the temperature range from 8 to 65 °C, the degenerate electron exchange reactions of the guanosine-5'-monophosphate cation $GMPH^+$ with the dication radical $GMPH^{++\bullet}$ at pH = 1.3, of the guanosine-5'-monophosphate anion $GMP(-H)^-$ with the neutral radical $GMP(-H)^\bullet$ at pH = 11.3, of the N-acetyl tyrosine anion $N-AcTyrO^-$ with a neutral radical $N-AcTyrO^\bullet$ at pH = 11.7 and of the tyrosine anion $TyrO^-$ with a neutral radical $TyrO^\bullet$ at pH = 11.7 were studied. In all cases, the radicals were formed in the reaction of quenching triplet 2,2'-dipyridyl. At each temperature the rate constant of the degenerate exchange in each system was determined. The reorganization energies were calculated using the Arrhenius equation. The rate constants of the reductive electron-transfer reactions for pairs $GMP(-H)^\bullet$/$TyrO^-$ and $GMP(-H)^\bullet$/$N-AcTyrO^-$ were found using Marcus cross-relation, the calculated values are higher than the experimental ones.

The rate of nuclear paramagnetic relaxation was found for the 3,5 and β-protons $TyrO^\bullet$ and $N-AcTyrO^\bullet$, the 8-proton $GMPH^{++\bullet}$ and $GMP(-H)^\bullet$ at each

temperature. The relaxation rates of the 8-proton in GMPH$^{++\bullet}$ and GMP(-H)$^\bullet$ coincide over the entire temperature range. In all cases, the dependences of the rate of nuclear paramagnetic relaxation on temperature are described by the Arrhenius dependence. The activation energy for β-protons TyrO$^\bullet$, N-AcTyrO$^\bullet$ is close to zero, and for 3,5-protons N-AcTyrO$^\bullet$ and 8-proton GMPH$^{++\bullet}$ and GMP(-H)$^\bullet$ its value coincided with the activation energy for the viscosity of the solvent. The activation energy for 3,5-protons TyrO$^\bullet$ is less than that for 3,5-protons N-AcTyrO$^\bullet$.

Singlet-Triplet Conversion in Molecular Hydrogen and its Role in Parahydrogen Induced Polarization

D. A. Markelov[1], V. P. Kozinenko[1], S. Knecht[2], A. S. Kiryutin[1], A. V. Yurkovskaya[1], K. L. Ivanova[1]

[1] International Tomography Center and Novosibirsk State University
[2] NVision-Imaging Technologies, Ulm, Germany

An analysis of singlet-triplet conversion in molecular hydrogen dissolved in solution with organometallic complexes used in experiments with parahydrogen (the H_2 molecule in its nuclear singlet spin state) is reported. We demonstrate that such conversion is an efficient process, which gives rise to the formation of orthohydrogen (the H_2 molecule in its nuclear triplet spin state) and also strongly reduces the resulting NMR (nuclear magnetic resonance) signal enhancement, here of ^{15}N nuclei polarized at high fields using special NMR pulse sequences. We make use of a simple improvement of the traditional pulse sequences, as shown in Fig. 1a, utilizing a single pulse on the proton channel and giving rise to an additional strong increase of the signal. Furthermore, the analysis of the enhancement as a function of the length of such pulse, see Fig. 1b, allows one to estimate the actual population of the spin states of H_2.

It should be noticed that enhancement factor strongly depends on the flip angle ϕ, consequently the H_2 nuclear spin-state is no longer a pure singlet-state (in this case enhancement would not change its value, since the singlet state does not evolve under the influence of rotation operators) but rather a combination of the singlet and central-triplet states. The experiments were performed with ^{15}N-Py as a to-be-polarized substrate.
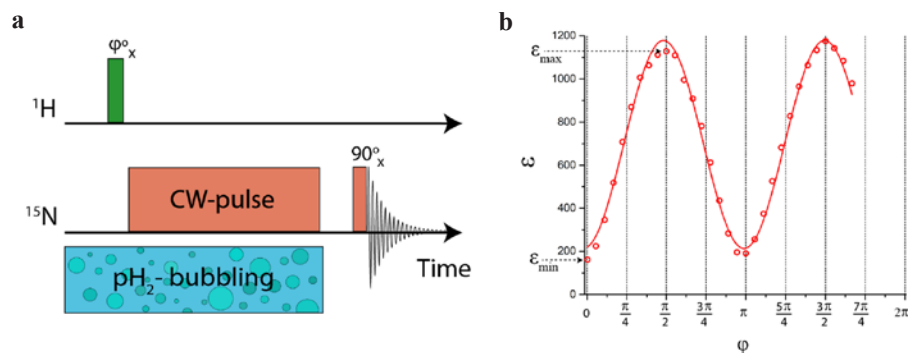
Fig. 1. a Experimental protocol used to run high-field SABRE experiments, aimed at enhancing ^{15}N signals [1]. Additional pulse with the flip angle ϕ on the proton channel is performed in order to study singlet-triplet conversion in molecular hydrogen. **b** The dependence of ^{15}N signal enhancement on the proton magnetization flip angle, ϕ.

We are also able to demonstrate that the spin conversion process in H_2 is strongly affected by the presence of ^{15}N nuclei. This observation allows us to explain the dependence of the ^{15}N signal enhancement on the abundance of 15N isotopes.

1. Knecht S., Kiryutin A.S., Yurkovskaya A.V., Ivanov K.L.: Mol. Phys. 2018, 2018, 1–10.

SECTION 6

LOW-DIMENSIONAL SYSTEMS AND NANO-SYSTEMS

Interaction of Spinons in $S = 1/2$ Chain Antiferromagnet Detected by ESR

A. I. Smirnov[1], K. Yu. Povarov[2], T. A. Soldatov[1], Ren-Bo Wang[3], O. A. Starykh[3]

[1] P. L. Kapitza Institute for Physical Problems RAS, Moscow 119334, Russian Federation,
smirnov@kapitza.ras.ru
[2] Laboratory for Solid State Physics, ETH Zürich, 8093 Zürich, Switzerland;
[3] University of Utah, Salt Lake City, Utah 84112, USA

The $S = 1/2$ Heisenberg antiferromagnetic spin chain has quantum critical ground state with an absence of ordered spin components and correlation function decay as power law. This ground state and it's excitations may be described in terms of quantized fractionalized dynamic spin structures referred to as spinons. The concept of spinons is formulated in terms of neutral spin-1/2 fermions, see, e.g. [1,2]. Consideration of free fermions is supported by numerous experiments, e.g., by observation of the continuum of $S = 1$ excitations (so called two-spinon continuum) in neutron scattering experiments [3] or by finding the field-dependent soft modes appearing within the continuum of longitudional fluctuations in a magnetic field [2]. A specific fine structure of the two-spinon continuum of transverse fluctuations was predicted for a spin $S = 1/2$ chain with a uniform Dzyaloshinsky-Moriya (DM) interaction. This interaction causes a shift of the continuum in q-space for a characteristic wavevector $q_{DM} = D/(Ja)$. The shift
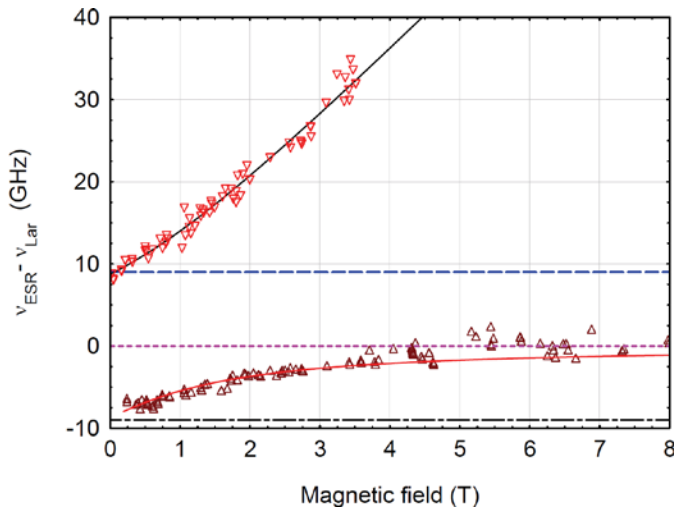
Fig. 1. ν_{ESR}-ν_{Lar} vs magnetic field at $T = 0.5$ K. Solid lines – theory, dashed – see text.
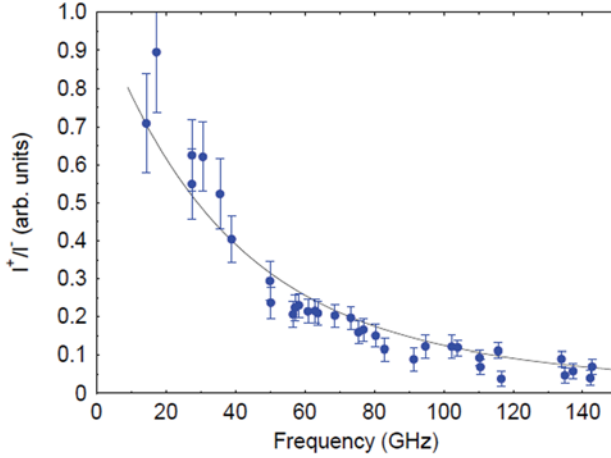
Fig. 2. Ratio of intensities of doublet components. Line – theory. $T = 0.5$ K

results in an energy gap $\Delta = \pi D/2$ and a doublet of electron spin resonance (ESR) frequencies

$$\nu_\pm = (g\mu_B H \pm \Delta)/2\pi\hbar \ . \tag{1}$$

Here D is the DM parameter and a – interspin distance. The frequencies $\nu_\pm$ correspond to lower and upper boundaries of the continuum of a purely Heisenberg (i.e. $D = 0$) chain at the wavevector q_{DM}. The ESR doublet $\nu_\pm$ was indeed experimentally observed [see, e.g., 4], confirming the fermion nature of the ground state and its excitations.

Now we report the measurements of ESR spinon doublet for an almost ideal 1D $S = 1/2$ Heisenberg antiferromagnet $K_2CuSO_4Br_2$ in a strong magnetic field. Here we observe a deviation of ESR modes $\nu_\pm$ from the simple relation (1). According to a recent theory [5], the continuum should be shifted from that of free (noninteracting) spinons due to the interaction of the backscattering type. This interaction, characterized by a parameter $u,$ describes backscattering of right/left moving spinons living near the right/left Fermi points of the one-dimensional Fermi surface, correspondingly [5, 6]. The interaction-induced gap between the lower and upper energies in the continuum is represented by $\Delta_{int} = uM/\mu_B$, where M is the magnetic moment per unit length. Using the results of [5] we explain the deviation of the experimentally observed [6] frequencies of the spinon doublet from the above interaction-neglecting relation (1). Fig.1 demonstrates the difference between the observed ESR frequencies and Larmor frequency $\nu_{Lar} = g\mu_B H/2\hbar$ measured in different magnetic fields. This difference should be constant for free spinons (see horizontal dashed lines at ± 8.7 GHz). The fit according to the predictions of [5] with the parameter $u = 3.5 \cdot 10^5$ cm/s

demonstrates a good quantitative correspondence of experiment and theory. Fig. 2 shows the frequency dependence of the ratio of intensities of the ESR doublet along with the theoretical prediction [5, 6] with the same value of u. At $u = 0$ (free spinons) this ratio should be equal to one in the whole frequency range. The theory explains a drastic drop of the upper component, which was a puzzling result of the experiment [4]. These consequences of the spinon-spinon interaction reveal a Fermi-liquid (not a Fermi-gas) behavior of quasiparticles in a 1D antiferromagnet. The excitations of 1D Heisenberg $S = 1/2$ antiferromagnetic chain demonstrate amazing analogy with the ensemble of electrons in a normal metal and specific Silin spin waves [7] in a normal metal.

1. Faddeev L., Takhtajan L.: Phys. Lett. A **85**, 375 (1981)
2. Dender D.C. *et al.*: Phys. Rev. Lett. **79**, 1750 (1997)
3. Tennant D.A. *et al.*: Phys. Rev. B **52**, 13368 (1995)
4. Smirnov A.I. *et al.*: Phys. Rev. B **92**, 134417 (2015)
5. Keselman A., Balents L., Starykh O.A.: Phys. Rev. Lett. **125** (2020)
6. Povarov K.Yu. *et al.*: arXiv:2108.02835
7. Silin V.P.: Sov. Phys. JETP **6**, 945 (1958); Silin V.P.: Sov. Phys. JETP **8**, 870 (1959)

Anisotropy-Induced Soliton Excitation
in Magnetized Strong-Rung Spin Ladders

**V. N. Glazkov[1,2,*], Yu. V. Krasnikova[1,2], S. C. Furuya[3],
K. Yu. Povarov[4], D. Blosser[4], A. Zheludev[4]**

[1] P. L. Kapitza Institute for Physical Problems, RAS, Kosygina 2, Moscow 119334, Russia
[2] Laboratory for Condensed Matter Physics, National Research University "HSE",
Myasnitskaya street 20, Moscow 101000, Russian Federation
[3] Condensed Matter Theory Laboratory, RIKEN, Wako, Saitama 351-0198, Japan
[4] Laboratory for Solid State Physics, ETH Zürich, Zürich 8093, Switzerland
*Corresponding author's email: glazkov@kapitza.ras.ru

Metal-organic compound $(C_5H_{12}N)_2CuBr_4$ (called BPCB for short) is a well-established strong-rung spin ladder with the rung coupling $J_{rung} = 12.7$ K and the couplings along the legs of the ladder $J_{leg} = 3.5$ K [2, 3]. The excitations of the spin ladder are gapped, the gap can be closed by an applied magnetic field $B_{c1} = \Delta/(g\mu_B)$, and up to the saturation field B_{c2} ideal 1D spin-ladder remains in a gapless Tomonaga-Luttinger spin liquid (TLL) state with the TLL interaction parameter determined by spin ladder exchange constants [1].

We have performed low-temperature ESR study of this magnet at the temperatures down to 400 mK. We report observation of the low-energy excitation with anomalous energy-vs-field dependency in the fields around 10 T, i.e. in the midst of the TLL phase (see Fig. 1).

Mapping of the Heisenberg strong-rung spin ladder on an equivalent "pseudospin" XXZ-chain [3] predicts equivalence of the magnetized spin ladder at $B^* = (B_{c1} + B_{c2})/2$ to the XXZ chain at zero field, i.e. zero excitation energy at B^*. Instead, we observed anisotropic gap at B^* with the asymptotic slope of $f(H)$ dependence corresponding to $g_{eff} \approx 3$:

$$2\pi\hbar\nu = \sqrt{\Delta^2 + [g_{eff}\mu_B(B - B^*)]^2} \ .$$

This behavior is explained by accounting for the Dzyaloshinskii-Moriya (DM). In the case of BPCB DM coupling is uniform along the legs of the ladder and Dzyaloshinskii vectors on the ladder's legs are exactly opposite. The ladder-to-chain mapping then yields XXZ-chain with uniform DM interaction. Excitations of the spin chain with uniform DM interaction are known to be gapped at $q = 0$ [4] in agreement with our observations.

However, the observed excitations turn out to be much more interesting. In the presence of DM interaction equivalent strongly anisotropic chain demonstrate transverse ordering of the "pseudospin" at B^* which allows for solitonic excitations of this anisotropic model. Our analysis proves that due to "real spins" to "pseudospin" transformation along the ladder-to-chain mapping only the solitonic "pseudospin" excitations remains ESR-active. Their frequency-field dependence is [5]

$$2\pi\hbar\nu = \sqrt{M^2 + [2Kg\mu_B(B - B^*)]^2} \ ,$$
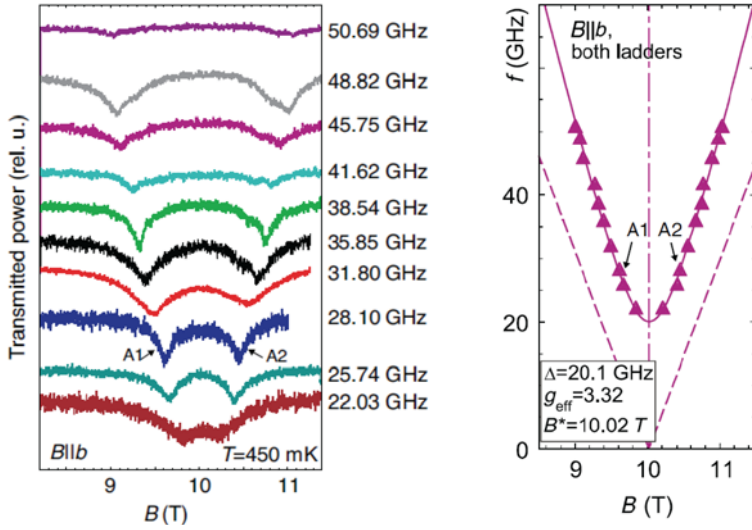
Fig. 1. (left) Examples of low-temperature ESR absorption curves in BPCB at various microwave frequencies. (right) ESR frequency-field diagram. Symbols – experimental data, dashed lines – excitations of isotropic model, solid curves – fit as described in the text. A1 and A2 marks indicate positions of the same absorption components on both panels.

here the soliton "mass" M is proportional to the squared component of Dzyaloshinskii vector transverse to the applied field and the asymptotic slope depends on Luttinger parameter K, which is equal to 3/4 for the BPCP exchange couplings constants. The predicted effective g-factor value $g_{eff} = 2Kg$ is in perfect agreement with the observed value (see Fig. 1) without any additional fitting parameter [6].

1. Jeong M. *et al.*: Phys. Rev. Lett. **117**, 106402 (2016)
2. Klanjšek M. *et al.*: Phys. Status Solidi C **247**, 656 (2010)
3. Bouillot P. *et al.*: Phys. Rev. B **83**, 054407 (2011)
4. Povarov K.Y. *et al.*: Phys. Rev. Lett. **107**, 037204 (2011)
5. Furuya S.C., Momoi T.: Phys. Rev. B **97**, 104411 (2018)
6. Krasnikova Yu.V. *et al.*: Phys. Rev. Lett. **125**, 027204 (2020)

Multiple-Quantum NMR in Quasi-One-Dimensional Zigzag Spin Chains of Hambergite

E. B. Fel'dman, E. I. Kuznetsova, <u>S. G. Vasil'ev</u>

Institute of Problems of Chemical Physics, Chernogolovka 142432, Russian Federation,
viesssw@mail.ru

Multiple quantum (MQ) NMR is recognized as an important technique for simplification of NMR spectra and complementation of structural information by establishing the spatial arrangement of atomic groups in solids with magnetic dipole-dipole interaction (DDI) [1]. MQ coherences are excited using a suitably designed pulse sequence which modifies the dipolar interaction naturally present in the system. Unlike the conventional excited single-quantum coherence, the observation of these forbidden MQ modes is achieved indirectly in the two-dimensional experiments exploiting the fact that different orders of coherences respond differently to the external magnetic field. The development of the MQ coherences is a dynamic process that proceeds pair by pair, requiring in each instance a finite time for propagation which is inversely proportional to the strength of DDI [1]. In general, the increase of the MQ excitation time τ results in the increase of the observable MQ coherence order, since more distant spins contribute to the correlated network. However, this is not the case for a spin chains in which the coupling presents only between nearest neighbors (nn). The number of spins involved in the network grows with extending MQ preparation time but the MQ coherence intensity is shared only between 0 and +/– 2 order in oscillatory manner with increasing time τ. Such behavior predicted theoretically is well supported by the experiments on ^{19}F in quasi-one-dimensional linear spin chains of fluorapatite, $Ca_5(PO_4)_3F$ [2, 3]. Nuclear spins are attractive as a model of qubits owing to good isolation from the environment and wide opportunities to manipulate spin system by radiofrequency electromagnetic fields. Though the actual addressing to individual spins in chains is lacking, the many-spin correlations present in MQ NMR experiments provide an exemplary model of multi-qubit cluster behavior.

More interesting and more sophisticated example of the spin chain is the zig-zag configuration. The protons in hambergite, Be_2BO_3OH, are example of such chain [4]. The chains along c-axis of the crystal lie in parallel planes. The angle between the vector connecting two nn protons and the c-axis of the crystal is approximately equal to 16.7°. Depending on the orientation in the external magnetic field, the chain can be considered as homogenous, with equal dipolar constants among all pairs of the nn spins, or inhomogeneous, where the dipolar coupling among nn alternates between two values for successive spin pairs. The unit cells of fluorapatite and hambergite are comparable in size but the latter contains 4 times as many protons [4]. This implies that the DDI between protons
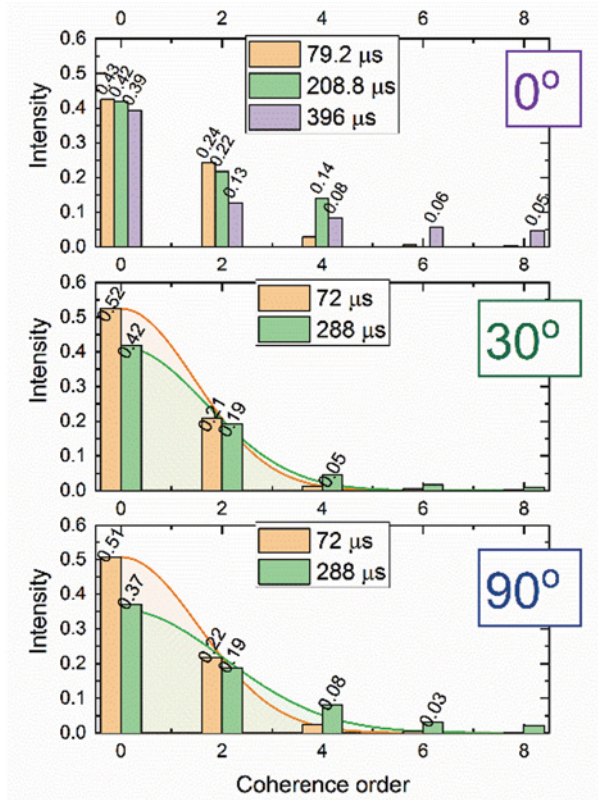
Fig. 1. ^{1}H MQ NMR spectra of hambergite at different orientations in the magnetic field. Different colors of bars correspond to different times τ.

in hambergite is much more intense. The possible drawback is the increased influence of the high order corrections to the average Hamiltonian of MQ pulse sequence [2]. The zig-zag arrangement also results in stronger interactions between next nearest neighbors (nnn) in the chain compared to linear case. In the present study we perform ^{1}H MQ NMR experiments on hambergite single crystals at different orientations in the magnetic field to compare the MQ dynamics with fluorapatite which is known to be a good model of one-dimensional spin chain. Three different orientations of the crystal in the field were chosen. The orientations were chosen to provide almost homogeneous chains. The MQ spectra are demonstrated in Fig. 1. The appearance of the coherences beyond the order two shows non-ideal behavior (compared to chain with nn DDI). In the case of 0° orientation the DDI is maximal and the non-ideal behavior is due to the high order corrections at longer times as well as nnn and interchain interactions at long times τ. For the orientations 30° and 90° the nn interactions are approximately the same and less than interaction in chain at 0° by a factor of 1.6. The "leakage" of the intensity towards high coherence order is less pronounced which can be ascribed to the smaller high order corrections to the

average Hamiltonian. The larger high order coherence intensities observed for 90° are due to the larger interchain interactions. The MQ dynamics in the spin chain can be described by the dimensionless parameter $D\tau$. Our results suggest that the dynamics of spin chains in hambergite can be described by a model of isolated spin chains with nn interactions up to relatively long times $D\tau \approx 5$–7.

1. Munowitz M., Pines A.: Science **233** (4763), 525–531 (1986)
2. Doronin S.I., Vasil'ev S.G., Samoilenko A.A. et al.: JETP Lett. **101**, 613–617 (2015)
3. Bochkin G.A., Fel'dman E.B., Lazarev I.D., Samoilenko A.A., Vasil'ev S.G.: Journal of Magnetic Resonance **301**, 10–18 (2019)
4. Bochkin G.A., Fel'dman E.B., Kuznetsova E.I., Lazarev I.D., Vasil'ev S.G., Volkov V.I.: Journal of Magnetic Resonance **319**, 106816 (2020)

Edge Electronic States in Nanostructured Graphene Oxide Derivatives: ESR, CESR and Magnetic Susceptibility Studies

A. M. Ziatdinov

Institute of Chemistry, Far Eastern Branch of the RAS, Vladivostok 690022, Russian Federation,
ziatdinov@ich.dvo.ru

Experimental finding of essentially novel properties of the electrons of π-states localized on the zigzag edges of honeycomb carbon structures [1, 2] motivated scientists to search of the methods for transferring them to the macroscopic level for subsequent use in the functional materials. One of the promising way for solving considered problem is shaping the edges of nanosized honeycomb carbon structures (nanographenes or few-layer nanographenes), which are already the elements of spatially extended structure (in particular, of percolation network in the nanostructured carbon materials), to predominantly zigzag form. Obviously, the beginning of the works in this direction should be preceded by search and investigations of carbon materials containing such structures. The principal results of our investigations in this direction are presented in this report.

In graphene oxide (GO) and its thermally reduced derivatives (rGO) the presence of various structures of nanoscale π-conjugated regions of the carbon framework, including their electrically connected percolation clusters, has been proven with the different structural methods of investigation [3]. For the case of the presence of distinguishable resonance signals from conduction electrons and from localized electrons in the EPR spectrum of such a phase rGO, the density of electronic states at the Fermi level $D(\varepsilon_F)$ of the sample can be estimated from comparing the intensities of these signals. Integrated intensities of the resonances on mobile (I_e) and localized (I_s) electrons, with their g-factors having the same value equal to 2, are, respectively, defined as:

$$I_e = C_1 \cdot \mu_B^2 \cdot D(\varepsilon_F) \tag{1a}$$

$$\text{and } I_S = C_2 \cdot \mu_B^2 \cdot N_s/k_B T , \tag{1b}$$

where μ_B is the Bohr magneton, k_B is the Boltzmann constant, values of the coefficients C_1 and C_2 depend on the experiment geometry, temperature, resonator Q-factor and other factors. In our experiments $C_1 = C_2$ as far as both considered resonances are observed in the same experimental conditions. Taking this into account, from (1a) and (1b) it follows:

$$D(\varepsilon_F) = (I_e/I_s) \cdot (N_s/k_B T) . \tag{2}$$

The estimations of $D(\varepsilon_F)$ using the expression (2) for nanostructured phases of rGO show that in them it exceeds the value of the corresponding parameter in macroscopic ordered graphite by certain orders (under these estimations we
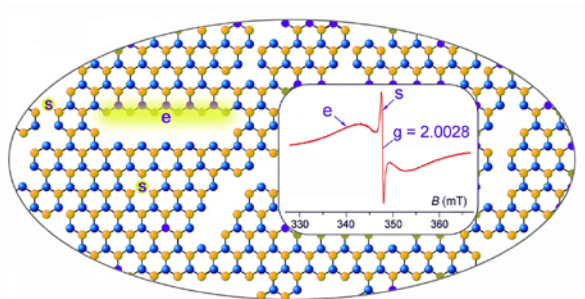
Fig. 1. The schematic images of nanofragmented carbon framework of rGO film. Letters "s" and "e" designate the localized electrons (spins) and mobile electrons of π-states stabilized on one of the zigzag edges of carbon network cracks (on the nanographene edge), respectively.

used the values of I_e and I_s determined from the EPR spectrum of studied film at 110 °C (Fig. 1, inset) and N_s value found from magnetic susceptibility measurements of a corresponding film at low temperatures). The values of $D(\varepsilon_F)$ found in this way are typical for the flat nanoscale honeycomb carbon structures with a large fraction of the zigzag edges. It has been shown that the reason for that may be the presence of π-electronic states stabilized near the zigzag regions of the carbon network cracks (near the zigzag edges of nanographenes).The conclusion has been drawn on the potential suitability of nanostructured derivatives of GO for the formation of percolation networks of nanographenes with predominantly zigzag edges in them and solving the problem of transferring peculiar quantum properties of electrons of the edge π-states to the macroscopic level.

1. Magda G., Jin X., Hagymasi I. *et al.*: Nature **514**, 608 (2014)
2. Kinikar A., Sai T.P., Bhattacharyya S. *et al.*: Nature Nanotech. **12**, 564 (2017)
3. Ziatdinov A.M.: Mat. Today: Proceedings **5**, 26183 (2019)

Optically Detected Mmagnetic Resonance of Chirality Sorted and Partially Oriented Single-Walled Carbon Nanotubes

I. Sudakov[1], E. Goovaerts[2], W. E. Wenseleers[2], J. L. Blackburn[3], J. G. Duque[4], S. Cambré[2]

[1] Chemistry Dep., University of Antwerp, 2610 Antwerp, Belgium
[2] Physics Dep., Univ. of Antwerp, 2610 Antwerp, Belgium, Etienne.Goovaerts@uantwerp.be
[3] National Renewable Energy Laboratory, Golden, Colorado 80401, United States
[4] Los Alamos National Laboratory, Los Alamos, New Mexico 87544, United States

The unique optical and electronic properties of single-walled carbon nanotubes (SWCNTs), which depend critically on their specific structure, have found many promising applications in optoelectronics [1]. Coulomb bound electron-hole pairs (excitons) are created under illumination, with a binding energy considerably higher (~400 meV) than the thermal energy at room temperature. While the singlet states have been studied in detail, less is known about the dark triplet excitons, while they may have a large impact in (opto)electronic applications. Optically detected magnetic resonance (ODMR) is the method of choice for characterization of such triplet excitons [2].

Here, we report the characterization by optically detected magnetic resonance (ODMR) of triplet excitons in pure-chirality samples of (6,5) and (7,5) SWCNTs. The zero-field splitting (ZFS) could be accurately derived from spectra of randomly oriented nanotubes (Fig. 1) as well as from drop cast samples with preferential in-plane orientation. In each of the chiralities two types of triplet excitons appear, both with axial symmetry but very different localization as derived from the magnitude of the ZFS. Finally, dependence on chirality of the SWCNTs and on changes in local environment of the SWCNTs will be discussed.

1. Jariwala D. *et al.*: Chem. Soc. Rev. **42**, 2824 (2013)
2. Stich D. *et al.*: Nature Phot. **8**, 139 (2014); Negyedi M. *et al.*: Rev. Sci. Instr. **88**, 13902 (2017); J. Palotás *et al.*: ACS Nano **14**, 11254 (2020)
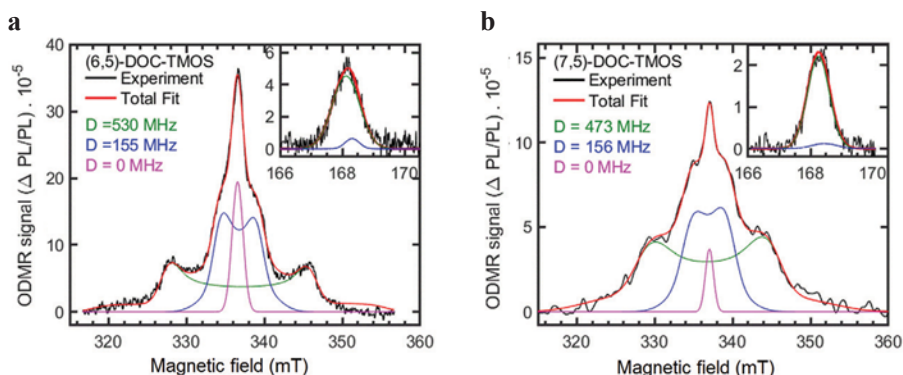
Fig. 1. ODMR spectra of (**a**) (6,5) and (**b**) (7,5) DOC-TMOS samples (T = 3.5 K, 561 nm and 635 nm excitation, resp.). Insets show the "half-field" transitions. Simulations (red) include three axial species with indicated *D*-values.

FMR of Pd-Fe Alloy Films with Inhomogeneous Composition Profiles

A. I. Gumarov[1,2], I. V. Yanilkin[1], I. A. Golovchanskiy[3], B. F. Gabbasov[1], R. V. Yusupov[1], R. I. Khaibullin[2], L. R. Tagirov[1,2]

[1] Institute of Physics, Kazan Federal University, Kazan 420008, Russian Federation, amir@gumarov.ru
[2] Zavoisky Physical-Technical Institute, FRC Kazan Scientific Center of RAS, Kazan 420029, Russian Federation
[3] National University of Science and Technology MISIS, Moscow 119049, Russian Federation

We have shown earlier that ion implantation of iron into epitaxial palladium films results in non-uniform magnetic structures across the film thickness [1]. Magnetic resonance studies revealed the emergence of several resonance lines (from 1 to 3 depending on the implantation dose), which we associated with a multiphase magnetic system (by spinodal decomposition) [1]. The proposed phases are isostructural sub-layers having different concentrations of iron impurities. The presence of several resonance lines can be explained by (i) resonance from non-interacting phases [2], (ii) coupled oscillation modes of phases [3], or (iii) manifestation of spin-wave resonance [4].

In this work, we aim to verify the third, spin-wave hypothesis of the resonance lines observed in [1]. For this, we synthesized model samples of epitaxial films of the Pd-Fe alloy with a given profile of the magnetic impurity distribution: (1) two films, 60 nm, and 120 nm thick, with a constant gradient of iron impurity concentration across the film thickness in the range from 2 to 9 at.%; (2) a trilayer heterostructure of the Pd-Fe alloy, each layer 20 nm thick with a fixed concentration of the magnetic impurity amounted to 2, 4, and 8 at.%. The first series of samples was a model for implanted samples without phase separation. The second series, on the contrary, simulated the presence of phase separation into three stable phases [1].

The results of FMR studies have shown that for samples with a constant gradient of the iron concentration, the number of resonance lines is determined by the film thickness (Fig. 1, solid blue and dash-dot red lines). In this case, the magnitude of the resonant field of signals linearly depends on the serial number n of the resonance (see the inset to Fig. 1). This indicates the spin-wave nature of the observed resonances. Resonances with a serial number $n > 0$ are, in fact, a manifestation of standing spin waves excited by a microwave field in an inhomogeneous ferromagnetic film [6, 7].

In the trilayer heterostructure with a stepped profile of iron distribution over the thickness, we also observed three resonances (dashed black line in Fig. 1). However: (1) the position of the resonance signals in the spectrum of the three-layer heterostructure differs from the position of the corresponding three modes of spin-wave resonances in the 60 nm thick Pd-Fe with a constant gradient of Fe impurity; 2) there is a nonlinear dependence of the magnitude of the resonance field on the serial number of the mode (see the inset to Fig. 1); 3) the positions
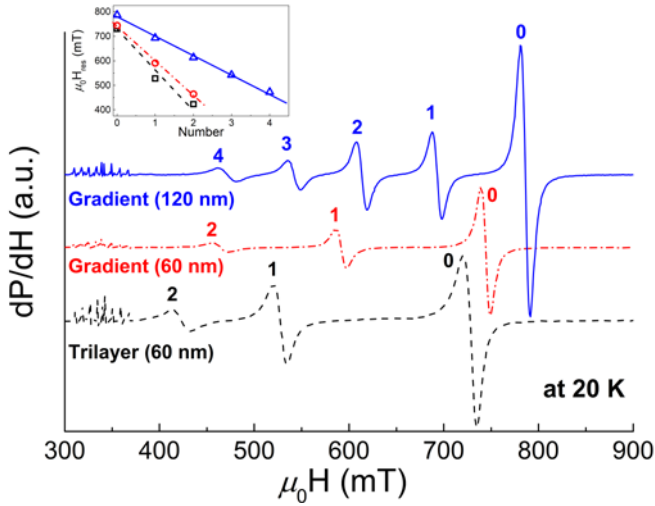
of the resonance lines of the model trilayer sample and the iron-implanted Pd film implanted with iron with the maximum dose almost coincide (compare with the data in Table S2 from [1]).

It follows from our FMR data that several spin-wave resonances are observed in the synthesized films with an iron concentration gradient, the number of which depends on the film thickness. At the same time, a quantitative coincidence with the experimental data for iron-implanted palladium films votes in favor of a stepped profile of the iron concentration distribution, which may confirm the hypothesis of spinodal decomposition in the implanted palladium films [1]. To lean towards one of the possible interpretations, additional samples will be synthesized, and magnetometry and magnetic resonance measurements carried out.

1. Gumarov A.I. *et al.*: Mater. Lett. **305**, 130783 (2021)
2. Esmaeili A. *et al.*: Sci. China. Matter. **64**, 1246 (2021)
3. Heinrich B., Bland J.A.C. (eds.): Ultrathin Magnetic Structures II. Measurement Techniques and Novel Magnetic Properties, Springer-Verlag Berlin Heidelberg 2005, 361 p.
4. Demokritov S.O., Slavin A.N. (eds.): Magnonics: From Fundamentals to Applications. Springer-Verlag Berlin Heidelberg 2013, 266 p.
5. Esmaeili A. *et al.*: Thin Solid Films. **669**, 338 (2019)
6. Rappoport T.G. *et al.*: Phys. Rev B **69**, 125213 (2004)
7. Portis A.M.: Appl. Phys. Lett. **2**, 69 (1963)

Spin-Wave and Classical Modeling of Diluted Magnetic Composite

K. Tsiberkin, E. Kovycheva, A. Sosunov, R. Ponomarev, V. Henner

Theoretical Physics Department, Perm State University, Perm, 614990, Russian Federation,
kbtsiberkin@psu.ru

We present a complex study of diluted magnetic composite (DMC) consisting of magnetic ions embedded into the dia- or paramagnetic lattice. The bulk atoms may interact each other and with the impurity by the dipole interaction; in addition, the RKKY coupling exist if the bulk lattice is a conductor. Our experiments show that functionalization of carbon nanocages and layered structures by H, N and F permits to synthesize materials with the properties of narrow-gap semiconductor. The experiments by our group allow to assume that such materials can be manipulated by the magnetic or electric field in further development [1–4]. Our theoretical research considers the magnetic response, magnetization waves and direct numerical spin simulations to find the reliable ways to synthesize such DMC [5–9].

The localized magnetic waves are well-established in ferromagnetic materials be and also may be realized in weak-coupled systems. We developed two continuous medium models of magnetization wave which can be applicable for the pure paramagnetic [5] and DMC [6, 7]. The Heisenberg equations for spin deviation operators can be averaged using the continuous medium approach. It leads to the equations analogous to the Landau–Lifshitz–Hilbert equations for the transversal magnetization which possible solutions are the magnetic traveling waves or localized solitons; their characteristic velocity is about of 10^{-3} nm/s and the wavelength is of order 10–100 nm. Such small velocity is because of weak RKKY and/or dipole coupling. The equation structure also allows another kinds of solutions related with the parametric instabilities.

The dynamics equations can also be considered within a spin-wave framework. Using the Fourier transform and linearizing the model, we obtain the dispersion relation for long magnetization waves. It has two branches corresponding the precession of the bulk and admixture ions. The transversal magnetic susceptibility and the free induction decay (FID) curve can be evaluated analytically using these dispersion law. It gives the universal $t^{-3/2}$ decay law at long times in the absence of spin wave relaxation mechanism. We assume that it occurs from the spin decoherence.

The direct numerical simulations are based on semi-classical spin dynamics as well as Schrödinger equation solution. It permits to model the magnetic resonance effects in the DMC. The numerical simulations of a classical spin system and the direct solution of the Schrödinger equation for a finite system of spins reveal a qualitative similarity of these two pictures. Nevertheless, there are some significant differences. The quantum problem is linear, therefore, the temporal spectrum of oscillations of any matrix element is finite (though large)

and discrete. The classical problem is nonlinear, and the spectrum of any observable quantity is typically either discrete with infinite number of frequencies (quasiperiodic motion) or continuous (chaotic motion), depending on the initial condition [8–10].

In addition, we consider the time evolution of magnetization of a single ion with large gyromagnetic ratio when it is placed into paramagnetic lattice taking into account the averaged dipolar interaction between them. We found from classical spin simulation that the precession of the dopant ion shows the long-time evolution is determined by the spin-spin interaction. The total spectrum of the system with single dopant ion includes a number of additional harmonics caused by mixing of the bulk lattice and dopant Larmor frequencies. Physically, such a spectrum originates due to non-linear interaction terms in the Hamiltonian.

1. Zhao R., Jayasingha R., Sherehiy A., Dharmasena R., Akhtar M., Jasinski J.B., Wu S.-Y., Henner V., Sumanasekera G.U.: J. Phys. Chem C **119**, 20150 (2015)
2. Zhao Afaneh T., Dharmasena R., Jasinski J., Sumanasekera G., Henner V.: Physica B Condens. Matter **490**, 21 (2016)
3. Rudakov G.A., Tsiberkin K.B., Ponomarev R.S., Henner V.K., Ziolkowska D.A., Jasinski J.B., Sumanasekera G.: J. Magn. Magn. Mat. **427**, 34 (2019)
4. Sosunov A.V., Ziolkowska D.A., Ponomarev R.S., Henner V.K., Karki B., Smith N., Sumanasekera G., Jasinski J.B.: New J. Chem. **43**, 12892 (2019)
5. Tsiberkin K.B.: J. Exp. Theor. Phys. **127**, 1059 (2018)
6. Tsiberkin K.B.: J. Magn. Magn. Mat. **523**, 167596 (2021)
7. Tsiberkin K.B.: Appl. Magn. Reson. (2021) in press
8. Henner V.K., Klots A., Belozerova T.S.: Eur. Phys. J. B **89**, 264 (2016)
9. Tsiberkin K.B., Belozerova T.S., Henner V.K.: Eur. Phys. J. B **92**, 140 (2019)
10. Henner V., Klots A., Nepomnyashchy A., Belozerova T.: Appl. Magn. Reson. (2021) in press

Electron Spin Resonance in a Strongly Correlated 2D Systems

A. R. Khisameeva[1], A. V. Shchepetilnikov[1], I. V. Kukushkin[1]

[1] Institute of Solid State Physics RAS, Chernogolovka 142432, Moscow district, Russian Federation

A detailed study of the spin resonance of two dimensional conduction electrons was performed on two different semiconductor heterostructures – narrow AlAs quantum wells and ZnO/MgZnO heterojunctions. In such 2DES a unique situation of strong electron-electron interaction occurs in the QHE regime when the cyclotron energy is small compared to the energy of the Coulomb interaction due to large effective masses of two-dimensional electrons. We used transport measurements as the main experimental method. In the QHE regime the longitudinal magnetoresistance of the two-dimensional channel R_{xx} is extremely sensitive to the absorption of microwave radiation.

Although it was commonly accepted that the ground state of the system should be paramagnetic at high electron concentrations, our main and the most surprising result was the observation of the ESR at the exact even filling factors [1]. Moreover, the ESR amplitude was comparable for even and odd filling factors. Such an anomalous ESR was observed at even filling factors both in AlAs quantum wells and in the ZnO/MgZnO heterojunction. It is worth noting that ESR splits into two well-resolved peaks near even filling factors in case of AlAs quantum wells. The obtained nontrivial results could be explained in terms of mixing of Landau levels with different numbers and spin projections caused by strong electron-electron interaction.

Furthermore, the detailed study revealed that such strong e-e interaction modifies not only the spin polarization of the ground state of the electronic system, but also the spin dynamics near odd filling factors in the case of narrow AlAs QW [2]. The spin relaxation was estimated from the analysis of the spin resonance linewidth in the regime of the quantum Hall ferromagnet. The measured spin dynamics is shown to undergo a radical modification in tilted magnetic fields. Increasing of the tilt angle resulted not only in the decrease of the relaxation time at the exact odd fillings by almost an order of magnitude, but also in the essentially different dependence of the relaxation rate on the filling factor ν at highest tilt angles. For perpendicular magnetic field, the relaxation rate reached its minimal value near the exact odd filling factor and slowly increased when the filling factor was altered. In contrast, at large tilt angles relaxation turned out to be the fastest at some ν in the close vicinity of the exactly odd numbers. The dependence of observed effects on electron density indicates the influence of the e-e interaction on the spin excitation spectra.

1. Shchepetilnikov A.V., Khisameeva A.R., Nefyodov Yu.A., Kukushkin I.V.: Phys. Rev. B **104**, 075437 (2021)
2. Shchepetilnikov A.V., Khisameeva A.R., Nefyodov Yu.A., Kukushkin I.V.: Phys. Rev. B **103**, 195313 (2021)

SECTION 7

ELECTRON SPIN-BASED METHODS
FOR ELECTRONIC AND SPATIAL STRUCTURE
DETERMINATION IN PHYSICS, CHEMISTRY
AND BIOLOGY

Vibronic Spins in Singlet Fissions

Y. Kobori[1,2]

[1] Molecular Photoscience Research Center, Kobe University, 1-1 Rokkodai-cho, Nada-ku, Kobe 657-8501, Japan
[2] Department of Chemistry, Graduate School of Science, Kobe University, 1-1 Rokkodai-cho, Nada-ku, Kobe 657-8501, Japan, ykobori@kitty.kobe-u.ac.jp

Singlet fission (SF) is expected to exceed the Shockley-Queisser theoretical limit with power conversion efficiencies (PCE) $\approx$ 33% of single junction organic solar cells because two separated triplet excitons (T+T) can be produced from one excited singlet state (S_1S_0) sharing its excitation energy with a neighboring ground-state chromophore. The intramolecular SF dynamics have widely been studied using the transient absorption spectroscopic methods together with theoretical modeling taking into account the vibronic effects in the ultrafast regimes.

The correlated triplet pair ^{1}(TT) with the singlet character is known to be converted to quintet state as ^{5}(TT) by the transient EPR method [1–3]. The above singlet and quintet TT pairs would separate into individual triplets as the T+T state. Because exchange coupling in TT is anticipated to be strong but dependent of T_AT_B conformation, it is expected that the specific molecular motions or phonon modes may play roles for the spin conversion and the ultimate T+T decoupling, as the vibronic effects. We present a theoretical tool to analyze electron spin polarization of the intramolecular multiexcitons of the quintet state and of the weakly coupled T+T state within a framework of the electron spin polarization transfer based upon the stochastic-Liouville equations [3, 4]. We have successfully interpreted the transient EPR spectra of the several multiexcitons observed for linked dimers and clarified that terahertz conformational motions play a role on generating the quintet state and the T+T state [4–6].

1. Sakai H., Nagashima H., Kobori Y. *et al.*: J. Phys. Chem. Lett. **9**, 3354–3360 (2018)
2. Saegusa T., Nagashima H., Kobori Y. *et al.*: J. Am. Chem. Soc. **141**, 14720–14727 (2019)
3. Matsuda S., Oyama S., Kobori Y.: Chem. Sci. **11**, 2934–2942 (2020)
4. Kobori Y., Fuki M. *et al.*: J. Phys. Chem. B **124**, 9411–9419 (2020)
5. Nakamura S., Fuki M., Kobori Y. *et al.*: J. Phys. Chem. Lett. 6457–6463 (2021)
6. Nakamura S., Fuki M., Kobori Y. *et al.*: J. Phys. Chem. C **125**, 18287–18296 (2021)

Radiospectroscopy of Non-Kramers Tb^{3+} Ions in Yttrium Aluminum Garnet

N. G. Romanov, R. A. Babunts, H. R. Asatryan

Ioffe Institute, Saint Petersburg, Russian Federation, nikolai.romanov@mail.ioffe.ru

The electronic structure of non-Kramers Tb^{3+} centers in single crystals of yttrium aluminum garnet (YAG) crystals was studied using a new-generation high-frequency magnetic resonance spectrometer that allows measurements of electron paramagnetic resonance (EPR), electron spin echo (ESE), the photon echo on hyperfine components of Stark levels in zero magnetic field, and optically detected magnetic resonance (ODMR). The results of cw EPR and ESE measurements at frequencies of 94 and 130 GHz will be presented, as well as a discussion of the effect of antisite defects in the YAG lattice on paramagnetic centers.

In YAG crystals containing terbium and cerium impurities, along with the main EPR signals of Tb^{3+} and Ce^{3+} ions located in the dodecahedral sites of the YAG lattice in a regular environment, EPR lines with a lower (several percent) intensity were observed that also belong to terbium and cerium centers with similar symmetry, but are characterized by slightly altered parameters – the initial level splitting for non-Kramers Tb^{3+} ions and g-factors for Ce^{3+} ions. It is shown that the nature of such centers and their number can be explained by the presence of Y_{Al} antisite defects, i.e. yttrium ions in the octahedral aluminum positions, in the environment of Tb^{3+} or Ce^{3+}.

In YAG crystals co-doped with Tb^{3+} and Ce^{3+}, ODMR of Tb^{3+} was observed via photoluminescence of Ce^{3+}. This result seems to be important, since these systems are of interest for quantum communication and computations.

Spatiotemporal Resolution of Conformational Changes in Biomolecules by Combining Pulsed Electron-Electron Double Resonance Spectroscopy with Microsecond Freeze-Hyperquenching

T. Hett[1], T. Zbik[2], S. Mukherjee[2], H. Matsuoka[1], W. Bönigk[2], D. Klose[3], Ch. Roullion[2], N. Brenner[2], S. Peuker[2], R. Klement[4], H.-J. Steinhoff[3], H. Grubmüller[4], R. Seifert[2], U. B. Kaupp[2], O. Schiemann[1]

[1] Institute of Physical and Theoretical Chemistry, University of Bonn, Wegelerstraße 12, Bonn 53115, Germany; schiemann@pc.uni-bonn.de
[2] Center of Advanced European Studies and Research (caesar), Ludwig-Erhard-Allee 2, Bonn 53175, Germany
[3] Fachbereich Physik, Universität Osnabrück, Barbarastraße 7, Osnabrück 49076, Germany
[4] Department of Theoretical and Computational Biophysics, Max Planck Institute for Biophysical Chemistry, Am Fassberg 11, Göttingen 37077, Germany

The function of proteins is linked to the structure and the conformational changes that they can undergo. X-ray crystallography and cryo electron microscopy are powerful methods for resolving protein structures at the atomic level. However, only a few methods like e.g., NMR or single molecule Förster Resonance Energy Transfer can provide the temporal order of intermediates and conformational changes, with each having its limitations.

In the talk, a new method will be presented that combines pulsed electron–electron double resonance spectroscopy (PELDOR or DEER) with a microsecond freeze-hyperquenching (MHQ) setup for achieving spatiotemporal resolution. Its capabilities will be shown on example of the ligand-induced conformational dynamics of the bacterial cyclic nucleotide-gated (CNG) K+ channel from Mesorhizobium loti (MloK1). This channel opens by binding of cyclic adenosine monophosphate (cAMP) to a cyclic nucleotide-binding domain (CNBD). Upon binding, the CNBD undergoes a conformational change, including a movement of the C-terminal Cα-helix. This movement has been inferred from X-ray and NMR structures of the CNBD in its apo and holo states and has also been predicted by atomistic simulations. With MHQ-PELDOR, this conformational change can be shown to occure within about 150 μs and can be resolved with angstrom precision. In addition, placing spin labels at different sites in the CNBD can provide a 4D picture of a conformational change with amino-acid resolution.

EPR-Spectroscopy of Monoisotopic ^{53}Cr^{3+} Ions in Orthosilicates Y$_2$SiO$_5$ and Sc$_2$SiO$_5$

V. Tarasov[1], K. Konov[1], R. Likerov[1], A. Sukhanov[1], A. Shestakov[1], I. Yatsyk[1], R. Eremina[1], Yu. Zavartsev[2], A. Kutovoy[2]

[1] Zavoisky Physical-Technical Institute, FRC Kazan Scientific Center of RAS, Kazan 420029, Russian Federation, tarasov@kfti.knc.ru
[2] Laser Materials and Technology Research Center, Prokhorov General Physics Institute of RAS, Moscow 119991, Russian Federation

Dielectric crystals doped with odd isotopes of transition ions are intensively studied since they are considered as promising materials for various quantum devices. For example, paramagnetic centers formed by rare-earth impurity ions in Y$_2$SiO$_5$ single crystals are regarded as the basis for optic quantum memory. We suppose that trivalent ions of Cr-53 isotope in Y$_2$SiO$_5$ and Sc$_2$SiO$_5$ crystals may be used for implementation of microwave quantum memory in superconducting quantum computers.

In this work methods of continuous wave and pulse EPR spectroscopy in the X-band were used to study Y$_2$SiO$_4$ and Sc$_2$SiO$_4$ single crystals doped with ^{53}Cr monoisotopic ions. The magnetic characteristics of paramagnetic centers formed by chromium ions replacing yttrium ions are determined. It is shown that the probabilities of allowed and forbidden transitions between hyperfine components of electron levels strongly depend on the orientation of the external magnetic field. In a certain range of magnetic field orientation, the probability of forbidden transitions with a change in the projection of the nuclear spin on the quantization axis is comparable with the probability of allowed transitions that occur without changing the projection of the nuclear spin.

The temperature dependences of spin-lattice and phase relaxation times of ^{53}Cr^{3+} ion in the Y$_2$^{28}SiO$_5$ single crystal are measured at the level anti-crossing point in the temperature range from 5 to 80 K. The effect of spin dynamical decoupling on the phase relaxation time is meaured using the Curr–Parcell–Meiboom–Gill (CPMG) multi-pulse sequence. Special features of hyper fine structure of the EPR spectra at the level anti-crossing are discussed.

Relaxation Mechanisms of Intrinsic Paramagnetic Centers VO^{2+}/FR in Heavy Oil Asphaltenes Combined with HYSCORE and DNP Measurements

F. Murzakhanov, D. Shurtakova, A. Alexandrov, A. Tajik, A. Vakhin, M. Gafurov, G. Mamin

Kazan Federal University, Kremlevskaya str. 18, Kazan 420008, Russian Federation,
murzakhanov.fadis@yandex.ru

Asphaltene constituents of petroleum affect all aspects of crude oil production and utilization. Undesirable asphaltene precipitation is a serious concern to the petroleum industry because asphaltenes can block catalyst active sites, plug up well bores and stop oil production, in addition to blocking pipelines [1, 2]. A fundamental condition for the development of effective processes for heavy oil production and processing is the understanding of the key factors that determine the aggregative behaviour and stability of oil disperse systems (ODS), behavior and chemical transformations of their components under various external conditions including elevated temperature [3, 4]. Therefore, the complex analytical study of each kind of ODS is in need both for the fundamental research and practical applications. A significant factor influencing the asphaltene aggregation and precipitation is their local environment, which determines the nature of intermolecular interactions of asphaltenes with other ODS components. It is evident that prediction of crude oil stability and solubility of asphaltenes under specified conditions requires the fundamental knowledge of the character of
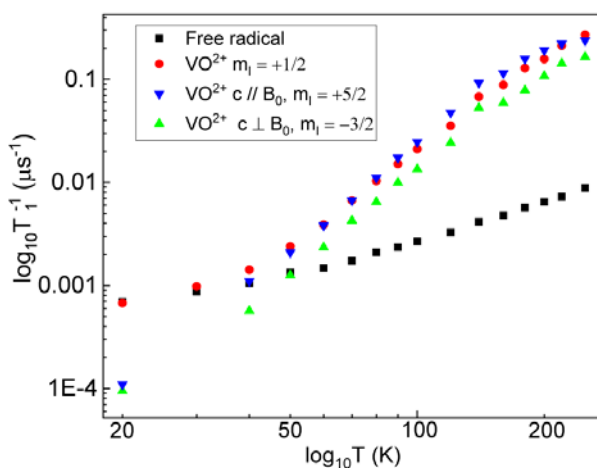
Fig. 1. T_1 temperature dependencies of VO^{2+} and FR centers.

intermolecular interactions between asphaltenes and other heavy oil components present in the local environment [5]. In this work, by investigating the mechanisms of electronic relaxation in a wide temperature range, as well as using the HYSCORE, ENDOR, DNP we aimed to expand the capabilities of magnetic resonance spectroscopy for analyzing the structural features of asphaltenes.

Asphaltenes and initial oil (bitumen) samples from Ashalchinskoe (Russia), Boca-Haruko (Cuba) and Athabasca (Canada) oilfields were studied by pulse EPR. The EPR spectra for all samples contain typical signals from the vanadium complexes (VO^{2+}) and carbon-centered organic free radical (FR). The full parameters of the spin Hamiltonian (the anisotropic hyperfine interaction constant A and the axial g-factor) were determined for each paramagnetic center. The temperature dependences of the relaxation times for VO^{2+} and FR were measured from the 297 K to 20 K in increments of 10 K. The analysis of the dependence curves revealed that paramagnetic centers have different mechanisms of spin-lattice (longitudinal) relaxation (Fig. 1). Additionally, it was found for the VO^{2+} center, the relaxation processes depend on the orientation of the complex in the magnetic field B_0.

HYSCORE was used to study weak electron-nuclear interactions. The 2D Fourier transform allowed to determine the types of surrounding nuclei ^1H, ^{14}N, ^{51}V (the second coordination sphere) and the values of their hyperfine and quadrupole interaction. Orientation-selective experiments were carried out for the VO^{2+} center to determine the anisotropic contributions to the value of the hyperfine coupling constant. The difference in the HYSCORE spectra for VO^{2+} and FR assume a various ionic environment. In the following experiments, under external influence (thermal or chemical treatment) on oil-containing materials, the paramagnetic centers VO^{2+} and FR will serve as two independent spin labels. The analysis of the spectroscopic values and relaxation can provide additional information about the structural changes of oil disperse systems [6].

DNP measurements at X-band at room temperature in initial oil samples reveal the both Overhauser-driven (OE) and solid-state (SE) DNP for FR and VO^{2+} [7]. It is found that the type, value, and relative contribution of OE/SE DNP depend on the oil origin and asphaltenes treatment.

1. Trukhan S.N., Kazarian S.G., Martyanov O.N.: Energy Fuels **31** (2017)
2. Ganeeva Yu.M., Yusupova T.N., Romanov G.V.: Russ. Chem. Rev. **80** (2011)
3. Gawel I., Bociarska D., Biskupski P.: Appl. Catal. A **295** (2005)
4. Shukla A.K.: Analytical Characterization Methods for Crude Oil and Related Products, pp. 101–124. JohnWiley & Sons Ltd, Hoboken, NJ 2018.
5. Martyanov O.N., Larichev Y.V., Morozov E.V., Trukhan S.N., Kazarian S.G.: Russ. Chem. Rev. **86** (2017)
6. Djimasbe R., Varfolomeev M.A. *et al.*: ACS Omega **6** (2021)
7. Gizatullin B., Gafurov M., Murzakhanov F., Vakhin A., Mattea C., Stapf S.: Langmuir 37 (2021)

EPR Studies of the Symmetry Lowering in the Cubic Phase of Strontium Titanate

R. V. Yusupov[1], B. F. Gabbasov[1], I. N. Gracheva[1], A. A. Rodionov[1], S. I. Nikitin[1], D. G. Zverev[1], A. G. Kiiamov[1], D. G. Zverev[1], A. Dejneka[2], V. A. Trepakov[3]

[1] Institute of Physics, Kazan Federal University, 420008 Kazan, Russian Federation,
Roman.Yusupov@kpfu.ru
[2] Institute of Physics, ASCR, v.v.i. 18221 Prague, Czech Republic
[3] Ioffe Physical-Technical Institute, RAS, St. Petersburg 194021, Russian Federation

Strontium titanate $SrTiO_3$ (STO) is a model representative of the family of highly polarizable ABO_3 perovskite-like oxides. At $T_c \sim 105$ K, STO undergoes a Pm3m $\rightarrow$ I4/mcm phase transition from the cubic to the antiferrodistorsive (AFD) tetragonal phase. For many decades, strontium titanate has been the subject of numerous academic studies, exhibiting a large number of effects under various external perturbations, doping, and various applications, in particular, being one of the most popular substrates for epitaxial thin films and heterostructures.

We report on the detection and study by the electron paramagnetic resonance (EPR) spectroscopy of impurity Mn^{4+} and Fe^{3+} ions of the previously unknown phenomenon of symmetry lowering in the temperature range generally associated with the cubic STO phase, in samples prepared in the form of rectangular parallelepipeds of the millimeter size (0.1–5 mm) [1–4]. EPR spectroscopy is a very sensitive experimental method, capable to detect and follow very small structural distortions of matrix crystals that are manifested in the structure and orientation dependences of the spectra of impurity centers serving as the probes. Thus, namely the studies of the EPR spectra of the impurity centers had first revealed the transition of STO to the AFD phase [1, 2], and the nature and temperature dependences of structural distortions in the tetragonal phase and its symmetry were determined [3, 4].

We found that already at room temperature the crystal structure of oriented millimeter samples of a certain geometry and size ratio with a shape of rectangular prisms (in particular, square (001)- or (110)-oriented plates with a thickness $h \sim 0.5$ mm and edge $a \gg h$) obtained from high-quality single crystals (Furuuchi Chemical Corp., Tokyo, Japan) has a tetragonal symmetry, different in structure from the AFD phase. The deformation magnitude depends on the quality of the sample surfaces, whose morphology was controlled by atomic force microscopy and was represented by two roughness values: ~150 nm and ~2 nm.

If the roughness of large platelet faces of STO: Fe^{3+} is identical, the deformation of the structure is practically uniform over the volume, with the possible exception of a thin near-surface layers, which unambiguously follows from the small inhomogeneous width of the fine structure components of the EPR spectrum and the investigated angular dependences. For a given identical faces roughness, a decrease in the thickness of the samples leads to an increase in the observed deformation, and the axial distortion is proportional to

the value $(1 - a/h)$ [5]. Thus, for samples in the form of a cube $(a = h)$ with faces perpendicular to the <100> directions, the cubic symmetry characteristic of STO at $T > 105$ K is retained. For plates with orientations (001) and (110), the structure is tetragonally distorted, and for {111}-oriented plates the structure always remains cubic, regardless of the surface roughness. In the experiments, during which the height of the samples h changed, the coexistence of the cubic and tetragonal phases manifested itself with a transition to the dominating of the latter on approaching the shape of a thin plate.

We find that the observed effect is not related to the residual stress, but rather is triggered by a combination of geometry, orientation, and surface quality of the samples. We argue that most likely the source of the observed symmetry lowering is the latent geometry-dependent structural instability of millimeter samples, due to the specific compliance of STO to tetragonal deformation with the possibility of exposing the corresponding metastable phase. In this case, a certain contribution to the effect is made by the interaction with the surface. The electric field effect in the EPR spectra of Mn^{4+} and Fe^{3+} ions has a quadratic character [6], which indicates the presence of an inversion center in the discovered tetragonal structure of millimeter STO samples.

1. Müller K.A.: Helv. Phys. Acta **31**, 173 (1958)
2. Unoki H., Sakudo T.: J. Phys. Soc. Japan **23**, 546 (1967)
3. Müller K.A., Berlinger W., Waldner F.: Phys. Rev. Lett. **21**, 814 (1968)
4. Müller K.A., Berlinger W., Capizzi M., Gränicher H.: Solid State Commun. **8**, 549 (1970)
5. Gabbasov B.F., Gracheva I.N., Rodionov A.A., Kiiamov A.G., Nikitin S.I., Zverev D.G., Trepakov V.A., Dejneka A., Jastrabik L., Yusupov R.V.: EPL **133**, 37002 (2021).
6. Gabbasov B.F., Rodionov A.A., Nikitin S.I., Trepakov V.A., Yusupov R.V.: Physics of the Solid State **63**, 248 (2021)

Molecular Organization of the Swelled Graphite Oxide and the Graphite Oxide Membranes According to Spin Probe Data

N. A. Chumakova[1,2], A. T. Rebrikova[2], A. Kh. Vorobiev[2], M. V. Korobov[2], T. S. Yankova[2], M. V. Matveev[2], A. V. Kaplin[2], D. A. Astvatsaturov[1,2], D. S. Popov[2]

[1] N. N. Semenov Federal Research Center for Chemical Physics, Russian Academy of Science, Kosygin St. 4, Moscow 119991, Russian Federation, harmonic2011@yandex.ru
[2] M. V. Lomonosov Moscow State University, Chemistry Department, Leninskiye Gory 1/3, Moscow 119991, Russian Federation

Graphite oxide (GO) is a layered material formed by graphene parallel planes decorated with oxygen-containing groups (–OH, –O–, –CO, –COOH, etc.) Swelling of GO in polar liquids is accompanied by intercalation of the liquids into the inter-plane space and increasing of the inter-plane distances from 6–7 Å to ~20–25 Å. Membranes formed by GO possess highly selective permeability. It was established that dry GO membrane can be easily penetrated by water and hydrated ions with radii less than 4.5 Å but they are practically not penetrative by other liquids and even gases. The cause of this unique behavior is still not clear. The hypothesis was proposed that the membrane permeability is connected with the molecular mobility of the intercalated water in the interplane spaces of GO [1]. The permeability can also depend on the orientational alignment of the membrane-forming layers. At present, the study of the GO materials is largely hindered by a lack of suitable experimental techniques. The adaptation of the widely used spin probe method for the investigation of the molecular organization of swelled GO and GO membranes is the aim of the present work.

EPR spectra of nitroxide spin probes in the systems "GO–polar liquid" include the signals of the nitroxides with high and slow rotational mobility (rotational correlation times come to $\sim 10^{-9}$ s and $\sim 10^{-7}$ s correspondently). The first signal was attributed to the spin probes located in the liquid, the second one to the radicals sorbed on the inner surface of GO. For the systems "BGO (Brodie synthetized graphite oxide) – polar liquid" it was shown that rotational mobility of the sorbed radicals changes considerably during the phase transformation. EPR spectra demonstrate that the transformation proceeds within a temperature range of ~30°. We suppose that this range reflects some inhomogeneity of the material [2].

The rotational mobility of the probes located in the intercalated liquid (water, acetonitrile, methanol) was found to be just a little slowed down compared to the rotation in the bulk liquid. This observation indicates that the intercalated liquid form the liquid-like medium between the graphene planes. The existence of a mobile liquid (water, acetonitrile, trifluoroethanol) in the inter-plane space of GO was confirmed reliably by NMR spectroscopy [3]. It was revealed that the spin probe method is more sensitive to a small amount of unfrozen liquid intercalated into GO than NMR spectroscopy.
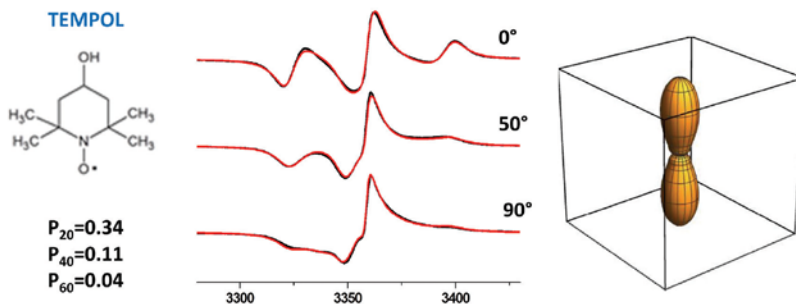
Fig. 1. The result of simulation of the EPR spectra angular dependence, orientational order parameters, and orientation distribution function of spin probe TEMPOL in GO membrane (thickness 50 μm, fabricated by vacuum filtration). Black lines – experimental spectra, red lines – result of simulation.

The spin probe method was found to be a unique technique for quantitative estimation of the layer ordering in the graphite oxide membranes. Until now, the alignment of the GO membranes was estimated only qualitatively (visually) by cross-sectional SEM and TEM. We propose to characterize the ordering of the membranes by orientation distribution of the spin probes sorbed on inner surface of GO (Fig. 1). It was shown that nitroxide radicals as well as paramagnetic complexes $[Cu(NH_3)_4]^{2+}$ adequately reflect the alignment of the membranes.

1. Joshi R.K. *et al.*: Science **343**, 752 (2014)
2. Chumakova N.A. *et al.*: Journal of Physical Chemistry C **122**, 22750 (2018)
3. Chumakova N.A. *et al.*: Physical Chemistry Chemical Physics **22**, 19969 (2020)

EPR of Crystalline $Pb_{1-x-y}Cu_xGdyS$ Semiconductor Alloy: Unusual Dependence of Resonant Lines Shapes on Microwave Power and Possible Reasons of the Effect

<u>V. A. Ulanov</u>[1,2], R. R. Zainullin[1], T. A. H. Housheya[1], I. V. Yatsyk[2]

[1] Kazan State Power Engineering University, Kazan 420066, Russian Federation,
ulvlad@inbox.ru
[2] Zavoisky Physical-Technical Institute, FRC Kazan Scientific Center of RAS, Kazan 420029,
Russian Federation

The object of this study was the narrow-gap semiconductor of the lead chalcogenide group, PbS, simultaneously doped with two magnetic impurities. The main features of the semiconductor under study are a direct narrow band gap (~0.3 eV) and high mobility of free charge carriers. PbS-based materials are widely used for the manufacture of electronic, nanoelectronic and thermoelectric devices [1]. Although the semiconductor PbS has been a subject of study for a long time, until now there are little studied materials made on the basis of PbS by double doping with impurity atoms of the transition group elements and the rare-earth group elements. It is known that the presence of any impurities in PbS dramatically changes its electrical and thermoelectric properties [2]. It seemed, the presence of two types of impurity atoms with unfilled electron shells would lead to the appearance of unusual properties of the semiconductor material thus created and would allow the creation new electronic devices.
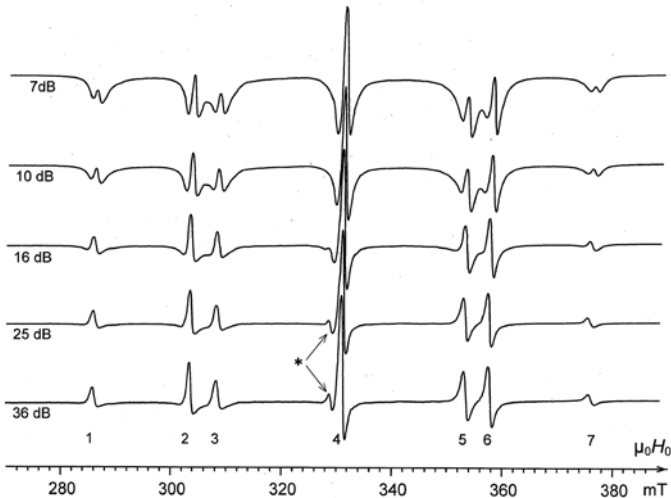
Fig. 1. EPR spectra of crystalline $Pb_{0,996}Cu_{0,0037}Gd_{0,0003}S$ semiconductor alloy at various values of microwave power (T = 4.2 K; $H_0 \parallel$ <001>; f_{EPR} = 932310 MHz)

The aim of this work was an experimental study the possibilities and results of simultaneous doping of a PbS crystal with copper and gadolinium impurities. Since at least one of these two impurity atoms is capable to form deep centers with nonzero magnetic moments in a PbS crystal, the method of electron paramagnetic resonance (EPR) was chosen as a method for studying the crystals under study. These crystals were grown by the Bridgman method in an induction type furnace. EPR spectra were recorded with "E-12 Varian" spectrometer. The most unusual results were observed in the crystalline $Pb_{0,996}Cu_{0,0037}Gd_{0,0003}S$ semiconductor alloy at $T = 4.2$ K. Fig. 1 shows the EPR spectra recorded in the $H_0 \parallel$ <001> orientation of the crystalline sample ($f_{EPR} = 932310$ MHz). In this figure, the asterisk marks the EPR line associated with electrons localized in clusters of sulfur vacancies. As it can be seen in Fig. 1, each of the EPR spectra as a whole can be represented as a superposition of two kinds of model spectra of paramagnetic centers with $S = 7/2$. Obviously, these model spectra can be associated with two groups of Gd^{3+} ions. The resonance values of the external magnetic field of the corresponding lines of these two spectra practically coincide each with other for any orientation of the crystal sample relative to the direction of the external magnetic field. The angular dependences of the positions of the lines of these two spectra correspond to the cubic symmetry of the crystal field acting at the positions of the gadolinium ions.

But, the resonant lines of one of the model spectra have the shapes of an inverted bell, while the lines of the second model spectra have Dysonian shapes. In addition, in the range of microwave power variation indicated in the figure, the intensities of lines with the Dyson shape change a little, while the intensities of the lines with the shape of an inverted bell decrease very quickly with decreasing power. The shape parameters of the observed lines and their dependences on the power were found.

It should be noted that the shapes of the lines, referred to here as "inverted bell", is very unusual for the EPR method. Obviously, these unusual shapes and their unusual dependencies on microwave power are associated with dinamical processes that have not yet been studied and, therefore, required careful study.

1. Mukherjee D.Li, Gautam A., Shi Z.: Transworld Research Network **37/661**, 88 (2010)
2. Pei Y.-L., Liu Y.: Journal of Alloys and Compounds **514**, 40 (2012)

SECTION 8

MAGNETIC RESONANCE INSTRUMENTATION

Multi-Extreme THz ESR: Current Status and Future

**H. Ohta[1,2], S. Okubo[1,2], E. Ohmichi[2], T. Sakurai[3], H. Takahashi[1,2],
S. Hara[3], M. Akaki[1]**

[1] Molecular Photoscience Research Center, Kobe University, Japan, hohta@kobe-u.ac.jp
[2] Graduate School of Science, Kobe University, Japan
[3] Research Facility Center for Science and Technology, Kobe University, Japan

We have developed the multi-extreme THz ESR, which can cover the frequency region between 0.03 and 7 THz [1], the temperature region between 1.8 and 300 K [1], the pulsed magnetic field region up to 55 T [1], and the pressure region up to 1.5 GPa [2] simultaneously.

Another direction of multi-extreme THz ESR is the developments of the high-sensitive force-detected ESR. We were able to observe ESR up to 1.1 THz using the micro-cantilever [3]. Then we extended our developments to the torque magnetometry [4] and ESR [5] measurements using a commercially available membrane-type surface stress sensor, and it is applied to the microliter solution sample (myoglobin) [6]. Recently we have achieved the sensitivity of 1012 spins/G at 0.154 THz and room temperature for the membrane ESR using the high power gyrotron at Fukui University and the static magnetic field [7].

Moreover we have developed the hybrid-type pressure cell, and achieved 2.5 GPa [8]. Using this pressure cell for our high-pressure THz ESR using the static magnetic field up to 10 T, we have discovered the first-order pressure-induced transition at 1.85 GPa in the Shastry-Sutherland Model Compound $SrCu_2(BO_3)_2$ [9], and extended its high pressure ESR system up to static 25 T in collaboration with the high field user facility in IMR, Tohoku University [10]. The high-pressure THz ESR up to 25 T is applied to Cs_2CuCl_4 in order to determine the pressure dependence of exchange interactions related to the new magnetic phases revealed under pressure [11]. Recently we have developed a new system which enables the simultaneous observations of the THz ESR and the pressure, and applied to the Co Tutton's salt under the static magnetic field [12].

Our multi-extreme THz ESR and other related topics on THz ESR are summarized in the special issue "Terahertz Spectroscopy" of Appl. Mag. Res. [13].

1. Ohta H. *et al.*: J. Low Temp. Phys. **170**, 511 (2013)
2. Sakurai T. *et al.*: Rev. Sci. Inst. **78**, 065107 (2007); Sakurai T.: J. Phys.: Conf. Series **215**, 012184 (2010)
3. Ohta H. *et al.*: AIP Conf. Proceedings **850**, 1643 (2006); Ohmichi E. *et al.*: Rev. Sci. Instrum. **79**, 103903 (2008); Ohmichi E. *et al.*: Rev. Sci. Instrum. **80**, 013904 (2009); Ohta H., Ohmichi E.: Appl. Mag. Res. **37**, 881 (2010); Ohmichi E. *et al.*, J. Mag. Res. **227**, 9 (2013); Ohmichi E. *et al.*: Rev. Sci. Instrum. **87**, 073904 (2016); Ohmichi E. *et al.*: J. Inorganic Biochemistry **62**, 160 (2016) (Invited paper); Takahashi H., Ohmichi E., Ohta H.: Appl. Phys. Lett. **107**, 182405 (2015)
4. Takahashi H. *et al.*: J. Phys. Soc. Jpn. **86**, 063002 (2017) (Editor's Choice)
5. Takahashi H. *et al.*: Rev. Sci. Intrum. **89**, 036108 (2018)
6. Okamoto T. *et al.*: Appl. Phys. Lett. 2018, **113**, 223702 (2018) (Editors Picks)

7. Takahashi H. *et al.*: Appl. Phys. Lett. **118**, 022407 (2021)
8. Fujimoto K. *et al.*: Appl. Mag. Res. **44**, 893 (2013); Sakurai T. *et al.*: J. Mag. Res. **259**, 108 (2015); J. Mag. Res. **280**, 3 (2017) (Invited review); Ohta H. *et al.*: J. Phys. Chem. B **119**,13755 (2015) (Invited paper)
9. Sakurai T. *et al.*: J. Phys. Soc. Jpn. **87**, 033701 (2018)
10. Sakurai T. *et al.*: J. Mag. Res. **296**, 1–4 (2018)
11. Zvyagin S.A. *et al.*: Nature Communications **10**, 1064 (2019)
12. Submitted to Appl. Mag. Res. 2021, Special Issue " Klaus Möbius and Kev Salikhov: On the Occasion of Their 85th Birthdays".
13. Ohta H., Sakai T., eds.: Appl. Mag. Res. 2021, **52**(4), 263-564, Special Issue "Terahertz Spectroscopy".

Simultaneous Mapping of the Partial Pressure of Oxygen and pH Using Electron Paramagnetic Resonance

H. Hirata

Division of Bioengineering and Bioinformatics, Hokkaido University, Sapporo 060-0814, Japan, hhirata@ist.hokudai.ac.jp

This talk presents the concept and the experimental results of simultaneous mapping of the partial pressure of oxygen (pO_2) and pH. The reason to develop this simultaneous mapping method is related to the importance of visualizing the physiological status of solid tumors. Low-oxygen supply in tumor tissue (hypoxia) and acidification in extracellular space (acidosis) are hallmarks of malignant tumors. These conditions often show resistance to chemotherapy and radiation therapy and lead to tumor growth and metastasis. Therefore, both quantities are crucial to understanding the pathophysiological status of solid tumors. EPR and other modalities can individually visualize pO_2 and extracellular pH. However, the measurements at different time points may show the different conditions for solid tumors, such as cycling hypoxia [1]. Thus, simultaneous mapping of pO_2 and pH is desired to minimize the difference in the conditions for mapping them [2]. The deuterated monophosphonated trityl radical p_1TAM-D was used in this simultaneous measurement (p_1TAM-D was synthesized and kindly provided by Dr. B. Driesschaert, West Virginia University, USA) [3]. Simultaneous mapping of solution samples was conducted with a home-built 750-MHz CW-EPR imager. Four-dimensional spectral-spatial imaging was applied to EPR signals from p_1TAM-D in solution samples with various conditions [4, 5]. In summary, this work demonstrated the feasibility of simultaneous mapping of pO_2 and pH using EPR and p_1TAM-D [6].

1. Matsumoto S. *et al.*: Cancer Res. **70**, 10019 (2010)
2. Gorodetskii A.A. *et al.*: Sci. Rep. **9**, 12093 (2019)
3. Dhimitruka I. *et al.*: J. Am. Chem. Soc. **135**, 5904 (2013)
4. Komarov D.A., Hirata H.: J. Magn. Reson. **281**, 44 (2017)
5. Komarov D.A. *et al.*: Anal. Chem. **90**, 13938 (2018)
6. Taguchi A. *et al.*: Analyst **145**, 3236 (2020)

In situ MW Heating: Design Considerations
of a Dual Mode X-band EPR Resonator

<u>E. Richards</u>[1], A. Folli[1], G. Magri[1], M. Barter[2], J. Harari[2], H. Choi[2], D. Slocombe[2], D. M. Murphy[1], A. Porch[2]

[1] EPR/ ENDOR Research Group, School of Chemistry, Cardiff University,
Cardiff CF10 3AT, UK, richardse10@cardiff.ac.uk
[2] Centre for High Frequency Engineering, School of Engineering, Cardiff University,
Cardiff CF24 3AA, UK

Most EPR detection methods, in particular at X-band frequencies, involve the use of resonant cavities where the MW magnetic component is used for spin excitation. Here we show that dual mode MW resonant cavities, using ca. 9.5 GHz frequency for EPR detection and ca. 6.1 GHz frequency for sample perturbation [1], can be used to induce rapid in-situ heating which offers new and exciting opportunities for sample interrogation and method development that are not possible with ordinary single mode resonant cavities. The 6.1 GHz MW electric field can be used to induce volumetric heating of a solution via electric dipole absorption, in theory via short MW pulses resulting in rapid T-jumps which can populate non-equilibrium reactive intermediate states for the study of reaction kinetics. The 9.5 GHz MW magnetic field simultaneously detects EPR spectra of the sampled paramagnetic species. Furthermore, this dual-mode design offers the possibility of using EPR resonators as MW reactors, thus accelerating reaction times during EPR detection enabling interrogation of molecular dynamics (as well as spin exchange phenomena) over much faster time frames when compared to conventional heating methods. This is exemplified here by probing heating effects on 16-DSE labelled SDS micelles, a model $Cu(acac)_2$ complex and activation of organic molecules to generate reactive radicals [2].

1. Slocombe D., Folli A., Choi H., Barter M., Harari J., Richards E., Murphy D.M., Porch A.: AMPERE Newsletter **102**, 1–8 (2020)
2. Folli A., Choi H., Barter M., Harari J., Richards E., Slocombe D., Porch A., Murphy D.M.: J. Magn. Reson. **310**, 106644 (2020).
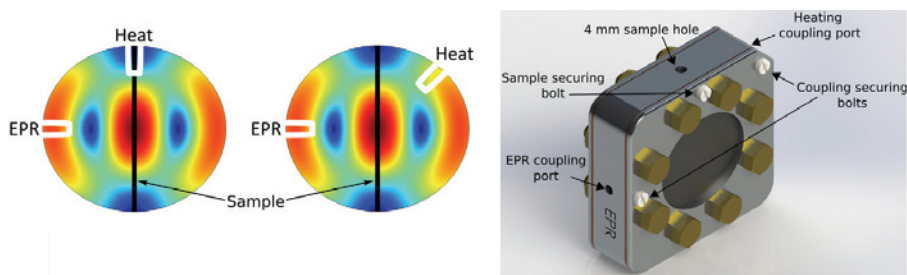
Fig. 1. Dual mode EPR resonator.

ENDOR with ESR Micro-Resonators

<u>A. Blank,</u> Y. Artzi, N. Dayan[1]

[1] Schulich faculty of chemistry, Technion – Israel Institute of Technology, Haifa 32000, Israel,
ab359@technion.ac.il

ESR micro-resonators are a class or resonators that enable to measure small amounts of paramagnetic samples with high signal-to-noise-ratio (SNR) [1–2]. While being around for several years, their scope of practical applications was limited, mainly due to their low concentration sensitivity. Here we introduce a possible new application of ESR micro-resonators that makes use of their small size to facilitate their combination with micro ENDOR coils. This enables to deliver very large B_2 (RF magnetic fields) to the sample, thus enabling to obtain ENDOR data for paramagnetic species with short ESR T_1. The new setup also supports the implementation of novel ENDOR sequences for efficiently exciting and detecting wide bandwidth of nuclear spins.

1. Dayan N., Ishay Y., Artzi Y., Cristea D., Reijerse E., Kuppusamy P., Blank A.: Review of Scientific Instruments **89**, 124707 (2018)
2. Dayan N., Ishay Y., Artzi Y., Cristea D., Driesschaert B., Blank A.: Journal of Magnetic Resonance Open, 100005 (2020)

Magnetic Properties of Colloidal Core-Shell CdSe/(Cd,Mn)S Nanoplatelets Studied by High-Frequency EPR, ENDOR

R. A. Babunts[1], Yu. A. Uspenskaya[1], N. G. Romanov[1], S. B. Orlinskii[2], G. V. Mamin[2], E. V. Shornikova[4], S. Shendre[3], S. Delikanli[3], H. V. Demir[3], P. G. Baranov[1], D. R. Yakovlev[1,4], M. Bayer[1,4]

[1] Ioffe Institute, St. Petersburg 194021, Russian Federation
[2] Kazan Federal University, Institute of Physics, 420008 Kazan, Russian Federation
[3] Department of Physics, Bilkent University, Ankara 06800, Turkey
[4] Experimental Physics 2, TU Dortmund University, Dortmund 44221, Germany

Nanoplatelets (NPLs) based on II-VI compounds are a new class of colloidal nanocrystals with a thickness of several monolayers. Mn doping of semiconductor nanoplatelets (NPLs) imparts new magneto-optical properties to these structures (see, for example, [1] and references therein). In this study, NPLs with a CdSe core and Mn doped CdS or (Cd,Zn)S shells were investigated by high-frequency EPR in continuous wave (CW) and pulsed (electron spin echo, ESE) modes.
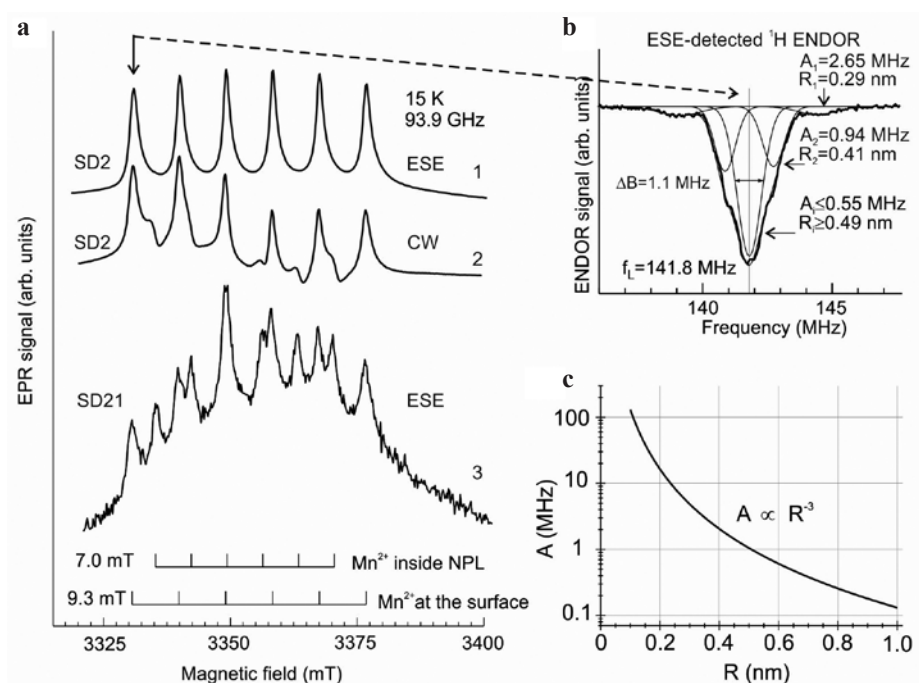
Fig. 1. a 93.9 GHz ESE-detected EPR spectra, recorded at 15 K in CdSe/(Cd,Mn)S NPLs sample SD2 (2/5 monolayers, 1% Mn) (1) and CdSe/(Cd,Zn,Mn)S NPLs sample SD21 (2/5 monolayers, 5% Mn) (3). The spectrum (2) was measured in CW mode (SD2). **b** ESE-detected ENDOR spectrum measured in a magnetic field corresponding to EPR of Mn^{2+} ions at the surface of NPLs, sample SD2. f_L is the Larmor frequency. **c** Hydrogen HF structure dependence on R between Mn^{2+} and ^1H nucleus.

Application of the ESE-detected electron nuclear double resonance (ENDOR) of Mn^{2+} ions allowed identification of ligands at the surface of NPLs.

Core-shell colloidal NPLs consisted of 2 monolayer (ml) CdSe core and 2 to 5 ml (Cd,Mn)S or (Cd,Zn,Mn)S shells with a nominal Mn^{2+} content of 1 to 5% were studied. EPR was measured at 94 GHz in a wide temperature range (1.5 to 300 K) using the high-frequency EPR-ODMR spectrometer developed in the Ioffe Institute and a Bruker E680 EPR spectrometer. It was shown that Mn^{2+} ions occupy positions both inside the shell and at the surface of NPLs, and are both in the form of single Mn^{2+} ions and complexes of interacting Mn^{2+} ions. These complexes are responsible for a large EPR line observed below 5 K. The individual Mn^{2+} ions inside the shell and at the surface differ in the hyperfine interaction constants – ca. 7 and 9.3 mT, respectively.

For Mn^{2+} at the surface ENDOR signals were found at the Larmor frequency of the ^{1}H nucleus (see Fig. 1b). The observed structure is due to hyperfine (dipole-dipole in this case) interactions between the electron and nuclear magnetic moments that depends on the distance R between Mn^{2+} and ^{1}H nucleus (Fig. 1c) and allows estimating these distances as being ca. 0.29 nm, 0.41 nm and > 0.49 nm.

1. Shornikova E.V., Yakovlev D.R., Tolmachev D.O. *et al.*: ACS Nano **14**, 9032 (2020)

Rapid Scan EPR Imaging

O. Tseytlin[1], A. Bobko[1], R. O'Connell[1], M. Tseytlin[1]

[1] Department of Biochemistry, West Virginia University, Morgantown WV, 26506, USA;
oxana.tseytlin@hsc.wvu.edu

Applications of rapid scan EPR imaging (RS EPRI) will be reported, including mapping of the magnetic field and photopolymerizations process. The latter project was recently initiated with the goal to address some of the challenges of 3D (bio) printing, such as visualization of the distribution and kinetics of oxygen during and after the printing process. Proof-of-principle imaging experiments demonstrate spatial propagation of the photopolymerization process, oxygen depletion as a result of post-curing, oxygen visualization in a 3D printed models manufactured by stereolithography and/or direct extrusion method. A lithium octa-n-butoxynaphthalocyanine (LiNc-BuO) probe was used as EPR oxygen reporter. Benefits of EPR application to bioprinting and tissue engineering are discussed.

SECTION 9

THEORY OF MAGNETIC RESONANCE

Static and Dynamic Vector Models in EPR of Anisotropic Centers

A. G. Maryasov[1], M. K. Bowman[1,2]

[1] Novosibirsk Institute of Organic Chemistry of the Siberian Branch of the Russian Academy of Sciences, 630090 Novosibirsk, Russian Federation, maryasov@nioch.nsc.ru
[2] Department of Chemistry & Biochemistry, The University of Alabama, Tuscaloosa, AL 35487, USA, mkbowman@ua.edu

Vector models in magnetic resonance are widely used to present important characteristics of the system studied by visualization of those. The most valuable dynamic model is Bloch type equation of magnetic moment motion in magnetic field which provides exact system description for non-interacting paramagnetic centers (PCs) with spin of ½. Reduction of a problem to such a model, even being approximate, provides intuitively clear description of system in question. Static vector models are also of importance, in some cases introduction of properly chosen quantization axes for electron and nuclei spins may solve system Hamiltonian thus giving a simple way to get analytical description with deep understanding of the system basic features. Rather useful quantities to analyze spin-spin coupling, either electron-electron or electron-nuclear, are effective spin vectors, si, which are mean values of electron spin vector $\mathbf{S}$ in i-th eigenstate of PC, ψ_i, $\mathbf{s_i} = \langle\psi_i|\mathbf{S}|\psi_i\rangle$. These quantities are useful in the case of high spin PCs with $S \geq 1$.

Here we consider both static and dynamic vector models for PCs with anisotropic spin Hamiltonians. PCs with effective spins of ½ having strong g-matrix anisotropy are analyzed, dynamics of their magnetic moments are described as compared to isotropic PCs behavior on the basement of generalized Bloch equations. Electron-electron dipole interaction and hyperfine interaction of high spin PCs are considered using effective spin vectors. Description is relevant for PELDOR/DEER and RIDME techniques in the case of electron-electron interactions, and either for cw-EPR or ESE EM techniques in the case of hfi.

Shift of the NMR Line Caused by the Interaction of Nuclei with Triplet Excitons

I. I. Geru

Academy of Sciences of Moldova, Exact and Engineering Section, Blvd Stefan cel Mare si Sfant 1, Chisinau MD-2001, Republic of Moldova, iongeru11@gmail.com

At high levels of optical excitation of semiconductor crystals, the generated electrons and holes in the main are bound into exitons. Under these conditions, the contribution of free charge carriers to the shift of the NMR line is negligible in comparison with the contribution of excitons [1].

In the representation of secondary quantization, the hyperfine interaction between nuclei and triplet excitons is considered. It is taken into account that the periodical parts of the electron Bloch wave function $U_{k,e}(0)$ and of the hole Bloch wave function $U_{k,h}(0)$ at location of the nucleus can be approximately considered independent of the wave vector [2]. We assume that the Bose-Einstein condensation of triplet excitons take place in the state with exciton wave vector $K = 0$ for the excitons from the lowest subband of the Zeeman triplet. In the crystal model in which the lower conduction band and the upper valence band are not orbitally degenerate, the shift of NMR line conditioned by condensed and overcondensed excitons is given by the expression

$$\Delta H = (4\pi/3)\hbar[\gamma_e|U_e(0)|^2 + \gamma_h|U_h(0)|^2]\{n_{ex}[1 - (T/T_c)^{3/2}] + m_{ex}^{3/2}\Delta_{ex}^{1/2}k_BT/\pi\hbar^3\} \ ,$$

where $\hbar$, γ_e, γ_h, m_{ex}, n_{ex}, Δ_{ex}, k_B, T_c, and T are the Planck constant, the electron gyro-magnetic ratio, the hole gyromagnetic ratio, the exciton mass, the exciton concentration, the exciton Zeeman splitting, the Boltzmann constant, the critical temperature of the exciton Bose-Einstein condensate, and the absolute temperature.

The Fig. 1 shows the temperature dependence of the resonant magnetic field for the NMR line of ^{63}Cu nuclei in a CuCl crystal, calculated for the following values of parameters: $\gamma_e = 1.76 \cdot 10^7$ Oe$^{-1} \cdot$s^{-1}, $\gamma_h = 7.3 \cdot 10^3$ Oe$^{-1} \cdot$s^{-1}, $|U_e(0)|^2 \sim 10^2$, $|U_h(0)|^2 = 0$, $m_{ex} = 20.4m_e$ (m_e is the free exciton mass), $n_{ex} = 10^{19}$ cm^{-3}, $\Delta_{ex} = 0.136$ cm^{-1}, and $T_c = 3$ K [1]. Due to the smallness of the exciton Bohr radius (7 Å) in the crystal CuCl, we used $n_{ex} = 10^{19}$ cm^{-3} (the maximum value of n_{ex} can be $4 \cdot 10^{20}$ cm^{-1} [3]). The value $|U_h(0)|^2$ is taken equal to zero because in the CuCl crystal there are no holes with s-type wave functions that could contribute to the exciton wave function. The additional magnetic field ΔH_{ex}, created by triplet excitons on nuclei, coincides in direction with the external magnetic field.

As can be seen in the plot of the temperature dependence in the Fig. 1, at temperatures below the critical temperature T_c, there is a sharp increase in the shift of the NMR line, which is due to the interaction of nuclei with triplet excitons of the Bose-Einstein condensate. The shifts of the NMR lines due to the interaction with the excitonic Bose condensate are significant not only in the case of triplet excitons. They also appear if the lowest exciton band is orbitally
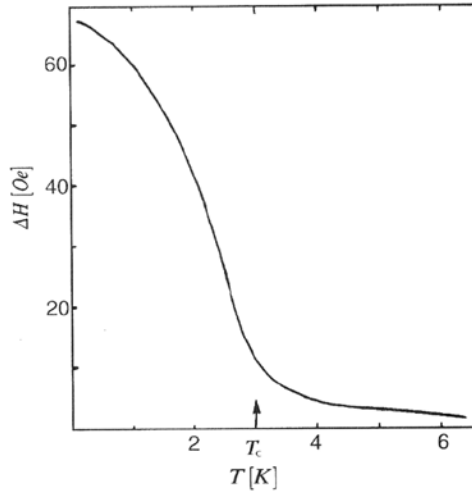
Fig. 1. Temperature dependence of the position of ^{63}Cu NMR line due to interaction of nuclei with triplet excitons in the CuCl crystal.

degenerate and the s-states of electrons (holes) contribute to the exciton wave function. The large shift of the NMR line at the interaction of nuclei with Bose condensed triplet excitons is due to the short-range nature of the contact hyperfine interaction. Shifts similar to this are also characteristic for the EPR spectrum lines in the case of a short-range exchange interaction of Bose condensed excitons with paramagnetic centers. A sharp increase in the shifts of the NMR and EPR lines due to the interaction of nuclei and paramagnetic centers with excitons at high levels of optical excitation of crystals is a criterion for the existence of a exciton Bose-Einstein condensate.

1. Geru I., Suter D.: Resonance Effects of Excitons and Electrons – Basics and Applications. Springer-Verlag, Berlin, Heidelberg, 283 pp. 2013.
2. Abragam A.: The Principles of Nuclear Magnetism. Clarendon Press, Oxford,), 614 pp. 1994.
3. Bivas A., Lévy R., Nikitine S., Grun J.B.: J. Phys. France **31** (2-3), 227–234 (1970)

Determination of the Electron Spin Relaxation Rate of Ni(II) Ions in the Crystalline Environment at 300 K

K. Amrutha, K. Velavan

Department of Applied Sciences, National Institute of Technology Goa, Ponda, 403 401, India,
amruthak@nitgoa.ac.in

Measuring the distance between sites in the biological system provides insight into some fundamental questions in molecular biology, including protein folding, dynamics, and how species cross the membrane. Electron Paramagnetic Resonance (EPR) spectroscopy is a popular method for measuring a longer distance with more precision. The knowledge of electron spin relaxation rate is essential for distance measurement by EPR spectroscopy. Ni(II) is an important trace element for living beings and is a non-Kramers ion with a d^8 electronic configuration. Due to its unusual relaxation features and large D value, the EPR transitions are usually observable in the liquid helium temperature range and also need HFEPR. Hence, the EPR property of Ni(II) ions is less understood till date.

Herein, the polycrystalline sample of Ni(II) ion magnetically diluted in Zn(4-chloropyrazole)$_6$(ClO$_4$)$_2$ [Ni/ZCPC] and Zn(pyrazole)$_6$(NO$_3$)$_2$ [Ni/ZPN] have been studied in detail by EPR spectroscopy to explore the electron spin relaxation time. The EPR signals corresponding to parallel and perpendicular orientations were monitored as a function of microwave power ranging from 0.01 to 200 mW at 300 K. The Progressive CW EPR power saturation study yielded 323
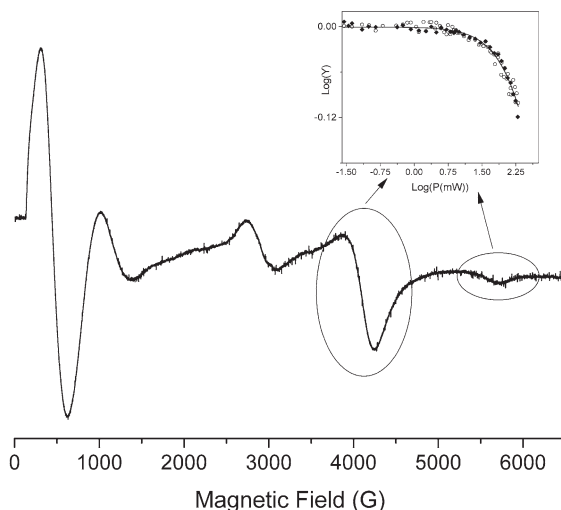
Fig. 1. CW EPR power saturation plot for Ni(II)/ZCPC at 300 K for transition corresponds to parallel orientation (○), perpendicular orientation (♦), and fit to the data (solid line); P$_{1/2}$ = 323 mW.

and 907 mW as the $P_{1/2}$ for Ni/ZCPC and Ni/ZPN, respectively. To overcome the difficulties in measuring the cavity constant (K_Q) of the resonator, a procedure has been developed to use a standard sample for measuring the product of relaxation time in the power saturation experiment. Using the tempol in polyvinyl alcohol-boric acid mixture glass [PVA-BA] as a reference sample, the product of relaxation time ($T_1 \cdot T_2$) was calculated as $3.51 \cdot 10^{-14}$ and $1.3 \cdot 10^{-14}$ s^2 for Ni/ZCPC and Ni/ZPN, respectively. The product of relaxation times for Ni/ZCPC is larger than the Ni/ZPN, indicating the ZCPC lattice is more rigid than ZPN. A significantly larger $T_1 \cdot T_2$ value even at 300 K for Ni/ZCPC and Ni/ZPN indicates that these samples can be used to measure the electron spin relaxation time of Ni(II) ions over a large temperature range to understand the relaxation mechanisms that contribute to the relaxation rate.

SECTION 10

SPIN-BASED INFORMATION PROCESSING

Quantum Magnonics

Yu. M. Bunkov

M-Granat, Russian Quantum Center, 30, B. Bulvar, Skolkovo, Moscow 121205, Russian Federation

Magnons are quasiparticles in magnetically ordered materials that describe elementary excitations of the ground state. They possess spin equal to 1 and accordingly obey Bose statistics. In thermal equilibrium, the density of magnons is not significant and their properties are well described in the linear approximation. However, the concentration of magnons can be enhanced up to a very high number by pumping them under magnetic resonance conditions. The deviation of magnetization of Yttrium Iron Garnet (YIG) up to a 3° leads to the formation of magnon Bose-Einstain condensation (mBEC) [1]. In the experiments carried out, we use out of plane magnetized epitaxial YIG film. Under these conditions, the magnons are repelled, the potential of which leads to the formation of the energy gap, and the stability of magnon supercurrent. Under these conditions, the properties of magnons are similar to their properties in the superfreight antiferromagnetic ³He-B, where mBEC and magnon superuidity were discovered for the first time [2]. The first results of our experiments with mBEC in YIG film are very promising [3–5].

We consider magnon BEC and magnon superfluidity as very promising candidates for a magnonic platform for quantum calculations. We are considering a few possible options for to form a magnonic qubit. First of all it is a qubit on the superposition of two circular magnon supercurrents. The stabilized domain boundary should change the phase of currents on π and, accordingly, form two quantum states with clockwise and counterclockwise circulation. These states should form two quantum states with a gap, similar to the case of a superconducting ring with Josephson junction. The second scheme is based on the interaction of two mBECs located in two YIG samples, which are connected by electromagnetic or acoustic interaction. The third scheme is based on composite magnon-photon qubit consisting of two or more samples with mBEC placed in high quality resonator. In this case, the interaction between mBECs can be controlled by changing the local magnetic field on each sample or selectively exciting magnons in the each of sample. And finally, the qubit can be formed by two states in the same sample under double frequency parametric pumping. In this case, the difference between states is a phase that is shifted to π. Parametric pump can support both states. The energy barrier between states determines by pump amplitude. Quantum manipulations between states can be made by RFe pulses. Adiabatic approach can be made by changing the amplitude of paramet-

ric pumping. The methods of optical reading out of qubit states, its phase and amplitude are also preview and are currently in development.

1. Bunkov Yu.M., Safonov V.L.: J. Mag. Mag. Mat. **452**, 30 (2018)
2. Bunkov Yu.M., Volovik G.E.: "Spin Superuidity and Magnon BEC" in Novel Superfluids" (eds. Bennemann & Ketterson), Oxford Univ. Press, Oxford 2013.
3. Bunkov Yu.M., Kuzmichev A.N., Safin T.R., Vetoshko P.M., Belotelov V.I., Tagirov M.S.: Scientific Reports, **11**, 7673 (2021)
4. Vetoshko P.M., Knyazev G.A., Kuzmichev A.N., Holin A.A., Belotelov V.I., Bunkov Yu.M.: JETP Lett. **112**, 299 (2020)
5. Kuzmichev A.N., Vetoshko P.M., Knyazev G.A., Belotelov V.I., Bunkov Yu.M.: JETP Lett. **112**, 710 (2020)

High Frequency Pulsed EPR/ENDOR Studies of NV⁻ Defects in Silicon Carbide

V. Soltamov[1], F. Murzakhanov[1], S. Orlinskii[1], G. Mamin[1], B. Yavkin[1], T. Biktagirov[2], U. Gerstmann[2], H. J. von Bardeleben[3]

[1] Institute of Physics, Kazan Federal University, Kazan 420008, Russian Federation, victrosoltamov@gmail.com
[2] Lehrstuhl für Theoretische Materialphysik, Universität Paderborn, Paderborn 33098, Germany, uwe.gerstmann@upb.de
[3] Sorbonne Université, Institut des Nanosciences de Paris, Paris 75005, France, vonbarde@insp.jussieu.fr

Intensive studies have been put forward to demonstrate the reliability of the approach to use optically polarized spin states of defects for quantum technologies. The most prominent results have been achieved on the negatively charged nitrogen-vacancy center (NV⁻) in diamond, stimulating a search of such kind defects in solids more technologically friendly then diamond [1]. Fairly fast, Silicon Carbide (SiC) has been recognized as a major material in this field [1, 2]. Its success is based on the special properties of the material and on the spin properties of silicon vacancies, divacancies and the more recently studied NV⁻ centers [1–3].

We have investigated the NV⁻ centers in SiC by means of 94 GHz EPR/ENDOR spectroscopy and correlated the results with ab-initio calculations [4]. Analysis of the NV⁻ ENDOR spectra allowed to determine the hyperfine interaction parameters with ^{14}N as $A_\parallel = -1.142$ MHz and $A_\perp = -1.184$ MHz. The value of the nuclear quadrupole interaction constant reflecting an interaction between the ^{14}N nuclear electric quadrupole moment with the electric field gradient was determined to be 2.44 MHz. A comparative analysis of the NV⁻ centers in SiC and in diamond shows a significant similarity of their ground state properties. The electron-nuclear parameters of the NV⁻ center in SiC can be obtained by rescaling the parameters of the NV center in diamond with the respective SiC lattice constants. These results are of significant interest in the rapidly growing field of solid-state qubits in semiconductors and to the broader condensed matter community.

1. Awschalom D., Hanson R., Wrachtrup J., Zhou B.B.: Nat. Photon. **12**, 516 (2018)
2. Soltamov V.A., Soltamova A.A., Baranov P.G., Proskuryakov I.I.: Phys. Rev. Lett. **108**, 226402 (2012)
3. von Bardeleben H.J., Cantin J.L., Rauls E., Gerstmann U.: Phys. Rev. B **92**, 064104 (2015)
4. Murzakhanov F.F., Yavkin B.V., Mamin G.V., Orlinskii S.B., von Bardeleben H.J., Biktagirov T., Gerstmann U., Soltamov V.A.: Phys. Rev. B **103**, 245203 (2021)

SECTION 11

MAGNETIC RESONANCE IMAGING

Rapid Scan EPR at L-Band

<u>G. R. Eaton</u>, L. Woodcock, G. Rinard, S. deGraw, S. S. Eaton

Department of Chemistry and Biochemistry, University of Denver, Denver, Colorado, USA 80208,
geaton@du.edu

Development of rapid scan EPR and a new image acquisition and reconstruction protocol for multiline spectra are a paradigm shift for imaging cancer and redox biology. Progress toward a benchtop rapid scan EPR imager, which will open the field of redox biology of cancer and other disease states and deliver new capability to end users, is illustrated Fig. 1. The original, 250 MHz imager occupies about 20×20 ft^2 of lab space. The new system occupies about 3×6 ft^2. The 700 MHz version of this spectrometer was reported in 2018 [1]. With new resonators and microwave sources the operation has been extended to 1 GHz. The present level of capability is illustrated by the signal to noise achieved with a 1 μM ^{15}N tempol sample in water (Fig. 2). The cross-loop resonator has 8 mm inside diameter and the sample contains ca. 1×10^{14} spins.

1. Buchanan L.A., Rinard G.A., Quine R.W., Eaton S.S., Eaton G.R.: Conc. Magn. Reson. B, Magn. Reson. Engin. **48B**, e21384, (2018).
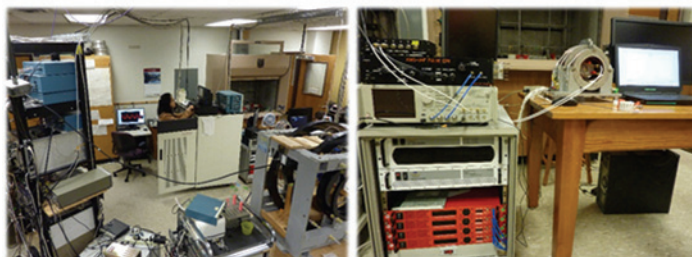
Fig. 1. 250 MHz spectrometer (left) and 1000 MHz table-top imager (right).
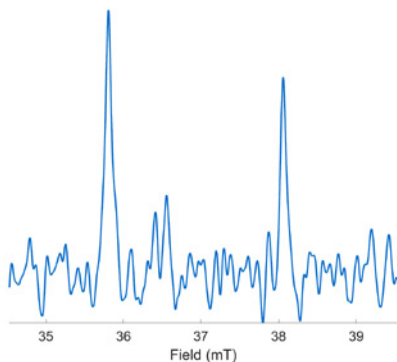
Fig. 2. Sinusoidal rapid scan spectrum of ^{15}N tempol obtained with 6.3 kHz scans, averaged for about 12 min.

Development of Methods for Early Detection of Rheumatoid Arthritis

D. Abdulganieva[1], N. Shamsutdinova[1], V. Mukhamadieva[1], Ya. Fattakhov[2], A. Fakhrutdinov[2], A. Bayazitov[2], R. Khabipov[2], V. Shagalov[2], V. Odivanov[2], A. Anikin[2]

[1] Kazan State Medical University, Kazan 420012, Russian Federation
diana_s@mail.ru
[2] Zavoisky Physical-Technical Institute, FRC Kazan Scientific Center of RAS, Kazan 420029,
Russian Federation, yfattakhov@yandex.ru

MRI in the average fields of 0.4–0.6 T has recently become widely used, due to the relative cheapness of the device and sufficiently high diagnostic capabilities. In this paper, we conducted research using a specialized MRI system with magnetic field induction of 0.4 T. Pulse sequences were used: T1-weighted images, T2-weighted images, the "fat suppression" mode.

The Clinical Guidelines "Rheumatoid arthritis", approved by the Ministry of Health of the Russian Federation, were adopted as a basis, which regulate the conduct of review radiography of the hands and feet during the initial examination to verify the diagnosis and establish the stage of the disease in all patients with RA. With acute onset and active inflammation in RA, periarticular osteoporosis and single cysts can be detected within 1 month of the disease; multiple cysts, narrowing of the articular crevices, and single erosions only 3 to 6 months after the onset of the disease. They provide detection of the disease at a later stage, since MRI of the hands is recommended only for patients with early RA or undifferentiated arthritis, in which diagnosis is difficult according to the ACR/EULAR criteria of 2010, for the detection of "subclinical " synovitis and erosive changes.

We selected patients with signs of inflammatory joint damage, with a disease duration of up to 6 months, and patients with verified rheumatoid arthritis receiving treatment. Further, a clinical examination was carried out and the indices of remission of the disease (DAS28-ESR, DAS28-CRP, SDAI, CDAI). Then the study was carried out by imaging methods: MRI of the hands and feet in high (1.5 T) and medium (0.4 T) fields [1], radiography [2].

1. The Utility of MRI for Assessing Structural Damage in Randomized Controlled Trials in Rheumatoid Arthritis. A&R, vol. 65, 2513 (2013)
2. Smirnov A.V.: Modern rheumatology, no. 4. 83 (2010)

Diagnostics and Rehabilitation of Patients with Voice Diseases

**M. Ya. Fattakhova[1], V. N. Krasnozhon[2], V. V. Fedorova[2],
R. Sh. Khabipov[1], E. S. Bekmacheva[3]**

[1] Zavoisky Physical-Technical Institute, FRC Kazan Scientific Center of RAS, Kazan 420029,
Russian Federation, mariam.fattakhova@gmail.com
[2] Kazan State Medical Academy PO, Kazan 420012, Russian Federation
[3] BarsMed LLC, Kazan 420138, Russian Federation

Functional and organic pathologies of the organs of voice formation are widespread among university professors, school teachers, vocalists, employees of enterprises with noise, chemical and dust pollution.

The paper describes the development of a method for diagnosing laryngeal pathologies using magnetic resonance imaging in high fields (3 T), stroboscopy and spectral analysis of the voice. Based on the received diagnostic information, methods of rehabilitation of patients with functional and organic pathologies of the larynx are being developed.

For the first time, a complex of modern complementary techniques was used: MRI in high fields, stroboscopy and spectral analysis of the voice for the diagnosis of functional and organic pathologies of the larynx.

With the use of magnetic resonance imaging in high fields of 3 T, studies of patients with pathologies of the larynx were carried out. This technique allows you to identify violations that lead to pain in the throat, difficulty in voice extraction. The dynamics of the larynx was also studied.

The stroboscopic technique allows you to obtain additional information: video recording of the functioning of the vocal apparatus. Spectral analysis of the voice allows you to record the patient's voice using special tests, conduct spectrum analysis, compare with the standard, identify deficiencies, and develop recommendations for the development of rehabilitation methods. The resulting database of sound samples and examination results will later be used to train the neural network to identify pathologies. Special rehabilitation programs have been developed for patients with functional and organic disorders of the larynx. At the same time, it is shown that it is possible to use the method of spectral analysis of the voice to control the dynamics of rehabilitation and adjust, if necessary, the process of rehabilitation.

SECTION 12

MODERN METHODS OF MAGNETIC RESONANCE

EPR in the Age of CryoEM: Two Recent Stories

H. S. Mchaourab

Vanderbilt University, 747 light hall 2215 Garland avenue, Nashville TN 37232, USA,
hassane.mchaourab@vanderbilt.edu

Structural and Dynamic Origins of ESR Lineshapes in Spin-Labeled GB1 Domain: the Insights from Experiments and Spin Dynamics Simulations Based on MD Trajectories

S. A. Izmailov[1], S. O. Rabdano[1], I. S. Podkorytov[1], O. O. Lebedenko[1], D. A. Luzik[1], Z. Hasanbasri[2], S. Saxena[2], <u>N. R. Skrynnikov</u>[1,3]

[1] Laboratory of Biomolecular NMR, St. Petersburg State University, St. Petersburg 199034, Russian Federation, n.skrynnikov@spbu.ru
[2] Department of Chemistry, University of Pittsburgh, Pittsburgh, PA 15260, USA
[3] Department of Chemistry, Purdue University, West Lafayette, IN 47907, USA

Site-directed spin labeling (SDSL) ESR is a valuable tool to probe protein systems that are not amenable to characterization by x-ray crystallography, NMR or EM. While general principles that govern the shape of SDSL ESR spectra are known [1], its precise relationship with protein structure and dynamics is still not fully understood. To address this problem, we designed seven variants of GB1 domain bearing R1 (MTSL) spin label and recorded the corresponding MD trajectories (net length 180 μs). The MD data were subsequently used to calculate time evolution of the relevant spin density matrix and thus predict the ESR spectra. The simulated spectra proved to be in good agreement with the experiment, suggesting that our MD-based models is a *bona fide* source of information that can be used to explore the relationship between the spectral lineshapes and the underlying structure/dynamics [2].

Subsequent analysis confirmed that the spectral shapes primarily reflect the degree of steric confinement of the R1 tag and, for the well-folded protein such as GB1, offers little information on local backbone dynamics. The rotameric preferences of R1 side chain are determined by the type of the secondary structure at the attachment site. The rotameric jumps involving dihedral angles χ_1
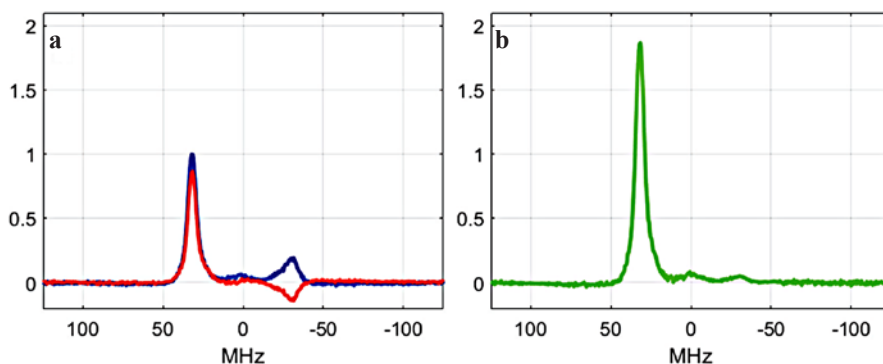
Fig. 1. a Pulse ESR spectra from the sample of GB1-(^{15}N)R1 in a form of in- and anti-phase doublets. **b** TROSY-type spectrum obtained by summation of the in- and anti-phase doublets.

and χ_2 are sufficiently fast to directly influence the ESR lineshapes. However, the jumps involving multiple dihedral angles tend to occur in (anti)correlated manner, causing smaller-than-expected movements of the R1 proxyl ring.

Of interest, ESR spectra of GB1 domain with solvent-exposed spin label can be accurately reproduced by means of Redfield theory. While broad applicability of Redfield theory to small-molecule radicals has long been established [3], here we present a comprehensive treatment involving 36×36 Redfield matrix evaluated in the operator basis for a (mobile) spin label attached to a protein molecule. In particular, we have found that the asymmetric character of the spectra is attributable to Redfield-type cross-correlations. This opens up an interesting possibility to emulate the popular NMR experiment TROSY [4] in the context of pulse ESR spectroscopy (illustrated in Fig. 1).

Finally, we have also tested the validity of our MD model of spin-labeled GB1 using paramagnetic relaxation enhancement (PRE) data [5]. For this purpose, we have measured the PRE effect in five MTSL-labeled variants of GB1 and additionally recorded MD trajectories of these constructs with the net length of 50 μs. For three constructs, the predicted PRE rates are in very good agreement with the experimental data, thus providing additional support to the MD models. On the other hand, the results from the remaining two constructs suggest that force-field parameters of the MTSL tag may need an improvement.

1. Mchaourab H.S., Lietzow M.A., Hideg K., Hubbell W.L.: Biochemistry **35**, 7692 (1996)
2. Izmailov S.A., Rabdano S.O., Hasanbasri Z., Podkorytov I.S., Saxena S., Skrynnikov N.R.: Sci. Rep. 10, 957 (2020)
3. Freed J.H., Fraenkel G.K.: J. Chem. Phys. **39**, 326 (1963)
4. Pervushin K., Riek R., Wider G., Wüthrich K.: Proc. Natl. Acad. Sci. USA **94**, 12366 (1997)
5. Gaponenko V., Howarth J.W., Columbus L., Gasmi-Seabrook G., Yuan J., Hubbell W.L., Rosevear P.R.: Protein Sci. **9**, 302 (2000)

The Role of Rotation in Diffusion NMR Experiments on Supramolecular Assemblies

B. B. Kharkov[1], I. S. Podkorytov[1], S. A. Bondarev[2], M. V. Belousov[2,3], V. A. Salikov[1], G. A. Zhouravleva[2], N. R. Skrynnikov[1,4]

[1] Laboratory of Biomolecular NMR, St. Petersburg State University, St. Petersburg 199034, Russian Federation, b.kharkov@spbu.ru
[2] Department of Genetics and Biotechnology, St. Petersburg State University, St. Petersburg 199034, Russian Federation
[3] Laboratory for Proteomics of Supra-Organismal Systems, ARRIAM, St. Petersburg 196608, Russian Federation
[4] Department of Chemistry, Purdue University, West Lafayette, IN 47907, USA

Pulsed-field gradient NMR is an important tool to measure diffusion of proteins and protein assemblies and thus obtain insight into their structure and dynamics. For extended objects, such as amyloid fibrils, these experiments become difficult to interpret because in addition to translational diffusion they are also sensitive to rotational diffusion. We have constructed a mathematical theory describing the outcome of PFG NMR experiments on rod-like fibrils. The analytical results proved to be in excellent agreement with the predictions from our random walk Monte-Carlo simulations. The effect of rotational diffusion is indeed significant, accounting for up to 30% of the diffusion-induced signal loss. However, just
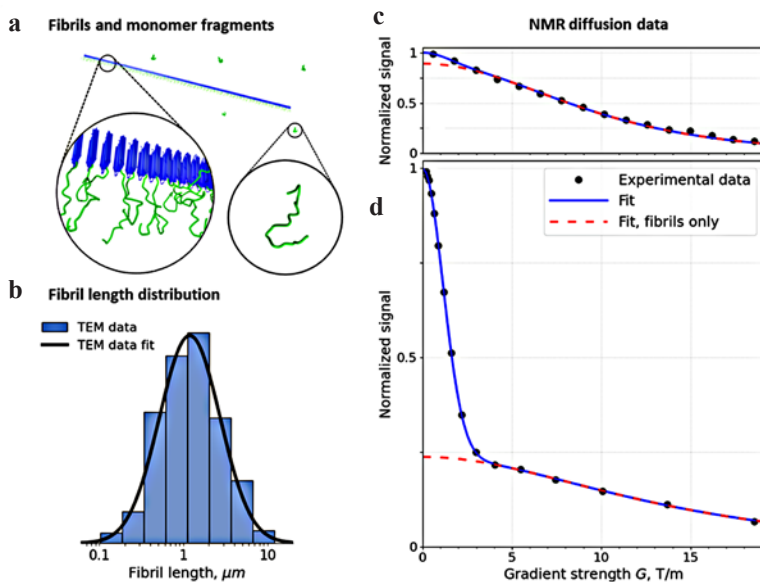
Fig. 1. a Fibrils and proteolytic fragments coexist in Sup35NM sample. **b** Fibril length distribution as obtained from TEM images. **c** Data from STE measurements on the sample of Sup35NM fibrils fitted by means of the new theory. **d** Data from STE measurements on another sample of Sup35NM fibrils spiked with recombinant Sup35M.

like translational diffusion, rotational diffusion of heavy fibril particles is a slow process and registers as such in the PFG NMR experiments. Contrary to certain literature claims, this allows one to separate spectral signals from fibrils and other species that may be present in the sample (monomers, proteolytic fragments, etc.) based on their different diffusion properties.

To test the validity of our theory, we have studied fibrils formed by Sup35NM fragment derived from yeast release factor Sup35. The presence of disordered M domain in Sup35NM fibrils makes it possible to observe spectral signals from the fibrils by means of solution-state NMR. Along with fibrils, the sample also contains a small fraction of proteolytic fragments, as schematically illustrated in Fig. 1A. The results of an NMR stimulated echo (STE) diffusion experiment on this sample are shown in Fig. 1C. The experimental data have been fitted using our new theory [1] that accounts for the effect of fibrils tumbling and, additionally, makes use of the fibril length distribution obtained by transmission electron microscopy (TEM), Fig. 1B. Furthermore, the fit accounts for the presence of 11% (as estimated from SDS-PAGE) of small-size soluble fragments broadly resembling the M-domain of Sup35NM.

To further address the presence of the rapidly diffusing species, we have spiked the sample of Sup35NM fibrils with recombinant Sup35M. The STE diffusion data from this sample are shown in Fig. 1D. The fast diffusion component is prominent in this graph, suggesting that various versions of diffusion ordered spectroscopy [2] can be readily implemented for multicomponent samples containing amyloid fibrils. This should facilitate future NMR studies of complex and intricate molecular processes underlying protein amyloidogenesis.

1. Kharkov B.B., Podkorytov I.S., Bondarev S.A., Belousov M.V., Salikov V.A., Zhouravleva G.A., Skrynnikov N.R.: Angew. Chem. Int. Ed. **60**, 15445 (2021)
2. Johnson C.S.: Prog. NMR Spectrosc. **34**, 203 (1999)

Abstract on Algorithm for Blind Recognition of EPR Spectra

S. O. Travin[1], A. I. Kokorin[1,2]

[1] Department of Dynamics of Chem-Bio Processes, N. N. Semenov Federal Research Center for Chemical Physics RAS, Moscow 119991, Russian Federation, travinso@yandex.ru
[2] Dept. of Chemistry, Plekhanov Russian University of Economics, Moscow 115093, Russian Federation

Resolution of EPR spectra of multi-component mixtures and determination of individual spectra are still important physicochemical tasks. It has a simple solution when either there are spectra of a preliminary known composition, or when reference spectra of all components are known. Without such information, the problem of so-called "blind" recognition becomes unsolvable using mathematical techniques alone and remains very difficult even after attracting additional chemical data.

There are currently two main approaches to solving these problems [1]: Principal Component Analysis (PCA) and Multivariate Curve Resolution with Alternating Least Squares (MCR-ALS). The MCR method, universally more suitable for "blind" recognition, decomposes the experimental data matrix D into the product of two smaller matrices C and S^T:

$$D = CS^T + E .\tag{1}$$

Here E is the error matrix, i.e., unexplained data change not associated with any chemical contribution.

The MCR-ALS approach is based on iterative step-by-step use of the least squares method where the object of variation changes on each even/odd cycle:

$$\min\|D^* - CS^T\|$$
variation of C taking into account it's limitations $\tag{2}$

$$\min\|D^* - CS^T\|$$
variation of S^T taking into account it's limitations $\tag{3}$

To our surprise, among thousands of publications, we could find only one paper [2] which described its application to the EPR spectra. Seems, the second work of this subclass was our publication [3]. We have tried to develop our own program package for 'blind' processing of spectroscopic sets focused on the use of the most efficient calculation methods. Thus, where it was possible to avoid iterative procedures, in particular, to abandon the basic use of the least squares method.

The most direct and reliable way to determine the eigenvalues (and vectors) of the data covariance matrix for bringing the matrix to the normal Frobenius form has been performed by the Danilevsky method. The obtained set of roots of the characteristic polynomial coincides with the number of linearly indepen-

dent basis vectors only for ideal spectra devoid of noise. In practice, the lower modulo eigen-values gives eigenvectors containing no information other than noise. Therefore, having received a set of eigenvalues, it is further necessary to discriminate and disengage them.

We used an algorithm that involves sequentially applying the following two procedures.

1) Alternately output all spectra to the positive region.

2) Alternating "removal" of common spectral lines so that ideally each line was contained in only one base spectrum.

The positive domain exit algorithm (procedure 1) includes iterative "blending" to the problem spectrum of other basis components having maximum positive values in the problem zone until all basis spectra become "mostly positive". Then, the maximum possible fraction of the remaining spectra is subtracted from each spectrum to avoid repeated maxima if possible (procedure 2). This set of steps is cyclically repeated for all base spectra in turn, until they are disengaged with the required accuracy. It is clear that this solves the task, since there remains so-called scale and, most importantly, rotational ambiguity.

The separated spectra DO NOT give the correct kinetic pattern. If there is a valid hypothesis about what a kinetic curve should look like (for example, an exponent for a first-order reaction), then from the whole variety of possible bases, one can go to the most plausible one using a pseudo-inverse transformation with the Moore-Penrose matrix. At the same time, an iterative procedure is not required and the determination of basic spectra with a kinetic curve fit passes simultaneously in one step.

1. Parastar H., Jalali-Heravi M., Tauler R.: Trends Anal. Chem. **31**, 134 (2012)
2. Abou Fadel M., de Juan A., Touati N., Vezin H., Duponchel L.: J. Magn. Reson. **248**, 27 (2014)
3. Kulak A.I., Travin S.O., Kokorin A.I.: Appl. Magn. Reson. **51**, 1005 (2020)

Sign-Sensitive Dipolar NMR Methods in Liquid Crystals

S. V. Dvinskikh[1,2]

[1] Department of Chemistry, KTH Royal Institute of Technology, Stockholm 11428, Sweden
[2] Laboratory of Biomolecular NMR, St Petersburg State University, St Petersburg 199034,
Russian Federation, sergeid@kth.se

Structural information in rigid solids and soft matter at the atomic level can be obtained by NMR spectroscopy through the measurements of dipole-dipole spin interactions. A wide range of NMR methods has been developed for estimating dipole couplings in anisotropic self-organising materials such as liquid crystals [1]. While the size of the coupling can be obtained from the splitting in the dipolar spectra, the sign of the constant is usually inaccessible. Such a limitation leads to structural and orientational ambiguities associated with the angular dependent term $(3\cos^2 - 1)$ of the dipolar interaction. Furthermore, experiments on static samples provide only the magnitude of the total spin-spin coupling $(J + 2d)$. Though the value and sign of scalar coupling constants J are known from other NMR studies, the ambiguity of determining the dipolar couplings d remains since the sign of the dipolar constant is unknown.

In this presentation, we review methods and introduce new approaches for the sign-sensitive determination of dipolar coupling constants in liquid crystals [2–5]. The suggested new experimental strategy includes the following components: (i) sign of dipolar coupling is determined in an off-MAS experiment; (ii) absolute values of spin coupling, which can be a combination $(J + 2d)$, is obtained with a high accuracy using advanced local field spectroscopy methods; (iii) if required, J coupling magnitude is determined from solution NMR spectra or from MAS spectra in mesophase.

1. Dvinskikh S.V. in: Modern Methods in Solid-State NMR: A practitioners' Guide (P. Hodgkinson, ed.), RSC, Abingdon, 2018.
2. Kharkov B.B., Chizhik V.I., Dvinskikh S.V.: J. Chem. Phys. **137**, 234902 (2012)
3. Majhi D., Dai J., Komolkin A.V., Dvinskikh S.V.: PCCP **22**, 13408 (2020)
4. Majhi D., Dvinskikh S.V.: Sci. Rep. **11**, 5985 (2021)
5. Majhi D., Kharkov B.B., Dvinskikh S.V.: Chem. Phys. Lett. (2021). In press.

Spin Kinetics of ^{3}He in Contact with DyF$_3$ Nanoparticles

**E. I. Kondratyeva[1,2], E. M. Alakshin[1,2], K. R. Safiullin[1,2],
V. V. Kuzmin[1,2], M. S. Tagirov[1,2]**

[1] Institute of Physics, Kazan Federal University, Kazan, 420008, Russian Federation,
katarina.kondratyeva@gmail.com
[2] Institute of Applied Research, Academy of Science of the Republic Tatarstan, Kazan, 420111,
Russian Federation, murat.tagirov@gmail.com

It is known that nanoscale objects have their own characteristics different from bulk. At nanoscale a matter has other properties, for example, the Curie temperature (T_C) or the Neel temperature (T_N), and coercive force (H_C) differ from the properties of a bulk material. In the DyF$_3$ single crystal at the temperature of T_C = 2.55 K, a transition from the paramagnetic to the ferromagnetic state was observed by measuring the specific heat [1] and magnetization [2]. It is interesting to compare the magnetic properties of dysprosium fluoride nanoparticles DyF$_3$ with the properties of a DyF$_3$ single crystal. In this work ^{3}He is used as a probe to study magnetic phase transition in DyF$_3$.

Earlier a significant change in the rates of the longitudinal and transverse nuclear magnetization relaxation of ^{3}He in the temperature region of the magnetic ordering in DyF$_3$ micrometer size powder was observed [3]. This report is devoted to the study of the effect of phase transitions in DyF$_3$ nanoparticles to the magnetically ordered states on the spin kinetics of ^{3}He used as a probe.

1. Holmes L.M., Hulliger F., Guggenheim H.J., Maita J.P.: Phys. Lett. A **50**, 163 (1974)
2 Savinkov A.V., Korableva S.L., Rodionov A.A., Kurkin I.N., Malkin B.Z., Tagirov M.S., Suzuki H., Matsumoto K., Abe S.: J. Phys.: Condens. Matter. **20**, 485220 (2008)
3. Alakshin E.M., Kondratyeva E.I., Kuzmin V.V., Safiullin K.R., Stanislavovas A.A., Savinkov A.V., Klochkov A.V., Tagirov M.S.: JETP Letters. **107**, 111 (2018)

Isotropic Mixing at Ultra-Low Field: a Way to Total Chemical Shift Correlation between All Magnetic Nuclei

I. V. Zhukov[1], A. S. Kityutin[1], F. Ferrage[2], G. Buntkowsky[3], G. Bodenhausen[2], A. V. Yurkovskaya[1], K. L. Ivanov[1]

[1] International Tomography Center, Novosibirsk 630090, Russian Federation, i.zhukov@tomo.nsc.ru
[2] Département de Chimie, École Normale Supérieure, Paris 75230, France
[3] Technical University of Darmstadt, Darmstadt 64277, Germany

Nowadays, 2D NMR methods are well-developed and used routinely in NMR research. For example, in a well-known TOCSY experiment, which highlights the network of coupled nuclei, a sufficiently strong spin-lock pulse provides the spin mixing due to scalar spin-spin coupling between locked nuclear spins of the same magnetic isotope. The heteronuclear version of TOCSY exists, which is known as HEHAHA (Heteronuclear Hartmann-Hahn) experiment [1]. It relies on polarization transfer between heteronuclei once Hartmann-Hahn conditions are met. However, in practice, the application of the HEHAHA pulse sequence is limited by technical problems since strong radiofrequency irradiation is necessary to cover the entire distribution of heteronuclei chemical shifts.

Recently, we realized an attractive idea to fulfill the condition of strong coupling for any heteronuclei by utilizing zero- to ultra-low field while keeping high-resolution NMR detection at high field. Here we present this novel approach to obtain a 2D chemical shift correlation spectrum with polarization transfer between heteronuclei named ZULF-TOCSY [2]. The mixing block of ZULF-TOCSY contains an interval of isotropic mixing at zero- to ultra-low field. This experiment in principle allows observing all possible correlations between signals of all magnetic nuclei with different gyromagnetic ratios. This unique feature assigns the application of the ZULF-TOCSY experiment for the straightforward determination of mixture components. In addition, ZULF-TOCSY allows rendering sequential assignments in peptides at natural abundance then no amide protons are present using a single 2D spectrum. The isotropic mixing at zero- to ultra-low field can be used to construct more sophisticated NMR pulse sequences in the future.

1. Morris G.A., Gibbs A.: Magn. Reson. Chem. **29**, 83 (1991)
2. Zhukov I.V. *et al.*: J. Phys. Chem. Lett. **11**, 7291 (2020)

POSTERS

Investigation of the Passage of Single-Photon States with an OAM Through a Turbulent Atmosphere

D. O. Akatiev, D. A. Turaikhanov, <u>A. V. Shkalikov</u>, I. Z. Latypov, A. A. Kalachev

Zavoisky Physical-Technical Institute, FRC Kazan Scientific Center of RAS, Kazan 420029, Russian Federation

Quantum key distribution (QKD), which provides absolutely secure communication between several parties, is one of the most promising and developing applications of quantum physics [1]. The security of the QKD is guaranteed by basic physical laws, which show that encrypted keys will remain safe even in the case of unlimited computing power from eavesdropping intruders, i.e. does not rely on mathematical complexity.

Since the inception of quantum cryptography in 1984 [2], QKD concepts have been demonstrated on various platforms such as fiber-optic networks [3], free-space communication lines [4], underwater [5]. However, in most QKD systems, information is encoded by the polarization degree of freedom, which is a two-dimensional Hilbert space that limits the information capacity to 1 bit per photon. Even in the case of high-brightness single-photon sources [6], two-dimensional QKD systems are still not efficient enough. For comparison, high-dimensional QKD systems are more efficient in terms of photons and are resistant to eavesdropping [7].

The orbital angular momentum (OAM) of photons is a promising degree of freedom for multidimensional QKD. However, the negative consequences of atmospheric turbulence are a constant problem in OAM systems operating in free space communication channels. In contrast to previous works devoted to the correction of simulated static turbulence, we additionally conduct studies in turbulence cells and the real atmosphere with adaptive optics (AO) correction in real time. Our AO system provides a small correction limited to 300 Hz to reduce errors caused by weak turbulence and establish a secure communication path. The coding of information on the states of orbital angular momentum can cover an infinite-dimensional Hilbert space, which has been experimentally demonstrated, and is promising both in multidimensional quantum cryptography [8] and in classical communication [9]. The c OUM state carries OAM units, has entwined spiral wavefronts, where l denotes the OAM quantum number and is an integer [10]. It should be noted that there are already fibers that support the propagation of high-order spatial modes, but they are at the stage [11]. Therefore, the most interesting from the applied point of view are channels in free space as the most flexible and universal. Since on states with OAM information is transferred in the phase profile, they are most vulnerable to atmospheric turbulence. Despite the fact that the propagation of states with OAM in a turbulent atmosphere has been widely studied both theoretically and experimentally, the

implementation of multidimensional one-photon states for QKD based on OAM and their propagation in a turbulent atmosphere is still a difficult problem.

The principle of operation of the adaptive optical system is based on the reproduction of the phase distribution by the surface of the mirror, which is conjugate to the corrected wavefront. The surface of the bimorph mirror is controlled by applying voltages to the electrodes. During system operation, the sensor measures the current wavefront. Any distortion of the wavefront, represented as a vector of spot displacements, can be expanded in a series of response functions, and the expansion coefficients will be the voltages that must be applied to the mirror electrodes, but with the opposite sign.

The process of creating a turbulent disturbance in the beam was divided into two parts: the creation of a turbulent upward flow using a 10×10 nozzle matrix 1 mm in diameter at an inlet pressure of 4.5 atm. and with the help of an oven heating up to a temperature of 95 degrees C. Initially, in the absence of turbulence, PV (peak-to-valley) was measured – the amplitude of the wavefront aberrations and RMS – the root-mean-square deviation P-V = 0.024 μm, RMS = 0.005 μm. The turbulence created with the nozzle array without heating is the least disturbing to the laser beam; the measured values were P-V = 0.087 μm, RMS = 0.037 μm. Under the conditions of creating a disturbance with the help of an oven located directly under the beam, the measured values reach P-V = 0.847 μm, RMS = 0.172 μm. Thus, the turbulence created by the stove is much greater.

In this work, on the basis of experimental modeling of a turbulent atmosphere, we study the passage of one-photon states with orbital angular momentum and superposition states through a turbulent medium. This work was supported by the Russian Foundation for Basic Research No. 18-29-20091.

1. Gisin N., Ribordy G., Tittel W., Zbinden H.: Rev. Mod. Phys. **74**, 145 (2002)
2. Bennett C.H., Brassard G.: Proc. IEEE Int. Conf. on Comput. Syst. Signal Process. 1984. P. 175.
3. Korzh B., Lim C.C.W., Houlmann R., Gisin N., Li M. J., Nolan D., Sanguinetti B., Thew R., Zbinden H.: Nat. Photonics **9**, 163 (2015)
4. Liao S.-K. *et al.*: Nature **549**, 43 (2017)
5. Bouchard F., Sit A., Hufnagel F., Abbas A., Zhang Y., Heshami K., Fickler R., Marquardt C., Leuchs G., Boyd R.W., Karim E.: Opt. Express **26**, 22563 (2018)
6. Dousse A., Suffczynski J., Beveratos A., Krebs O., Lemaitre A., Sagnes I., Bloch J., Voisin P., Senellart P.: Nature **466**, 217 (2010)
7. Sheridan L., Scarani V.: Phys. Rev. A **82**, 030301 (2010)
8. Vallone G., D'Ambrosio V., Sponselli A., Slussarenko S., Marrucci L., Sciarrino F., Villoresi P.: Phys. Rev. Lett., **113**, 060503 (2014)
9. Wang J. *et al.*: Nat. Photonics **6**, 488 (2012)
10. Allen L., Beijersbergen M.W., Spreeuw R., Woerdman J.: Phys. Rev. A **45**, 8185 (1992)
11. Flaes D.E.B., Stopka J., Turtaev S., de Boer J.F., Tyc T., Cižmár T.: Phys. Rev. Lett. **120**, 233901 (2018)

The Structure of Radicals in Mechanically Activated Calcium Gluconate

M. M. Akhmetov[1], G. G. Gumarov[1], V. Yu. Petukhov[1], R. B. Zaripov[1], G. N. Konygin[2], D. S. Rybin[2]

[1] Zavoisky Physical-Technical Institute, FRC Kazan Scientific Center of RAS, Kazan 420029, Russian Federation, mansik86@mail.ru
[2] UdmFRC Ural Branch of RAS, Izhevsk 426067, Russian Federation, dsrybin@mail.ru

Mechanical action on a substance can cause multiple structural transformations [1], such as amorphization, polymorphic transitions, conformational transformations, as well as the formation of free radicals. Earlier, it was reported about the presence of an EPR signal with $g = 2.0051 \pm 0.0004$ and a width $\Delta H = 8.7 \pm 0.5$ Oe from calcium gluconate (CG) subjected to mechanochemical treatment. It is assumed that paramagnetic centers are free radicals, the appearance of which is probably associated with the cleavage of the Ca–OR bond with the subsequent formation of delta-gluconolactone (δ-GL). It was found that with an increase in the grinding time, the accumulation of paramagnetic centers occurs without changing their physicochemical nature [2]. The ^{1}H NMR method revealed conformational transformations of the CG molecule, which are a consequence of the formation of intermolecular hydrogen bonds with an increase in the concentration of an aqueous solution. It was found that CG molecules in solution exist in the form of two conformations: zigzag 1-P and cyclic $_3$G$^+$ [3].

Earlier, using pulsed EPR methods and quantum-chemical calculations, the structures of radicals formed during the mechanochemical activation of calcium gluconate were proposed [4]. No final conclusions have been drawn – the experimental data can be described by several models. In addition, it was necessary to
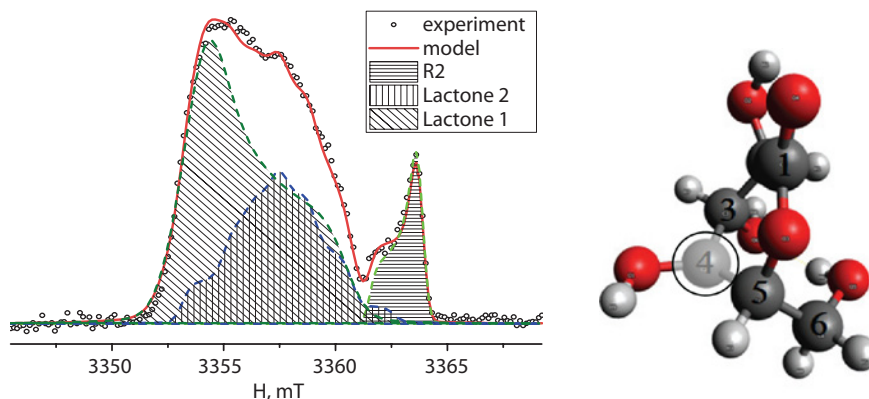
Fig. 1. EPR of the W-band for MACG and the structure of the radical on δ-GL (Lactone 1).

establish whether HFC with magnetic nuclei is the main mechanism of EPR line broadening in the system under study. The aim of this work was to elucidate the structure of the radical (radicals) arising during the mechanoactivation of CG, using EPR spectroscopy in various ranges, including the W-band.

CG monohydrate produced by the Tyumen Chemical-Pharmaceutical Plant was used as the initial samples. Mechanically activated powders were obtained by mechanical grinding in a planetary ball mill "LAIR" cooled by running water for 1 hour. To match the model and experiment, a quantum-chemical calculation of the geometric and electronic structure of various fragments of metal gluconates was carried out using the Orca program.

It is known that the interaction of radicals arising during mechanical activation with environmental components can significantly affect their appearance and stabilization. In this case, it is also possible to accept radicals, which prevents further free radical reactions due to a change in the structure of the molecule. In order to clarify the nature of radicals in MACG, measurements were carried out not only in X and Q, but also in the W-band (Fig. 1). The measurement was carried out in a pulsed mode, the duration of the 90°-pulse is 80 ns, and the temperature is 80 K. The observed spectrum can be described by three components. The corresponding EPR spectrum was calculated using the Easyspin software package.

As can be seen from Fig. 1, the spectrum corresponding to the radical R2 describes only a part of the spectrum in the W-band, and is typical for powder samples. It should be noted that R2 is a fragment of molecule calcium gluconate formed upon the rupture of the Ca-O bond and containing a calcium atom. Quantum-chemical calculation for the remaining fragment of the gluconate anion gives rather large values of the HFC-tensor, which are not observed experimentally. Previously, it was indicated that there is a small amount of delta-gluconolactone in the original sample and MACG. It is assumed that smaller margin area of the spectrum in the W-band corresponds to the radicals formed during the mechanoactivation of calcium gluconate, when the gluconate anion is transformed into the δ-GL-radical with the abstraction of one of the hydrogen atoms. The most suitable were two structures of the radical on the C4 carbon atom, formed upon the termination of the C-H bond (Lactone 1, Lactone 2). The values of the g-tensor for such radicals differ from the proposed structure R2 by such an amount that their joint contribution describes well the experimental EPR spectrum in the W-band. The weak splitting in the X and Q ranges does not allow one to detect the contributions of the tensors of the HFC and the g-factor for the MACG sample, since the location of the π-radicals on the C4 atom (Lactone 1-2) is close to 90° to the neighboring beta-protons, and according to the Mac-Connell, the value of their HFC is extremely small.

Thus, during the mechanoactivation of calcium gluconate monohydrate, molecular transformations occur, which can be conditionally divided into several stages: the decomposition of the crystal hydrate, the destruction of intermolecular and intramolecular bonds. Mechanoactivation of calcium gluconate is accompanied by insignificant formation of δ-GL-radical, due to the destruction of the chemical bond between calcium and gluconic acid. While the line corresponding

MD Study of Structural Anomaly of Dibutyl Phtalate at Different Temperatures

D. V. Alimov[1], S. Pylaeva[2], M. Yu. Ivanov[1], M. V. Fedin[1]

[1] International Tomography Center, Siberian Branch of the Russian Academy of Sciences,
Russia and Novosibirsk State University, Novosibirsk 630090,
Russian Federation, d.alimov@g.nsu.ru
[2] Dynamics of Condensed Matter and Center for Sustainable Systems Design,
Chair of Theoretical Chemistry, University of Paderborn, Warburger Str. 100, Paderborn, Germany,
svetlana.pylaeva@gmail.com

In the T_g vicinity the majority of glasses are heterogeneous and consists of immobile "solid-like" and mobile "liquid-like" domains with different dynamic properties. Recently molecular mobility and radical libration value near T_g of ionic liquid (IL) which is assigned to structural rearrangements of glassy ILs on the nanometer scale was researched[1]. The coexistence of two types of IL environments was observed by EPR in the temperature range from (T_g − 60 K) to T_g. At temperatures close to T_g there is formation of areas where the radical is more compressed and rotates more slowly and areas where the radical is less compressed and rotates faster. As a result, this leads to a decrease in the average librations. Local minimum of the spin probe librations has been correlated with decreasing of macroscopic density. This is uncommon behavior (structural anomaly), since most of known substances, become less dense upon temperature increase.

To establish the features of the IL dynamics we carried out an MD experiment, where we also noted a decrease in librations at a temperature T_g. Dibutyl phthalate (DBP) with a TEMPO nitroxyl radical in it as a spin probe was chosen as a model system. Calculations were carried out in the ORCA, Multiwfn, pack-
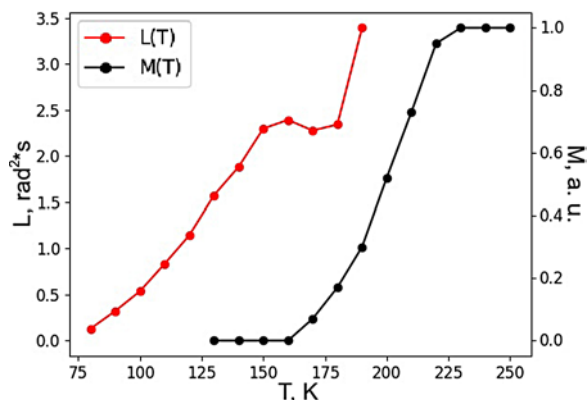
Fig. 1. $L(T)$ and $M(T)$ for TEMPO in dibutyl phta-late.
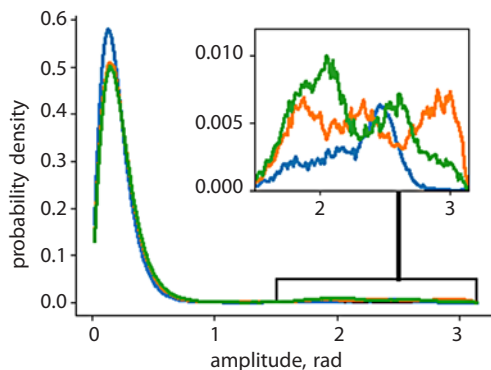
Fig. 2. TEMPO rotational spectra.

mol and GROMACS packages; mdtraj and plumed were used for data analysis. After energy minimization 400 ns NVT trajectory was calculated at 300 K, from which 80 snapshots were taken. For each snapshots after shock freezing to temperatures in the vicinity of T_g the system NVT evolution was observed during 15 ns. Various types of radical movement were identified depending on the amplitude of movement of the ON group. It was shown that three essentially different types of arrangement can be distinguished: clamping of a radical - librations at small angles, a free radical – librations at large angles and intermediate states. We have examined the features of the mutual of radical – solvent arrangement and the dependce of of the radical movement from its environment. The rdf distributions from the radical to various atom groups of solvent were analyzed and it was shown that the probability of simultaneous approach of the radical with the oxygen atoms of DBP and DBP chains corresponding to the radical compression is the highest at T_g. Onward, the prevalence of fractions of different types of radical-solvent arrangements was calculated. Despite the fact that for each of the fractions, the average amplitude of the radical movement increases with increasing of T, at T_g the clamped fraction is more widespread. Therefore, on average, the libration amplitude decreases, what correlates with the EPR experiment. Further, a correlation was established between the dynamics of the radical and the features of the geometry of the bulk of dibutyl phthalate. It was shown that the anomalous distribution of librational fractions is caused by structural rearrangement of the solvent at T_g. The formation of DBP clusters of various types was analyzed: at T_g TEMPO is situated at surface of clusters, what leads to the suppression of librations.

The MD calculation has improved the understanding of the nature of the structural anomaly. An article has been published in Nanoscale Advances.

1. Ivanov M.Y., Poryvaev A.S., Polyukhov D.M., Prikhod'ko S.A., Adonin N.Y., Fedin M.V.: Nanoscale, **12**(46), 23480–23487 (2020)
2. Ivanov M.Y., Bakulina O.D., Alimov D.V., Prikhod'ko S.A., Veber S.L., Pylaeva S., Adonin N.Y., Fedin, M.V.: Nanoscale Advances **3**(17), 4973–4978 (2021)

to R2 can be described by one component, the weak-field contribution can be described by 2 components. The first component corresponds to a radical with the structure R2 ($C_6H_{11}O_7Ca^*$) – a radical containing a calcium ion and formed as a result of the rupture of the Ca-O bond, the second and third components to the remainder of the calcium gluconate molecule, presumably transforming into the δ-GL-radical forms.

1. Boldyrev V.V.: Journal of materials science **39**, 5117–5120 (2004)
2. Gumarov G.G., Petukhov V.Yu., Konygin G.N., Rybin D.S., Zheglov E.P., Akhmetov M.M., Porsev V.E.: Journal of Physical Chemistry **87**, (9), 1578–1581 (2013)
3. Akhmetov M.M., Konygin G.N., D.S. Rybin, V.Yu. Petukhov, G.G. Gumarov, A.B. Konov: Applied Magnetic Resonance **48**, Iss. 10, 971–979 (2017)
4. Zaripov R.M., Aminova, Salikhov K.M.: Applied magnetic resonance **35**, Iss. 2, 337–358 (2008)

EPR Spectra of Metal Ions on Graphite Oxide

D. A. Astvatsaturov, A. Kh. Vorobiev

Moscow State University, Moscow 119991, Russian Federation,
ASTVaaaa@yandex.ru

Graphite oxide is a non-stoichiometric derivative of graphite prepared by oxidation of pure graphite in acidic conditions. Graphite oxide could be used as a precursor of graphene as well as a starting material for membrane fabrication. Today, the investigation of physico-chemical properties of graphite oxide membranes attracts a lot of attention. Graphite oxide membranes are layered materials consisted of packages of graphene oxide sheets. The thickness of the membrane and its interlayer distance are often used to characterize the material. The degree of graphene oxide sheets ordering in the membrane is also an important characteristic of the material. The most detailed way to describe the degree of ordering of a material is to use the order parameters, which are values of Legendre functions averaged over all possible orientations. It is known that graphite oxide membranes demonstrate selective permeation of liquids and gases. The correlation of permeating ability and separation selectivity of membranes with the degree of layer ordering is a question of interest. However, there are few works that employ the quantitative approach for determination the degree of layer ordering in graphite oxide membranes [1, 2]. In work [2], the authors use the EPR method and obtain quantitative data using TEMPOL radical as a spin probe. The values of the second and fourth rank order parameters (P_{20} and P_{40}) were obtained by computer simulation of the EPR spectra recorded at different orientations of the sample in the magnetic field [2]. The goal of this contribution is to investigate if paramagnetic metal ions could be used as spin probes to
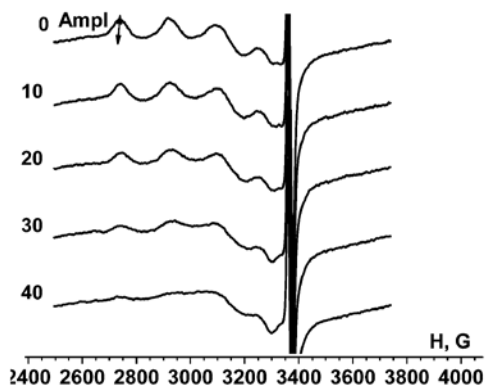
Fig. 1. Angular dependence of the EPR spectrum of $[Cu(NH_3)_4]^{2+}$ complex on the membrane.

study the degree of layer ordering in the graphite oxide membranes. Paramagnetic metal ions are known to demonstrate higher anisotropy of magnetic parameters than nitroxide radicals and can be sorbed by graphite oxide and membranes.

In our work, four samples of the graphite oxide membranes were studied. Three samples were prepared by the vacuum filtration of graphite oxide water dispersion. The one additional sample was fabricated by evaporation of the graphite oxide water dispersion. Mn^{2+}, Cr^{3+}, VO^{2+}, Cu^{2+} complexes were tested as spin probes. The concentration of paramagnetic species in membranes was taken to be enough for spectra recording but to avoid the dipole-dipole broadening of the EPR spectra. EPR spectra were registered in the X-range and at 100K.

We found that the most reliable results are obtained if the copper hexaammonia complex $[Cu(NH_3)_4]^{2+}$ is used as a spin probe. EPR spectra of the membranes treated with copper ammonia solution demonstrated hyperfine structure typical for Cu^{2+} ions. The typical angular dependence of the EPR spectrum of $[Cu(NH_3)_4]^{2+}$ adsorbed on the membrane is presented in Fig 1.

The numerical simulation of the spectrum angular dependence was found to be impossible because of a complex shape of base line depending on the orientation of a sample. To overcame that trouble we used simplified method based on the measurement of the angular dependence of the amplitude of the parallel component ($m_I = -3/2$) of the experimental EPR spectra (this amplitude is marked as "Ampl" in the Fig. 1) and numerical prediction of this angular dependence for different orientation distributions. The matching of the orientation distribution satisfactory describing the experimental angular dependence of parallel component of spectrum allows to estimate the order parameters. The values of the order parameters of studied graphite oxide membranes were found to be in range: $P_{20} = 0.020 \div 0.55$; $P_{40} = 0.033 \div 0.30$; $P_{60} = 0.03 \div 0.10$. It was found that membranes fabricated by different methods have different degree of graphene oxide layers ordering.

1. Akbari A., Sheath P., Martin S.T., Shinde D.B., Shaibani M., Banerjee P.C., Tkacz R., Bhattacharyya D., Majumder M.: Nature Communications **7**, 10891 (2016)
2. Chumakova N.A., Rebrikova A.T., Talyzin A.V., Paramonov N.A., Vorobiev A.Kh., Korobov M.V.: J. Phys. Chem. C **122**, 22750 (2018)

Investigation of Layered Perovskite-Like Oxides Sr_2TiO_4 Doped with La and Cu by EPR

T. I. Chupakhina[1], R. M. Eremina[2], I. V. Yatsyk[2], T. P. Gavrilova[2], Yu. A. Deeva[1], A. A. Sukhanov[2]

[1] Institute of Solid State Chemistry of the Ural Branch of the Russian Academy of Sciences, Ekaterinburg 620990, Russian Federation
[2] Zavoisky Physical-Technical Institute, FRC Kazan Scientific Center of RAS, Kazan 420029, Russian Federation

Strontium titanates $Sr_{n+1}Ti_nO_{3n+1}$, (Ruddlesden-Popper homologous series) have structural similarity with the anatase phase of TiO_2. The Ti atoms in these ternary oxides, are located in a six-coordinated octahedral environment, as well as in TiO_2. Strontium titanates were found to be suitable materials for use in photo-systems [1, 2]. Copper oxides (CuO/Cu_2O) are known to be 2.0 eV band gap wide. Introduced into titanium oxide sublattice structure, copper has an effective influence to the electronic and intrinsic defectiveness of titanates, for example the concentration of oxygen vacancies that regulate the semiconductors catalytic activity [3, 4]. The use of the conjugate substitution La/Cu for the cationic Sr/Ti sublattices in Sr_2TiO_4, will make it possible to control the band gap width and influence the toxic products photooxidation shift of to the visible range.

The aim of this work is investigation of copper valence and crystal field dynamic in $La_xSr_{2-x}Ti_{1-x}/2Cu_x/2O_4$ ($x = 0.2, 0.3, 0.5$) ceramics. The EPR spectra were measured at temperature range from 5 to 300 K in the continuous wave mode in the X-band using an ELEXYS E-680 EPR and EMXPlus spectrometers. The samples were irradiated with a laser with an average power of 120 mW with
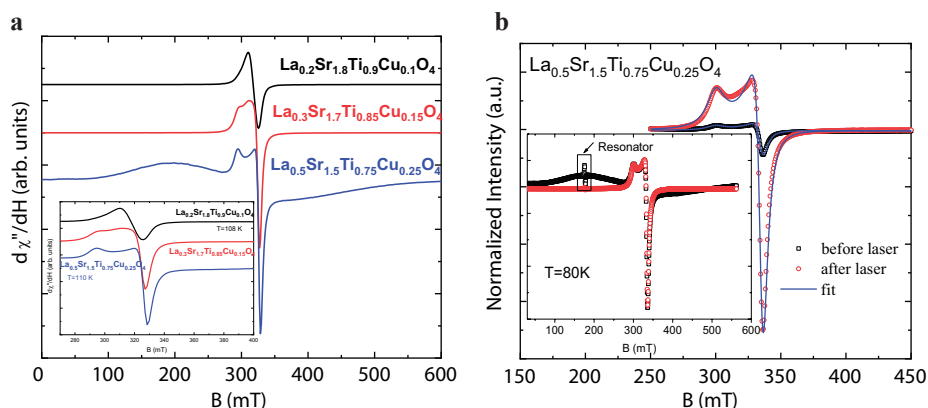
Fig. 1. a EPR spectra in $La_xSr_{2-x}Ti_{1-x}/2Cu_x/2O_4$ ($x = 0.2, 0.3, 0.5$) ceramics at 108 K–110 K. Inset shows the same data on a larger scale; **b** EPR spectra of $La_{0.5}Sr_{1.5}Ti_{0.75}Cu_{0.25}O_4$ ceramics before and after laser irradiation at 80 K. The inset shows the EPR signals normalized to the maximum; the signal from the resonator is shown by an arrow.

a wavelength of 355 nm in an ampoule with an external diameter of 4 mm. The photocatalytic activity of the obtained oxides $La_xSr_{2-x}Ti_{1-x}/2Cu_x/2O_4$ (x = 0.0; 0.2; 0.3) is caused by the presence in them of copper cations of different valences. To determine the valence state of Cu ions the EPR spectra of $La_xSr_{2-x}Ti_{1-x}/2Cu_x/2O_4$ (x = 0.2, 0.3, 0.5) ceramics were obtained at temperature 110 K, (Fig. 1a) and the effect of laser irradiation (λ = 355 nm) on the $La_{0.5}Sr_{1.5}Ti_{0.75}Cu_{0.25}O_4$ compound was investigated (Fig. 1b). We suggest that the observed resonance line is related to Cu^{2+} ions ($3d^9$, S = 1/2), which exist in all samples. The EPR lineshape is typical for the powder EPR spectrum, which is characterized by simultaneous observation of two components with $g_\parallel$ and $g_\perp$, which represent the absorption line and the first derivative of the absorption line, respectively. As can be seen from the Fig. 1a, the degree of anisotropy (the difference between $g_\parallel$ and $g_\perp$) of the EPR line varies greatly with increasing dopant concentration that can be due to the distortion of the ligand octahedron of the copper ions nearest environment with increasing x. Observed signals were fitted by the powder EPR lineshape and the theoretical curves are shown as solid lines in Fig. 1b. The degree of anisotropy of the EPR signal in $La_{0.2}Sr_{1.8}Ti_{0.9}Cu_{0.1}O_4$ ceramics is small $g_\parallel$ = 2.2; $g_\perp$ = 2.11 and the linewidth is 80 Oe, while for $La_{0.3}Sr_{1.7}Ti_{0.9}Cu_{0.15}O_4$, the degree of anisotropy increases – $g_\parallel$ = 2.25; $\Delta H_\parallel$ = 85 Oe, and $g_\perp$ = 2.08; $\Delta H_\perp$ = 50 Oe, fit parameters of the ESR signal in $La_{0.5}Sr_{1.5}Ti_{0.75}Cu_{0.25}O_4$ are equal to $\Delta H_\parallel$ = 85 Oe, $g_\parallel$ = 2.25 and $g_\perp$ = 2.015. The additional broad resonance line with the linewidth value ΔH = 1500 Oe was observed in $La_{0.5}Sr_{1.5}Ti_{0.75}Cu_{0.25}O_4$ sample at T = 110 K (Fig. 1a). The number of paramagnetic Cu^{2+} centers observed in the EPR spectrum was estimated for all samples. For this purpose the EPR spectra integral intensity of the sample was compared with the integral intensity of the reference sample with a known number of paramagnetic spins. It was found that the ratio of the number of paramagnetic centers N_{Cu2+} to all copper ions N (both Cu^+ and Cu^{2+}) in $La_xSr_{2-x}Cu_x/2Ti_{1-x}/2O_4$ is N_{Cu2+}/N = 1.5% for x = 0.2; N_{Cu2+}/N = 13% for x = 0.3, and N_{Cu2+}/N = 21.3% for x = 0.5.

1. Lu L.W., Lv M.L., Wang D., LiuG., Xu X.X.: Applied Catalysis B-Environmental **200**, 412–419 (2017)
2. Lu L.W., Lv M.L., Liu G., Xu X.X.: Applied Surface Science **391** 535–541 (2017)
3. Sun Q.N., Peng Y.P., Chen H.L., Chang K.L., Qiu Y.N., Lai S.W., Journal of Hazardous Materials **319** 121–129 (2016)
4. Xi Z.H., Li C.J., Zhang L., Xing M.Y., Zhang J.L.: International Journal of Hydrogen Energy **39**(12) 6345–6353 (2014)

The Dobryakov-Lebedev Relation Applied to Partially-Resolved EPR Spectra

M. M. Bakirov[1], I. T. Khairutdinov[1], B. Bales[2]

[1] Zavoisky Physical-Technical Institute, FRC Kazan Scientific Center of RAS, Kazan 420029, Russian Federation, pinas1@yandex.ru
[2] Western Institute of Nanoelectronics, University of California, Los Angeles 18111, USA

The Dobryakov-Lebedev relation which relates the line width of the first-derivative of a Gaussian-Lorentzian convolution to the linewidths of its Gaussian and Lorentzian components for an unresolved line is extended to resolved lines. Applying this extension to nitroxide free radicals in solutions of low-viscosity solvents offers an opportunity to study interactions of the spins with the microwave field and spin-spin interactions previously inaccessible except by tedious numerical methods.

We have shown that an experimental partially resolved line may be analyzed in the same manner as an unresolved inhomogeneous nitrogen manifold line as detailed in [1].

1. Bales B.L. in: Biological Magnetic Resonance (L. J. Berliner and J. Reuben, Editors). Plenum, New York 1989.
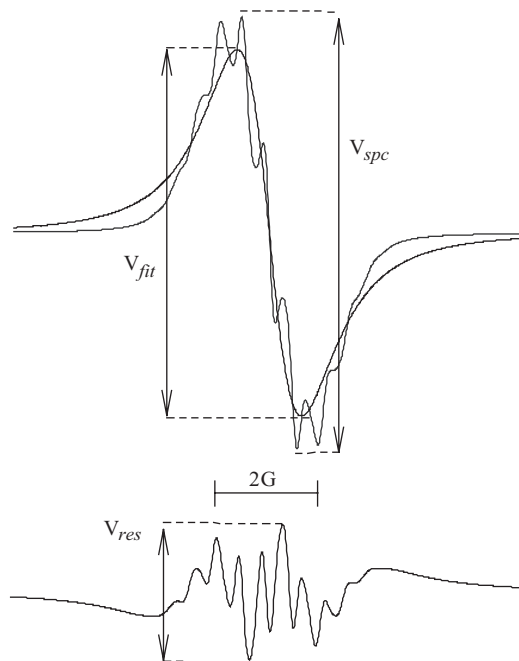
Fig. 1. Simulated spectra of one of three ^{14}N lines for Tempol with inequivalent proton coupling constants.

Nanostructural Anomalies and Heterogeneities in Organic Glasses Revealed by EPR

O. D. Bakulina, M. Yu. Ivanov, M. V. Fedin

International Tomography Center, Novosibirsk State University, Novosibirsk 630090, Russian Federation, o.bakulina@tomo.nsc.ru

Phthalic acid esters, or phthalates, are widely used in industry. For instance, they apply as plasticizers – substances added to plastics to increase their strength, transparency and flexibility. Phthalates are also found in medical devices, toys, detergents, cosmetics and many other household items. Therefore, there are many studies of their impact on human health, on the environment, and so on. However, no attention has been paid to the study of nanostructuring of phthalic acid esters.

Electron paramagnetic resonance (EPR) spectroscopy helps to obtain unique information about the structural organization of matter at the molecular level. With this approach, a paramagnetic probe (in most cases, nitroxyl radicals) dissolves in IL in insignificant "undisturbed" concentrations.

Earlier, our group studied heterogeneities in ionic liquids (IL) by EPR methods [1]. In the vicinity of the glass transition temperature (T_g), suppression of molecular mobility associated with unusual structural rearrangements of ILs on the nanometer scale was found. Pulsed and stationary EPR clearly indicate the presence of heterogeneities near T_g in the temperature range of ~50 K.

Despite the fact that the structure of phthalates differs from IL, similar rearrangements were found for phthalic acid esters, which is the subject of this work. In addition, the structural rearrangements in saturated alcohols and substituted benzenes were studied. In this case, their nanostructuring was investigated, and the results were compared with the corresponding ILs [2].

1. Ivanov M.Yu. *et al.*: J. Phys. Chem. Lett. **9** (16), 4607–4612 (2018)
2. Ivanov M.Yu. *et al.*: Nanoscale Adv., 2021, Advance Article

Spatial Structure of PAP (85-120) Peptide Forming SEVI Fibrils by NMR Spectroscopy

D. Blokhin, D. Sanchugova, V. Klochkov

Institute of Physics, Kazan Federal University, Kazan 420008, Russian Federation, dblohin@kpfu.ru

Semen is the major vehicle for the spread of the HIV-infection [1]. Accumulating evidence shows that semen boosts HIV-infection [2]. One factor that contributes to the HIV-enhancing effect of semen is an amyloid fibrils SEVI (semen-derived enhancer of virus infection). SEVI forms from peptide fragments of prostatic acid phosphatase (PAP): PAP(248-286) and PAP(85-120). SEVI captures viral particles and promotes their attachment to target cells to boost viral fusion and infection [2].

In the last few years, the considerable attention has been given to the semen amyloid fibrils for further understanding of molecular mechanisms of the HIV infectivity [3,4]. Understanding the molecular mechanisms of fibrils interaction with virions and cells is based on the structural characteristics of the peptide.

To date, the spatial structures of prostatic acid phosphatase (PDB: 1CVI) [5] and PAP(248-286) peptide (PDB: 2L3H) [6] have been determined. Analysis of 1CVI was showed that both fragments PAP(248-286) and PAP(85-120) contain two helical regions and one beta sheet in prostatic acid phosphatase. 2L3H is different from PAP(248-286) structure obtained from full PAP. (ex., significantly reduced helix fragments). Based on this, for the analysis of SEVI fibrillation, it is necessary to determine the structure of PAP peptide fragments in solution.

The purpose of our work was to determine the spatial structure of PAP(85-120) peptide in solution by NMR spectroscopy. Assignment of ^{1}H, ^{13}C NMR signals was performed using 2D ^{1}H-^{1}H TOCSY, 2D ^{1}H-^{1}H NOESY, ^{1}H-^{13}C HSQC, ^{1}H-^{13}C HMBC, ^{1}H-^{13}C TOCSY-HSQC experiments. Internuclear distances were determined from NOESY spectrum analysis. The spatial structure of PAP(85-120) was determined by the molecular dynamics method in the XPLOR-NIH program [7]. Internuclear distances were used as input parameters for the calculation.

1. Haase A.T.: Nat. Rev. Immunol. **5**, 783 (2005)
2. Münch J. *et al.*: Cell **131**, 1059 (2007)
3. Widera M., Klein A.N., Cinar Y., Funke S.A., Willbold D., Schaal H.: AIDS Res. Ther. **11**, 1 (2014)
4. Xun T, Li W, Chen J, Yu F, Xu W, Wang Q, Yu R, Li X, Zhou X, Lu L, Jiang Sh, Li L, Tan S, Liu Sh: Antimicrob. Agents Chemother **59**, 5123 (2015)
5. Jakob C.G., Lewinski K., Kuciel R., Ostrowski W., Lebioda L.: Prostate **42**, 211 (2000)
6. Nanga R.P., Brender J.R., Vivekanandan S., Popovych N., Ramamoorthy A.: J. Am. Chem. Soc. **131**, 17972 (2009)
7. Schwieters C.D., Kuszewski J.J., Tjandra N., Clore G.M.: J. Magn. Reson. **160**, 65 (2003)

$T_2 \times T_{2eff}$ Low-Field NMR-Relaxometry for Solids

A. V. Bogaychuk[1,2], T. H. Farkhutdinov[1]

[1] Institute of Physics, Kazan Federal University, Kazan, 420008, Russian Federation
[2] Tatarstan Academy of Sciences, Kazan, 420111, Russian Federation,
aleksandr.bogaychuk@gmail.com

Multi-dimensional correlation experiments are ubiquitous in low-field NMR-relaxometry for studies of molecular structure and dynamics [1]. $T_1 \times T_2$ is the most used and informative technique. T_2 is sensitive to slow frequencies of molecular motions, and T_1 to fast ones at frequencies close to Larmor's frequency ω_0 [2]. In case of solids the effective spin-spin relaxation time T_{2eff}, which is sensitive to molecular motions at frequencies ω_1, can serve as an additional relaxation parameter [3]. This relaxation time can be estimated from experiments on narrowing the spectral line for a solid: MW-2, MW-4, WHH-4, MREV-8, etc.

The samples for the investigation were as follows: the polyethylene $(C_2H_4)_n$ (PE), the polyvinyl chloride $(-CH_2-CHCl-)_n$ (PVC). The measurements
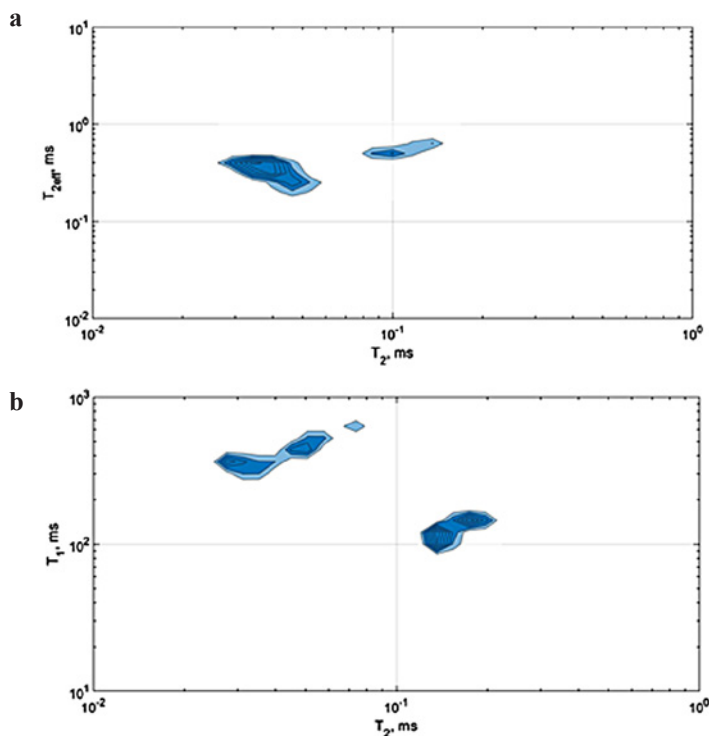
Fig. 1. $T_{2eff} \times T_2$ (**a**) and $T_1 \times T_2$ (**b**) correlation maps for a mixture of polyethylene and polyvinyl chloride samples.

were carried out in average value of the magnetic field of 598.0 mT and a half-width of 226.9 ppm [4]. The $\pi/2$-pulse duration was 3 µs ($\omega_1 \approx 83$ kHz). The measurements of T_1 were carried out by the saturation method and amounted to $T_{1\,PE} = 111.9$ ms and $T_{1\,PVC} = 535.71$ ms. T_2 was measured by solid state echo: $T_{2\,PE} = 100$ µs and $T_{2\,PVC} = 30$ µs. $T_{2\text{eff}}$ was estimated using the MW-2 pulse sequence with delay between pulses 120 µs: $T_{2\text{eff}\,PE} = 545$ µs, $T_{2\text{eff}\,PVC} = 352$ µs.

Fig. 1 is showed correlation maps for $T_1{\times}T_2$ and $T_2{\times}T_{2\text{eff}}$ for a mixture of polyethylene and polyvinylchloride samples. Errors in the numerical determination of relaxation times may be due to the peculiarities of the inverse Laplace transform [5].

1. Ernst R.R., Bodenhausen G., Wokaun A.: Principles of Nuclear Magnetic Resonance in One and Two Dimensions. Oxford University Press, New York, US, 1994.
2. Song Y.Q., Venkataramanan L., Hürlimann M.D., Flaum M., Frulla P., Straley C.: J. Magn. Reson. **154**, 261–268 (2002)
3. Ursu I., Balibanu F., Demco D.E., Bogda M.: phys. stat. sol. (b) **136**, 309 (1986)
4. Bogaychuk A., Kuzmin V.: Review of Scientific Instruments **91**(10), 103904 (2020)
5. Fricke S., Seymour J., Battistel M., Freedberg D., Eads C., Augustine M.: Journal of Magnetic Resonance **313**, 106704 (2020)

Determination of Position of Impurity Er³⁺ Ion at Cubic Sites in CsCaF₃ Single Crystals

M. L. Falin[1], V. A. Latypov[1], S. L. Korableva[2]

[1] Zavoisky Physical-Technical Institute, FRC Kazan Scientific Center of RAS, Kazan 420029, Russian Federation, falin@kfti.knc.ru

[2] Kazan (Volga Region) Federal University, Kazan 42008, Russian Federation

Double fluoride crystals with perovskite structure $A^+B^{2+}F_3^-$ (A = Cs, B = Ca) are very interesting because, on the one hand, they find extensive application in practice, and, on the other hand, they are convenient model systems for studying magneto-optical properties of impurity dopant ions. In principle, it is possible to substitute two various cations in inequivalent positions in these matrices. This enables one to carry out investigations of impurity dopant ions in sixfold or twelvefold coordination. The recent research indicates that on certain conditions of the CsCaF₃ crystals growth it is possible to form fluorite nano- or microcrystallites [1]. This report is concerned with the further investigation of impurity paramagnetic centers formed by Er³⁺ ions by EPR method.

The crystals were grown using the Bridgman-Stockbarger method. The concentration of the impurity ions was 0.1–1.0 w%. EPR experiments was carried out using an X-band spectrometer ERS-231 (Germany) at $T = 4.2$ K.

The complete coincidence of EPR spectra of new centers Er³⁺ in CsCaF₃ and Er³⁺ of cubic symmetry in CaF₂ was discovered. This implies the existence of self-organized fluorite nanocrystals in CsCaF₃ crystals, the concentration of which may vary arbitrarily. The given supposition rejects a possibility of position-
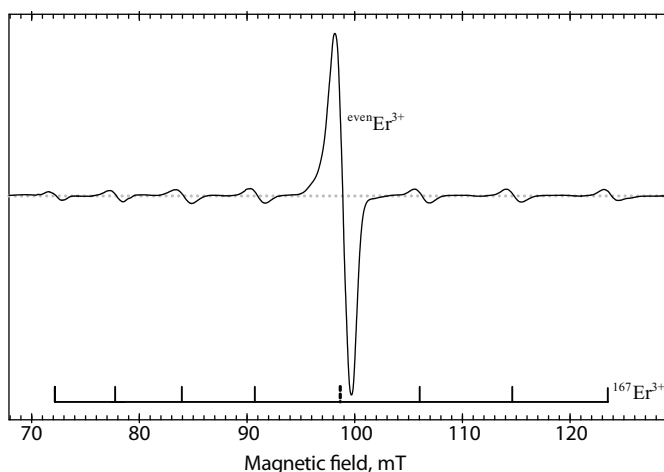
Fig. 1. EPR spectrum of centers Er³⁺ in CsCaF₃ at $T = 4.2$ K.

ing Er^{3+} ion at Cs site, as the crystal field of twelvefold coordinated complexes cannot coincide with coordination in CaF_2 nanocrystal.

The parameters of the corresponding spin Hamiltonians, the ground states and their wave functions were determined. Structural models of the observed complexes were proposed.

1. Falin M.L., Latypov V.A., Gerasimov K.I.: Appl. Magn. Reson. **45**, 707 (2014)

Incoherent-Light Pulse Annealing of Nanoporous Germanium Layers Formed by Ion Implantation

**B. F. Farrakhov, A. L. Stepanov, Ya. V. Fattakhov, D. A. Konovalov, V. I. Nuzhdin, V. F. Valeev**

Zavoisky Physical-Technical Institute, FRC Kazan Scientific Center of RAS, Kazan 420029, Russian Federation, bulat_f@mail.ru

The study addresses the monocrystalline c-Ge substrates implanted by Ag^+ ions with the energy of 30 keV, irradiation dose of $7.5 \cdot 10^{16}$ ion/cm^2 and annealed by incoherent-light pulse. By scanning electron microscopy and optical spectroscopy measurements it was shown that after ion implantation an amorphous porous Ag:PGe layer of a spongy structure with nanowires on the c-Ge substrate were formed. The spongy pulse light annealed structure of the Ag:PGe layer was not destroyed, however the diameters of nanowires increased by about 1.5 times.

Monocrystalline c-Ge (100) n-type plates 150 |mkm thick were selected as substrates. Implantation was carried out by Ag^+ ions with $E = 30$ keV, $D = 7.5 \cdot 10^{16}$ ion/cm^2 at current density $J = 8$ mkA/cm^2 using an ILU-3 ion accelerator at room temperature of the irradiated substrate and normal angle of incidence of the ion beam on the irradiated c-Ge surface. The implanted Ag:PGe samples were annealed in air by ILP by special "Impuls-6" equipment with halogen lamps located in a sealed reaction chamber as heating elements (Fig. 1). Annealing of implanted Ge was realized with 1 light pulse, duration 5 s. The power density of the light pulse was 30 W/cm^2. The surface sample temperature was measured to be near 600 °C.

The surface morphology of the Ag:PGe samples was studied using Merlin (Carl Zeiss) scanning electron microscope (SEM). Elemental chemical analysis was performed using X-Max energy dispersive (EDX) spectrometer (Oxford Instruments) in the same microscope. Optical reflection spectra were measured by AvaSpec-2048 spectrometer (Avantes) at the normal angle of incidence of the probe and reflected light beam to the surface of the samples through a paired waveguide in the spectral range from 220 to 1100 nm at room temperature.
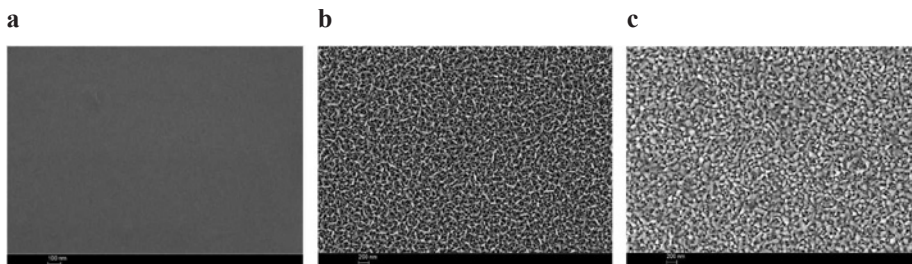
Fig. 1. SEM-images of surfaces (**a**) c-Ge, (**b**) c-Ge implanted by Ag^+ ions at $E = 30$ keV, $J = 8$ mkA/cm^2, $D = 7.5 \cdot 10^{16}$ ion/cm^2 and (**c**) and same implanted sample treated by ILP annealing.
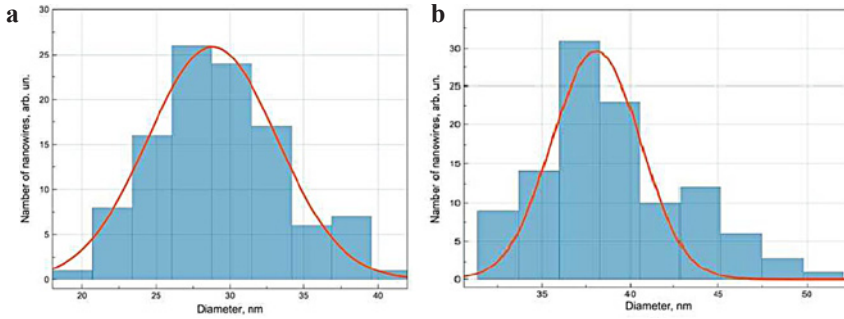
Fig. 2. Histograms of the nanowire diameters for the c-Ge implanted by Ag^+ ions at $E = 30$ keV, $J = 8$ mkA/cm², $D = 7.5 \cdot 10^{16}$ ion/cm² (**a**) and the same implanted sample treated by ILP annealing (**b**).

Fig. 1 shows SEM images of the surfaces for the virgin c-Ge, Ag:PGe layer formed by implantation with Ag^+ ions and the same sample after ILP annealing. The surface of the c-Ge substrate was flat and smooth (Fig. 1a). Ion implantation leads to the formation of an amorphous Ag:PGe layer of a spongy structure consisting of nanowires with the diameter of ~29 nm (Fig. 1b), as it was described in detail earlier.

ILP annealing of Ag:PGe sample does not dramatically modify the spongy layer with nanowires (Fig. 1b), only their average diameter size increased by about 1.5 times relative to the implanted surface. Such quantitative dimensional difference could be clearly recognized from the histograms of the nanowire diameter distribution (Fig. 2a and b). To explain the changes of nanowire diameter after annealing, it may be assumed that when the implanted layer with a sponge structure is heated during the interaction with light pulses the individual narrowest nanowires partially melted. After that, melted materials sinter together with unmelted nanowires and caused the appearance of nanowires of a larger diameter. Apparently, this process is similar to Ostwald ripening observed usually in a
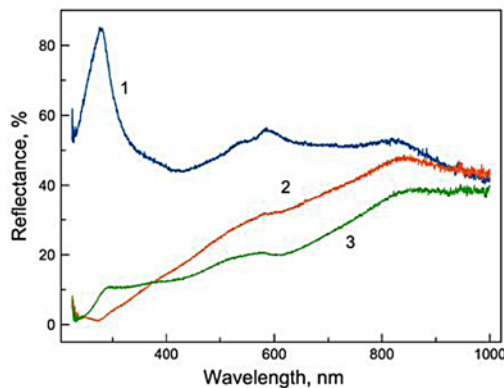
Fig. 3. Optical reflection spectra from various samples: (1) c-Ge, (2) c-Ge implanted by Ag^+ ions at $E = 30$ keV, $J = 8$ mkA/cm², $D = 7.5 \cdot 10^{16}$ ion/cm² and (3) and same implanted sample treated by ILP annealing.

colloidal solution, implanted, lithography prepared materials with nanoparticles, in which after increasing solution temperature smallest particles melt, and their constituent material is gettered to enlarge bigger particles. Thus, in the present case of the implanted Ag:PGe layer heating by ILP, such process could occur because the melting temperature for Ge nanoobjects essentially decreases in dependence of their size from the value of melting point corresponding to the bulk material 938 °C, which leads to the predominant melting of thinnest nanowires. It should be mentioned that Ostwald ripening mechanism was also used to explain the growth and reconstruction of nonvoids in the electrochemically fabricated meso-porous Ge layers during equilibrium thermal annealing.

The optical reflection spectra was measured in the visible range for the qualitative estimation of changes in crystallinity of Ag:PGe sample surface after ILP annealing. Spectra of the virgin c-Ge, Ag:PGe layer formed by implantation with Ag^+ ions and the same sample after ILP annealing are presented in Fig. 3. The reflection spectra of Ge implanted with Ag^+ ions in a wide range of D were described in detail earlier in the work. These data allow concluding that the reflection spectrum of the crystalline surface of the virgin c-Ge substrate (curve 1, Fig. 3) changes after the ion implantation to the reflection characteristic of the implanted amorphous a-Ge layer (curve 2, Fig. 3). For this case, a sharp decrease in the intensity of the reflection bands responsible for the interband transitions and spin orbit interaction in Ge with the maxima at 276 nm and a double peak at 564 nm respectively. Amorphization of the near surface layer of Ge and a decrease in the intensity of the corresponding fundamental optical reflection bands after irradiation with O^+ and Ni^+ ions measured from flat and smooth implanted surfaces were also observed earlier in the works. Additionally, such intensity decrease in the ultraviolet spectral region is also caused by the formation of a dark PGe layer on the surface of the c-Ge substrate called in a literature as "black Ge". As follows from Fig. 3 (curve 3), after ILP annealing the intensity of the band increases at 276 nm in the reflection spectra, that indicates a partial recovery of the Ge crystal lattice in nanowires from the amorphous state. A similar partial recrystallization of the Ge was detected after heating with He-Ne laser amorphous nanowire PGe layers fabricated by electrochemical etching in aqueous solutions and by ion implantation in a vacuum.

Thus, the present research discusses the experimental study of c-Ge substrates implanted by Ag^+ ions at $E = 30$ keV, $J = 8$ mkA/cm^2, $D = 7.5 \cdot 10^{16}$ ion/cm^2 and annealed by ILPs. Fast ILP annealing, which gives the achievement against to equilibrium thermal annealing, indicates the practical effectiveness of this technique for the industrial use. It was shown that as a result of ion implantation an amorphous porous Ag:PGe layer of a spongy structure with nanowires is formed on the c-Ge surface. ILP annealing of the implanted samples leads to partial melting and recrystallization of the surface Ag:PGe layer. While the spongy structure of the annealed layer is retained, the diameters of Ge nanowires increase by about 1.5 times.

Distribution of ^{14}N NQR Relaxation Times in Sulfonamide Polymorphs

M. Fedotov[1], I. Mershiev[1], G. Kupriyanova[1], N. Sinyavsky[1,2]

[1] Immanuel Kant Baltic Federal University, Kaliningrad 236016, Russian Federation,
mfedotov1994@gmail.com
[2] Kaliningrad State Technical University, Kaliningrad 236022, Russian Federation

The development of new methods for studying the polymorphism of solid forms is an actual problem. Different polymorphic modifications of the same drug may require using of different technologies to obtain the substance, determine its stability, biological compatibility, therapeutic efficacy, and drug resistance to destruction and aging.

Understanding polymorphism remains a contemporary scientific issue in solid state chemistry. Polymorphic transformations cause serious issues with the proposal of mechanisms that could explain what actually happens to molecules in time and space.

As follows from the literature, the features of polymorphic states and the phase transition mechanisms in sulfonamide have not been elucidated in detail. This work is devoted to the study of the dynamics of sulfonamide polymorphic modifications by determining the distribution functions of the spin-lattice and spin-spin relaxation times of ^{14}N NQR. This information is important for the development of recommendations for identification, quality control of a substance in the required polymorphic form, and determination of the mixed polymorphic states composition.

There are three polymorphic forms of sulfanilamide: α, β and γ. The most stable polymorph is the β-polymorph. Sulfanilamide polymorphism has been previously studied by many methods, including NMR and NQR. The first NQR
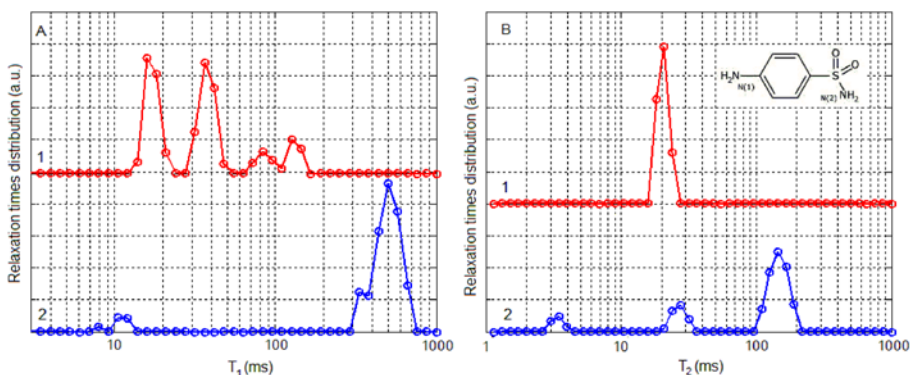
Fig. 1. Distribution of ^{14}N NQR relaxation times for the $\nu_- = 2.495$ MHz line of the N(1) atom (curve 1) and the $\nu_- = 2.565$ MHz line of the N(2) atom (curve 2) for the β-form of sulfanilamide.

measurements of nitrogen in β-sulfonamide at $T = 77$ K were carried out in [1]. The review [2] demonstrated a clear difference between three known polymorphic modifications of sulfanilamide; the complete ^{14}N NQR spectra at $T = 295$ K are given for two different nitrogen positions of all three polymorphs.

Relaxation experiments were performed on a Tecmag Apollo NQR spectrometer at $T = 295$ K with subsequent inversion of Laplace transform. The NQR relaxation times of nitrogen atoms in the amino group and sulfonamide group make it possible to characterize the dynamics of the crystal lattice and the environment of these atoms.

The results of determining the distributions of the spin-lattice relaxation times T_1 and spin-spin relaxation T_2 for the resonance lines on frequency ν- of the atoms N(1) and N(2) of ^{14}N NQR in the β-phase of $C_6H_8N_2O_2S$ are shown in Fig. 1.

If the traditional method for determination the times T_1 for N(1) and N(2) gives 25 ms and 400 ms [2], respectively, then the spectrum of times T_1 obtained by the Laplace transform inversion method is much more complicated. Thus, the T_1 distribution for the N(1) atom consists of four lines. This means that there are several para-amino groups in the crystal lattice with different mobility. The distribution of T_1 times for nitrogen of the sulfonamide group is practically unimodal.

The spin-spin relaxation times T_2 are determined by the interaction of spins with each other, and also, to some degree, for much the same reasons as T_1. The T_2 distribution for nitrogen N(1) consists of one peak, while the T_2 spectrum for N(2) gives three peaks of different intensities. This is due to the fact that in the crystal the spins N(2) of different molecules are reside at different distances and interact with each other in different ways.

In this work, the distribution of relaxation times for different polymorphic states of sulfanilamide is presented and analyzed. This allows us to make assumptions about the structure and dynamics of polymorphs.

1. Subbarao S.N., Bray P.J.: J. Med. Chem. **22**, 111 (1978)
2. Trontelj Z., Pirnat J., Jazbinšek V. *et al.*: J. Crystals **10**, 450 (2020)

Chain Fe (III) Complexes with Tetradentate Ligands

E. Frolova, O. Turanova, L. Gafiyatullin, L. Bazan, A. Turanov, I. Ovchinnikov

Zavoisky Physical-Technical Institute, FRC Kazan Scientific Center of RAS, Kazan 420029, Russian Federation, fro-e@yandex.ru

This work is devoted to the UV-vis and EPR study of chain Fe (III) spin-variable complexes with tetradentate ligands. The general formula of the compounds is $[Fe(L)(tvp)]BPh_4 \cdot nCH_3OH$, where L = dianions of N_2O_2 tetradentate ligands containing a different number of aromatic groups: N,N′-ethylenebis(salicylaldimine) (salen), N,N′-ethylenebis(acetylacetone)2,2′-imine (acen), N,N′-ethylenebis(benzoylacetylacetone)2,2′-imine (bzacen). The photosensitive bidentate ligand tvp = 1,2-di(4-pyridyl)ethylene was used as the axial bridging ligand. The aim was to reveal the effect of the equatorial ligand on the SCO properties of chain Fe (III) complexes with unchanged axial ligand and counterion.

The values of exchange interactions, thermodynamic parameters of spin-crossover and electronic structure features of the Fe (III) complexes were estimated from the EPR data.

Shown, that in the presence of aromatic fragments in the equatorial ligand salen, HS Fe(III) complexes are formed. In the complex with bzacen, the equatorial ligand of which contains both aromatic and aliphatic groups, the spin transition occurs in the range 130–230 K. The presence of only aliphatic groups in the acen equatorial ligand leads to a change in the spin state of Fe (III) complexes to LS at higher temperatures ($T_{1/2} \sim 328$ K), so that the spin transition started at temperatures above 300 K and almost completed at 150 K at cooling. At temperatures below 150 K, ~1% of the complexes are in the HS state and do not participate in the spin transition.

Thus, the structural changes associated with the substitution of a fragment of the equatorial ligand L in the series salen–acen–bzacen change the local symmetry of the complex in the 1-D chain, thereby affecting the spin variable properties. The achieved results provide information for the molecular design of SCO material based on Fe (III) complexes with tetradentate Schiff bases and bridging ligands of the pyridine family.

EPR Study of the Content of Nitric Oxide and Copper in the Hippocampus of Rats in the Acute Phase of Ischemic Stroke

Kh. L. Gainutdinov[1,2], G. G. Yafarova[1,2], V. V. Andrianov[1,2], A. S. Zamaro[3], Y. P. Tokalchik[3], L. V. Bazan[1], T. Kh. Bogodvid[2,4], V. S. Iyudin[1], V. A. Kulchitchky[3]

[1] Zavoisky Physical-Technical Institute, FRC Kazan Scientific Center of RAS, Kazan 420029, Russian Federation, kh_gainutdinov@mail.ru
[2] Institute of Fundamental Medicine and Biology of Kazan Federal University, Kazan 420008, Russian Federation
[3] Institute of Physiology of Nat. Acad. of Sci. of Belarus, Minsk 220072, Belarus
[4] Volga Region State University of Physical Culture, Sport and Tourism, Kazan 420010, Russian Federation

Brain ischemia can be caused by a decrease in the oxygen content, or disruptions of the cerebral blood flow can lead to a lack of oxygen supply to parts of the brain, which can culminate in ischemic insult defined as acute damage of brain tissue, with a disruption of its functions due to the difficulty or cessation of blood flow to brain areas [1, 2]. Therefore the study of pathogenesis, treatment and the mechanisms of stroke are important from both the theoretical and practical points of view [3, 4]. The functioning of neurotransmitter systems, including the nitric monoxide system, is disrupted during hypoxia and brain ischemia. Nitric oxide (NO) is known as one of the most important signaling molecules regulating the physiological functions of the organism and the metabolism of cells [5, 6]. There is interest in the participation of NO in the mechanisms of development of various pathological processes [2, 7–9]. NO performs its physiological functions by binding to iron (Fe) ions in heme, or through S-nitrosylation of proteins, and also participates in a number of biochemical reactions. Currently, the development of brain ischemia and the subsequent occurrence of stroke is associated with disorders of cerebral blood flow, as well as with violations of its regulation by the NO system [3, 4, 6, 7]. In addition to regulating the NO level, antioxidant enzymes are another way to protect against highly toxic oxygen radicals. This is the cytosolic enzyme Cu, Zn-SOD (superoxide dismutase – SOD), which serves as the primary and main protection against free radical oxidation processes [10]. Therefore, the purpose of this work was to study the intensity of NO and copper production in the rat hippocampus by electron paramagnetic resonance (EPR) spectroscopy in the simulation of brain ischemia.

Brain ischemia was modeled by ligation of the common carotid arteries at the bifurcation level in male Wistar rats ($n = 10$) under ketamin-xylazine-acepromazine anesthesia [11]. The second group consisted of intact animals ($n = 10$) that were not subjected to surgical manipulations in the brain area. The method of EPR spectroscopy was used to estimate the NO production by the integral intensity of the complex $(DETC)_2\text{-}Fe^{2+}\text{-}NO$ in rat hippocampal tissues [12]. Formation of a complex $(DETC)_2\text{-}Fe^{2+}\text{-}NO$ was described earlier [6, 13].

The components of the spin trap NO (DETC-Na, $FeSO_4$, sodium citrate) was injected 30 minutes before the extraction of studied tissue. The main measurements were carried out on the EPR spectrometers of the 3-centimeter range of the Bruker company ER 200 SRC and EMX/plus with the temperature prefix ER 4112HV in the X range (9.50 GHz).

It was shown that the NO content in the hippocampus decreased by an average of 50% on the next day after modeling brain ischemia, and the NO content in the hippocampus was restored 2 days after modeling brain ischemia. No significant changes were found in the copper content associated with the superoxide dismutase content.

1. Donnan G.A., Fisher M. *et al.*: Lancet **371**, 1612–1623 (2008)
2. Manukhina E.B., Malyshev I.Y. *et al.*: Nitric Oxide **3**, 393–401 (1999)
3. Terpolilli N.A. *et al.*: J. Cereb. Blood Flow Metab. **32**, 1332–1346 (2012)
4. Andrianov V.V., Yafarova G.G. *et al.*: Appl. Magn. Reson. **51**, no 4, 375–387 (2020)
5. Vanin A.F.: Nitric Oxide **54**, 15–29 (2016)
6. Gainutdinov Kh.L., Gavrilova S.A. *et al.*: Appl. Magn. Reson. **40**, no 3, 267–278 (2011)
7. Bolanos J.P. , Almeida A.: Biochim. Biophys. Acta. **1411**, 415–436 (1999)
8. Pacher P., Beckman J.S., Liaudet L.: Physiol. Rev. **87**, 315–427 (2007)
9. Reutov V.P., Okhotin V.E. *et al.*: Uspekhi Physiol. Nauk **38**, no 4, 39–58 (2007)
10. Miller A.F.: FEBS Lett. **586**, 585–595 (2012)
11. Shanko Y., Zamaro A. *et al.*: J. Sci. Tech. Res. **7** (5), MS.ID.001567 (2018)
12. Vanin A.F., Huisman A. *et al.*: Methods in Enzymology **359**, 27–42 (2003)
13. Ismailova A.I. *et al.*: Appl. Magn. Reson. **28**, 421–430 (2005)

DFT-Assisted Study of Conformation of γ-Irradiated Calcium Gluconate

A. R. Gafarova, G. G. Gumarov, V. Yu. Petukhov, R. B. Zaripov, M. M. Bakirov

Zavoisky Physical-Technical Institute, FRC Kazan Scientific Center of RAS, Kazan 420029, Russian Federation, Albina-gafarova@gmail.ru

Calcium gluconate is widely used in the chemical and food industries, it is used as a drug for the treatment of diseases associated with a lack of calcium in the body. Also, interest in the study of this compound is high in connection with the development of a mechanically activated modified nanodispersed amorphous form of calcium gluconate (MACG), the treatment efficiency of which is much higher. It is assumed that an increase in the bioavailability of the drug may be associated with a change in the conformation of the calcium gluconate (GC) molecule. Given the high importance of calcium gluconate for industrial and medical applications, it is surprising that its structure has remained unexplored for a long time. In this regard, it seems attractive to use quantum chemical methods to study the structure of calcium gluconate.

The starting material was a calcium gluconate powder manufactured by Sigma Aldrich. The samples were placed in a special cuvette and irradiated with photons on a Rokus gamma-therapeutic apparatus with an average energy of 1.25 MeV. The resulting radiation doses were 400, 600, 800 and 1000 Gy. EPR spectra were measured in the X- and Q-bands at room temperature.

Quantum-chemical modeling was carried out using the ORCA software package [1], [2]. For the calculation, the density functional theory (DFT) method was used, namely the unrestricted Kohn-Sham method. We took the X-ray diffraction data as the coordinates of the atoms [3]. The IGLO III basis was used to calculate the hyperfine coupling (HFC) parameters and the g-factor. To refine the HFC parameters and the g-factor, the model spectra (calculated from the ORCA data) were fitted to the experimental EPR spectra using EasySpin package [4].
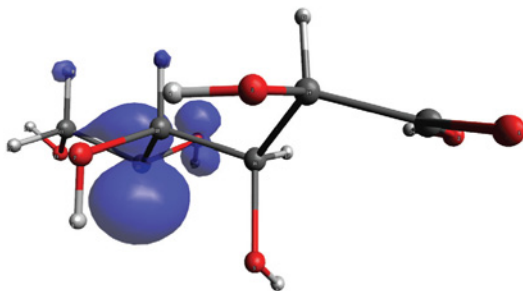

Fig. 1. Spin density distribution of radical on gluconate anion.

The dependence of the isotropic HFC on the torsion angle between the axis of the π-radical and the direction of the beta bond of the proton with carbon turns out to be more complicated than the square of the cosine of the angle. This is due to the preservation of a certain degree of tetrahedrality of valence bonds when the hydrogen atom is removed from the carbon. In this case, the hybridization changes from sp3 to sp2, and a π-radical is formed. Here it is necessary to take into account that the calcium gluconate molecule remains bound in the crystal structure. This does not allow the carbon atom and its three neighbors to be in the same plane - a certain degree of tetrahedrality will remain. In addition, this leads to a violation of the axial symmetry of the spin density distribution, as well as a difference in this density above and below the plane passing through the nodal point of the radical perpendicular to the axis (Fig. 1). Nevertheless, a quantum chemical calculation makes it possible to establish a relationship between the torsion (and valence) angles and the values of the parameters of the HFC and the g-factor. In combination with the refinement of these parameters on the basis of EPR spectra in two bands, this method makes it possible to identify radicals formed when gluconates are irradiated with gamma quanta. In particular, it was found that the EPR spectra of GC irradiated in the range of 400–1000 Gy can be decomposed into three components corresponding to radicals on the C2, C3, C5 atoms, (numbering starting from the carbon atom closest to the calcium atom). The calculated values of the hyperfine splitting of the radical at the C4 carbon atom turned out to be much higher than those observed by us experimentally. This confirms our earlier conclusion that there is no radical on the C4 atom.

This indicates the possibility of using this method for the conformational analysis of the studied compounds.

1. Neese F.: The ORCA program system, WIREs Comput. Mol. Sci. **2**, 73–78 (2012). https://doi.org/10.1002/wcms.81
2. Neese F.: Software update: the ORCA program system, version 4.0, Wiley Interdiscip. Rev.: Comput. Mol. Sci. **8** (2017), e1327. https://doi.org/10.1002/wcms.1327
3. Bugris V., Dudas Cs., Kutus B., Harmat V., Csanko K., Brockhauser S., Palinko I., Turner P., Sipos P.: Acta Cryst (2018) https://doi.org/10.1107/S2052520618013720
4. Stoll S., Schweiger A.: J. Magn. Reson. **178** (1), 42 (2006)

Peculiarities of the *ac*-Susceptibility in the Vicinity of Level Anticrossing

R. T. Galeev

Zavoisky Physical-Technical Institute, FRC Kazan Scientific Center of RAS, Kazan 420029, Russian Federation, galeev_rt@rambler.ru

A model system the ground state of which has level anticrossing is considered. The dependence of ac-susceptibility on the frequency of the non-resonance magnetic field was calculated for the system. This dependence has a maximum at a frequency equal to the relaxation rate. It is shown that the position of the maximum ac-susceptibility can depend on the value of the anticrossing. At certain ratios between the rates of population relaxation and coherence decay, two peaks may appear in the frequency dependence. Two peaks are usually explained by the presence of two relaxation mechanisms with different distribution of relaxation times. However, the manifestation of two peaks in the given model dependencies is associated with the nonlinearity of the response in the vicinity of the anticrossing. Such manifestations can lead to incorrect interpretation of the relaxation data in the system.

Iron Oxidation State in La$_{0.7}$Sr$_{1.3}$Fe$_{0.7}$Ti$_{0.3}$O$_4$ and La$_{0.5}$Sr$_{1.5}$Fe$_{0.5}$Ti$_{0.5}$O$_4$ Layered Perovskites

T. P. Gavrilova[1], Yu. A. Deeva[2], I. V. Yatsyk[1,3], I. F. Gilmutdinov[3], M. A. Cherosov[3], F. G. Vagizov[3], T. I. Chupakhina[2], R. M. Eremina[1,3]

[1] Zavoisky Physical-Technical Institute, FRC Kazan Scientific Center of RAS, Kazan 420029, Russian Federation, tatyana.gavrilova@gmail.com
[2] Institute of Solid State Chemistry of the Russian Academy of Sciences (UB), Ekaterinbur, 620990, Russian Federation
[3] Institute of Physics, Kazan Federal University, Kazan 420008, Russian Federation

Layered perovskite structures with the chemical formula A2BO$_4$, (where A is a rare earth or alkaline earth element, and B is d-metals of the IV period of the periodic table), are widely known and intensively studied, since they possess a multifunctional set of properties that are promising for practical applications. In the A$_2$BO$_4$ structure, the ABO$_3$ layers with the perovskite structure are separated by A-O layers of rock salt, and the B-O-B electronic interactions can occur only in the plane. Variations in electrical, magnetic, catalytic, and other properties are possible both by isomorphic substitution of cations in the B positions, and by conjugate substitution in the B and A positions.

The investigated here Sr$_{2-x}$La$_x$Ti$_{1-x}$Fe$_x$O4 (x = 0.5 and 0.7) are materials with a high dielectric constant $\varepsilon \approx 10^5$ [1]. One of the reasons for the high values of the dielectric constant of these oxides was the small polaron hopping conduction mechanism presumably due to the different valence state of Fe that requires a detailed investigation of their magnetic properties. So the magnetometry, electron spin resonance and Mossbauer spectroscopy measurements of La$_x$Sr$_{2-x}$Fe$_x$Ti$_{1-x}$O$_4$ (x = 0.5 и 0.7) oxides were performed to prove the existence of mixed-valence iron ions and study the associated effects [2].
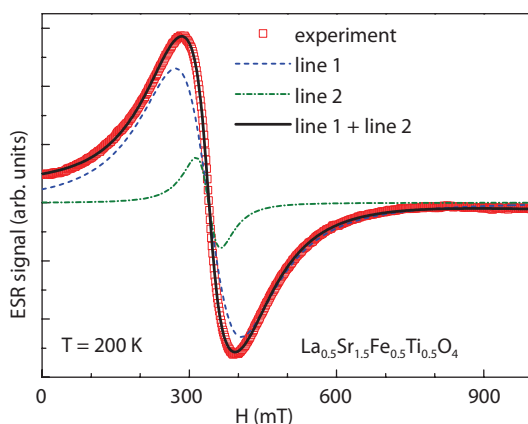
Fig. 1. Decomposition of the ESR spectrum of La$_{0.5}$Sr$_{1.5}$Fe$_{0.5}$Ti$_{0.5}$O$_4$ at T = 200 K in X-band.
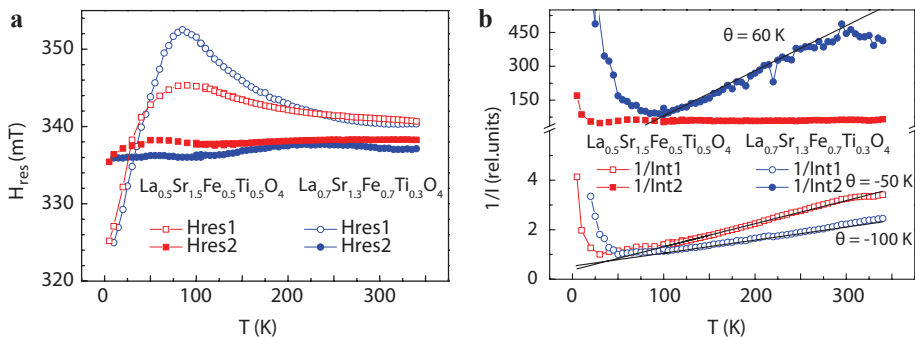
Fig. 2. Temperature dependence of (**a**) resonance field, (**b**) inverse normalized integral intensity I^{-1} of two lines in ESR spectra of $La_{0.5}Sr_{1.5}Fe_{0.5}Ti_{0.5}O_4$ and $La_{0.7}Sr_{1.3}Fe_{0.7}Ti_{0.3}O_4$.

Based on our magnetization and electron spin resonance measurements it was suggested the presence of the electronic phase separation in the investigated samples – the simultaneous existence of the paramagnetic phase and magnetically correlated regions. Two types of signals in ESR spectra were clearly detected (Fig. 1): from paramagnetic phase – line 1 and from magnetically correlated regions – line 2. One can see from Fig. 2 that the integral intensity of the ESR signal from the paramagnetic phase (line 1) is two orders of magnitude higher than from magnetically correlated phase (line 2) assuming that samples are in a paramagnetic phase with a small inclusion of magnetically correlated regions.

Detailed investigations of obtained experimental data showed that the significant proportion of samples volume is a paramagnetic phase which is ordered antiferromagnetically at the phase transition temperature, while the second phase is ferromagnetically correlated regions in $La_{0.5}Sr_{1.5}Fe_{0.5}Ti_{0.5}O_4$ and canted ferrimagnetically correlated regions in $La_{0.7}Sr_{1.3}Fe_{0.7}Ti_{0.3}O_4$. The electronic phase separation can be realized due to the mixed-valence iron ions that mean the presence of Fe^{4+} ions in addition to trivalent iron ions and that was exactly confirmed by Mossbauer spectroscopy investigations [2].

1. Chupakhina T.I., Melnikova N.V., Kadyrova N.I. *et al.*: Journal of Solid State Chemistry **292**, 121687 (2020)
2. Gavrilova T.P., Yagfarova A.R., Deeva Yu.A. *et al.*: Journal of Physics and Chemistry of Solids **153**, 109994 (2021)

NMR Study of Size Effects in Ferromagnetic Nanoparticles

A. Yu. Germov, D. A. Prokopyev, K. N. Mikhalev, A. S. Konev

M. N. Miheev Institute of Metal Physics of Ural Branch of Russian Academy of Sciences, 620108, Russian Federation, germov@imp.uran.ru

Magnetic nanoparticles are of interest with increasing number of their practical applications. Fundamental research of pure metals of the iron group in the nano state faces significant technical difficulties [1], for example, due to the impossibility of avoiding surface oxidation when interacting with an environment. It is difficult to separate the chemically driven surface effects from the fundamental physical properties associated with size. At a certain size of nanoparticles corresponding to a transition to a single-domain state [2], abnormal magnetic properties of the iron group metals should be observed. In a number of applications, such as using of magnetic particles in suspensions, it is important to distinguish whether the particles remain multidomain or single domain, since this affects the stability of the suspensions. Therefore, for practical applications of magnetic nanoparticles, it is very important to identify these states.

We performed ^{57}Fe, ^{59}Co, ^{61}Ni NMR in ferromagnetic nanoparticles based on pure metals and bimetallic alloys [3, 4]. It has been shown that nanoscale effect consists in an increase of the hyperfine field in ferromagnetic single domain state. This change is connected with additional demagnetizing field. Estimates of the proportion and size of single domain particles have been made. Combination of NMR and Mossbauer spectroscopy can provide quantitative information about phase composition of magnetic iron nanoparticles [5].

1. Uimin M.A. *et al.*: Phys. Met. Metallogr. **120**, 228–232 (2019)
2. Leslie-Pelecky D.L., Rieke R.D.: Chem. Mater. **8**, 1770–1783 (1996)
3. Mikhalev K.N. *et al.*: J. Phys. Conf. Ser. 1389 (2019)
4. Mikhalev K.N. *et al.*: Mater. Res. Express **5**, 055033 (2018)
5. Germov A.Yu. *et al.*: Materials Today Communications **27**, 102382 (2021)

Anisotropy of the Paramagnetic Susceptibility in the 3D Dirac Semimetal Cd_3As_2 Caused by Chromium Impurity: the ESR on Cr^{3+} Ions

Yu. Goryunov[1], A. Nateprov[2]

[1] Zavoisky Physical-Technical Institute, FRC Kazan Scientific Center of RAS, Kazan 420029, Russian Federation, gorjunov@kfti.knc.ru
[2] Institute of Applied Physics, Chisinau, MD-2028, Moldova, nateprov@phys.asm.md

The influence of Cr impurities on the properties of 3D topological Dirac semi-metal Cd_3As_2 has been studied by ESR. Ions of transition d-metals (Fe and Mn) with the $3d^5$ configuration are in the S-state, and the total orbital angular momentum of their electrons is zero. Therefore, the magnetic state of these ions is traditionally considered purely spin with a g-factor equal to that of a free electron (2.0023). In the case of the $3d^3$ configuration Cr^{3+} ion with spin $S = 3/2$, the magnetic state of the ion is not purely spin and there is a significant admixture of the orbital angular momentum with $L = 3$. I.e. the influence of the orbital degree of freedom and hybridization of various valence states of chromium ions with the wave functions of free electrons of the Cd_3As_2 matrix on the properties of the material is obvious.

Cd_3As_2 ingots alloyed with 1–5 at% Cr were synthesized at 1023 K by both direct reaction of components, Cd (purity 99.999%), As (99.9999%), and Cr (99.99%), and via Cd–Cr alloys in glass–graphite crucibles placed in evacuated sealed-off quartz ampoules. The crystal structure and stoichiometry was verified by EDX analysis and powder X-ray diffraction (PXRD). The electron spin resonance (ESR) were measured on a standard Bruker modulation ESR spectrometer in the X range (9.3 GHz). ESR signals from Cr^{3+} ions were observed in the temperature range of 10–300 K. A single ESR signal had a distorted almost symmetric shape, in which one could see signs of a hyperfine structure. Note that in the natural mixture of chromium isotopes there is only 9% of the isotope with a nonzero nuclear spin, but the appearance of a hyperfine structure may be due to the interconfigurational interaction [2] with the nuclei of ligands Cd and As. It can be argued with a sufficient degree of confidence that the spectrum of the powder sample consists of at least 3 unresolved ESR lines with a width of about 300 Oe. The rapid decreasing of the resonance field H_0 was observed at low of temperature after a jump of H_0 at 120 K. In this case, it is passed a significant broadening of the spectrum. But the most interesting is the observation of the angular dependence of the position and width of the ESR signal (see Fig. 1). The fact is that the sample is a powder with a particle size of about 4 microns placed in paraffin and a cylindrical ampoule. The sample was rotated in a magnetic field around the ampoule axis. For the Cr ion, a small anisotropy of the g-factor is typical (typical values of g_x, g_y, g_z ~ 1.95–1.98). In Fig. 1 g-factor ranges from 2.13 to 2.18. In the case of a powder, where all crystallographic directions are equally probable, rotation of the ampoule cannot lead to a change in the position of the ESR signal. In our experiment, the angular dependence in
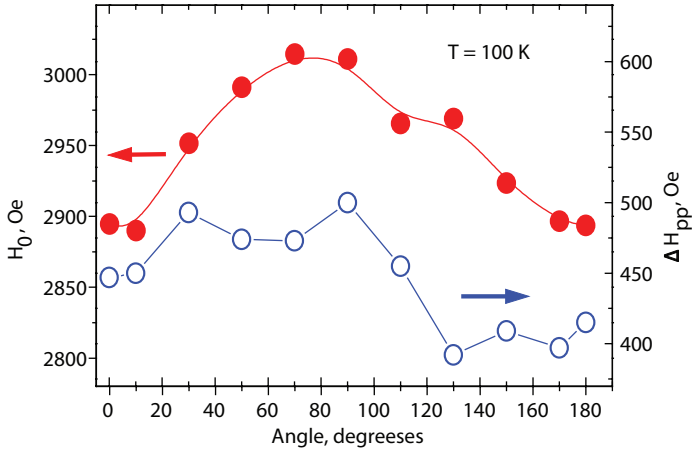
Fig. 1. Angle dependence of the resonance field and linewidth pic-to-pic.

Fig. 1 was obtained after melting the paraffin and holding the sample in a field of 13 kOe at a temperature of about 400 K for 15 min. and cooling in this field. This means that at a given temperature (~400 K), the magnitude of the induced magnetization of chromium ions depends on the crystallographic direction. We underline that pure Cd_3As_2 is strong diamagnet. Such, the magnetic state of the Cr^{3+} ion is significantly influenced by the orbital degrees of freedom, and in the case of Dirac quasiparticles, it can be expected that this effect will be enhanced due to the exchange interaction between localized magnetic moments and free carriers whose spins are rigidly related to their orbital moments. This leads to an increase in the g-factor of localized moments and to the appearance of anisotropy of the induced magnetization in the paramagnetic state. The report is devoted to a discussion of these results.

1. Goryunov Yu.V., Nateprov A.N.: Phys. Solid State **62**, 100 (2020)
2. Abragam A.: Phys. Rev. **79**, 534 (1950)

EPR of $Pb_{1-x}Ni_xS:Mn^{2+}$ Semiconductor Alloy Powder: Results of Double Doping of Galena

T. A. H. Housheya[1], A. V. Shestakov[2], I. V. Yatsyk[2], <u>V. A. Ulanov</u>[1,2]

[1] Kazan State Power Engineering University, Kazan 420066, Russian Federation,
ulvlad@inbox.ru
[2] Zavoisky Physical-Technical Institute, FRC Kazan Scientific Center of RAS, Kazan 420029,
Russian Federation

The lead chalcogenides represent an important family of functional materials, in particular due to the high-temperature thermoelectric performance. A number of recent investigations, experimental and theoretical, have aimed to gather insight into their unique lattice dynamics and electronic structure [1]. But, as we know, so far no research has been carried out on lead chalcogenide semiconductors aimed at studying the possibilities of obtaining new properties by doping them with polyvalent metals. We are also not aware of any work related to the doping of lead chalcogenides with two or more paramagnetic ions. In this work, galena (PbS), which belongs to the group of lead chalcogenides, was chosen as the basis material. Nickel was selected as the polyvalent impurity metal, and manganese was selected as the second impurity. The choice of the second impurity was dictated by the fact that this element was very widely used for doping various semiconductor materials to impart certain magnetic properties to them. The EPR method was used as a method for studying the properties of nickel and manganese ions formed in samples under study.

The purpose of this work was to find some effects associated with mutual dependences of properties of paramagnetic centers of nickel and manganese ions in the sample under study.

The $Pb_{1-x}Ni_xS:Mn^{2+}$ alloy was prepared from mixture of PbS and MnS with purities of 99.99 by a vertical zone melting with a very thin zone (5–10 mm) and low speed (1 mm/h). After the ingot was prepared it was powdered in an agate mortar to perform the experiment with a powder-like sample. This powder was sealed in a quartz capillary, which was then placed in the resonator of the spectrometer in the antinode of microwave magnetic field lines.

The EPR spectra of the sample under study were recorded by EPR spectrometer "Varian E-12" at temperatures of 4.2, 77, and 300 K. The main experimental results of this study are presented in Fig. 1. It can be seen in Fig. 1 that the general view of the EPR spectrum varies greatly with temperature. At the temperature of 4.2 K, the spectrum of the powder sample contains a number of rather narrow lines corresponding to different values of the external dc magnetic field and, consequently, to different values of the effective g-factor. There is no doubt about the origin of a group of six lines of equal intensity with a center of gravity at the point $B_0 = 331$ mT. These are the EPR lines of the manganese paramagnetic center. It was found that the Mn^{2+} ions are located in a crystal field of cubic symmetry and can be characterized by parameters $g = 2.008 \pm$
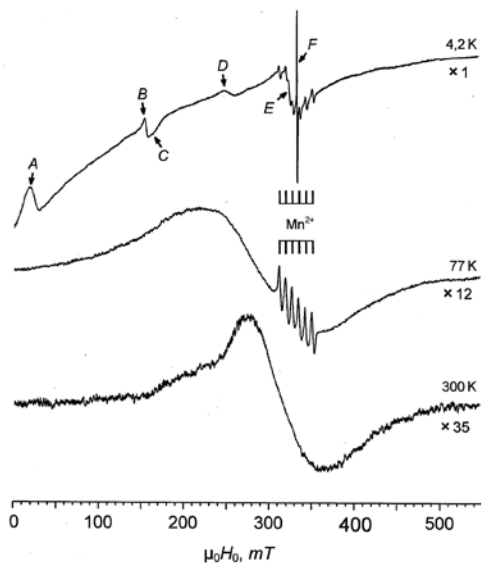
Fig. 1. EPR spectra of $Pb_{1-x}Ni_xS:Mn^{2+}$ alloy powder (f_{MW} = 9320 MHz).

0.001 and AHFI = 223 MHz. Regarding the line marked with the letter A, our previous studies clearly indicate that this line corresponds to non-resonant absorption of microwave power by microscopic inclusions of metallic lead. At the temperature of liquid helium, these particles are in a superconducting state.

Using the methods of decoding the powder EPR spectra, we determined the values of the g-factors for the observed EPR lines: g_B = 4.226 ± 0.005; $g_C \approx$ 4.015; g_D = 2.628 ± 0.005; g_E = 2.055 ± 0.005; g_F = 2.0026 ± 0.0003. The results of theoretical analysis of these values of the g-factors of the B-F lines indicate the following. The line B is associated with nickel centers in the (+3) valence state and localized in the positions of Pb^{2+} cations substituted by them. The coordination polyhedron of such Ni^{3+} (^4F, $3d^7$) ion is an octahedron at the vertices of which there are six S^{2-} ions. The positions of the D and E lines in the spectrum apparently determine the values of the principal components of the g-tensor of the Ni^+ (2D, $3d^9$) centers: $g_\parallel$ = 2.628 ± 0.005; $g_\perp$ = 2.055 ± 0.005. It is assumed that the tetragonal distortion of the coordination octahedron of an Ni^+ ion is due to the Jahn-Teller effect. The nature of the F line and unusual changes in the EPR spectrum with increasing temperature of the sample under study are discussed.

1. Pei Y.-L., Liu Y.: Journal of Alloys and Compounds **514**, 40 (2012)

Enhanced Intersystem Crossing due to Resonant Energy Transfer to a Remote Spin

## Yu. E. Kandrashkin[1], A. van der Est[2]

[1] Zavoisky Physical-Technical Institute, FRC Kazan Scientific Center of RAS, Kazan 420029, Russian Federation, yuk@kfti.knc.ru
[2] Department of Chemistry, Brock University, St. Catharines, Canada

A new mechanism for enhanced intersystem crossing (ISC) in coupled three-spin systems consisting of a chromophore with rigidly attached paramagnetic species is discussed [1]. It is based on resonant energy transfer from the chromophore to the radical involving a singlet to triplet transition of the chromophore. Two properties are significant for this mechanism: 1) The difference in the exchange interactions of the remote radical with the two unpaired electrons of the chromophore (ΔJ interaction) should be non-zero so that the singlet − triplet transitions of the chromophore become partially allowed, and 2) The energy gap for the S_1–T_1 transition ($\Delta E(S_1 - T_1) \approx J_0$) should be approximately in resonance with the excitation energy of the stable radical (ΔE_{uv}). Under these conditions, spin-orbit (SO) coupling on the remote spin can promote the ISC on the chromophore. In total, the ΔJ and SO interactions result in a concerted transition in which the chromophore undergoes a transition from its excited singlet state to its triplet state, while the radical is excited from the ground state to its lowest excited state. This process is shown schematically in Fig. 1.

The resonance condition is expected to be achieved in systems such as the lanthanide dyes in which the paramagnetic species exhibits significant SOC and NIR emission. In addition, the energy matching conditions for ΔE_{uv} for with higher excited states $\Delta E(S_n - T_k)$ could potentially lead to violation of the Vavilov-Kasha rule.

1. Kandrashkin Yu.E., van der Est A.: J. Phys. Chem. Lett. **12**, 7312–18 (2021)
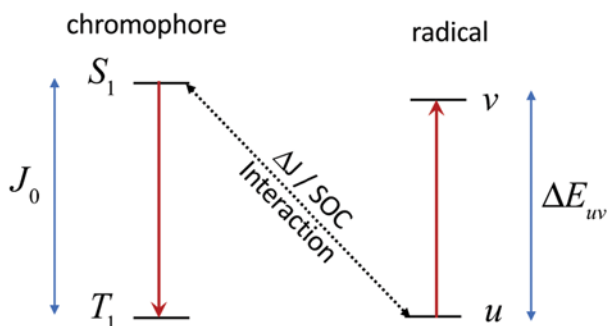
Fig. 1. The S_1–T_1 ISC pathway enchanced by the resonant energy transfer from the chromophore to the radical.

Phase Transformations in the System "Graphite Oxide – Acetonitrile" According to Spin Probe Technique

## A. V. Kaplin, A. T. Rebrikova, D. Popov

Chemistry Department, Moscow State University, Moscow, Russian Federation, avkaplin97@mail.ru

Graphite oxide (GO) is a layered material obtained by oxidation of graphite in an acidic environment. There are two main ways to obtain graphite oxide – Hammers' and Brodie's methods. The materials obtained by these methods (HGO and BGO) differ in degree of oxidation, composition of the oxygen-containing groups as well as ability to swell in polar liquids – HGO swells more easily compared to BGO. The membranes based on GO capable of retaining gases and sorbing, separating, and purifying many polar solvents.

In the systems "BGO–polar liquid" for acetonitrile, DMFA and alcohols the reversible phase transformations were observed with release of part of the sorbed liquid and decrease of the inter-plane distance. The aim of the present work was to establish the dependence of the phase transformations on the oxidation level of the material. Figure 1 shows the temperature dependence of the rotational mobility of the nitroxide spin probe sorbed on inner surface of BGO for one-stage (BGO1) and two-stage (BGO2) oxidized materials. In the case of BGO2 the anomaly at the temperature dependency is observed. The area of the temperature dependence of the radical's mobility reflects the phase transformation in the system.
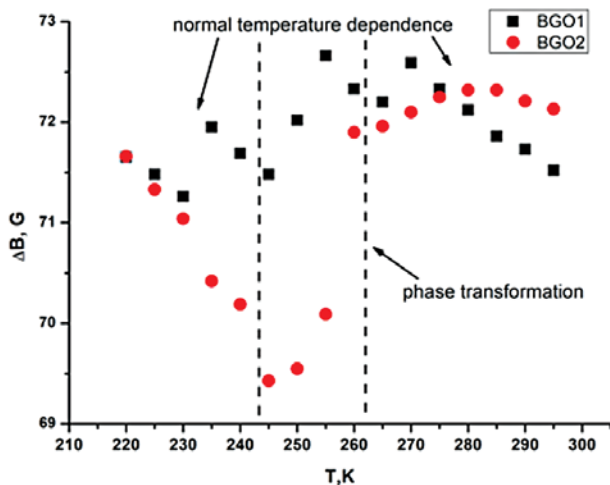
Fig. 1. Temperature dependence of the rotational mobility of the nitroxide spin probe sorbed on inner surface of BGO1 and BGO2.

Three Pulse ELDOR Simulation for the Case of Overlapping EPR Spectra of Spin Labels Taking into Account "Flip-Flop" Terms of Dipole-Dipole Interaction

I. T. Khairutdinov, K. M. Salikhov

Zavoisky Physical-Technical Institute, FRC Kazan Scientific Center of RAS, Kazan 420029, Russian Federation, semak-olic@mail.ru

The current theory of the four-pulse electron double resonance (PELDOR) has been extended to take into account two effects: (1) overlapping of the electron paramagnetic resonance (EPR) spectra of paramagnetic spin ½ particles (spin labels) in pairs and (2) overlapping of the excitation bands by the pump and echo forming pulses [1]. In our theoretical calculations nonsecular part of the dipole-dipole interaction has been taken into account. It has been shown that the PELDOR signal contains additional terms in contrast to the situation considered in the current theory, when the EPR spectra of the spin labels in the pairs and the excitation bands do not overlap [2]. The largest additional terms originates from the fact that both spins in pairs can be excited by the echo forming pulses when the EPR spectra of the partners in pairs do essentially overlap. When the difference of Zeeman frequencies greater than the spin-spin interaction all terms oscillate with the same frequency, which is the characteristic dipolar interaction frequency. In a situation where the difference of Zeeman frequencies becomes comparable with the value of the spin-spin interaction new oscillation frequencies appear in the PELDOR signal. The results of the numerical calculations, which illustrate the possible scale of the effect of these additional terms and additional frequencies on the PELDOR signal are presented.

1. Salikhov K.M., I.T. Khairuzhdinov I.T.: Appl. Magn, Reson. **46**, 67–83 (2015)
2. Salikhov K.M., Khairuzhdinov I.T., Zaripov R.B.: Appl. Magn, Reson. **45**, 573–620 (2014)

Stimulation of Plant Stress Resistance of Agricultural *Solanum Tuberosum L.* Using Metal-Containing Bionanocomposites Based on Polysaccharides

S. S. Khutsishvili[1], A. I. Perfil'eva[2], O. A. Nozhkina[2], N. I. Tikhonov[3]

[1] N. N. Vorozhtsov Novosibirsk Institute of Organic Chemistry, Novosibirsk 630090, Russian Federation, khutsishvili_sp@yahoo.com
[2] Siberian Institute of Plant Physiology and Biochemistry SB RAS, Irkutsk 664033, Russian Federation
[3] A. E. Favorsky Irkutsk Institute of Chemistry SB RAS, Irkutsk, 664033, Russian Federation

The potato is an important agricultural plant about a very sensitive organism to various types of stress, including phytopathogen, such as *Clavibacter michiganensis* bacteria (*Cms*). During the study of potato tissues the EPR spectra of plant tissues showed a singlet with a *g*-factor of 2.004(2) and a line width (ΔH) 8(1) G, see Fig. 1. The signal parameters are characteristic of stable semiquinone radicals. The level of semiquinone radicals can serve as an indicator of plant resistance to stress and is determined by the degree of damage to the cell structure, moisture loss, and other processes. To evaluate the stress state of plants under the action of the obtained (Mn, Fe and Cu)-containing bionanocomposites (NCs) based on natural polysaccharides (arabinogalactan, starch, *κ*-carrageenan), the following biochemical parameters were studied: peroxidase activity in the tissues of potato leaves, the content of reactive oxygen species (ROS), and the amount of lipid peroxidation (LPO) products, diene conjugates (DC) and malonic dialdehyde (MDA) in tissues of roots and leaves. Peroxidase is a very sensitive enzyme towards various stress factors. Therefore, changes in the activity of this enzyme can often be used to assess the body's resistance to stress. The activity
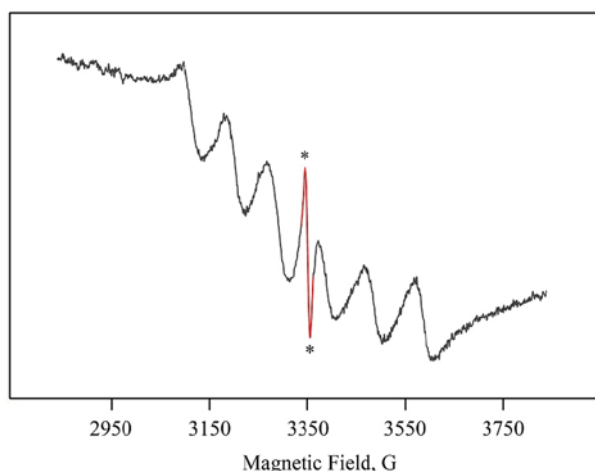
Fig. 1. The EPR spectra for leaves materials (the additional line is indicated by the asterisks symbols).
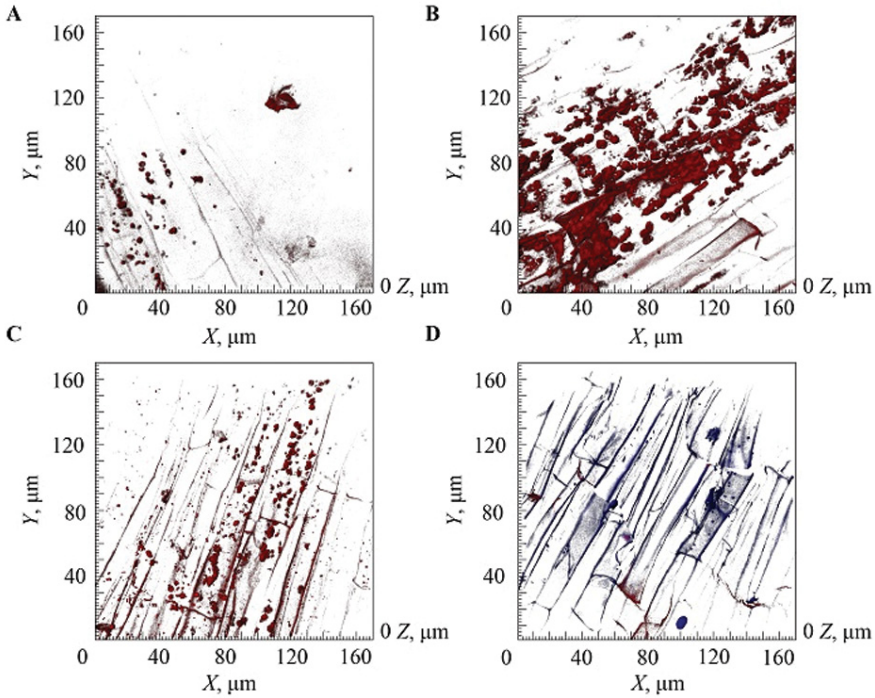
Fig. 2. TEM images of the effect of NCs on ROS production in plant tissues (A) of control, (B) infected with *Cms*, (C) treated with NCs, (D) treated with NCs and infected with *Cms*.

of guoyacol-dependent peroxidase was determined by the Boyarkin method at the end of plants co-incubation with NCs.

Plants suffering from ring rot were used to assess the level of stress using ROS. They were completely colonized by the pathogen, since four days have passed since the moment of their infection, and during this period of time, no increase in ROS in the root tissues was recorded in them (Fig. 2). The observed picture is quite understandable, since it is known that the ROS level rises significantly at the initial stage of the plant's response to the stress factor. If healthy plants were treated with NCs, a significant increase in the amount of ROS in the potato root tissues was observed by more than 4 times as compared with the control values. Obviously, this indicates an increase in the protective reaction of plant cells to stress due to the influence of NCs. In the case of NCs treatment of plants with ring rot, a decrease in the ROS content was also noted (Fig. 2). The obtained result indicates the activation of the protective functions of the plant organism under stress.

Experiments to estimate the amount of DC in the tissues of potato roots and leaves showed that all studied NCs also reduced the content of DCs in leaves of infected plants, which indicated the inhibition of LPO processes, probably due to the antioxidant effect of NCs. In the case of assessing the level of MDA, there

was practically no effect in the presence of NCs in healthy plants, however, in infected plants, the level of MDA decreased. The obtained results show that NCs have a pronounced antiradical action. Treatment of infected plants with this composite reduced the content of ROS, DC and MDA in tissues, indicating the intensity of destructive processes under the influence of ROS, among which there were radicals. Thus, it can be concluded the available results indicate that NCs improve the protective functions of the plant organism due to an increase in the activity of antioxidant enzymes.

Transport Properties of Quasi-One-Dimensional Iron Chalcogenide $KFeS_2$

A. G. Kiiamov[1], M. D. Kuznetsov[1], Z. Seidov[2], V. Tsurkan[3,4],
H.-A. Krug von Nidda[4], D. Croitori[3], L. R. Tagirov[1,5], D. A. Tayurskii[1]

[1] Institute of Physics, Kazan Federal University, Kazan 420008, Russian Federation
[2] Institute of Physics, Azerbaijan National Academy of Sciences, Baku AZ-1143, Azerbaijan
[3] Institute of Applied Physics, Chisinau MD-20208, Moldova
[4] Experimental Physics V, Center for Electronic Correlations and Magnetism, Institute of Physics, University of Augsburg, Augsburg D-86135, Germany
[5] Zavoisky Physical-Technical Institute, FRC Kazan Scientific Center of RAS, Kazan 420029, Russian Federation

Iron chalcogenide $KFeS_2$ is a linear chain antiferromagnet with T_N = 250 K [1] which belongs to the group of quasi-one-dimensional compounds $AFeX_2$ (A = K, Rb; X = S, Se), consisting of linear chains of edge-sharing $[FeX_4]$ tetrahedra along the c direction, cross-linked by A atoms [1]. It is reasonable to assume that the iron-chain compound to be a conductor. According to simple band theory, once the one-dimensional band is partially filled, the compound should exhibit one-dimensional metallic conduction. However, in real crystals, this picture is modified in a non-trivial way by the presence of disorder and defects: interruptions of the chains by defects such as vacancies or impurities localize the electrons within the resulting chain segments [2]. The experimental measurements of the electrical resistivity of $KFeS_2$ show that the transport properties of the compound depend on the preparation and synthesis method [3]. The annealed sample shows semiconductor-like behavior, whereas the conductivity of the quenched samples can be characterized as metal and semiconductor above and below the temperature of 250 K, respectively [3]. Our *ab initio* density functional theory calculations of $KFeS_2$ band structure within the non-magnetic approach give zero bandgap which represents the sample in the paramagnetic state above the Neel temperature. On the contrary, for the antiferromagnetic state, we obtained a non-zero bandgap, which depends on the Hubbard U parameter. Our *ab initio* results suggest that the paramagnet-antiferromagnet transition is accompanied by the metal-semiconductor transition, that is with the opening of the bandgap. That prediction is in good qualitative agreement with the experimentally measured temperature dependence of the quenched samples of $KFeS_2$ reported in [3]. We digitized the experimental temperature dependence of the electrical resistivity below T_N and fitted it with the intrinsic semiconductor model. The obtained band gap amounted to 0.13 eV. The experimental bandgap value can be used to get initial guess of the Hubbard U parameter for further calculations of thermal and magnetic properties of the $KFeS_2$ compound similar to refs. [4, 5].

1. Bronger W., Kyas A., Müller P.: Journal of Solid State Chemistry **70**, 2 (1987)
2. Zeller H.R.: Phys. Rev. Lett. **28**, 22 (1972)
3. Nishioka S., Kuriyaki H., Hirakawa K. Synthetic Metals **71**, 1 (1995)
4. Seidov Z. *et al.*: Phys. Rev. B **94**, 134414 (2016)
5. Kiiamov A.G. *et al.*: Phys. Rev. B **98**, 214411 (2018)

Paramagnetic Centers and Rhodamine Dye Luminescence of Titania-Based Nanoheterostructures

E. A. Konstantinova[1], V. B. Zaitsev[1], E. V. Kytina[1], A. V. Marikutsa[2]

[1] Physics Department, M. V. Lomonosov Moscow State University, Russian Federation, liza35@mail.ru
[2] Chemistry Department, M. V. Lomonosov Moscow State University, Russian Federation

Over the past decades, titania has been the object of close attention of scientists all over the world [1, 2]. Titania is a wide-gap semiconductor with a band gap varying from 3.2 to 3.4 eV, and continuous illumination by UV radiation must be used for reactive electrons and holes generation [1, 2]. The way to improve the photocatalytic characteristics of titania is doping with ions of metals or nonmetals and to prolong the lifetime of photoexcited carriers (electrons and holes) by their spatial separation in nanoheterostructures, thus prevent recombination. In this work we have obtained nanoheterostructures effectively absorbing light in the visible spectral region and accumulating photoexcited charge carriers, providing rather long catalytic activity of the produced structures after illumination is turned off. At the same time we have seriously checked out the behavior of the used nanoheterostructures after adsorbtion of organic dye molecules on their surface. Organic dye molecules adsorption is involved in a standard method for the photocatalytic activity measurements.

Nanocrystalline nitrogen-doped titanium dioxide and TiO_2-MoO_3, $TiO_2-V_2O_5$, TiO_2-WO_3, $TiO_2-MoO_3-WO_3$, and $TiO_2-MoO_3-V_2O_5$ nanoheterostructures were prepared by the method described in detail in [2]. The electron paramagnetic resonance (EPR) spectra were recorded by ELEXSYS-E500 spectrometer (Bruker, Germany). Fluorescence and diffuse reflection spectra were recorded using an LS-55 Perkin Elmer spectrometer (spectral range from 250 to 900 nm). The photocatalytic activity (oxidizing power) of the samples was investigated with the reaction of the photodegradation of rhodamine dye. The dye was applied to the sample surface from aqueous and ethanol solutions. To obtain the visible spectral range (from 450 to 750 nm) for the photocatalysis study YG-16 glass filter was used. Changes in the surface concentration of the dye were monitored according to the diffuse reflectance R value at a wavelength of the maximum light absorption by the adsorbed dye. The diffuse reflectance was recalculated to a value proportional to the surface concentration using the Kubelka-Munk approach [3].

Nanoparticles average diameter in the nanoheterostructures was approximately 10 nm according our XRD investigatrion and the specific surface area of all samples was in the range of 100–110 m^2/g. Paramagnetic centers of $N^{\bullet}$, Ti^{3+}, Mo^{5+}, V^{4+}, and W^{5+} were detected and characterized in the samples under investigation. The defect concentrations calculated by us had the following values: $1.3 \cdot 10^{18}$ g^{-1} (TiO_2-WO_3), $2.1 \cdot 10^{18}$ g^{-1} ($TiO_2-V_2O_5$), $2.2 \cdot 10^{18}$ g^{-1} (TiO_2-MoO_3), $1.6 \cdot 10^{19}$ g^{-1} ($TiO_2-MoO_3-V_2O_5$), $1.4 \cdot 10^{19}$ g^{-1} ($TiO_2-MoO_3-WO_3$).

It is revealed that nanoheterostructures consisting of several metal oxides have high photocatalytic activity in the visible spectral region and the ability

to accumulate photogenerated charge carriers. As a result, catalytic reactions in the samples take place even after illumination is turned off and thus do not require continuous illumination. These results correlate with the data obtained by EPR. It is found that samples with high radical concentration have a high light absorbance and photocatalysis rate in visible range. The energy position of the different radicals in the band gap of nanooxides was determined using our original EPR method with illumination of samples *in situ*. We have performed for the first time a comparative study of the luminescence of dye molecules adsorbed on nanoheterostructures surface and these structures catalytic activity. We have shown that under illumination of nanoheterostructures with the adsorbed rhodamine dye at the dye absorption wavelength (500 nm), photocatalytic reactions are mainly determined by the light absorption by the nanostructures themselves, and not by the energy transfer from the dye. Since the strong quenching of the initial fluorescence is observed on the surface of all studied nanoheterostructures, it can be stated that the nonradiative energy transfer from dye molecules associated with such quenching occurs, but does not lead to a significant additional acceleration of photocatalysis. This important result shows that high photocatalytic activity of the material is the primary criterion for creating energy-efficient photocatalysts. The research was carried out with financial support of the Russian Foundation for Basic Research within the framework of research project no. 18-29-23051.

1. Zhao W., Liu S., Zhang S., Wang R., Wang K.: Catal. Today **337**, 37 (2019)
2. Konstantinova E.A., Zaitsev V.B., Kytina E.V., Marikutsa A.V.: Semiconductors **55**, 219 (2021)
3. Wedland W., Hecht H.: Reflectance Spectroscopy. Interscience, New York, 1966.

Highly Efficient MOF-Based Catalyst for Ortho-Para Hydrogen Conversion

N. A. Kudriavykh[1,2]**, A. S. Kiryutin**[1]**, A. S. Poryvaev**[1]**, M. V. Fedin**[1]
D. M. Polyukhov[1]

[1] International Tomography Center, Novosibirsk 630090, Russian Federation
[2] Novosibirsk State University, Novosibirsk 630090, Russian Federation

Metal-organic frameworks (MOFs) demonstrate great attention nowadays. Metal-organic frameworks consist of metal units and organic polydentate ligands (linkers). MOFs have porous structure and their functional properties can be fine-tuned by varying large number of linkers and metal units. These properties make MOFs promising materials for such application fields as gas adsorption and storage, heterogeneous catalysis and other. Hydrogen takes part in many technological processes. *Para-* nuclear spin isomer of hydrogen is used in such nuclear hyperpolarization methods as PHIP and SABRE [1, 2]. These methods are promising way to drastically increase sensitivity of NMR and MRI. However, ortho-para conversion process requires a catalyst for carrying out this process in high velocity flows.

MOF-74 contains open metal sites which makes them perspective materials for hydrogen *ortho-para* conversion purposes. In this work we studied influence of metal ion replacement in series of (Zn, Mn, Ni, Cu, Co)-MOF-74 on *ortho-para* conversion efficiency. We used plug flow reactor to find kinetic parameters of the catalysts and compared the results with industrially used catalyst FeO(OH). It was shown that MOF-74 samples demonstrate much higher conversion efficiency compared to FeO(OH). Noticeably, Ni-MOF-74 turned up to be the most effective catalyst among studied series. It's effective rate constant more than in 200 fold higher than that for industrially actual FeO(OH). Also, we determined the origin of ortho-para conversion over initially diamagnetic Zn-MOF-74. Zn-MOF-74 was found to contain paramagnetic defects that provide *ortho-para* conversion.

1. Hübler P. *et al.*: J. Am. Chem. Soc. **121**, 22, 5311–5318 (1999)
2. Eshuis N. *et al.*: J. Am. Chem. Soc. **136**, 7, 2695–2698 (2014)

Validating MD Models of Disordered Proteins Using NMR Data on Translational Diffusion

O. O. Lebedenko[1], S. A. Izmailov[1], V. A. Salikov[1], N. R. Skrynnikov[1,2]

[1] Laboratory of Biomolecular NMR, St. Petersburg State University, St. Petersburg 199034, Russian Federation, o.lebedenko@spbu.ru

[2] Department of Chemistry, Purdue University, West Lafayette, IN 47907, USA

Long molecular dynamics (MD) trajectories provide a powerful tool to analyze the behavior of intrinsically disordered proteins (IDPs). However, MD simulations generally suffer from inadequate statistics and imperfect nature of force fields that have not been originally intended to model IDPs. Therefore, it is highly important to benchmark such MD models against the experimental data. The choice of suitable experimental metrics is, in fact, rather limited. One of the most relevant parameters is the translational diffusion coefficient D_{tr}, measurable by pulsed-field gradient (PFG) NMR. The D_{tr} value provides a measure of peptide chain's compactness, which is especially useful for small proteins (molecular weight < 5 kDa), where small-angle X-ray scattering (SAXS) data are unavailable.

Of note, prediction of D_{tr} requires two modifications to the standard MD modeling scheme. First, the predicted D_{tr} value scales linearly with the inverse linear size of the simulation box. Therefore, one needs to set up a series of simulations in the boxes of increasing size and extrapolate the obtained D_{tr} values to an infinitely large box. In our study, we first recorded a long trajectory in a box of a relatively small size and then used the snapshots from this trajectory to start many short simulations in bigger boxes. This strategy ensures adequate conformational sampling of the modeled peptide. Second, accurate determination of D_{tr} is impossible under the standard NPT setup using Langevin thermostat. More specifically, Langevin thermostat applies random force to the system, which generates non-zero translation and interferes with the calculation of D_{tr}. We circumvented this problem by employing the so-called Bussi thermostat [1], which we implemented for the latest release of the MD simulation program Amber [2].

The computational scheme was first tested on the well-known globular protein ubiquitin. Two series of simulations have been conducted, one using TIP4P-Ew [3] water (advanced general-use model) and the other using TIP4P-D [4] water (recent *ad hoc* model developed specifically for disordered proteins). The extracted D_{tr} values fall within 10% of the experimental result obtained in-house using the double-stimulated-echo (DSTE) experiment [5]. The differences between the MD predictions and the experimental result are due to the trivial viscosity effects, with TIP4P-Ew underestimating and TIP4P-D slightly overestimating the viscosity of water. The same conclusion was reached by analyzing the rotational diffusion coefficient of ubiquitin, D_{rot}.

As a next step, we have simulated the dynamics of the intrinsically disordered N-terminal fragment of human histone H4 (residues 1-25, termed N-H4). The net

length of the MD trajectories recorded for this peptide was 60 μs. It has been found that the simulations in TIP4P-Ew water overestimate D_{tr} of N-H4 by ca. 20%, whereas the simulations in TIP4P-D water underestimate it by ca. 30%. In part, this effect is attributable to water viscosity, similar to ubiquitin. However, alongside with the trivial viscosity effect a major source of the discrepancy is a misrepresentation of N-H4 conformational ensemble in the MD simulations: the peptide is exceedingly compact in the TIP4P-Ew simulation, but overly extended in the TIP4P-D simulation. This observation underscores the usefulness of D_{tr} data for validation of the MD-based models of intrinsically disordered proteins. While D_{rot} cannot be meaningfully defined for the strongly disordered N-H4 peptide, relevant information on local dynamics can be extracted from the ^{15}N relaxation rates. We found that the simulated rates from the TIP4P-D trajectory employing Bussi thermostat are in good agreement with our prior experimental results [6].

1. Bussi G., Donadio D., Parrinello M.: J. Chem. Phys. **126** (2007)
2. Case D.A., Belfon K., Ben-Shalom I.Y., Brozell S.R., Cerutti D.S., Cheatham T.E. *et al.*: Amber 2020. San Francisco: University of California 2020.
3. Horn H.W., Swope W.C., Pitera J.W., Madura J.D., Dick T.J., Hura G.L. *et al.*: J. Chem. Phys. **120**, 9665-78 (2004)
4. Piana S., Donchev A.G., Robustelli P., Shaw D.E.: J. Phys. Chem. B. **119**, 5113-23 (2015)
5. Jerschow A., Muller N.: J. Magn. Reson. **125**, 372-5 (1997)
6. Kämpf K., Izmailov S.A., Rabdano S.O., Groves A.T., Podkorytov I.S., Skrynnikov N.R.: Biophys. J. **115**, 2348-67 (2018)

Magnetic Interactions and Spin Dynamics of the ^{53}Cr in the Orthosilicate Host Crystals

R. Likerov, A. Sukhanov, I. Yatsyk, V. Tarasov

Zavoisky Physical-Technical Institute, FRC Kazan Scientific Center of RAS, Kazan 420029, Russian Federation, rodionlikerov@gmail.com

Recently, much attention has been paid to finding ways of practical implementation of various algorithms of quantum informatics. An active search is carried out of quantum systems for practical implementation of quantum computers. To transfer quantum information over long distances and create a universal quantum computer, quantum memory devices capable to remember and to reproduce quantum information are needed. Rare-earth impurity ions with a nonzero nuclear spin in oxide crystals (in particular, the yttrium orthosilicate Y_2SiO_5 (YSO)) are widely studied [1–3] as a possible material basis for practical implementation of quantum memory in optic range. In the field of quantum computing, significant progress has been associated with the creation of systems of coupled quantum bits (Q-bits) based on superconductor devices.

In this work, we measured the orientation dependencies of the EPR spectra of ^{53}Cr impurity monoisotopic ions in YSO and determined principal values and orientations of the principal axes of the D-tensor that determines anisotropy of the electron levels of trivalent chromium in YSO single crystal. Values of isotropic g-factor and the energy of the hyperfine interaction between electron and nuclear spins were also determined. Temperature dependencies of spin-lattice relaxation time and memory phase time were measured and estimated.

1. Rancic M. *et al.*: Nature Physics **14**, 50–55, (2018)
2. Jobez P. *et al.*: Phys. Rev. Lett. **114**, 230502 (2015)
3. Zhong M. *et al.*: Nature **517**, 177–181 (2015)
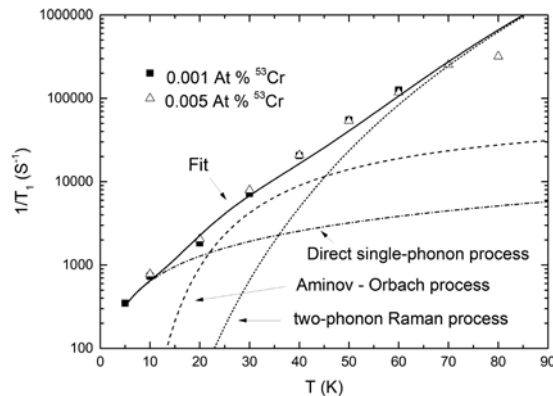
Fig. 1. Inversion – recovery T_1 rate measurements.

Electron Spin Polarization Dynamic in a Bay-Substituted Perylene Bisimide upon Photoexcitation

A. Mambetov[1], A. Sukhanov[1], V. K. Voronkova[1], X. Zhang[2], J. Zhao[2]

[1] Zavoisky Physical-Technical Institute, FRC Kazan Scientific Center of RAS, Kazan 420029,
Russian Federation, vio@kfti.knc.ru
[2] State Key Laboratory of Fine Chemicals, School of Chemical Engineering, Dalian University of
Technology, 116024, P. R. China

We present the results of TR EPR investigation of two substituted perylene bisimide: PBI-Br2 and PBI-Br-NH upon photoexcitation. The electron spin polarization (ESP) dynamic of the excited triplet state for PBI-Br–NH is shown in the Fig. 1. The initially observed TR EPR spectrum is typical spectrum of the excited triplet state with (e, e, e, a, a, a) ESP pattern characteristic of the spin−orbit-coupling-induced ISC (SO-ISC) mechanism. The pattern of the TREPR spectrum remains unchanged up to approximately 450 ns after laser flash. The initial polarizations of triplet spin states evolve over time to the opposite ESP. The spectrum with inverted polarization is observed distinctly starting from 900 ns and is characterized by a sufficiently long lifetime.

The parameters of the zero field splitting (ZFS), the sublevel decay rate constants and the relative populating rates were determined by fitting the experimental spectra and their time and temperature dependences with the model spectra.

Quite accurate mathematical model for spectrum calculations was used and the ESP dynamic was reproduced good. It was found in both systems that inverted polarization can be explained mostly by introducing different lifetimes of ZFS sublevels – τ_X, τ_Y and τ_Z, where τ_X for PBI-Br-NH is about 0.35–0.45 microseconds and it is 10 times (or more) shorter than τ_Y and τ_Z.
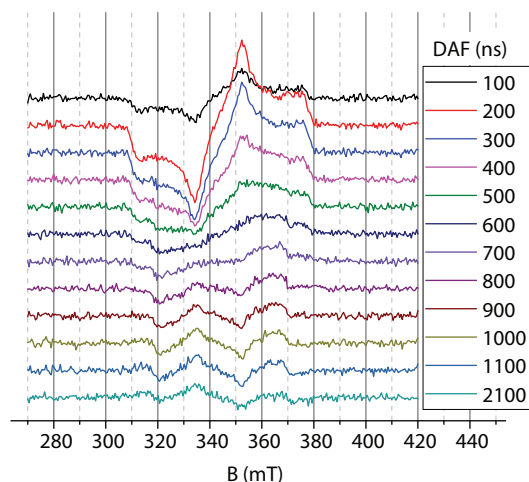
Fig. 1. TREPR spectra of PBI-Br-NH at 80 K, X-band for different delay after laser flash (DAF).

Nuclear Quadrupole Resonance Spectra of Nitrogen-Based Heterocycles

S. Mamadazizov[1,2], G. S. Kupriyanova[2]

[1] School of Arts and Sciences, University of Central Asia, Khorog 736000, Tajikistan, sultonazar.mamadazizov@mail.ru
[2] I. Kant Baltic Federal University, Kaliningrad 236041, Russian Federation, galkupr@yandex.ru

Nitrogen-based heterocycles are widely used in the development of novel drugs and biologically active substances. About 75% of drugs approved by the Food and Drug Administration of the USA contain nitrogen [1]. Hence the application of ^{14}N Nuclear Quadrupole Resonance (NQR) in pharmaceutics seems very prospective.

In previous papers [2–3], we have provided detailed theoretical and experimental research for tetrazole derivatives, which are used as isosteric substitutes for other functional groups in drug development. In the current work, a ^{14}N NQR investigation of β-lactams, which are containing four-membered ring heterocycles will be provided. Ezetimibe and Clavulanic acid (Fig. 1) are well-known antibiotics. Moreover, ezetimibe is used as a cholesterol absorption inhibitor and the acid is β-lactamase inhibitor. However, further research of β-lactams is a relevant task due to the development of bacterial resistance to known β-lactams.

The application of ^{14}N NQR provides insights on molecular dynamics, structure, h-bond formation. The ^{14}N NQR spectra directly depend on the Electric Field Gradient. Thus it is sensitive to any changes in the environment of the nuclei. Hence NQR allows differentiating between isomorphic structures and similar compounds with various radicals. Therefore investigation of novel β-lactams [4] will be carried on the next step.
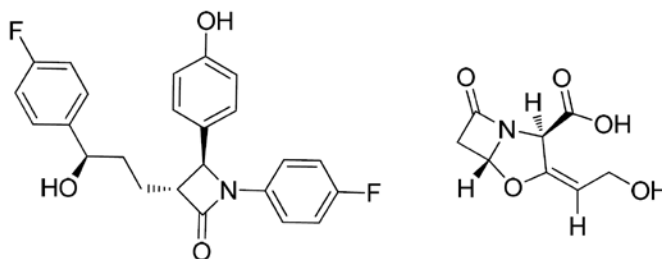
Fig. 1. Ezetimibe on the left, clavulanic acid on the right.

Theoretical calculations are performed with the GAUSSIAN09 package [5]. Structural information for ezetimibe and clavulanic acid are given in [6] and [7] respectively. Calculation were done on the B3LYP level of theory.

1. Kerru N. *et al.*: Molecules **25** (8), 1909 (2020)
2. Mamadazizov S. *et al.*: Chemical Physics **506**, 52–60 (2018)
3. Mamadazizov S. *et al.*: "⁴N NQR Study of Tetrazole Derivatives for Potential Applications in Security, Detection of Counterfeit Drugs and Pharmaceutics. 2019 PhotonIcs & Electromagnetics Research Symposium-Spring (PIERS-Spring). IEEE 2019.
4. Malebari A.M., Darren F., Nathwani S.M., O'Connell F., Noorani S., Twamley B., O'Boyle N.M., O'Sullivan J., Zistere, D.M., Meegan M.J.: Eur. J. Med. Chem. **189**, 112050 (2020)
5. Frisch M.J. *et al.*: Gaussian, revision B. Gaussian Inc., Pittsburg 2003.
6. Bruning J., Alig E., Schmidt M.U. CCDC 786811: Experimental Crystal Structure Determination, 2010, DOI: 10.5517/ccvdr0z
7. National Center for Biotechnology Information. "PubChem Compound Summary for CID 5280980, Clavulanic acid" PubChem, https://pubchem.ncbi.nlm.nih.gov/compound/Clavulanic-acid. Accessed 1 September, 2021.

Magnetic Properties of Double Perovskites $Ba_xSr_{2-x}TiFeO_6$ ($x = 0, 0.1, 0.15, 0.25$)

D. V. Mamedov[1], R. M. Eremina[1], F. G. Vagizov[2], T. Maiti[3]

[1] Zavoisky Physical-Technical Institute, FRC Kazan Scientific Center of RAS, Kazan 420029, Russian Federation, javi-m@yandex.ru
[2] Institute of Physics, Kazan Federal University, Kazan 420008, Russian Federation
[3] Department of Materials Science and Engineering Indian Institute of Technology Kanpur, Kanpur 208016, UP, India

Currently, thermoelectric materials such as chalcogenides (Bi_2Te_3, Sb_2Te_3, Zn_4Sb_3, Bi_2Se_3, SnTe and others) and intermetallics are mainly used to convert heat into electricity [1]. They have disadvantages, such as toxicity, decomposition, at high temperatures ($T > 600$ K), evaporation, melting and oxidation. As a result, the efficiency of converting heat to electricity at high temperatures is low. However, most of the heat is generated by various sources at temperatures above 900 K. For these temperatures, oxides are a more suitable alternative because of their greater stability at high temperatures, lower cost, and higher oxidation resistance. Among oxide materials, good thermoelectric properties are shown, for example, by Na_xCoO_2, $Ca_3Co_4O_9$ and others [2]. Several oxides of double perovskites have shown promising high temperature thermoelectric properties.

Double perovskite oxides have the formula $A_2B'B''O_6$, where A is alkaline earth metals, lanthanides; B', B'' are transition metals.

One of the representatives of double perovskites is $Ba_xSr_{2-x}TiFeO_6$. In this work, we investigate the magnetic properties of $Ba_xSr_{2-x}TiFeO_6$ ($x = 0, 0.1, 0.15, 0.25$). This substance has a cubic structure.

EPR and Mössbauer studies of the samples were carried out. From the EPR and Mössbauer spectroscopy data, we have shown the presence of two magnetic centers of iron (Fe^{3+}, Fe^{4+}) in this substance. The temperature dependences of the magnetization were obtained. It can be seen from the dependence that the magnetic phase transition to ordering state occurs at temperatures of about ~ 17.5 K, 14.5 K, 13.5 K, and 13.0 K for $Ba_xSr_{2-x}TiFeO_6$ ($x = 0, 0.1, 0.15, 0.25$, respectively.

1. Maiti T., Saxena M., Roy P.: J. Mater. Res. **34**, 107 (2019)
2. Roy P., Waghmare V., Maiti T.: RSC Adv. **6**, 54636 (2016)

Application of Low-Field NMR-Relaxometry for Soybean Lecithin

A. Minsafina[1], A. Bogaychuk[1,2]

[1] Institute of Physics, Kazan Federal University, Kazan 420008, Russia, mins.adelina@gmail.com
[2] Tatarstan Academy of Sciences, Kazan 420111, Russian Federation

Soybean lecithin is a multicomponent system, 70% of which are phospholipids. Lecithin is widely used in the food industry, agriculture, and medicine and there are many factors that lead to its degradation [1, 2]. The aim of this research is to measure the spin-lattice T_1 and spin-spin T_2 relaxation times of soybean lecithin samples in order to adapt the methods of low-field ^{1}H NMR relaxometry for its identification and quality control.

Nuclear magnetic resonance (NMR) and high-performance liquid chromatography-mass spectrometry (HPLC-MS) were chosen to study the chemical composition of soybean lecithin.

Relaxation times were measured using inversion-recovery and CPMG methods. ^{1}H NMR experiments were conducted on the multifunctional NMR-pulsed spectrometer [3] with a hand-assembled magnetic system called Halbach [4]. Measurement data were processed by the RILT script [5], executed in the MathLab environment. The ^{1}H time distributions of T_2 were obtained by applying the RILT algorithm.

In HPLC-MS we obtained complete chromatograms for each sample for two registration methods: positive and negative. From these spectra, peak area values for each phospholipid were obtained. Four types of phospholipids have
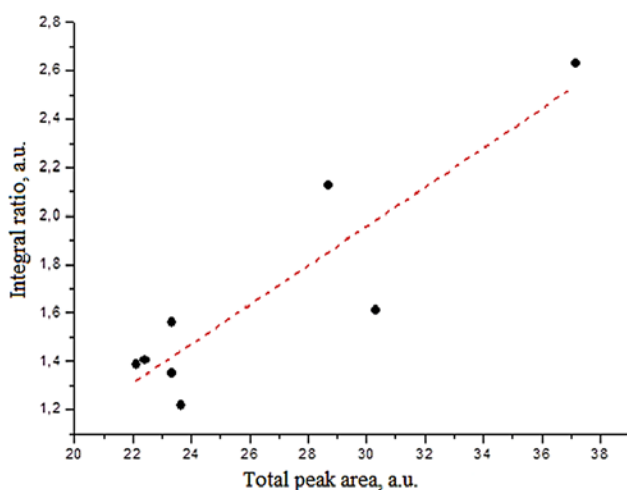
Fig. 1. Graph of dependence of the total peak area and the integral ratio, negative method of registration.

been found and identified using the Metlin Scripps database: PI – Phosphati-dylinositol, PE – Phosphatidylethanolamine, PC – Phosphatidylcholine, PS – Phosphatidylserine [6].

It was assumed that the data from HPLC spectra and the two peaks $T_{2,1}$ and $T_{2,2}$ in NMR T_2-distributions could correlate. The direct correlation between the total peak area and the integral ratio for the two time peaks for all samples have been found. This can be seen from the correlation coefficient, which is close to 0.89.

1. Xia X. *et al.*: Journal of Food Research 116–125, Canada, 2017
2. Saha S. *et al.*: Biocatalysis and Agricultural Biotechnology **20**, 2–8, 2019
3. Kuzmin V.V. *et al.*: Magnetic resonance in solids **21**(1), art. №19104 (2019)
4. Bogaychuk A.V. *et al.*: Review of Scientific Instruments 2020.
5. Marino I.: Regularized Inverse Laplace Transform (RILT) 2014, URL: https://www.mathworks.com/matlabcentral/fileexchange/6523-rilt, (accessed: 25.08.2021)
6. Metlin Scripps: URL: https://metlin.scripps.edu, (accessed: 25.08.2021)

Modern MRI Methods in the Diagnostics of Brain Diseases

A. Nikitina, Yu. Bogachev, M. Shishkina

Physics Department, St.-Petersburg Electrotechnical University, 197376, Russian Federation,
nastya_nikitina1996@mail.ru

Modern MRI techniques used in the early diagnosis of brain diseases are considered.

Magnetization transfer imaging (MTI). MTI allows you to detect the presence of microscopic damage to the white matter, which looks normal on a conventional MRI [1]. The development of research in the direction of obtaining quantitative characteristics of normal and pathological tissues in vivo on the basis of nuclear magnetization transfer seems promising, since the available data suggest that the efficiency of magnetization transfer is very sensitive to pathological changes in the structure of biopolymers, including those forming cell membranes. The quantitative assessment of the effect of magnetization transfer is usually carried out using the magnetization transfer ratio (MTR). One of the current applications of magnetization transfer is to determine the age of lesions in patients with multiple sclerosis (MS). In the early stages, acute MS lesions, mainly edematous and inflamed, show a small level of demyelination. Unlike standard sequences, MTI shows greater specificity for macromolecules, such as myelin. Over time, large macromolecules of myelin proteins disintegrate in the MS lesions, and gliosis and demyelination occur. Magnetization transfer imaging shows a correlation with these pathological changes, showing small changes in MTR in early MS lesions and significantly reduced MTR in old, chronic lesions.

Diffusion-weighted imaging (DWI). DWI is used for the differential diagnosis of acute and chronic MS lesions by measuring the apparent diffusion coefficient (ADC) and fractional anisotropy (FA). In patients with MS, most lesions show an increased diffusion coefficient compared to normal white matter. The increase in diffusion reflects the increased volume of free water contained in the lesion, although it is difficult to say whether this is a relative contribution from edema, demyelination or axon loss [2]. Acute lesions have a significantly higher diffusion coefficient in contrast to chronic lesions, reflecting cytotoxic edema. Basically, MS lesions have a reduced level of fractional anisotropy in the images of diffusion tensor imaging (DTI) compared to normal white matter. A decrease in the FA level in the lesions shows the destruction of myelin and axonal structures, which leads to destruction and increased intercellular space. Some researchers believe that the decrease in FA in lesions accumulating a contrasting agent is less than in non-accumulating lesions, which indicates the possibility of DTI to show the activity of the disease. Another method for studying diffusion images is based on 3D reconstruction of fiber bundles using tractography [3].

Susceptibility weighted imaging (SWI). This method is a highly sensitive imaging method that is able to display the distribution of the magnetic susceptibility of a substance in tissues. The SWI method implements a sequence of

three-dimensional gradient echo (GRE), which uses the dependence on the level of oxygen in the blood (BOLD) and phase information to increase the contrast in the resulting images. In a broader sense, SWI involves combining the amplitude and filtered phase data for further post-processing when constructing projection images with minimal intensity to display smaller hemorrhages that are not visible when visualizing T_2^*. Higher magnetic fields enhance the effects of magnetic susceptibility and, consequently, create SW images with a higher signal-to-noise ratio, which allows better visualization of small brain structures, blood vessels and tumors. However, the ultra-high magnetic field induction (more than 7 T) in the SWI method can distort the size of brain structures in areas characterized by high concentrations of iron. Phase images can be used to distinguish between diamagnetic (i.e., calcium) and paramagnetic (deoxyhemoglobin, hemosiderin and ferritin) substances.

Numerous studies have shown that the SWI method is more sensitive than conventional MRI when examining the vascular network, detecting metastases or hemorrhages in a tumor. The SWI method provides extensive information about patients with brain tumors that cannot be obtained using other MRI sequences. The SWI method is not limited to the detection of a lesion, it can be used to demonstrate the response to treatment, monitor recovery after a stroke and predict the results, as well as for better anatomical localization in neurosurgery when using a gamma knife [4].

Multimodal MRI/PET technique allows simultaneous MRI and PET signal detection of MRI markers and radioligands [5]. This technology has great potential in the investigation of specific aspects of inflammation, axonal degeneration or repair and changes in neurometabolism for characterization of MS and testing of potential intervention therapies.

1. Bogachev Yu.V., Marchenko Ya.Yu. *et al.*: Izvestia SPbETU "LETI" **6**, 19–33 (2013)
2. Celso Hygino da Cruz Jr. L., Batista R.R. *et al.*: Neuroimag. Clin. **21**, 71–88 (2011)
3. Sbardella E., Tona F. *et al.*: Hindawi Publ. Corporation. Article ID 671730, **11** (2013)
4. Di Ieva A., Lam T. *et al.*: J. Neurosurg. **123**, 1463–1470 (2015)
5. Cho Z.H., Son Y.D., Choi E.J. *et al.*: MAGMA **26**(1), 71–79 (2013)

The Localization of Co Dopant in the Structure of TlInS$_2$ Ternary Semiconductor Obtained from EPR Investigations

E. Okumuş[1], S. T. Öztürk[1], M. Yu. Seyidov[1]

[1] Department of Physics, Gebze Technical University, Turkey
esraokumus_84@hotmail.com

TlInS$_2$ is always a p-type semiconductor at normal conditions and a great deal of efforts have been made to achieve a reliable n-type conductivity in this compound [1]. A conversion from p-type conduction to n-type by doping do not alter its p-type conduction.

In this work we study the properties of 3d transition metal dopant in TlInS$_2$ layered crystal in order to understand why transition metal defects incorporated into TlInS$_2$ can't change the conductivity type of TlInS$_2$ semiconductor. We have investigated the properties of 0.1% Co transition metal impurities in TlInS$_2$ semiconductor by an electron paramagnetic resonance (EPR) technique.
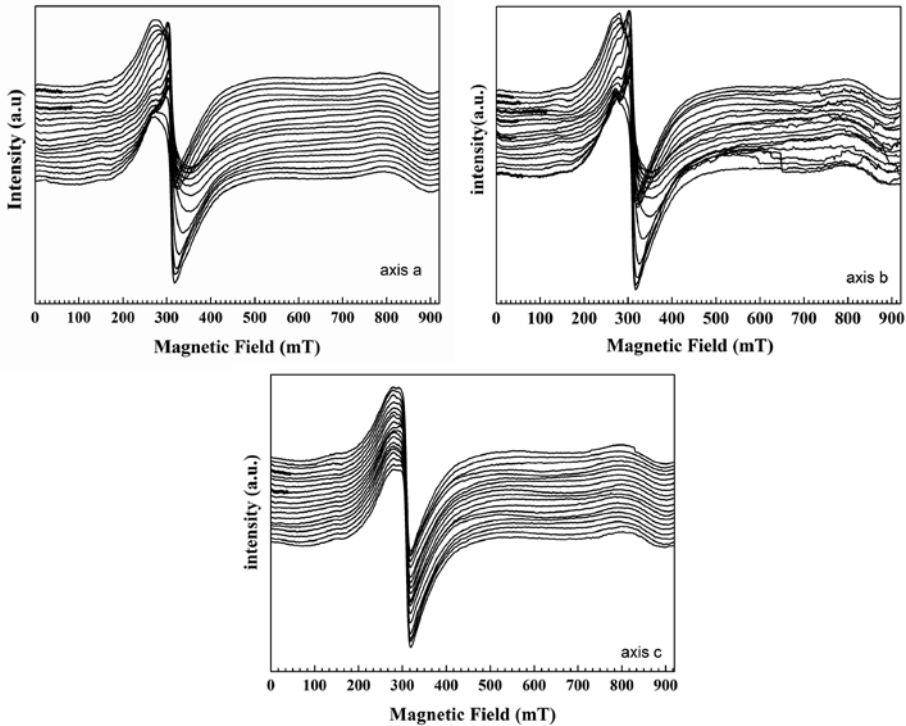
Fig. 1. The angular dependence of the magnetic field on the bc*, ac* and ab planes of Co-doped TlInS$_2$ crystals, respectively.

EPR measurements were performed using a standard X-band (9.12 GHz) Jeol model JES FA-300 spectrometer in magnetic field from 0 to 900 mT at room temperature.

Angular variations were studied by rotating the sample along its three crystalline axes. The angular dependence of the magnetic field in the bc*, ac*, and ab planes of the Co-doped $TlInS_2$ crystal is shown in Fig. 1, respectively.

An EPR lines arising from Co ions are identified in the 0.1% Co $TlInS_2$ system. Spin states of paramagnetic Co atom in $TlInS_2$, its location and local site symmetry of cobalt ion in the lattice host as well as the electron Lande g-factor values were experimentally studied. The ESR spectra were analyzed using a suitable spin Hamiltonian including the Zeeman and the hyperfine interactions. A uniform picture of the cobalt center in this semiconductor host material is thus derived.

A key aspect of these experiments was to understand the defect chemistry role of foreign Co cations in the structure host $TlInS_2$ semiconductor crystal. The EPR spectra revealed that Co – ions are located inside a low symmetry sites of host $TlInS_2$ semiconductor crystal. Thus, EPR study of $TlInS_2$ with Co guest concentration is completely similar to behavior of a donor electron in $TlInS_2$ semiconductor. Our findings could be further supported by measurements of the conductivity and thermal properties.

1. Aliev V.A., Bagırzade E.F., Gasanov N.Z., Guseinov G.D.: Physıca Status Solidi (a) applications and materials science **102**, K109-K112 (1987)

Free Induction Decay (Hahn Echo) in Deuterated PEO Melts

<u>I. K. Ostrovskaya</u>[1], K. Lindt[2], N. F. Fatkullin[1], C. Mattea[2], S. Stapf[2]

[1] Institute of Physics, Kazan Federal University, Kazan 420008, Tatarstan, Russian Federation, Nail.Fatkullin@kpfu.ru
[2] Dept. Technical Physics II/Polymer Physics, TU Ilmenau, PO Box 100 565, Ilmenau D-98684, Germany, kevin.lindt@tu-ilmenau.de

An intrasegmental origin of deuteron spin relaxation mechanism and one dimensional reptation diffusion of polymer chains inside a stable tube postulated in tube reptation model at times $t < \tau_1$, where τ_1 is the polymer chain terminal relaxation time, lead to specifics [1] of Free Induction Decay (FID) or Hahn Echo $g(t)$ at time interval $T_2^{\text{eff}} < t < \tau_1$, where T_2^{eff} is an effective spin-relaxation time defined as $g(T_2^{\text{eff}}) = e^{-1}$ [1]. For low molecular polymer melts, when the Redfield limit is satisfied, FID has power low character $g(t) \propto t^{-1}$ reflecting a frequency nature, i.e., increasing with observing time, of the dynamical heterogeneity of segments of polymer chain created by existence of the end segments [2]. For longer polymer chains, when the Redfield limit is violated ($\tau_1 < T_2^{\text{eff}}$), FID at discussed time interval takes with accuracy of a logarithmic corrections the extended exponential character $g(t) \propto \exp(-(t/\widetilde{T})^{\alpha})$, where $\widetilde{T}$ = const, $\alpha = 1/4$ in the region of incoherent reptations and $\alpha = 1/2$ in the region of coherent reptations at initial times, which approaching again to $\alpha = 1/4$ due to the frequency nature of the end effects [3]. Our original experimental data with deuterated PEO melts with molecular masses M_w = 3410, 34400, 310000 Da at temperatures 70 °C, 80 °C and 100 °C show a qualitative agreement, and some discrepancies with mentioned features will be presented and discussed.

1. Fatkullin N.F., Körber T., Rössler E.A.: Polymer **142**, 310 (2018)
2. Ostrovskaya I.K., Fatkullin N.F.: Polym. Sci., Ser. A **62**, 138 (2020)
3. Ostrovskaya I.K., Fatkullin N.F., Körber T., Rössler E.A., Lozovoi A., Mattea C., Stapf S.: J. Chem. Phys. **152**, 184904 (2020)

Similarities and Differences of ^{169}Tm in LiTm$_{(0.02)}$Y$_{(0.98)}$F$_4$ and LiTmF$_4$: NMR Study

**<u>A. S. Parfishina</u>[1], A. V. Egorov[1], A. G. Kiiamov[1], S. L. Korableva[1],
D. S. Nuzhina[1], A. A. Rodionov[1], I. V. Romanova[1], K. R. Safiullin[1],
M. S. Tagirov[1,2]**

[1] Institute of Physics, Kazan Federal University, Kremlyovskaya 18, Kazan 420008,
Russian Federation
[2] Tatarstan Academy of Sciences, Institute of Applied Research, Kazan 420111, Russian Federation

Both of the LiTm$_{(0.02)}$Y$_{(0.98)}$F$_4$ and LiTmF$_4$ are Van Vleck paramagnets (VVP) with singlet ground state and non-magnetic excited doublet state of the ground multiplet in a paramagnet rare-earth ion [1]. Van Vleck paramagnets could be researched by NMR method due to gigantic induced magnetic moment at the 4f-shell and, consequently, a huge hyperfine magnetic field at the its own nucleus. We reported the first NMR observation and study of ^{169}Tm nucleus in the diluted single crystal VVP LiTm$_{0.02}$Y$_{0.98}$F$_4$ and comparing results with our newest NMR-obtained data of LiTmF$_4$.

Both of VVP LiTm$_{0.02}$Y$_{0.98}$F$_4$ and LiTmF$_4$ have tetragonal structure of scheelite (CaWO$_4$) with the space group C$_{4h}^6$ [2]. NMR studying of VVP single crystals were carried out by pulse home-built spectrometer. Magnetic field range was 0–0.8 T, working frequencies were 14.15 MHz and 8.43 MHz, temperature region was 2–4.2 K.

As a result of a series of experiments, an anisotropy of the spin-lattice relaxation rate (T_1^{-1}) close to the direction [001] were obtained for the LiTm$_{0.02}$Y$_{0.98}$F$_4$. Angular dependence of the spin-spin relaxation rate (T_2^{-1}) were measured and calculated for both VVP single crystals. The inhomogeneous linewidth was obtained for the LiTm$_{0.02}$Y$_{0.98}$F$_4$ and compared with the results for the concentrated VVP LiTmF$_4$.

Temperature dependencies of T_1^{-1} and T_2^{-1} were measured for the LiTm$_{0.02}$Y$_{0.98}$F$_4$. The interval between the singlet ground state to the first excited doublet state was determined equals to 25.9±0.2 cm^{-1} in approach of two-phonon Aminov-Orbach relaxation process. The value of splitting between the ground singlet and excited doublet for the concentrated LiTmF$_4$ is 31 cm^{-1} [3]. According to this result, we assumed different roots of correlation time in cases of diluted and concentrated Van Vleck paramagnets LiTmF$_4$.

1. Aminov L.K., Teplov M.A.: Sov. Phys. Usp. **28**, 762–783 (1985)
2. Garcia E., Ryan R.R.: Acta Cryst.C. **49**, 2053–2054 (1993)
3. Romanova, I.V., Tagirov, M.S.: Magn. Reson. Solids **21**, 19412 (2019)

Magnetization Precession in Three-Layer PdFe/W/PdFe Heteroepitaxial Structure with Perpendicular Magnetic Anisotropy

M. V. Pasynkov[1], A. A. Busse[1], A. V. Petrov[1], R. V. Yusupov[1], S. I. Nikitin[1], A. I. Gumarov[1], I. V. Yanilkin[1], A. G. Kiiamov[1], L. R. Tagirov[1,2]

[1] Institute of Physics, Kazan Federal University, Kazan 420111, Russian Federation, mike_p95@mail.ru
[2] Zavoisky Physical-Technical Institute, FRC Kazan Scientific Center of RAS, Kazan 420029, Russian Federation

Magnetic materials based on thin-film structures with perpendicular magnetic anisotropy (PMA) can be used for ultrahigh-capacity magnetic non-volatile memory devices. In trilayer F/N/F systems (F – ferromagnet, N – normal metal), by varying material and thickness of the intermediate N-layer one can obtain structures with both ferromagnetic and antiferromagnetic couplings between F-layers. Here, we report on a synthesis, static and dynamic magnetic properties of the F/N/F-type structure with antiferromagnetic coupling and high PMA, which can be used in data storage media with the information recorded by ultrafast laser pulses [1].

A trilayer structure of $L1_0$-PdFe/W/PdFe with layer thicknesses of 12/0.7/12 nm, respectively, was synthesized on a single crystal MgO (001) substrate. Thin continuous layers of the ordered $L1_0$-phase of PdFe compound were deposited by co-evaporation of Fe and Pd from high-temperature effusion cells in ultrahigh vacuum setup. For the tungsten layer deposition, the electron beam evaporation process was used. Each PdFe layer was deposited with the substrate temperature of 150 °C and annealed after deposition at 650 °C for 1 hour. The tungsten interlayer was grown with a substrate temperature of 300 °C. Epitaxial growth of the PdFe layers on both the chromium underlayer and tungsten interlayer with the tetragonal c-axis perpendicular to the film plane was verified by X-ray diffractometry.

Magnetization reversal curves (hysteresis loops) were measured at room temperature with a vibrating sample magnetometer (with the magnetic field applied both out-of-plane and in the plane of the structure) and with the magneto-optical Kerr effect (MOKE) setup in polar geometry. A butterfly-like shape of the hysteresis loop in the out-of-plane geometry clearly indicates the PMA of the film and the AFM coupling between the PdFe layers that can be overcome by the applied magnetic field. Comparison of the $M(H)$ loops for a single-layer $L1_0$-PdFe and trilayer FePd/W/FePd structure measured with the field lying in the sample plane allowed to estimate the principal magnetic parameters of the sample: magnetocrystalline anisotropy constants K_{u1}, K_{u2}, saturation magnetization M_s and the exchange interaction integral J.
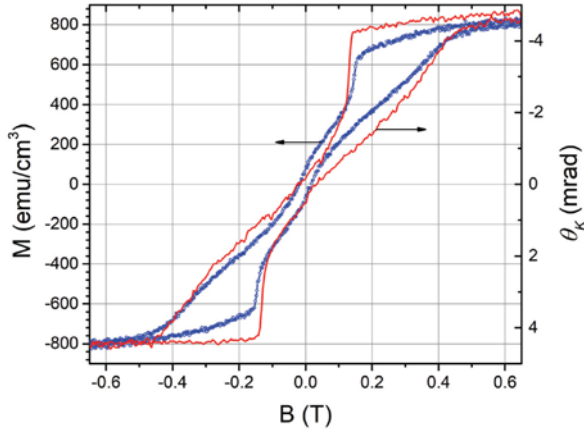
Fig. 1. Magnetization hysteresis loop of the $L1_0$-structure-based PdFe/W/PdFe heteroepitaxial trilayer structure.

Further, magnetization precession in the $L1_0$-PdFe film and PdFe/W/PdFe artificial antiferromagnet induced by the femtosecond laser pulses was studied with time-resolved MOKE spectroscopy. It was found that the precession frequency is different for the $L1_0$-PdFe film and studied F/N/F structure. The dependence of the frequency on the applied magnetic field for both samples was studied.

Mathematical modeling of the magnetization precession within the Landau-Lifshitz-Gilbert approach was performed. As it was expected for a system of coupled FM layers, two precessional modes coexist in the investigated three-layer structure, the oscillations of the magnetization of the FM layers occurring either in-phase or out-of-phase. The experimental dependence of the precession frequency on the magnitude of the applied magnetic field has been successfully described. The results show that the experimentally observed Kerr angle oscillations correspond to the antiphase low-frequency mode.

The possibility of creating an artificial ferrimagnet with PMA based on $L1_0$-FePd, a prototype medium for an optically driven magnetic storage of ultrahigh density and speed, has been demonstrated.

1. Petrov A.V. *et al.*: Magnetic Resonance in Solids **21**, 19503 (2019)

Application of EPR Method to Study of Binary Systems Graphite Oxide – Polar Liquids

A. T. Rebrikova[1], N. A. Chumakova[2,1], V. Kh. Vorobiev[1], M. V. Korobov[1]

[1] Department of Chemistry, Moscow State University, Moscow 119991, Russian Federation,
niccolumtesla@mail.ru
[2] N.N. Semenov Federal Research Center for Chemical Physics,
Russian Academy of Science, Kosygin St. 4, Moscow 119991, Russian Federation

Careful examination of the systems Brodie graphite oxide (B-GO) – polar liquids was carried out by using spin probes. Nitroxide radicals TEMPOL and TEMPO were embedded in swelled B-GO. Experimental EPR spectrum of the system "B-GO – polar liquid– spin probe" is a superposition of the three individual spectra, namely of the intrinsic spectrum of B-GO and the spectra of radicals characterized by fast and slow rotational mobility. Fast rotation is typical for the radicals dissolved in the liquid CH_3CN or CH_3OH while slow rotation can be attributed to the radicals sorbed at the internal surface of B-GO.

Incongruent melting of the swelled structures was detected in the systems B-GO – CH_3CN and B-GO – CH_3OH using DSC and XRD [1,2]. In the system B-GO – CH_3CN the reversible transition was found on heating at $T = 285–300$ K. Temperature dependence of EPR spectrum in the system showed a sharp decrease of rotational mobility of the sorbed radicals at 267~300 K. Hence, EPR measurements are more sensitive compared to XRD and DSC and detect the beginning of phase transformation at much lower temperatures.

Much attention was attracted to the properties of polar liquids, sorbed into the confined inter-plane space of GO. B-GO with TEMPO samples equilibrated with the unsaturated vapors of polar liquids showed the presence of the triplet signal which is typical for radicals located in a bulk liquid. The signal of the radicals in the liquid medium was visible only in the swelled samples and was detected at the vapor pressures 24–50% of the saturated value. Based on the results obtained we claim that the polar liquids intercalated into the inter-plane space of GO form liquid-like mobile media.

1. You S.: J. Phys. Chem. Lett. **3**, 812–817 (2012)
2. Talyzin A.V.: Nanoscale **7**, 12625–12630 (2015)

General Adiabatic Pulses for Transferring Singlet Order to Heteronuclear Magnetization: Application to Fumarate Hyperpolarized with Parahydrogen

B. A. Rodin[1,2,3], **V. P. Kozinenko**[1,2], **J. Eills**[4], **K. Ivanov**[1,2], **A. Yurkovskaya**[1,2]

[1] International Tomography Center SB RAS, Novosibirsk 630090, Russian Federation
[2] Novosibirsk State University, Novosibirsk 630090, Russian Federation
[3] Laboratoire des biomolécules, LBM, Département de chimie, École normale supérieure, PSL University, Sorbonne Université, CNRS, Paris 75005, France
[4] Helmholtz Institute Mainz, Johannes Gutenberg University, Mainz 55099, Germany

Singlet order can be defined for a coupled spin pair as the difference between the singlet state population and the mean population of triplet states. Singlet order often relaxes much slower than magnetization, i.e., it is often long-lived, which allows one studying various slow processes and preserving hyperpolarized spin order in the singlet state. A particularly interesting and relevant problem in this area is given by transfer of the singlet order of two protons to polarization of a neighboring heteronucleus. Several methods were proposed achieve such a transfer, including techniques using adiabatic adiabatic rf-pulses or B_0-field pulses. Here we propose a significant improvement of such adiabatic methods by using "constant-adiabaticity" temporal profiles of the pulses* which were originally proposed to generate singlet order in a spin pair. All constant-adiabaticity methods were implemented for the important metabolite [1-13C]fumarate, representing an AA'X-type spin system.

First of all, we have generalized and improved the procedure to evaluate constant-adiabaticity ramps by using a pertinent restriction of the space of spin states. With this method, we have introduced constant-adiabaticity rf-field ramps to manipulate spin order in high-field experiments, allowing us to reach an excellent efficiency of 96.2% for singlet order to heteronuclear polarization transfer. In experiments with parahydrogen, such rf-pulses allowed us to obtain 6.8% 13C polarization. Last but not least, the same optimization method has been utilized in ultralow-field experiments, using field cycling (FC) and field sweeping (FS) to convert the proton spin order into the 13C polarization. The constant adiabaticity profiles have demonstrated a much better performance in comparison with their linear analogues used before: one can achieve efficient polarization transfer in much shorter times, getting around the problem of relaxation losses of spin order during the field pulse.

---

* B.A. Rodin, K.F. Sheberstov, A.S. Kiryutin, J.T. Hill-Cousins, L.J. Brown, R.C.D. Brown, B. Jamain, H. Zimmermann, R.Z. Sagdeev, A.V. Yurkovskaya, K.L. Ivanov: Constant-adiabaticity RF-pulses for generating long-lived singlet spin states in NMR, J. Chem. Phys. **150**, 064201 (2019)

The highly efficient polarization transfer techniques used here are of a more general scope and can be exploited to generate heteronuclear spin hyperpolarization in various molecules, notably, in metabolites.

1. Smith J.R., Brown P.L.: Phys. Rev. B **150**, 123 (2004)
2. Suzuki I.W.: EPR Investigations, vol. 3, pp. 12-34. New York: Plenum 2004.

The Bulk Transport Properties of the $Bi_{1.08}Sn_{0.02}Sb_{0.9}Te_2S$ Topological Insulators as Revealed from ESR and Resistivity Data

V. O. Sakhin, E. F. Kukovitskii, Yu. I. Talanov, G. B.Teitel'baum

Zavoisky Physical-Technical Institute, FRC Kazan Scientific Center of RAS, Kazan 420029, Russian Federation, sahin@kfti.knc.ru

Studies of topological insulators (TI) are marked by a growing interest to the strong impact of various defects and local charge inhomogeneities on the fundamental properties of surface and bulk current carriers. We report the comprehensive studies of such phenomena in bulk transport in one of the best 3D TI $Bi_{1.08}Sn_{0.02}Sb_{0.9}Te_2S$ (BSSTS) [1, 2].

The first part of our research consisted in the contactless visualization of local charge and spin inhomogeneities using electron spin resonance (ESR) of the bulk charge carriers. An analysis of the observed ESR signal revealed that the current carriers participating in the resonance represent a random spaced array of electron or hole droplets of nanoscale sizes. It is expected that charge carriers from these droplets don't participate in the ordinary transport, since they cannot travel freely from one droplet to another.

Our transport measurements give evidence that for BSSTS at relatively high temperatures conduction due to electrons and holes follows the activation behavior with resistivity $\rho = \rho_0 \exp(\Delta/k_B T)$, but corresponding activation energies (Δ_e and Δ_h) are much smaller than the half of forbidden band, $E_g/2$. Analysis of our data revealed, that Δ_e and Δ_h may be as low as ~60 meV. Note, that for BSSTS $E_g/2 = 175$ meV [1, 2] and one obtains the estimate $\Delta = E_g$.

It is important, that at sufficiently low temperatures (<100 K) electrons and holes can tunnel between the droplets, so that variable range hopping (VRH) replaces activated transport. In the low temperature limit the resistivity should obey the Efros-Shklovskii (ES) law [3, 4] $\rho = \rho_0 \exp\{(T_{ES}/T)^{1/2}\}$, where T_{ES} is the characteristic ES temperature. For the BSSTS we estimated $T_{ES} \sim 2300$ K, and crossover to VRH ES regime takes place at 50–60 K.

1. Kushwaha S.K. *et al.*: Nat. Comm. **7**, 11456 (2016)
2. Sakhin V.O. *et al.*: JETP Letters **109**, 465 (2019)
3. Efros A.L., Shklovskii B.I.: J. Phys. C **8**, L49 (1975)
4. Skinner, Chen T., Shklovskii B.I.: Phys. Rev. Lett. **109**, 176801 (2012)

Improved Processing Scheme for Diffusion NMR Data Implemented in Web Server DDfit

V. A. Salikov[1], N. R. Skrynnikov[1,2], I. S. Podkorytov[1]

[1] Laboratory of Biomolecular NMR, St. Petersburg State University, St. Petersburg 199034, Russian Federation, st044619@student.spbu.ru
[2] Department of Chemistry, Purdue University, West Lafayette, IN 47907, USA

Pulsed-field gradient nuclear magnetic resonance (PFG-NMR) is extensively used for characterization of macromolecules and macromolecular assemblies. The range of problems addressed by PFG NMR includes protein-ligand interactions, protein oligomerization and aggregation, protein folding, formation of supramolecular assemblies and a host of other applications. Oftentimes, PFG NMR measurements are conducted on samples with low concentration as dictated by limited solubility of the species of interest or high cost of the material. Given poor signal-to-noise ratio of the experimental data, accurate determination of diffusion parameters becomes a challenge. The situation is compounded by baseline distortions, caused by residual solvent signals or various instrumental reasons. Under these circumstances, it is important to develop a robust data processing scheme, which would allow one to improve the accuracy of the experiment.

In this contribution, we present a new data processing scheme [1] to treat the data from 1D diffusion NMR experiments. The algorithm can be briefly described as follows. First, the user defines the boundaries of the spectral region intended for signal integration. The two boundary points are used to perform linear baseline correction. Next, the spectra are integrated in a standard fashion yielding the approximate values of signal intensities, $I_0(G_k)$. In order to obtain more accurate integral intensities, we generate the so-called model spectrum and then fit all of the individual spectra to this model spectrum. The model spectrum is constructed as a weighted average of all individual spectra in the series, with weights set to $I_0(G_k)$. This design is based on the concept of optimal filtration [2], which allows one to maximize the signal-to-noise ratio of the model spectrum. Fitting of the individual spectra to the model spectrum produces a set of refined integrals, $I(G_k)$, which can be interpreted using Stejskal-Tanner equation [3] or another appropriate formalism.

The new data processing scheme has been implemented in a form of web server named DDfit (Diffusion Data fit; https://ddfit.bio-nmr.spbu.ru). In order to use this service, the user needs to upload the files with spectral data from the Bruker TopSpin program and enter several relevant parameters (e.g. the boundaries of the integration region). The server obtains $I(G_k)$ values as described above. For stimulated-echo (STE), as well as double-stimulated-echo (DSTE) experiments the results can be fitted using the appropriate equations [3, 4] and the extracted diffusion coefficient is reported. The entire treatment is fast, taking just a few seconds.
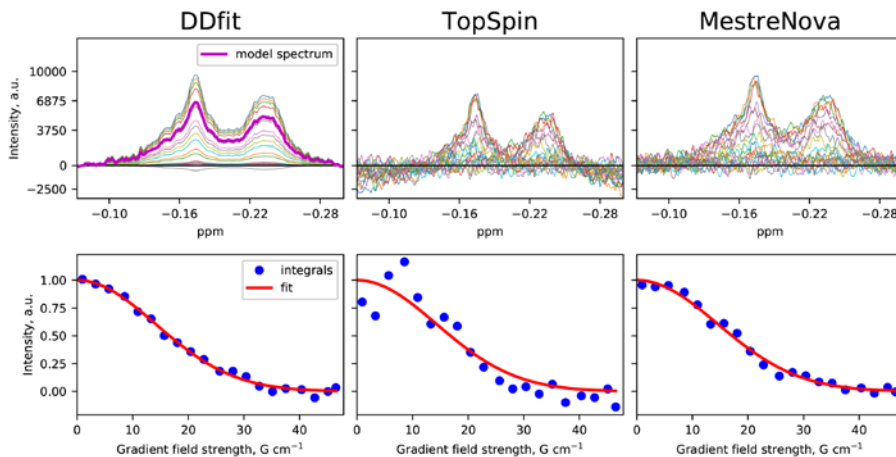
Fig. 1. Processing of DSTE data from a sample of lysozyme using DDfit, TopSpin and MesterNova.

The server has been tested on the simulated spectral data from the protein ubiquitin, as well as the experimental data from protein lysozyme collected in house. The new processing scheme proved to be both more accurate and more precise compared to the standard schemes available in the programs TopSpin and MestreNova.

1. Kharkov B.B., Podkorytov I.S., Bondarev S.A., Belousov M.V., Salikov V.A., Zhouravleva G.A., Skrynnikov N.R.: Angew. Chem. Int. Ed. **60**, 15445 (2021)
2. Ernst R.R., Bodenhausen G., Wokaun A. Principles of nuclear magnetic resonance in one and two dimensions. Oxford: Oxford University Press 1987.
3. Stejskal E.O., Tanner J.E.: J. Chem. Phys. **42**, 288 (1965)
4. Jerschow A., Muller N.: J. Magn. Reson. **125**, 372 (1997)

The Structure of Fibril-Forming SEM1(68-85) Peptide Increasing the HIV Infection

D. A. Sanchugova, V. V. Klochkov, D. S. Blokhin

Kazan Federal University, Kazan 420008, Russian Federation,
d.sanchugova@yandex.ru

The SEM1 (68-85) peptide is the N-terminal domain of the SEM1 (68-107) peptide. Peptide SEM1 (68-107) is a cleavage product of semenogelin 1 (SEM1) expressed in seminal vesicles. SEM1 (68-107) forms amyloid fibrils [1] that increase the infectious activity of HIV. To understand the process of fibrillation, it is necessary to have information about the spatial structure of the peptide and its domains.

This work presents the information about the SEM1(68-85) in aqua solution structure obtained by the Nuclear Magnetic Resonance (NMR) spectroscopy. Based on the NMR spectra it was done assignment chemical shifts of ^1H, ^{13}C, ^{15}N and identifies internuclear distances for SEM1 (68-85). Secondary structure prediction is also made using NMR spectrometry parameters [2] in the CCP-NMR [3] program. The analysis showed that SEM1(86-107) secondary structure refers to a random coil, but in the region from 76His to 78Gln, the presence of an alpha-helix turn is possible.

The obtained values of internuclear distances were used as input data for calculating the spatial structure of the peptide SEM1(68-85) in aqua solution using the XPLOR-NIH [4] program. The calculated structure also confirmed the presence of a disordered secondary structure, but a 310 helix is formed in the region from 73Ala to 76His.

The previously predicted secondary structure of SEM1(68-85) is consistent with calculations. We may assume that a fragment of 73Ala to 76His has low mobility and can participate in the process of fibrillation.

1. Munch J., Rucker E., Standker L. *et al.*: Cell **131**, no. 6, 1059–1071 (2007)
2. Wishart D.S., Sykes B.D., Richards F.M.: Biochemistry **31**(b) 1647–1651 (1992)
3. Vranken W.F., Boucher W., Stevens T.J. *et al.*: Proteins **59**, 687–696 (2005)
4. Schwieters C.D., Kuszewski J.J., Tjandra N., Clore G.M.: Journal of Magnetic Resonance **160**, no. 1, 65–73 (2003)

Tunable EPR Spectroscopy of Non-Kramers Ions in a YAlO$_3$ Crystal

**G. S. Shakurov[1], H. R. Asatryan[2], A. G. Petrosyan[3],
K. L. Hovannesyan[1], M. V. Derdzyan[3]**

[1] Zavoisky Physical-Technical Institute, FRC Kazan Scientific Center of RAS, Kazan 420029, Russian Federation, shakurov@kfti.knc.ru
[2] Ioffe Institute, Russian Academy of Sciences, St. Petersburg, 194021, Russian Federation
[3] Institute for Physical Research, National Academy of Sciences of Armenia, Ashtarak-2, 0203, Armenia

YAlO$_3$ crystal with paramagnetic impurities finds applications in laser physics and is the subject of numerous studies. Most of the known works on EPR spectroscopy are associated with the study of Kramers ions. The local symmetry of positions where impurity enter is CS for Y^{3+} and Ci for Al^{3+}. We have undertaken a study of a crystal YAlO$_3$ with an iron impurity by the method of tunable 37–850 GHz EPR spectroscopy. Two non-Kramers ions were found.

One of the centers observed in the 37–87 GHz frequency range belonged to the Tb^{3+} ion, which entered the crystal as an uncontrolled impurity. This is evidenced by the shape of the spectrum, which consists of four lines of the allowed hyperfine structure. The observed spectra are due to resonance singlet-singlet transitions. By measuring the angular and frequency-field dependences of the EPR spectra, we concluded that terbium replaces yttrium and obtained a set of spectral parameters that describe well the experimental results.

The second center is registered in the frequency range 200–230 GHz. Presumably, this EPR spectrum is due to the Fe^{2+} ion. The angular dependences of the spectra indicate the substitution of the aluminum ion. However, the value of the g-factor differs sharply from those known for Fe^{2+} in the octahedron. In addition, the frequency-field dependence of the spectrum indicates resonance transitions of the singlet-doublet type. Under low symmetry conditions, the doublet should be split. We measured the value of energy gap between singlet and doublet (215.2 ± 0.5 GHz), and did not find the splitting of the doublet. The report discusses the possible reasons for the disagreement with the literature data for the Fe^{2+} ion.

The Region of Existence of Nanoscale States with Magnetic and Ferroelectric Ordering

T. Shaposhnikova, R. Mamin

Zavoisky Physical-Technical Institute, FRC Kazan Scientific Center of RAS, Kazan 420029, Russian Federation, t_shap@kfti.knc.ru

The magnetoelectric effect (ME), i.e. the appearance of magnetization when an electric field is applied or the appearance of polarization when a magnetic field is applied, has been actively studied [1]. But the practical application of ME was difficult, since it was observed at low temperatures, and the resulting magnetization and polarization were small. In recent years, new materials with more attractive characteristics for practical use have been synthesized [2]. In addition, ME was found in heterostructures, composite materials [3] and multi-ferroics (MF), for example, in some manganites, boracites and hexaferrites [2].

The charge and phase separation in the MF near the phase transition leads to the formation of small bounded regions with a magnetic order. Inhomogeneous magnetic ordering in these regions, as well as the presence of a boundary between the phases, can lead to a magnetoelectric response. A similar mechanism for the appearance of polarization is observed in domain walls in magnetically ordered materials. In this paper, we consider the possibility of electric polarization in small spherical magnetic particles located in a paramagnetic matrix.

The inhomogeneous vortex distribution of magnetization and the associated inhomogeneous electric polarization in such small magnetic particles was obtained earlier in the framework of a phenomenological model [4]. The microscopic mechanism of the magnetoelectric effect is due to the Dzyaloshinskii-Moriya interaction [5, 6]. The specific type of expressions for magnetization and polarization is determined by the geometric shape of the nano-regions. Within the framework of this report, the region of the existence of such states is determined.

1. O'Dell T.H.: The Electrodynamics of Magneto-Electric Media. Amsterdam 1970.
2. Fiebig M., Lottermoser T., Meier D., Trassin M.: Nat. Rev. Mater. **1**, 16046 (2016)
3. Zhou Z., Zhao S., Gao Y. *et al.*: Sci. Rep. **6**, 20450 (2016)
4. Shaposhnikova T., Mamin R.: Ferroelectrics **576**, 62 (2021)
5. Dzyaloshinskii I.: JETP **10**, 628 (1960)
6. Morya T.: Phys. Rev. **120**, 91 (1960)

Intermolecular Mobility of Pillar[5]arene – α-Lipoic Acid Complex by NMR Spectroscopy Data

L. V. Sharipova[1,2], E. A. Ermakova[1], <u>A. N. Turanov</u>[3], B. I. Khayrutdinov[1,2], Y. F. Zuev[1]

[1] Kazan Institute of Biochemistry and Biophysics, FRC Kazan Scientific Center of RAS, Kazan 420008, Russian Federation, gilbert.robs@yandex.ru
[2] Institute of Physics, Kazan Federal University, Kazan 420008, Russian Federation
[3] Zavoisky Physical-Technical Institute, FRC Kazan Scientific Center of RAS, Kazan 420029, Russian Federation

The creation of new macrocyclic compounds and the study of their ability to molecular recognition is one of the rapidly developing areas of modern supramolecular chemistry. Pillar[5]arenas are unique compounds that have high symmetry, a rigid frame, planar chirality, and also capable of forming host-guest complexes [1]. The aim of the work is to study the intramolecular mobility of the decaammonium salt 4,8,14,18,23,26,28,31,32,35-deca (carboxymethoxy) – pillar[5]arene (hereinafter pillar[5]arene 1) with encapsulated biologically active substance α-lipoic acid.

Within the framework of this work, the complex of pillar[5]arene 1 with α-lipoic acid was studied by NMR spectroscopy. The proton mobility of the guanidine fragment of pillar[5]arene 1 in complex with α-lipoic acid was characterized by determining the chemical exchange rate constant from the CPMG (Carr-Purcell-Meiboom-Gill) spectra. The temperature dependence of the chemical exchange rate constant was used to determine the thermodynamic parameters of the conformational exchange of protons in the guanidine fragment of the pillar[5] arene 1. The dissociation constant of the pillar[5]arene 1 – α-lipoic acid complex was determined by the Benesi-Hildebrand method. The 3D model of complex was simulated by semiempirical methods of quantum chemistry.

1. Ogoshi T.: J. Am. Chem. Soc. **130**, 5022–5023 (2008)

Direct Measurements of Magnetic Polarons in $Hg_{1-x}Mn_xTe$ (*x* = 0.135) by Magnetic Resonance Method

A. V. Shestakov[1], I. I. Fazlizhanov[1], I. V. Yatsyk[1,3], M. A. Cherosov[3], I. I. Ibragimova[1], R. M. Eremina[1,3]

[1] Zavoisky Physical-Technical Institute, FRC Kazan Scientific Center of RAS, Kazan 420029, Russian Federation, tatyana.gavrilova@gmail.com
[2] Institute of Solid State Chemistry of the Russian Academy of Sciences (UB), Ekaterinburg, 620990, Russian Federation
[3] Institute of Physics, Kazan Federal University, Kazan, 420008, Russian Federation

$Hg_{1-x}Mn_xTe$ as a typical narrow-gap semimagnetic semiconductor has found applications in infrared photonic devices. The interesting magnetic properties of magnetic semiconductors $Hg_{1-x}Mn_xTe$ originates in the strong sp-d exchange interactions that exist between carrier spins (i.e., band electrons and holes with s- and p-type wave functions) and the local 3d spins of embedded paramagnetic dopant atoms. In $Hg_{1-x}Mn_xTe$, the defects form magnetic polarons at low temperatures because the sp-d exchange interaction between Mn ions and the carriers localized at defects may induce magnetization in their vicinity [1]. The binding energy of magnetic polarons decreases as temperature or magnetic field increases in the dilution regime. Moreover, owing to the spin-polarization of Mn^{2+} ions and thermodynamic fluctuations of magnetization, the average moment of magnetic is usually not zero.

The aim of this work is investigation of magnetic polaron in $Hg_{1-x}Mn_xTe$ (*x* = 0.135) by magnetic resonance method. The EPR spectra were measured at temperature range from 5 to 300K in the continuous wave mode in the X-band using an EMXPlus spectrometer. The temperature dependence of the magnetic resonance spectra of these samples was studied. It was found that the magnetic resonance spectrum contains signals belonging to different spin systems. Three signals are distinguished in the spectrum. Two signals, with a strong temperature dependence of the *g*-factor and a width that increases with temperature, are due to magnetic polarans. For the third signal, broadening is observed with decreasing temperature and approaching the ordering temperature, which is characteristic of exchange-coupled spins. We assume that this signal belongs to manganese ions, whose spins are linked by exchange interaction. The temperature dependence of the Hall constant was measured.

1. Zhu L., Shao J., Lin T., Lu X., Zhu J., Tang X.: J. Chu: J. of App. Phys. **111**, 083502 (2012)

Variation Perturbation Scheme for Calculating Temperature Dependence of the Unconventional Spin-Singlet Superconductors

F. Siraev, M. Avdeev, Yu. Proshin

Theoretical Physics Department, Institute of Physics,
Kazan Federal University, Kazan, Russian Federation, siraevfail@mail.ru

A variational perturbation theory [1] is proposed for is the framework of calculating the temperature dependence d-wave and higher-harmonic components of the superconducting order parameter in unconventional superconductors. Up to two-loop diagrams, the variational free energy functional was calculated. Angular dependence of the order parameter along the Fermi contour was tried in the form of series [2]

$$\Delta(\varphi) = \Delta_s + \sum_{n=1} \Delta_n \sqrt{2} \cos(2n\varphi) \ \ ,$$

where components Δ_s and Δ_n are determined by minimizing procedure of the functional at fixing temperature T. Moreover, the spin-singlet superconducting pairing potential we tried in form of the series as follows

$$V(\varphi_1 - \varphi_2) = \lambda \sum_{n=1} \frac{2\sin(n\delta)}{n(\pi - \delta)} \cos(2n(\varphi_1 - \varphi_2)) \ \ ,$$

where λ is coupling constant and δ is phenomenological coupling parameter. It was shown that this pairing potential leads to the appearance of $\cos(2\varphi)$, $\cos(6\varphi)$ and $\cos(10\varphi)$ order parameter harmonics, which is in agreement in [2]. The temperature dependences of these harmonics were also calculated. It is shown that the temperature dependence of higher harmonics differs significantly from the BCS ones.

1. Sissakian A., Solovtsov I., Shevchenko O.: Int. J. Mod. Phys. A **9**(12), 1929–1999 (1994)
2. Parker D., Balatsky A.V.: Phys. Rev. B **78**, 214502 (2008)

^{13}C NMR High Resolution Spectrometry and Relaxometry for Soybean Oil Research

M. Smirnov, I. Mershiev, G. Kupriyanova

Institute of Physics, Mathematics and Information Technology, Immanuel Kant Baltic Federal University, 236041, Kaliningrad, Russian Federation,
galkupr@yandex.ru; smirnov.mark2015@yandex.ru

Vegetable oils are an important part of the daily human diet. Soybean oil has one of the largest market shares of vegetable oils. However, the composition and quality of soybean oil depends on the living conditions of the soybeans, processing techniques and storage methods. Therefore, the problem of the qualitative composition of consumed soybean oil is quite acute. NMR has a number of advantages over chemical methods (mass spectroscopy, for example), since it does not require special sample preparation and is a non-destructive method. This method has good prospects for studying multicomponent systems. High resolution ^{1}H NMR has already been successfully used to determine a qualitative composition of various oils as well as processed soybean oil based on the quantitative analisys of essential fatty acids. ^{1}H NMR relaxometry in a low magnetic field made it possible to reveal the differences between the samples subjected to extraction and hydrogenation, based on their relaxation profile [1]. It should be noted that the determination of the composition of oils by NMR spectroscopy methods is complicated by the fact that individual signals of various fatty acids, such as linolenic, oleic, stearic, and palmitic acids, overlap. This made it difficult to quantify stearic and palmitic acids, the important technological indicators.
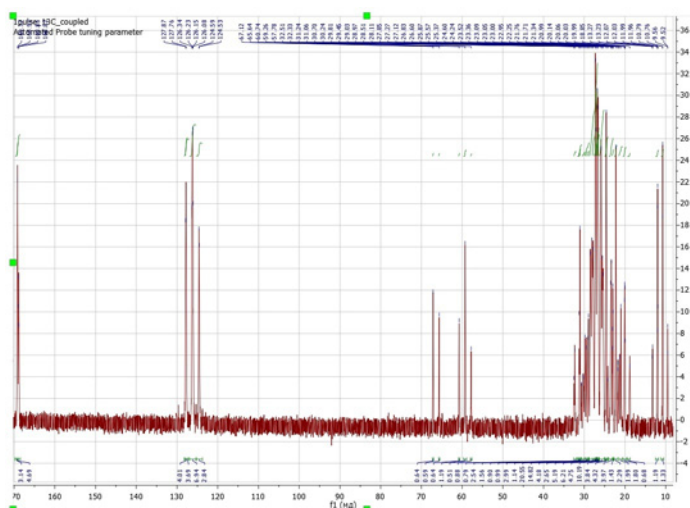
Fig. 1. ^{13}C NMR spectra of soybean oil without proton decoupling.

13C T1, Proton decoupling: OFF
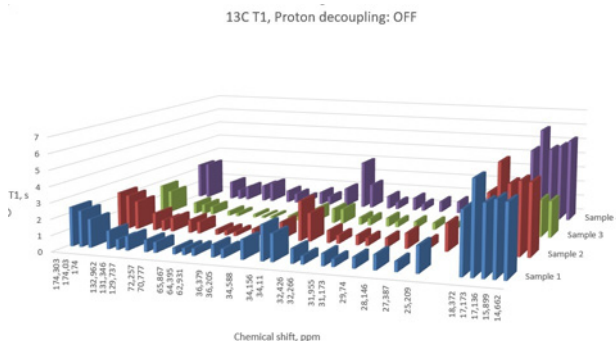
Fig. 2. ^{31}P NMR spectra of soybean oil.

The aim of this work was to study the processed samples of soybean oil by NMR methods ^{1}H, ^{31}P, ^{13}C in order to obtain more complete information about their qualitative composition and dynamic behavior of ^{13}C belonging to the CH_2 group of various changes in fatty acids, to identify indicators that determine the composition of oils after hydration and extraction.

High resolution ^{13}C NMR spectra were obtained on a Varian 400 MHz Premium Shielded instrument with $B = 9$ T. Spectra of soybean oil were recorded using standard parameters: 250.0 ppm spectral width, 1 s. relaxation delay, 45 degrees pulse width, 256 scans. Spectra were recorded with and without proton decoupling (Fig. 1). The inversion-recovery method was used to measure the spin-lattice relaxation times (64 scans, 20 s relaxation delay). The processing of the spectra and the calculation of the relative integral intensities of ^{1}H and ^{13}C signals were carried out using the MestreNova program. Additionally, ^{31}P NMR spectra were recorded for 4 oil samples previously studied by chemical methods. The chemical analysis data are given in the Table 1.
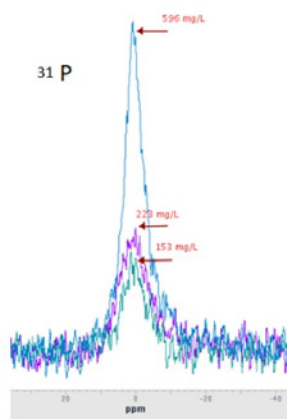
Fig. 3. Distribution of ^{13}C NMR longitudinal relaxation times for 4 soybean oil samples.

Table 1. The chemical analysis data for soybean oil samples.

№ soybean oil	phosphorus content (mg/kg)	stearin
1 extraction	596	1,52
2 hydrated	223	0,57
3 hydrated	153	0,39
4 hydrated	6,6	0,02

^{13}C, ^{1}H NMR, ^{13}C NMR {^{1}H} and ^{13}C-^{1}H COSY spectra of soybean oil samples were recorded and used to assign ^{13}C and ^{1}H signals (Fig. 1). The assignment of signals in the ^{13}C spectrum to the functional groups of fatty acids was carried out both on the basis of experimental data [1] and literature data [2, 3]. Using a chemometric approach and data on the intensities of the ^{13}C signal lines without suppression of protons, a qualitative change in fatty acids in the composition of the samples was revealed. The ^{31}P NMR spectrum data showed that the phosphorus content in the samples correlates with the data obtained by chemical methods and can be used to authenticate soybean oil samples. The inversion-recovery method was used to measure the spin-lattice relaxation times of carbon nuclei. ^{13}C relaxation profiles of each sample were obtained. The analysis showed that the relaxation profiles of the samples are different (Fig. 3) and can be used to authenticate soybean oil samples that are subjected to processing.

1. Smirnov M., Mershiev I., Kupriyanova G.: ^{1}H high-resolution NMR spectrometry and relaxometry for soybean oil research. Magnetic Resonance and its Applications. Spinus-2021. Proceedings. Saint Petersburg State University, 2021. 282 pp. ISSN 2542-2049
2. Chira N.-A., Todasca M.-C., Nicolescu A., Rosu A., Nicolae M., Rosca S.-I.: Evaluation of the Computational Methods for Determining Vegetable Oils Composition using ^{1}H NMR Spectroscopy. Revista de Chimie, 2011, 62.
2. Sacchi R., Addeo F., Paolillo L.: ^{1}H and of Virgin Olive Oil: ^{13}C NMR An Overview. MAGNETIC Resonance in Chemistry **35**, 133–45 (1997)

Investigation of Pyrochlore Structure Compounds: $Tb_2Ti_2O_7$ and $(Y_{0.95}Er_{0.05})_2Sn_2O_7$ Synthesis, Magnetic Measurements and *ab initio* Calculations

A. V. Spiridonova, M. A. Cherosov, B. F. Gabbasov, A. G. Kiiamov, R. V. Yusupov, O. V. Nedopekin, I. V. Romanova

Institute of Physics, Kazan Federal University, Kazan, 420111, Russian Federation, phys.dep@kpfu.ru

Pyrochlores with the general formula $A_2B_2O_7$ have face centred cubic structure with the $Fd\overline{3}m$ space group. Compounds with such structure where A = Er^{3+}, Dy^{3+}, Tb^{3+}, Ho^{3+}, Sm^{3+}, Yb^{3+}, Tm^{3+} stands for a rare-earth ion show exotic magnetic behaviors such as dipolar spin ice and spin liquid phases, a first order transition in the spin dynamics, complex antiferromagnetic and frustration at the low temperatures [1]. Investigations on pyrochlores mainly contain calculations of Hamiltonians based on the crystal field theory, while the lack of modern ab initio calculations on these materials delays understanding of these magnetic model Hamiltonians [2–3]. However, nowadays phonon spectrum can be successfully reproduced from modern ab initio calculations of periodic structures, what subsequently allows the reproduction of all modes of a given structure.

In the present work are reported the results of ab initio calculations of the $Tb_2Ti_2O_7$ pyrochlores crystal structure and the phonon density and mode spectra. The calculations were performed MedeA software. The GGA–PBE-sol functional was choosing as a basic for using within the density functional theory method [4]. Single crystal of $Tb_2Ti_2O_7$ and microsized powder of $(Y_{0.9}5Er_{0.05})_2Sn_2O_7$ were synthesized by the optical floating zone method. All samples were analysed by X-ray diffraction. Magnetic properties were determined by vibrating magnetometry in the magnetic fields up to 90 kOe and the temperature range of 5 K to 300 K. EPR measurements were made using a laboratory spectrometer it the magnetic fields up to 5000 Oe. The experiments and analysis for microsized powder $(Y_{0.95}Er_{0.05})_2Sn_2O_7$ were held for the first time. The obtained data for $Tb_2Ti_2O_7$ is in agreement with previous results [5]. This work is supported by the Russian Science Foundation, Grant No. 19-12-00244.

1. Petit S. **et al.**: Phys. Rev. Let. **119**, 187202 (2017)
2. Klekovkina V.V., Malkin B.Z.: Optics and Spectroscopy **116**, 6 (2014)
3. Deilynazar N., Khorasani E., Alaei M., Hashemifar S.J., e-print arXiv:1502.01814v1 (2015)
4. Kresse G., Furthmuller J.: Phys. Rev. B **54**, 11169 (1996)
5. Chernyshev V.A., Petrov V.P., Nikiforov A.E., Phys. Solid State **57**, 5 (2015)

Time Resolved EPR Study of Some Photoexcited Twisted Molecules

A. A. Sukhanov[1], V. K. Voronkova[1], Yuxin Yan[2], Z. Mahmood[2], J. Zhao[2]

[1] Zavoisky Physical-Technical Institute, FRC Kazan Scientific Center of RAS, Kazan 420029, Russian Federation, vio@kfti.knc.ru

[2] State Key Laboratory of Fine Chemicals, School of Chemical Engineering, Dalian University of Technology, 116024, P. R. China, zhaojzh@dlut.edu.cn

Triplet photosensitizers (PSs) have attracted much attention in fundamental photochemistry studies, as well as in applications in photocatalysis, photodynamic therapy (PDT), photovoltaics, photon upconversion, etc. For these applications, it is crucial to design organic triplet PSs showing strong visible-light absorption, efficient intersystem crossing (ISC), and long-lived triplet states. ISC is an electron spin-forbidden electronic transition, whose efficiency relies on the magnitude of the spin−orbit coupling (SOC) effects in organic compounds. Several mechanisms for enhancing ISC are known, each of the mechanisms has its own advantages and disadvantages. One of the possible ways to create effective triplet PSs is to use nonplanar chromophores. To develop a heavy-atom-free organic triplet PSs design strategy it is needed to study the relationship between the twisting of the π-conjugation framework of chromophore and the ISC efficacy, and to find out whether a twisted molecule will always show more efficient ISC than the corresponding planar structures.

Here we present the results of an TREPR study of two Bodipy derivatives: BDP-B and BDP-P with a minor and with a significantly twisted π-conjugated framework, respectively. The electron spin selectivity of the ISC of the derivatives is different, manifested by the phase pattern of the TREPR spectra as AAEAEE and EEEAAA for BDP-B and BDP-P, respectively. The study of these Bodipy derivatives demonstrated that the twisted π-conjugated framework does not necessarily induce efficient ISC [1].

The results of TREPR studies of two perylenebisimide (PBI) derivatives with anthryl and carbazole moieties fused at the bay position, showing twisted π-conjugation frameworks are also presented [2].

The obtained data are useful for in-depth understanding of the ISC efficiency of molecules with a twisted π-conjugated framework and for the design of heavy-atom-free triplet PSs.

1. Yan Yu., Sukhanov A.A. *at al.*: J. Phys. Chem. B **125**, 6280−6295 (2021)
2. Mahmood Z., Sukhanov A.A. *at al.*: J. Phys. Chem. B **125**, 9317−9332 (2021)

On the Manifestation of the Le Chatelier-Braun Principle in Trehalose Matrices Photosystem 1

A. Sukhanov[1], M. Mamedov[2], A. Semenov[2], K. Salikhov[1]

[1] Zavoisky Physical-Technical Institute, FRC Kazan Scientific Center of RAS, Kazan 420029, Russian Federation
[2] A. N. Belozersky Institute of Physical-Chemical Biology, Moscow State University, Moscow, Russian Federation

Disaccharide trehalose prevents protein denaturation caused by freezing, heating, and drying [1]. The existing paradigm of the protective mechanism of the native protein structure by trehalose is based on the assumption that this sugar inhibits protein dynamics [2]. Although this assumption seems to be very interesting, it requires additional details and evidences. Based on our experimental results and analysis of the data available in the literature, we proposed a phenomenological molecular model of the stabilizing and cryoprotective effect of trehalose on the functioning of the reaction center (RC) of photosystem I (PSI) [3]. This model assumes the existence of two pathways for the adsorption of trehalose – endothermic and exothermic, which may differ due to the conformation of this disaccharide or due to the different realization types of formation of the hydrogen bonds of trehalose with surrounding molecules. In doing so, the effect of trehalose on the functioning of the RC can be explained by the Le Chatelier-Brown principle. To justify the model, the influence of 4Fe-4S clusters on the spin-lattice relaxation of separated charges in the RC of PS I is of fundamental importance.

Earlier, using the out-of-phase ESEEM, we measured the distance between the separated charges on the primary donor P700+ and the phylloquinone acceptor A1− in the PS I RC, lacking terminal 4Fe-4S clusters FA and FB, embedded into a dry trehalose matrix. It was shown that this distance does not change when heated from 150 K to room temperature [4].

In this work, we measured the distance in the PS I RC with iron–sulfur complexes removed. It was found the modulation frequency of the out-of-phase ESEEM signal depends on the temperature. We assume that this change in frequency can be explained by rather fast hopping of electrons between branches A and B, so that only the averaged modulation frequency appears.

1. Palazzo G., Mallardi A., Hochkoeppler A., Cordone L., Venturoli G.: Biophys. J. **82**, 558 (2002)
2. Savitsky A., Gopta O., Mamedov M., Golbeck J.H., Tikhonov A., Möbius K., Semenov A.: Appl. Magn. Reson. **37**, 85 (2010)
3. Sukhanov A.A., Mamedov M.D., Möbius K., Semenov A.Y., Salikhov K.M.: Appl. Magn. Reson. **49**, 1011–1025 (2018)
4. Sukhanov A.A., Mamedov M.D., Möbius K., Semenov A.Y., Salikhov K.M.: Appl. Magn. Reson. **51**, 909–924 (2020)

Fluorine and Sodium MRI on 0.5 T Clinical Scanner

**A. A. Tarasova[1], N. V. Anisimov[2], O. S. Pavlova[1,2], M. V. Gulyaev[2],
I. A. Usanov[1], Yu. A. Pirogov[1]**

[1] Faculty of Physics, Lomonosov Moscow State University, Moscow 119991, Russian Federation;
arina.tarasova99@mail.ru
[2] Faculty of Fundamental Medicine, Lomonosov Moscow State University, Moscow 119991,
Russian Federation

Typical MR scanners are focused on the detection of proton (^{1}H). Detection of other nuclei provides additional diagnostic information – about the state of tissues, cellular processes, etc. Sodium is of considerable interest – the natural abundance of the ^{23}Na isotope is 100%, and the gyromagnetic ratio is 3.8 times lower than of proton. However, the sodium content in living tissues is 2-3 orders of magnitude lower than that of hydrogen, which determines the low sensitivity of the method. The detection of fluorine signals is also of interest in MRI. The ^{19}F isotope has 100% natural abundance and its gyromagnetic ratio is only 6% less than of proton. So, ^{1}H and ^{19}F MRI are comparable in sensitivity. The content of fluorine in living tissues is extremely low, therefore, it is very productive to detect signals from fluorine-containing substance injected into the body, for example, a drug, as well as from gases in the lungs, since there is no background from normal tissues in the images. The use of strong fields – from 3 T and more increases the sensitivity of multinuclear methods. However, such fields are unattainable with open-type magnets and compact portable MRI systems. Therefore, it is of interest to evaluate the productivity of multinuclear research on low-field equipment. We carried out these studies on a 0.5T clinical scanner Bruker Tomikon S50 (1H NMR frequency is 21.1 MHz). The technical rework concerned only the coils, which were used as modified proprietary prototypes, originally intended for the detection of protons [1, 2].

In experiments on ^{19}F MRI (19.8 MHz) of human lungs, we used octafluorocyclobutane gas C_4F_8 [1]. The patient inhaled a gas mixture (80% C_4F_8 + 20% O_2) and during the breath holding, scanning was performed. Since this gas has $T_1 \sim 50$ ms, we use FSE method (TE_{min} = 8 ms, ETL = 4). There were 2D FSE in 3 projections (TR = 69 ms, NA = 30, in-plane resolution of 1×1 cm^2, no slice selection, scan time of one projection of 20 s), SNR up to 43) and 3D FSE (TR = 42 ms, NA = 4, voxel size = $1\times1\times1$ cm^3, scan time = 33 s, SNR up to 11). Measurements were carried out on 6 volunteers: females – 23 and 27 y.o. and males – 23, 23, 40 and 71 y.o. The 3D scan data were used to calculate the volumes of lung lobes and their volumetric reconstructions. Real-time studies of lung filling during inhalation and exhalation have also been conducted. For this, 2D scans (TR = 45 ms) were carried out 16÷30 times every 5÷7 seconds, NA = 16÷20. 2D scan data was used also to create maps of T1, ventilation and perfusion.

^{23}Na MRI (5.6 MHz) was done using 3D GRE technique (TR/TE = 44.7/12 ms, FA = 45°, NA = 1, voxel size = $6\times6\times6$ mm^3, scan time = 24.5 min) [2, 3].
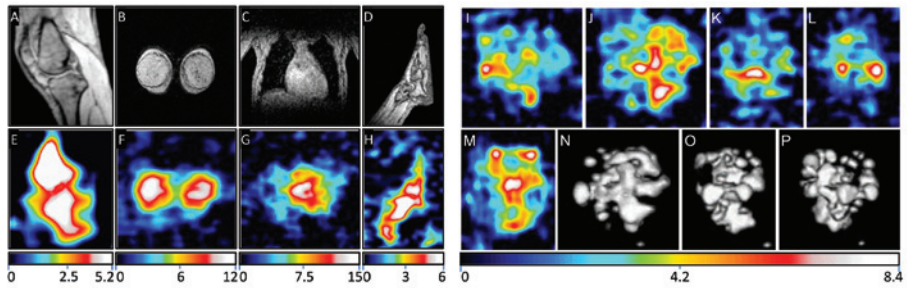
Fig. 1. MR images of different human organs: ^{1}H (A-D) and ^{23}Na (E-O).

To increase the SNR by an order of magnitude, the k-space data were exponentially apodized. To eliminate external RF interference, scans were performed at specific times of the day, and pulse noise bursts detected in k-space were edited [4]. Fig.1 shows examples of MRI of different human organs. Images A,E, I-M were obtained using a saddle coil and B-D, F-H using a solenoid coil. These coils are optimized for extremities and breast studies, respectively. For assignment of anatomical structures on ^{23}Na images E (knee, sagittal), F (breast, coronal), G (heart, coronal), H (foot, sagittal), corresponding ^{1}H images are shown: A-D. The right panel shows MRI of the head – separate slices: I,J (sagittal), K,L (coronal), M(axial), as well as 3D reconstruction – rendering at different azimuthal angles: –90°(N), 0°(O), 10°(P). The brightness scale corresponds to the SNR values. Optimization of the transceiver path can increase the SNR by more than 2 times [3].

^{19}F MRI on a 0.5 T clinical scanner is easy to implement. ^{23}Na MRI on it is also possible, but it is necessary to pay attention to the design of the coils and setting up the transceiver path.

1. Pavlova O.S., Anisimov N.V., Gervits L.L. *et al.*: Magn. Reson. Med. **84**, 2111 (2020)
2. Anisimov N.V., Tarasova A.A., Pavlova O.S. *et al.*: Appl. Magn. Reson. **52**, 221 (2021)
3. Anisimov N.V., Tarasova A.A., Pavlova O.S. *et al.*: Achiev. Mod. Radioel. **75**, 37 (2021)
4. Anisimov N.V., Tarasova A.A., Usanov I.A. *et al.*: Electromagn. Waves & El. Syst. **26**(6), 3 (2021)

Rotating-Frame Overhauser Enhancement Using Long-Lived Coherences

F. Teleanu[1,2], A. Topor[1,3], D. Serafin[4], A. Sadet[1], P. R. Vasos[1,2]

[1] Extreme Light Infrastructure - Nuclear Physics ELI-NP, Laser Gamma Experiments Department (LGED), "Horia Hulubei" National Institute for Physics and Nuclear Engineering IFIN-HH, 30 Reactorului Street, 077125-Bucharest-Măgurele, Romania
[2] Interdisciplinary School of Doctoral Studies, University of Bucharest, Regina Elisabeta Blvd., Bucharest, Romania
[3] Inorganic Chemistry Laboratory, Faculty of Chemistry, University of Bucharest, 23 Dumbrava Rosie Street, Romania
[4] Faculty of Physics, University of Bucharest, 405 Atomistilor Street, Măgurele, Romania

The nuclear Overhauser effect is omnipresent in the structural investigations of small and large molecules using nuclear magnetic resonance. The through-space dipolar coupling provides a good estimation of the internucleus distance between nuclei up to 5–6 Å. This limitation is due to the weak dipolar interaction and short lifetime of magnetization to be transferred among nuclei. The latter impediment can be overcome by employing long-lived magnetization reservoirs known as long-lived states (LLS) [1] and coherences (LLC's) [2]. Here, we present the theoretical evidence for the enhanced rotating-frame Overhauser transfer from a pair of two J-coupled spins (I, S) to a third one (K) resembling the protons' configuration in a small dipeptide. It is shown that by using the magnetically active LLC's ($I_x - S_x$) as magnetization source instead of the transverse magnetization ($I_x + S_x$), the former can lead to an enhanced magnetization accumulation at the K spin compared to the transfer from the later, from a certain correlation time characteristic to large proteins. Also, an oscillation behavior of the transfer from LLC's is predicted and proved experimentally.

1. Carravetta M., Johannessen O.G., Levitt M.H.: Phys. Rev. Lett. **92**, 153003 (2004)
2. Sarkar R., Ahuja P., Vasos, P.R., Bodenhausen G.: Phys. Rev. Lett. **104**, 053001 (2010)
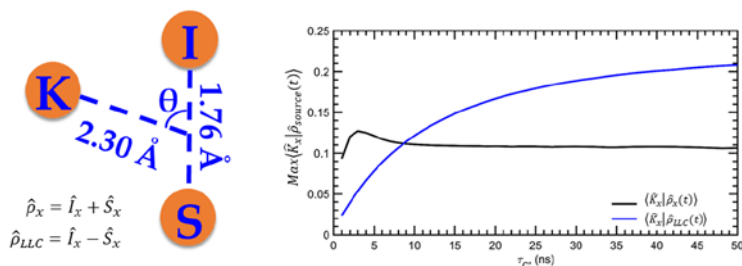
Fig. 1. (Left) Spins' configuration used for simulation. (Right) Predicted maximum amplitude of the ROE transfer from transverse magnetization (black curve) and from LLC (blue curve) towards the transverse magnetization of the third spin K_x as a function of the rotational correlation time τ_C. LLC-based transfer of magnetization becomes more effective than the transfer based on transverse magnetization at rotational correlation time values $\tau_C > 10$ ns.

Critical Temperature of Superconductor/Ferromagnet Nanostructure Containing Magnetic Skyrmion

V. A. Tumanov, V. E. Zayceva, Yu. N. Proshin

Theoretical Physics Department, Kazan Federal University, Kazan 420008, Russian Federation,
tumanvadim@yandex.ru

This research addresses the proximity effect of a superconductor with a chiral ferromagnetic metal. We theoretically study the effect of skyrmions and chiral bobbers [1] on a critical temperature of superconductor/ferromagnet (S/F) hetero-structure. In recent years many very small scale (1–100 nm) magnetic skyrmions and skyrmion lattices have been experimentally discovered in specially created materials [2, 3]. In contrast to the previously discovered micron-scale spin vor-tices, such structures can have a significant effect on the critical temperature of the superconducting transition.

We have studied the S/F systems in the dirty limit, since this approxima-tion is consistent with most experimental systems. We started with rotation of the matrix Usadel function $\hat{F}(r, \omega)$[4] in spin space. The transformed Usadel equation has the form

$$\frac{D_f}{2}\widehat{\mathcal{D}}^2\tilde{F}(r,\omega) - |\omega|\tilde{F}(r,\omega) - \frac{iI}{2}\mathrm{sgn}\omega\{\tilde{F}(r,\omega),\hat{\sigma}_3\} = 0,$$

where $\tilde{F}(r,\omega) = \hat{U}\hat{F}(r,\omega)\hat{U}^{-1}$, $\widehat{\mathcal{D}}\hat{f} = \nabla\hat{f} + [\widehat{\mathbf{A}},\hat{f}]$, $\widehat{\mathbf{A}} = \hat{U}\nabla\hat{U}^{-1}$, D_f is the diffusion constant, ω is the Matsubara frequency, I is the effective exchange field. The rotation matrix $\hat{U}$ is chosen in such a way that in the transformed equation the term responsible for the interaction with localized spins becomes diagonal. Boundary conditions on S/F interface have the form

$$\frac{4D_s}{v_s\sigma_s}\left(\nabla\widetilde{F}_s, \mathbf{n}\right) = \frac{4D_f}{v_f\sigma_f}\left(\widehat{\mathcal{D}}\widetilde{F}_f, \mathbf{n}\right) = \widetilde{F}_f - \widetilde{F}_s,$$

where $v_{S(f)}$ is the Fermi velocity, $\sigma_{S(f)}$ is the transparency parameters of the bound-ary for the S and F layers, respectively. The normal vector $\mathbf{n}$ is directed from S to F layer. On the external surfaces the boundary conditions have the form

$$\left(\nabla\widetilde{F}_s, \mathbf{n}\right) = 0, \left(\widehat{\mathcal{D}}\widetilde{F}_f, \mathbf{n}\right) = 0.$$

Self-consistency equation is invariant under such transformations and has conventional form (see, for example [5]). We use a generalization of the approach constant within the layer of the order parameter, so this procedure simplifies the boundary value problem in many practical cases. For complex spin textures, such as spin vortices and domain walls, the Usadel equation does not reduce to an equation with constant coefficients after the unitary rotation. However, the transformed Usadel function phase changes much weaker along the SF bound-ary. This allows us to use an approximate approach to solve boundary value
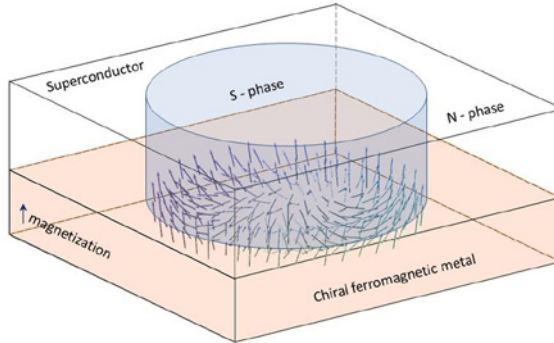
Fig. 1. Schematic representation of a superconducting phase localized near a chiral skyrmion.

problem by neglecting some terms in the Usadel equation for the ferromagnetic layer. This approach allowed us to obtain a quantitative estimation of the effect on the superconducting critical temperature for almost any spin texture.

Using our approach, we calculated the critical temperature for S/F systems containing conical magnetization, Neel, Bloch, chiral skyrmions, chiral bobbers. As expected, the impact on critical temperature near the magnetic inhomogeneity is determined by its scale compared to the superconducting coherence length. According to our calculations, the described effect is very sensitive to the thickness of the superconducting layer and the border transparency. By special choice of layer thicknesses, it is possible to achieve that superconductivity occurs only in the spin vortex localization region (see Fig.1). In this case the critical temperature is about 10-20% of the bulk superconductor critical temperature.

The significant effect of nanoscale spin vortices on the critical temperature, combined with topological stability and low current density required for their movement [3], makes it possible effectively to use such systems as superconducting spin valves.

1. Borisov A.B.: Physics-Uspekhi **63**, 269 (2020)
2. Romming N. *et al.*: Science **341**, 636 (2013)
3. Baumard J. *et al.*: Physical Review B **99**, 014511(2019)
4. Fominov Y.V., Volkov A.F., Efetov K.B.: Physical Review B **75**, 104509 (2007)
5. Efetov K.B. *et al.*: Springer Tracts in Modern Physics **227**, 251 (2008)

Application of High Frequency Magnetic Resonance Spectrometer for Study of Recombination Centers by Microwave Spin Dependent Photoconductivity

Yu. A. Uspenskaya, R. A. Babunts, L. S. Vlasenko

Ioffe Institute, Russian Academy of Sciences, St. Petersburg, Russian Federation,
yulia.uspenskaya@mail.ioffe.ru

Electrical Detection of Magnetic Resonance (EDMR) using the spin dependent change of microwave photoconductivity of semiconductors is a few orders of magnitude more sensitive compare to usual Electron Paramagnetic Resonance (EPR) method for detection paramagnetic recombination centers, as well as to EDMR methods utilized the electrical contacts applied to samples and detection of dc-photocurrent changed under magnetic resonance. The microwave photoconductivity detection of magnetic resonance is based on the effects of spin dependent recombination when the recombination rate and, consequently the concentration of photo excited carriers, or sample photoconductivity, are changed under magnetic resonance of recombination centers. The change of photoconductivity is detected by absorption of the electrical component of microwave field while the magnetic resonance is excited by microwave magnetic component [1].

The main goal of this work is to demonstrate the advantages of high frequency EDMR for investigation of recombination centers in semiconductors and to determine the optimal experimental conditions for microwave EDMR detection. Experiments were performed with pure high resistance (300 $\Omega \cdot$ cm) float zone (FZ) grown silicon crystals irradiated by γ-rays with dose $\approx 10^{17}$ cm^{-2}. The dominant spin dependent recombination process in these samples is the recombination through the excited triplet states of carbon related centers showing strong microwave detected EDMR signals with well resolved fine- and hyperfine structures. The change of microwave photoconductivity is observed not only at the magnetic resonance, but at zero-field and at the magnetic fields corresponding to the anticrossing points of magnetic sublevels of triplet centers.

1. Vlasenko L.S.: Appl. Magn. Reson. **47**, 813 (2016)

Magnetic Study of the Dendrimeric Iron(III) Carbazole Complexes

V. E. Vorobeva[1], D. V. Starichenko[2], M. S. Gruzdev[3], U. V. Chervonova[3], A. M. Kolker[3]

[1] Zavoisky Physical-Technical Institute, FRC Kazan Scientific Center of RAS, Kazan 420029, Russian Federation, vvalerika@gmail.com
[2] M. N. Mikheev Institute of Metal Physics of the Ural Branch of the Russian Academy of Sciences, Ekaterinburg 620108, Russian Federation
[3] G. A. Krestov Institute of Solution Chemistry, Russian Academy of Sciences, Ivanovo 153045 Russian Federation

The combination of various structural units in one molecule to obtain new properties required for technological applications is an interesting and important task. In this work the EPR spectroscopy and the SQUID magnetometry have been used to study magnetic properties of three novel azomethine Fe(III) dendrimeric complexes and the influence of the counterions NO_3^- (**1**), Cl^- (**2**), PF_6^- (**3**) on the structure and the spin transition.

Magnetic measurements reveals that at room temperature compounds **1** and **3** contains high spin ($S = 5/2$) and low-spin ($S = 1/2$) centers and undergo partial spin crossover ($S = 5/2 \leftrightarrow 1/2$). Compound **2** is only in the HS centers. All three compounds demonstrate AFM spin interactions between the neighboring Fe(III) ions.

The X-band EPR spectra were recorded in a wide range of temperatures from 5 to 340 K. The procedure of spectra decomposition was carried out by using EasySpin Matlab program.

At 340 K EPR spectra of all three compounds are similar and consist of intense broad line with $g_{eff} \sim 2$. The broad resonance line is typical for high-spin ions with a weakly distorted octahedral environment. With lowering temperature, the line widens and shifts toward weaker fields. Its temperature dependence of I passes through a broad maximum. The broad signal from III-type of HS centers can be interpreted as an exchange line from chains of antiferromagnetically coupled iron(III) centers.

With the temperature decrease become distinguishable and grow in intensity signals with $g_{eff} = 6$, $g_{eff} \sim 4.2$ and narrow anisotropic low spin signal. The number of these centers are low and we can assume that these centers are isolated individual paramagnetic centers.

EPR Study of the Mononuclear Iron(III) Complexes with Biphenyl-Bisubstituted Schiff Base Ligand

V. E. Vorobeva[1], R. B. Zaripov[1], M. S. Gruzdev[2], U. V. Chervonova[2]

[1] Zavoisky Physical-Technical Institute, FRC Kazan Scientific Center of RAS, Kazan 420029, Russian Federation, vvalerika@gmail.com
[2] G. A. Krestov Institute of Solution Chemistry, Russian Academy of Sciences, Ivanovo 153045б Russian Federation

In this work the magnetic properties of novel azomethine complexes of iron(III) based on esters of biphenyl-4-carboxylic acid with Cl^-, NO_3^- and PF_6^- counter ions will be presented. Synthesis and properties were presented earlier [1].

The X- and Q-band EPR spectra were recorded in a wide range of temperatures (4 to 340 K – X-band, at 50 K, 100 K and 300 K – Q-band). The EPR spectra were simulated by using EasySpin program. EPR results showed that compounds with Cl^- and PF_6^- counter ions consist of the $S = 5/2$ high-spin (HS) centers. The centers with strong low-symmetry octahedral crystal fields are individual paramagnetic centers and their number decreases with increasing temperature. While the number of Fe(III) centers with weakly distorted octahedral environment increase and they form formations with ferromagnetic order. The X-band EPR spectra from compound with NO_3^- counter ions demonstrate unusual magnetic behavior – a very broad line strongly shifted in a low field region with effective g-factor ~ 8.3 with a minimum at 2000 G. Most likely, it can be interpreted as a result of spontaneous ferromagnetic magnetization (weak ferromagnetism).

1. Gruzdev M.S.: J. Mol. Struct. **1176**, 529 (2019)
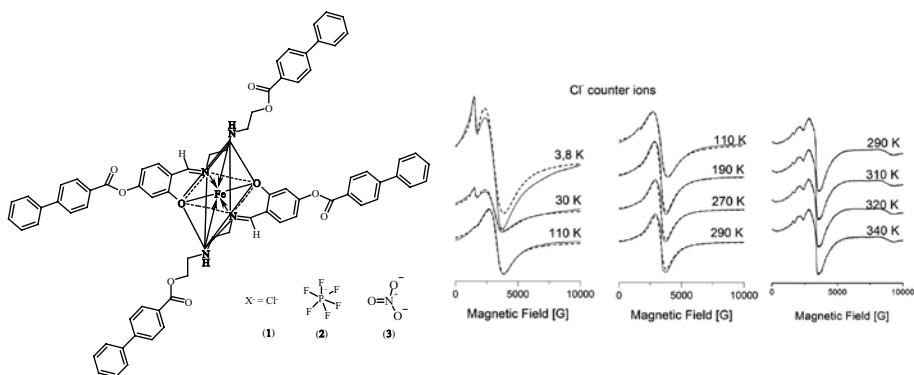
Fig. 1. Schematic representation of the iron(III) complexes (left) and EPR spectra of the compound with Cl^- counter ions (right).

Site-Specific Spin Probing of Graphite Oxide Membrane Using 4-AminoTEMPO

T. S. Yankova[1], N. A. Chumakova[2]

[1] Department of Chemistry, Lomonosov Moscow State University, Moscow 119991, Russian Federation, ya.tatiana@gmail.com

[2] N.N. Semenov Federal Research Center for Chemical Physics, Moscow 119991, Russian Federation

Graphite oxide membranes (GOM) are materials with versatile useful properties. Nevertheless many details of internal structure of the membranes are still unclear. Until now the orientational ordering of the planes in GOMs was studied only visually by cross-sectional SEM imagines. We showed that the ordering of GOMs can be investigated quantitatively using spin probe technique [1].

The present work is devoted to quantitative characterization of the orientational order of the graphite oxide membrane fabricated by vacuum filtration. Spin probes TEMPO, TEMPOL, and 4-aminoTEMPO were used for this purpose. The radicals were introduced into the membrane from acetonitrile. It was revealed that 4-aminoTEMPO cannot be further removed by washing the membrane with acetonitrile or water as opposed to TEMPO and TEMPOL. The slower rotational mobility of 4-aminoTEMPO, sorbed on inner surface of the membrane, compared with TEMPOL was also found. These facts were interpreted as site-specific binding of 4-aminoTEMPO molecules with carboxylic groups of GOM. Analysis of angular dependences of EPR spectra (Fig. 1) showed that orientational ordering of 4-aminoTEMPO in the membrane is significantly less than ordering of TEMPOL. Apparently, 4-aminoTEMPO mainly reflects the alignment of the membrane areas containing carboxylic groups, while TEMPO and TEMPOL characterize the average orientation of the membrane.

1. Chumakova N.A., Rebrikova A.T., Talyzin A.V., Paramonov N.A., Vorobiev A.Kh, Korobov M.V.: J. Phys. Chem. C. **122**, 22750 (2018)
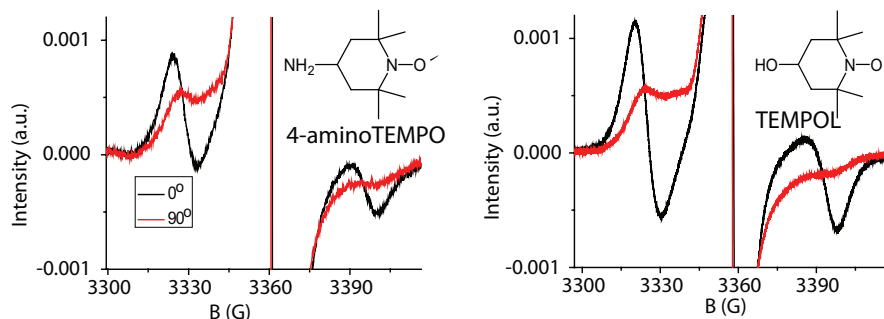
Fig. 1. EPR spectra of the spin probes in GOM recorded at 0° (black lines) and 90° (coloured lines) between the membrane surface normal vector and the magnetic field direction.

Chemisorption Study of Nitrogen Monoxide into Radical-Containing Xerogel by EPR Spectroscopy

A. Yazikova[1,2], A. Poryvaev[2], E. Gjuzi[3], D. Polyukhov[2], F. Hoffmann[3], M. Froba[3], M. Fedin[1,2]

[1] Novosibirsk State University, Novosibirsk 630090, Russian Federation, a.yazikova@tomo.nsc.ru
[2] International Tomography Center SB RAS Novosibirsk 630090, Russian Federation
[3] Institute of Inorganic and Applied Chemistry University of Hamburg Martin-Luther-King-Platz 6, 20146 Hamburg, Germany

Anthropogenic air pollution is a significant problem nowadays. One of the most widespread toxic waste gases is NOx mixture. Nitric oxides are detrimental for ecosystems and human health. The prime source of NOx emission is fuel combustion. Adsorption of NOx from the flue gas is a good method in order to reduce negative affection to environment. As a result this field is attracted interest of the scientific community and industry.

Organosilica materials have established themself as perspective sorbents that find applications in many areas. The materials are perspective for specific sorption application due to the ease of morphology tailoring and surface functionalization. In particular, the introduction of paramagnetic sites in material is promising way for development sorbent that capture paramagnetic gases effectively.

Electron paramagnetic resonance is a spectroscopic technique for studying systems having unpaired electrons. Thus EPR is suitable approach for monitoring radical centers behavior during paramagnetic gas sorption and desorption.

In this work we studied NO sorption in Blatter radical-containing silica xerogel. We showed that properties of such paramagnetic xerogels are significantly different depending on the synthesis conditions. We demonstrated that Blatter radical-containing silica xerogel is able to interact with NO forming diamagnetic product. We studied desorption by heating up to different temperatures and monitoring numeric change of radical centers by EPR. Quantitative EPR analysis of radical content during repetitive sorption/desorption revealed gradual decreasing of sorption capacity. Selective capturing of nitric oxide from flue gas model mixture by radical containing xerogel was approved by EPR spectroscopy.

FMR Signals in Cultivated Cells *Fagopyrum Tataricum*

S. V. Yurtaeva[1], I. V. Yatsyk[1], A. I. Valieva[2], E. A. Gumerova[2], N. I. Rumyantsev[2]

[1] Zavoisky Physical-Technical Institute, FRC Kazan Scientific Center of RAS, Kazan 420029, Russian Federation, S.Yurtaeva@kfti.knc.ru
[2] Kazan Institute of Biochemistry and Biophysics, FRC Kazan Scientific Center of RAS, Kazan, Russian Federation

Iron (Fe) is an obligate requirement for the life of all multicellular organisms. In most eukaryotic cells, iron-requiring proteins are abundantly present in mitochondria, cytosol, and nucleus; they function in electron transfer, ribosome maturation, DNA replication and repair, and cell cycle control [1]. Iron removal out of cells by chelators courses the inhibition of DNA synthesis [2, 3].

When studying mitosis in HeLa cells, it was shown that iron ions in interphase of the cell cycle are concentrated in nucleoli, and in metaphase are detected in chromosomes [3]. It was found that one of the main places of iron localization in plant cells is the nucleolus [4]. Iron concentration found in the nucleolus of pea (Pisum sativum) embryo cells was higher than in the expected iron-rich organelles such as plastids or vacuoles.

Recently, it was shown by Hilo et al. [5] that iron promoted meristematic cell division during adventitious root formation in Petunia hybrida. The authors revealed an enhanced allocation of Fe to the nuclei of meristematic cells in adventitious root initials.

Since the 1960s it is known about the phenomenon of the appearance of ferromagnetic (FMR) signals with simultaneous changes of the static magnetic susceptibility in the yeast cell cultures at certain stages of cell culture growth. It is reported that ferromagnetism in semi-synchronized yeast cultures has been observed in the period immediately preceding the beginning of the intensive budding. After cell division, the signal disappears [6–8].

In this research, the phenomenon mentioned above was detected for the first time in actively dividing non-morphogenic cultures Fagopyrum tataricum.

Cultures of non-morphogenic plant cells in their physiologic characteristics are similar to tumor cells. That allows us to consider these cultures as a potential model to study the mechanisms of proliferation in tumor cells.

In this study, the dynamics of growth of cell cultures in two ways of cultivation: callus-cells – on solid agar medium, and suspension culture – in a liquid medium, were investigated by X-band EPR spectroscopy (Bruker EMX). The samples were frozen at 77 K.

When using both ways of cultivation, at a certain stage of cell culture growth (namely at the 4th day of callus passage and the 3rd day of cell suspension passage) ferromagnetic signals appeared (the example in Fig. 1a). There were no such signals either in initial cell cultures or in media. This stage of cell growth correlates with the phase of a maximum cell division activity in culture. In the following days, the signal disappeared.
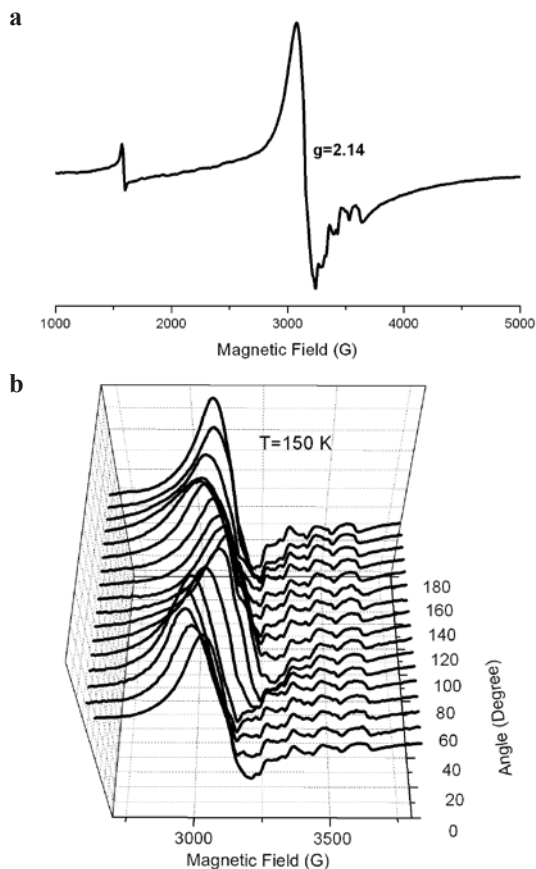
Fig. 1. a FMR signal, arising in the cell culture at the 4-th day of cell division, **b** the angular dependence of the signal.

The observed signal was characterized by resonance field anisotropy (Fig 1b), which is character to the ferromagnetic nature of the signal, by non-monotonic temperature behavior of amplitude, line width, and resonance field within temperature interval 100–270 K.

The origin of detected signals and their relation with aggregated forms of iron are discussed.

The investigation of cell division processes with EPR spectroscopy may contribute to understanding the role of iron in these processes.

1. Zhang C. *et al.*: Protein Cell. **5**, iss. 10, 750–760 (2014)
2. Le E., Richardson S.T.: Biochim. Biophys. Acta **1603**, 31–46 (2002)
3. Robbins E., Peterson S.T.: Proc. Nat. Acad. Sci. USA **66**, 1244–1251 (1970)
4. Roschzttardtz H., Grillet L. *et al.*: The Journal of Biol. Chemistry **286**, 27863–27866 (2011)
5. Hilo A., Shahinnia F. *et al.*: J. Exp. Bot. **68**, iss. 15, 4233–4247 (2017)
6. Samoilova O.P., Blumenfeld L.A.: Biofizika (in Russian) **6**, iss. 1, 15–19 (1961)
7. Tsapin A.I., Samoilova O.P., Blumenfeld L.A.: Biofizika (in Russian) **34**, iss. 4, 15–19 (1989)
8. Samoilova O.P., Tsapin A.I., Blumenfeld L.A.: Biofizika (in Russian) **40**, iss. 2, 383–388 (1995)

EPR Study of Endohedral Fullerene $Sc_2@C_{80}(CH_2Ph)$

R. B. Zaripov[1], Yu. E. Kandrashkin[1], K. M. Salikhov[1], B. Büchner[2,3], F. Liu[2], M. Rosenkranz[2], A. A. Popov[2], V. Kataev[2]

[1] Zavoisky Physical-Technical Institute, FRC Kazan Scientific Center of RAS, Kazan 420029, Russian Federation
[2] Leibniz IFW Dresden, Dresden, D-01069, Germany
[3] Institute for Solid State and Materials Physics, TU Dresden, Dresden, D-01062, Germany

Encapsulating the spin system within the robust molecular container is an appealing strategy to isolate spins from the surrounding media. As the carbon cage can stabilize endohedral spin units chemically and magnetically, fullerenes have been playing a prominent role in this field. In this work, we report on the stabilization of the single electron Sc–Sc bond in the stable benzyl monoadduct $Sc_2@C_{80}(CH_2Ph)$, which enabled comprehensive CW and pulsed ESR studies of this unique spin system [1, 2]. A full localization of the spin density inside the fullerene cage at the Sc_2 dimer results in an extraordinary large hyperfine coupling of the unpaired spin $S = 1/2$ with two equivalent ^{45}Sc nuclear spins $I = 7/2$ of the metal centers amounting to $a = 18.2$ mT (510 MHz). This yields a fully resolved hyperfine-split EPR spectrum comprising 64 lines, which can be excellently resolved in the ESR experiments at X-, Q- and W-band frequencies over a broad temperature range. Pulse ESR experiments demonstrate coherent spin dynamics of the electron-nuclear system in $Sc_2@C_{80}(CH_2Ph)$ enabling manipulation of the quantum states on dedicated resonant transitions.

1. Zaripov R.B., Kandrashkin Yu.E., Salikhov K.M., Büchner B., Liu F., Rosenkranz M., Popov A.A., Kataev V.: Nanoscale **12**, 20513 (2020)
2. Kandrashkin Yu.E., Zaripov R.B., Liu F., Büchner B., Kataev V., Popov A.A.: Physical Chemistry Chemical Physics **23**, 18206 (2021)
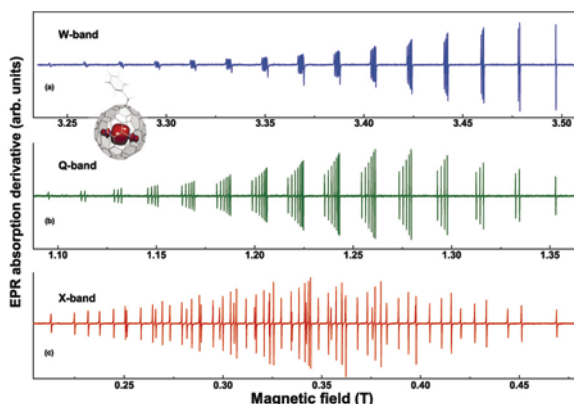
Fig. 1. EPR spectra recorded at frequencies of 94.1 GHz (top), 34.2 GHz (middle) and at 9.8 GHz (bottom) at room temperature.

In situ EPR Study of the Mechanisms and Kinetics of Intercalation of Molybdenum Pentafluoride Molecules from the Liquid Phase into Graphite

A. M. Ziatdinov, A. K. Tsvetnikov

Institute of Chemistry, Far Eastern Branch of the RAS, Vladivostok 690022, Russian Federation,
ziatdinov@ich.dvo.ru

Understanding the mechanisms of insertion of "guest" molecules into graphite is an important stage at developing methods for the synthesis of its new intercalated compounds. One of the effective methods for studying the kinetics and mechanisms of insertion of "guest" molecules into graphite is the EPR. To date, *in situ* studies by this method of the mechanisms of insertion of a number of molecules from the gas phase into graphite have already been implemented [1–4]. At the same time, there is still no information in the literature on EPR studies of the process of insertion into graphite of molecules from the liquid phase of a substance. This report presents the results of the first *in situ* studies by EPR of kinetics and
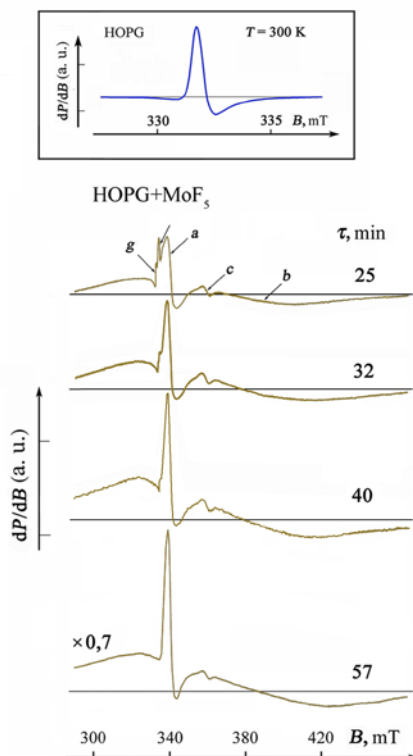
Fig. 1. Evolution of the EPR spectrum of a system (HOPG + MoF$_5$) at 360 K (>T_m). τ is the reaction time. The X-band.

mechanisms of insertion into the highly oriented pyrolytic graphite (HOPG) plate of molecules from the liquid phase of molybdenum pentafluoride (MoF_5).

Up to the melting temperature of intercalate (T_m) the asymmetric signal of spin resonance on conduction electrons (CESR) of the graphite plate (Fig. 1, inset)) is characterized by a g-factor value 2.0413 ± 0.0002 and by a width at half height of an intense peak 0.45 ± 0.05 mT. From the moment of melting of the MoF_5 powder, which completely covers the graphite plate, it monotonically decreases in intensity up to the disappearing after ~45 min. In this time interval of reaction, several new resonances appear in the EPR spectrum of the (graphite + MoF_5) system, the parameters of which vary with time (Fig. 1).

The "a" component of the EPR spectrum (Fig. 1) represents the resonance on the conduction electrons of the carbon layers adjacent to the two-dimensional solid layers of the intercalate. From the moment of the first registration until the end of the reaction, it is characterized by one and the same value g = 2.001 ± 0.001. Its intensity, shape and width smoothly change during the reaction. The broad "b" component of the EPR spectrum (Fig. 1) belongs to Mo^{5+} ions in the solid intercalate layers and is characterized by g ~ 1.95. Its width is ~70 mT at the beginning of the reaction and decreases to ~100 mT at its completion. The symmetric low-intensity "c" component (Fig. 1) also belongs to Mo^{5+} ions, but to those that are outside the graphite plate – in the liquid phase of the intercalate. This component is characterized by the values of g-factor and width, equal to 1.89 ± 0.02 and ~3.7 mT, respectively. The weakly asymmetric "d" component of the EPR spectrum (Fig. 1) belongs to electrons localized on the p_z-orbitals of the atoms of carbon layers near the front of the MoF_5 intercalation. The phase of this component is the opposite of the phase of the graphite CESR signal. During the reaction, it narrows and the ratio of its peak intensity to that of the graphite CESR signal increases. All this happens at a constant value of its g-factor 2.035 ± 0.002.

The presence in the EPR spectrum of intercalated graphite plate simultaneously of resonances on the conduction electrons of the carbon layers of both unintercalated and already intercalated regions indicates that the current carriers of both of these regions in the EPR time scale are localized within their regions. This fact indicates the existence of a high-resistance barrier between the regions under consideration. The observation of resonance on electrons localized on the p_z-orbitals of the atoms of the carbon network near the front of the MoF_5 intercalation into graphite is consistent with this point of view. The simultaneous observation in the reaction product – in the 1st stage intercalated compound of the graphite with MoF_5 – of resonances on the π-electrons of the carbon layers and on the d-electrons of the intercalated molecules indicates a weak exchange interaction between them (a negligible mixing of the wave functions of current carriers and MoF_5), which is unusual for paramagnetic conductors.

1. Davidov R., Milo O., Palchan I., Selig H.: Synth. Met. **8**, 83 (1983)
2. Nakajima M., Kawamura K., Tsuzuku T.: J. Phys. Soc. Jpn. **57**, 1572 (1988)
3. Ziatdinov A.M., Sviridova A.G., Sereda V.V. *et al.*: Appl. Magn. Reson. **35**, 221 (2008)
4. Ziatdinov A.M., Mishchenko N.M.: J. Phys. Chem. Solids **58**, 1572 (2019)

Anisotropic Ferromagnetism in High Dose Iron Implanted Magnesium Oxide

A. L. Zinnatullin[1], B. F. Gabbasov[1], R. V. Yusupov[1], R. I. Khaibullin[2], F. G. Vagizov[1]

[1] Institute of Physics, Kazan Federal University, Kazan 420008, Russian Federation,
almaz.zinnatullin@gmail.com
[2] Zavoisky Physical-Technical Institute, FRC Kazan Scientific Center of RAS, Kazan 420029, Russian Federation

The observation of ferromagnetism ($T_C \leq 200$ K) in Mn-doped indium and gallium arsenides stimulated studies of magnetism in other semiconductor materials doped with magnetic ions [1]. It was theoretically predicted that in wide-gap semiconductors with a 3d-element impurity, the Curie temperature may be even higher than room temperature [2]. Meanwhile, one of the possible mechanisms of high-temperature ferromagnetism in such compounds is the formation of magnetically ordered clusters from implanted 3d-elements [3]. New multifunctional devices may be developed on the basis of such nanostructured systems [4].

Here we present the results of a study of single-crystal magnesium oxide (MgO) implanted with iron ions (^{57}Fe – 40 %) with an energy of 40 keV and to a fluence of $1.5 \cdot 10^{17}$ ions/cm^2. The valence state and local environment of the introduced iron impurity were studied by Mössbauer spectroscopy at room and low (80 K) temperatures. The magnetic properties of the sample were investigated by vibration magnetometry in the temperature range of 10–300 K and ferromagnetic resonance (FMR) at room temperature in various geometries.

It was found that MgO single crystal implanted with iron ions exhibits a strong ferromagnetic response at room temperature and fourth-order in-plane magnetic anisotropy. The implanted iron impurity was found in different valence and phase states. A significant part of the impurity forms α-Fe nanoparticles. They are the main source of the observed ferromagnetism at room temperature. We suppose that these nanoparticles are coherently buried into the MgO host matrix. This explains the discovered magnetic anisotropy in the plane of the implanted surface.

1. Wolf S. *et al.*: Science **294**, 1488 (2001)
2. Dietl T. *et al.*: Science **287**, 1019 (2000)
3. Okay C. *et al.*: Appl. Magn. Reson. **48**, 347 (2017)
4. Dietl T.: Nature Materials **9**, 965 (2010)

Coil to Globule Transition in PNIPAM and Its Copolymer Solutions: EPR Spin Probe Technique Study

E. M. Zubanova, T. A. Ivanova, E. N. Golubeva

Chemistry Department, Lomonosov Moscow State University, Moscow 119991, Russian Federation, kate_zub@mai.rul

Continuous-wave electronic paramagnetic resonance spectroscopy using spin probe technique with amphiphilic TEMPO radical was applied to determine temperature ranges of the coil to globule transition in the thermoresponsive polymers aqueous solutions. Such polymers exhibit changes of physical properties, e.g., solubility, with temperature. Thermoresponsive polymers with low critical solubility temperature (LCST) below soluble in water are more common. Near LCST, they undergo coil to globule transition in aqueous solutions. In the present work, classical thermoresponsive polymer poly-N-isopropylacrylamide (PNIPAM) and its statistical copolymer with N-tert-butylacrylamide (NTBA) and graft-copolymer with D,L-polylactide (PLA) were studied.

Adding probe molecules to the polymer solution leads to self-distribution of these guest molecules between hydrophobic and hydrophilic regions in polymer solutions. EPR spectroscopy of probe molecules shows that globules start to form in considered thermoresponsive polymers solutions at temperatures before thermal collapse detected by DSC or turbidimetry methods. In copolymers of PNIPAM with hydrophobic NTBA and PLA inhomogeneities exist already at temperatures 275–280 K in contrast to 295–300 K measured by turbidimetry. Hydrophobic modification of PNIPAM by PLA and NTBA leads to decreasing LCST and, according to EPR spin probe data, leads to increasing the coil to globule transition interval. If the temperature range of coil to globule transition for PNIPAM in aqueous was 1-2 degrees, then PNIPAM-NTBA and PNIPAM-PLA temperature ranges were about 20 degrees. A theoretical simulation of obtained EPR spectra at higher temperatures after the globule collapsed was performed and showed further reorganization of solutions changing the globule to a denser state.

Multi-Pulse Protocols in Solid-State ^{1}H NMR in Cu- and Ni-Oxamidato Complexes

Yu. Slesareva[1], Yu. Kandrashkin[1], R. Zaripov[1], T. Ruffer[2], E. Vavilova[1]

[1] Zavoisky Physical-Technical Institute, FRC Kazan Scientific Center of RAS, Kazan 420029, Russian Federation
[2] Technische Universität Chemnitz, Chemnitz, Germany

Metal-oxamidato complexes are considered as structural units for new materials for spintronics and quantum computing applications. CPMG pulse protocol is usually applied to increase the coherence time in presence of spectral diffusion [1]. Here we present the results of ^{1}H NMR study of Cu(II)-oxamidato complex in comparison with its diamagnetic Ni(II)-containing analog. The experiments have shown the influence of inhomogeneous broadening on the process of suppression of nuclear spin decoherence and registration of parasitic echo components. An improved CPMG pulse protocol suggested in [2] was applied for the elimination of unwanted echoes.

1. Zaripov R. *et al.*: Phys. Rev. B. **88**, 094418 (2013)
2. Zaripov R. *et al.*: Beilstein J. Nanotechnol. **8**, 943–955 (2017)

AUTHOR INDEX

Отпечатано с оригиналов заказчика